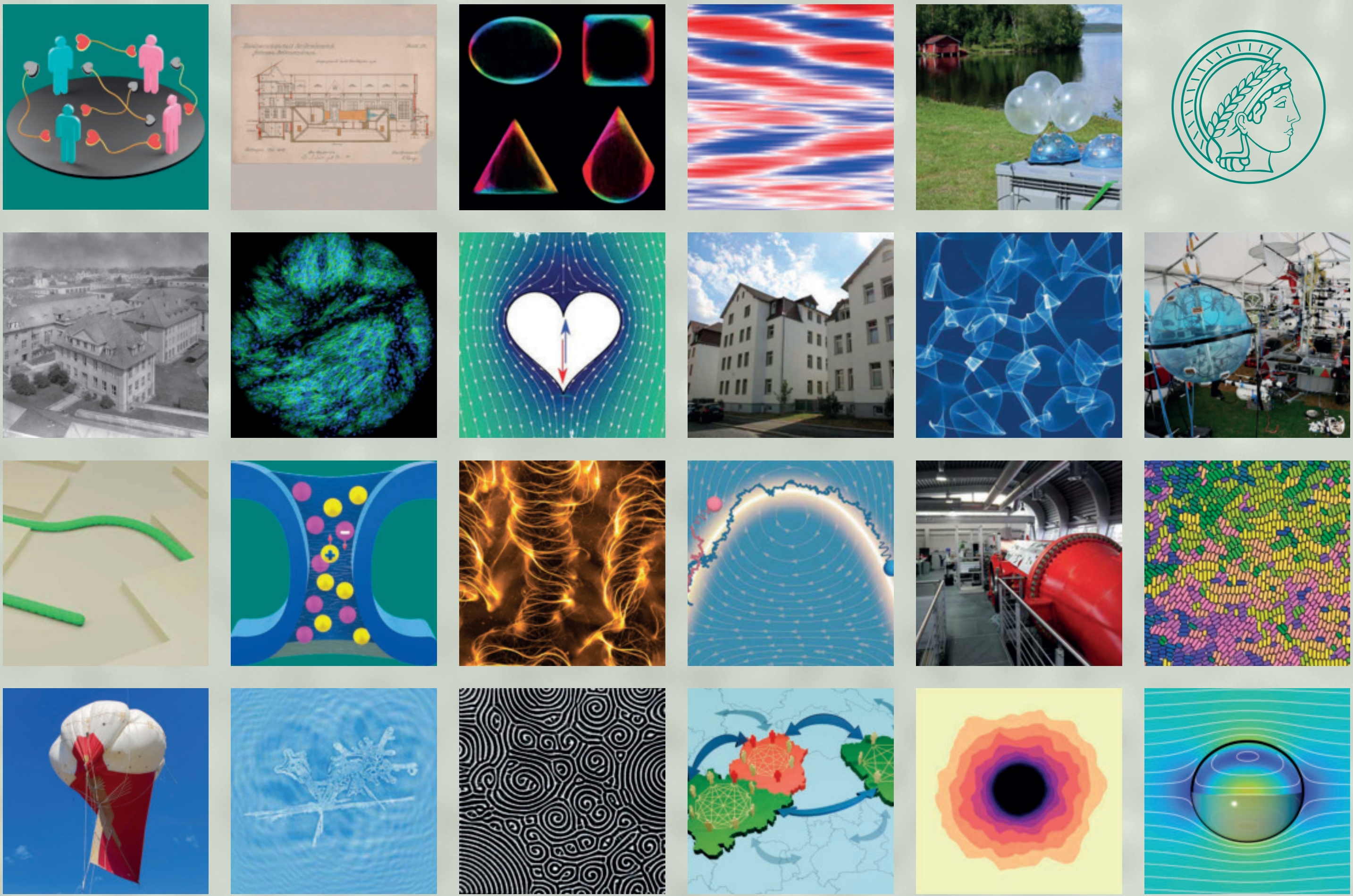

Max Planck Institute for Dynamics and Self-Organization

Research Report 2025

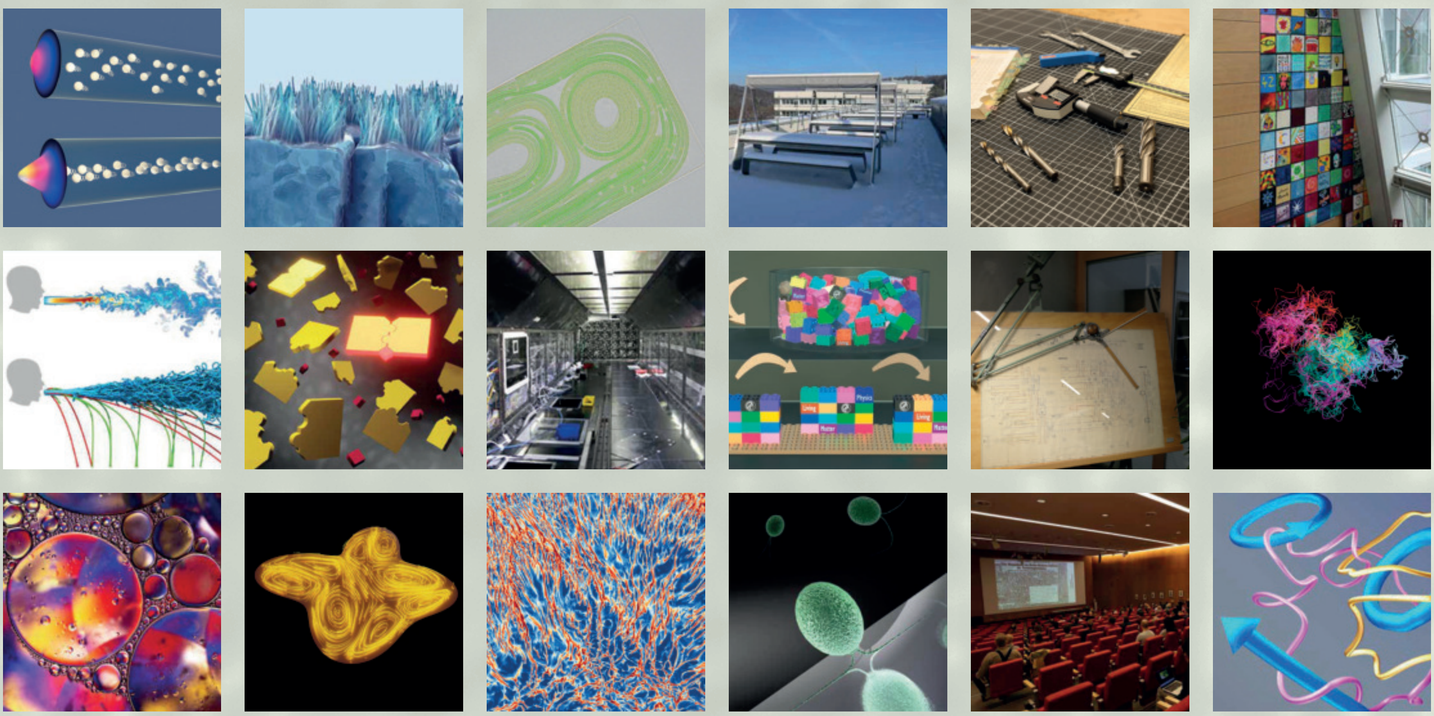

Max Planck Institute

for

Dynamics and Self-Organization

RESEARCH REPORT

2025

Directors

Prof. Dr. Dr. h.c. Eberhard Bodenschatz (Managing Director)
Prof. Dr. Ramin Golestanian

Scientific Advisory Board

Prof. Dr. Seth Fraden, Brandeis University, Waltham, USA
Prof. Dr. Marileen Dogterom, Delft University of Technology, The Netherlands
Prof. Dr. Hugues Chaté, Institut Rayonnement Matière de Saclay, France
Prof. Dr. Leticia F. Cugliandolo, Université Pierre et Marie Curie – Paris VI, France
Prof. Dr. J. Michael Kosterlitz, Brown University, Providence, USA
Prof. Dr. Udo Seifert, Universität Stuttgart, Germany
Prof. Dr. John Toner, University of Oregon, Eugene, USA
Prof. Dr. Regine von Klitzing, Technische Universität Darmstadt, Germany

No matter how well we understand how a single droplet of water is formed in the laboratory, we cannot predict how countless droplets form clouds that substantially affect the Earth's climate. And although we can accurately characterize a single neuron's impulse, we do not yet understand how billions of them form a single thought. In such systems, animate or inanimate, processes of self-organization are at work: Many interacting parts organize themselves independently, without external control, into a complex whole. At our institute we explore the mechanisms underlying these processes in order to gain a detailed understanding of complex systems. Also the major challenges of the 21st century, from climate change and economic crises to problems in energy supply and transport, are closely linked to these scientific questions. Without a deep understanding of dynamics and self-organization in complex and highly networked systems we cannot face these challenges. With our basic research not only do we want to deepen our understanding of nature, but also want to contribute to a sustainable existence on this planet.

CONTENTS

PART I
MPI-DS IN A NUTSHELL

PART I

MPI-DS IN A NUTSHELL

INTRODUCTION

1

In 2025, the Max Planck Institute for Dynamics and Self-Organization (MPI-DS) will celebrate its centennial. Originally founded as the Kaiser Wilhelm Institute for Flow Research (Strömungsforschung) in late 1923, the institute advanced the field of fluid dynamics under the leadership of Ludwig Prandtl, Albert Betz, and Walter Tollmien. Among our alumni is Klaus Hasselmann, the 2021 Nobel Prize in Physics laureate. He received his doctorate in 1957 under Tollmien's supervision. As early as then, the focus was on the nonlinear dynamics of fluid dynamical systems, a topic that remains one of the institute's key research areas today. In the 1970s, under the direction of Jan-Peter Tonnies, Hans Pauly, and Heinz-Georg Wagner, the institute expanded its focus to include the study of molecular interactions, atomic and molecular physics, and reaction kinetics. Meanwhile, Ernst-August Müller continued fundamental fluid dynamics research, particularly focusing on aeroacoustics. After the previous directors retired, Theo Geisel arrived in 1996 and shifted the focus to nonlinear dynamics and its applications to neuroscience and network dynamics. In 2003, Stephan Herminghaus established the Department of Dynamics of Complex Fluids, and Eberhard Bodenschatz founded the Department of Fluid Physics, Pattern Formation, and Biocomplexity. Research shifted its focus to studying dynamics and self-organization in a variety of areas, ranging from cell biology to granular matter, turbulence, cloud physics, and even public transportation. In 2004, the institute was renamed the Max Planck Institute for Dynamics and Self-Organization. Following Theo Geisel's retirement, Ramin Golestanian established the active matter physics research area at the institute within the Department of Living Matter Physics. The former neuroscience research focus continues at the Göttingen Campus Institute for Dynamics of Biological Networks. Following Stephan Herminghaus's retirement, the institute's research shifted to focus on dynamics and self-organization in active matter.

Active matter is all around us. It is the building block of life. For instance, cells self-organize to form organisms, organs, and people, which then interact with each other. Active matter exists outside of thermodynamic equilibrium. It requires constant local energy input to generate function at larger spatial and temporal scales. The dynamics and properties of a system or systems are self-organized by nonlinear interactions outside of equilibrium all in the absence of a guiding body. These nonlinear, complex interactions unite the research at the institute. Though the topics presented in this report seem vast, they are not when it comes to dynamics and self-organization. The

commonality of the physical principles and their mathematical descriptions combine our diverse research program seamlessly. This common language enables us to transcend traditional disciplinary boundaries. Our advanced experimental facilities and computational infrastructure provide a breeding ground for scientific breakthroughs in the dynamic and diverse environment of the Max Planck Institute for Dynamics and Self-Organization.

Göttingen, June 2025,

Eberhard Bodenschatz
Managing Director

The two directors of MPI-DS (from left): Eberhard Bodenschatz and Ramin Golestanian (Burg Ludwigstein, Witzenhausen, March 2025).

INITIATIVES

2

Contents

2.1 PHYSICS AND LIFE

Living matter, unlike its inanimate counterpart, is not naturally in equilibrium. To sustain and thrive, it must constantly convert the energy present in the environment to move, grow or reproduce, exhibiting unique properties that are impossible in thermal equilibrium. The implications of this non-equilibrium activity are already apparent at the nanoscale level of enzymes and proteins, or the complex interplay of self-organising processes within cells or complex organelles such as cilia, but can also be studied at the level of organs and complete organisms, or even at the level of populations of living organisms.

At MPI-DS, we study dynamics and self-organization of a large variety of living systems, across multiple scales. Building on the century-long legacy of flow research at our institute, we study the complex spatiotemporal patterns of the cilia-driven cerebrospinal fluid flow in the third ventricle of mouse brain using particle image velocimetry (PIV) (Fig. 2.1) alongside theoretical research that uncovers how cilia can use the non-reciprocal nature of hydrodynamic interactions to quickly synchronize and generate robust metachronal waves [1]. We have also performed a multi-scale theoretical study of how to properly quantify dissipation in active matter systems, including the introduction of a new hydrodynamically consistent many-body Harada-Sasa relation [2], a minimum dissipation theorem that incorporates the internal dissipation in microswimmers [3], development of a thermodynamically consistent framework to quantify the dissipation in micro- and nanoscale swimmers [4], and a field theoretical description to present exact fluctuation dissipation relations that involve entropy production [5, 6].

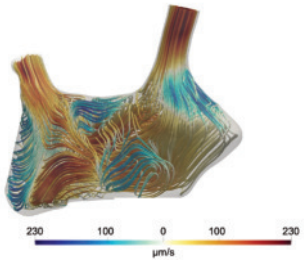

Figure 2.1: Simulation of v3V streams in wild type adult mice. Note the whirl in the lower right and difference in velocities. The areas of low velocities are where tanycytes reside. Streamlines are color-coded using the horizontal component of the local velocity, with red indicating anterior to posterior and blue indicating posterior to anterior.

Living filaments have been studied extensively (see Fig. 2.2) and shown to exhibit novel collective behavior including mechanical instabilities, collective cell migration, and self-organization within virtual cages due to phototactic response [7]. Other experimental investigations include flight dynamics of bees and developing an innovative flat cell imagining technique.

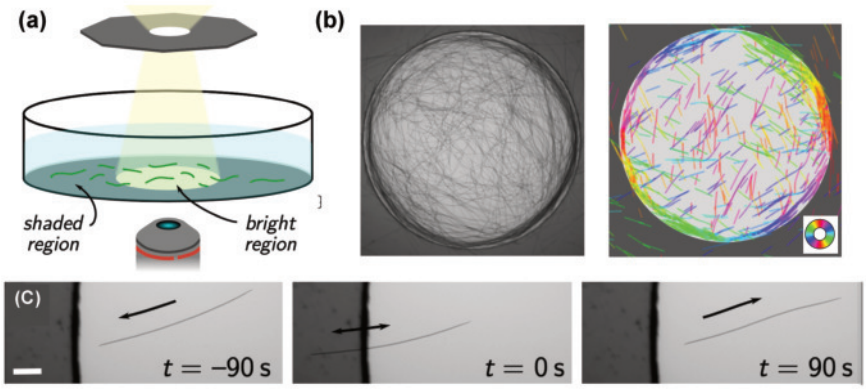

Figure 2.2: (a) Schematic of the experimental setup: Filaments glide at the bottom of a Petri dish, submerged in medium and are illuminated from above with a masked light pattern. (b) Ring formation in the experiment (left) and simulations (right), with the color wheel showing the local orientation of filaments. (c) Velocity reversal of *O. lutea* gliding into the dark. Scale bar: 100 μm.

Non-reciprocal active matter has been at the focus of extensive investigations at MPI-DS [8]. We have uncovered a surprising connection between the non-reciprocal Cahn-Hilliard (NRCH) model that describes scalar fields to Toner-Tu-like theories of polar active matter and the

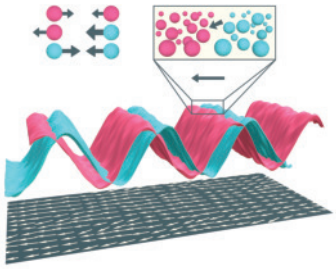

Figure 2.3: The reciprocal attraction between particles can give rise to phase separation of every species into coexisting dense and dilute domains and the non-reciprocal interaction will make them form bands that chase each other, leading to the emergence of global polar order and motion in the system while breaking both parity and time-reversal (PT) symmetries.

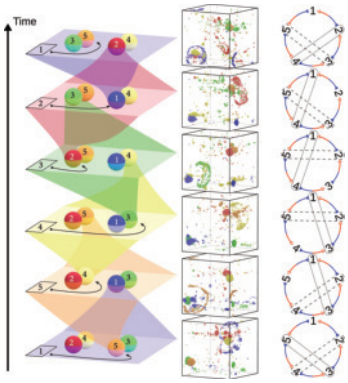

Figure 2.4: A collection of a number of enzymes with chasing interactions can lead to spontaneous formation of a swarm with a cyclic pattern of collapse and explosion. (left) Schematic representation of the dynamics, (middle) snapshots of Brownian dynamics simulations, and (right) diagrammatic representation of the non-reciprocal interactions, with the dashed and dotted lines representing respectively the pairs on the left and right of the schematic picture.

Kardar-Parisi-Zhang (KPZ) equation that describes the dynamics of growing rough interfaces [9]. This formal mapping has allowed us to prove the existence of true long-range polar order in 2D NRCH model in violation of the Mermin-Wagner theorem, which even persists upon introduction of hydrodynamic interactions [10]. The NRCH model has been extended in various forms to include the effect of nonlinear non-reciprocal interaction terms, which lead to the emergence of effervescence [11], the role of multi-species non-reciprocal interactions that can stabilize complex metabolically active suspensions [12], and the defect solutions that break the symmetries of the system and destroy polar order [13]. We have also introduced and studied a model that describes quorum-sensing active matter with non-reciprocal aligning interactions, which exhibits a remarkable similarity to the phenomenology of NRCH together with additional chaotic features [14, 15]. Non-reciprocal chemically active systems remain a major focus of research. Among many notable achievements in these studies, we can highlight the proposed scenario in which non-reciprocal active matter may have led to fast and efficient emergence of metabolic cycles at the origin of life [16] (see Fig. 2.4). Moreover, non-reciprocal interactions have been shown to enable choreographed shape-shifting transitions between different structures in multifarious self-assembly [17].

At the cellular and tissue scale, growth as a source of activity can give rise to a rich phenomenology, in the context of the nematic structure of growing cell colonies [18], statistical properties of the displacements of dividing cells [19] or the consequences of specific mechanical interactions [20, 21]. On the other hand, at the molecular scale, enzymes have been extensively studied as stochastic oscillators, and a proposal has been developed for mechanistic rules that can provide opportunities for de novo design and control [22].

In summary, physics is essential for understanding the dynamics and self-organization of life from molecular processes to whole organisms and their interaction. Only with physics in combination with biomolecular chemistry can life-like processes be created from the bottom up, such as building synthetic molecular motors [23–25]. To help with our strategic focus on this vision, we have invested in a strong partnership with the Max Planck School Matter-to-Life graduate school since its inception.

[1] D. J. Hickey, R. Golestanian, A. Vilfan, Proc. Natl. Acad. Sci. USA **120**, e2307279120 (2023)
[2] R. Golestanian, Phys. Rev. Lett. **134**, 207101 (2025)
[3] A. Daddi-Moussa-Ider, R. Golestanian, and A. Vilfan, Nat. Commun. **14**, 6060 (2023)
[4] M. Chatzittofi, J. Agudo-Canalejo, R. Golestanian, Phys. Rev. Research **6**, L022044 (2024)
[5] M. K. Johnsrud and R. Golestanian, arXiv:2409.14977
[6] M. K. Johnsrud and R. Golestanian, arXiv:2502.02524
[7] M. Kurjahn, L. Abbaspour, F. Papenfuß, P. Bittihn, R. Golestanian, B. Mahault, S. Karpitschka, Nat. Commun. **15**, 9122 (2024)
[8] R. Golestanian, Europhys. News **55**, 12 (2024)
[9] G. Pisegna, S. Saha, R. Golestanian, Proc. Natl. Acad. Sci. USA **121**, e2407705121 (2024)

[10] G. Pisegna, N. Rana, R. Golestanian, S. Saha, arXiv:2501.01330
[11] S. Saha, R. Golestanian, Nat. Commun., *in press*
[12] L. Parkavousi, N. Rana, R. Golestanian, S. Saha, Phys. Rev. Lett. **134**, 148301 (2025)
[13] N. Rana, R. Golestanian, Phys. Rev. Lett. **133**, 158302 (2024)
[14] Y. Duan, J. Agudo-Canalejo, R. Golestanian, B. Mahault, Phys. Rev. Lett. **131**, 148301 (2023)
[15] Y. Duan, J. Agudo-Canalejo, R. Golestanian, B. Mahault, Phys. Rev. Research **7**, 013234 (2025)
[16] V. Ouazan-Reboul, J. Agudo-Canalejo, R. Golestanian, Nat. Commun. **14**, 4496 (2023)
[17] S. Osat, R. Golestanian, Nat. Nanotechnol. **18**, 79 (2023)
[18] J. Isensee, L. Hupe, R. Golestanian, P. Bittihn, J. R. Soc. Interf. **19**, 20220512 (2022)
[19] S. R. Lish*, L. Hupe*, R. Golestanian, P. Bittihn, arXiv:2409.20481
[20] T. Sunkel, L. Hupe, P. Bittihn, Commun. Phys. **8**, 179 (2025)
[21] J. Isensee, P. Bittihn, Soft Matter **21**, 4233 (2025)
[22] M. Chatzittofi, J. Agudo-Canalejo, R. Golestanian, Chem Catalysis (2025)
[23] A.-K. Pumm et al., Nature **607**, 492 (2022)
[24] X. Shi et al., Nat. Phys. **18**, 1105 (2022)
[25] X. Shi et al., Nat. Nanotechnol. **19**, 338 (2023)

2.2 PHYSICS AND MEDICINE

"Insight must precede application."

Max Planck

Global health faces significant challenges from neurological, cardiovascular, and infectious diseases, which are a major source of disability and death worldwide. The MPI-DS conducts basic and applied research to develop innovative tools and concepts for disease diagnosis, therapy, and prevention thereby helping to address these global challenges. Physicists have made groundbreaking contributions to medicine by devising quantitative techniques to measure biological functions. These techniques have led to many diagnostic tools that medical professionals use every day. For instance, the invention of the electrometer paved the way for the first electrocardiogram and the development of modern quantitative electrophysiology. X-ray imaging enables computerized tomography scans of the entire body. Ultrasound imaging is also used daily in medical practice. Magnetic resonance imaging (MRI) has revolutionized our ability to characterize anatomical structures and functions without impacting the biological tissue under investigation. Researchers at MPI-DS leverage their expertise in the dynamics of complex systems to develop the next generation of measurement technologies. Examples include recent advances in real-time MRI (by MPI-DS external scientific member Jens Frahm) and 4D imaging of cardiac electromechanical function (Sec. 6.27), techniques that visualize the spatiotemporal dynamics of biological systems with unprecedented detail. Building on advances in measuring biological function and the ever-growing amount of dynamical data, MPI-DS researchers apply their expertise to advance our understanding of dynamics and self-organization principles in biological systems. This allows for new approaches to diagnosing, treating, and preventing diseases. MPI-DS researchers conduct research ranging from basic theoretical and experimental studies to initial clinical trials with patients and the development of biomedical devices. MPI-DS is partner in the interdisciplinary biomedical research at Göttingen Campus, including the Campus Institute for Dynamics of Biological Networks, the Faculty of Physics, the University Medical Center (UMG), the Heart and Brain Research Center, the German Primate Center (DPZ), and the German Center for Cardiovascular Diseases (DZHK). In the following, we provide a brief overview.

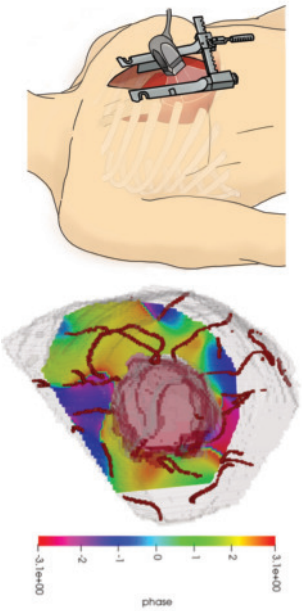

Figure 2.5: 4D electromechanic imaging of human ventricular fibrillation (VF) during bypass surgery (top). Snapshot of 4D rotors and phase singularities (red) during human VF (bottom).

Cardiac arrhythmias are a prominent example of a "dynamic disease", i.e., a medical condition characterized by a significant change in the dynamic behavior of a physiological system. Arrhythmias are associated with the propagation of chaotic excitation waves in excitable cardiac tissue. Researchers at the MPI-DS study arrhythmias using concepts of nonlinear dynamics and develop new diagnostic and therapeutic approaches. Research topics include the dynamics of waves in excitable media (Sec. 5.11) [1–3], the dynamics of chaotic transients, the spatial-temporal organization of human ventricular fibrillation, and the optimal spatial-temporal control (Sec. 8.8) [4–6]. Methods range from time series analysis (Sec. 7.9) numerical simulations and preclinical (optogenetic) studies and simulations [4, 7–9] to clinical trials (Sec. 8.8). MPI-DS is supported by the MPG's Technology Transfer Funds and Max

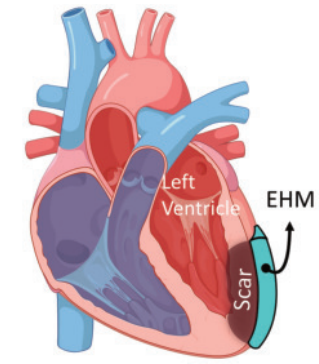

Figure 2.6: Schematic illustration of an infarcted heart with a scarred left ventricle and engineered heart muscle (EHM) patch over it.

Planck Innovation GmbH to advance innovative arrhythmia control for atrial and ventricular arrhythmias to clinical application (Sec. 3.2.2).

Heart failure (HF) is a complex clinical syndrome characterized by the heart's inability to pump blood. In the CRC 1002 "Modulatory Units in Heart Failure," researchers at the MPI-DS team up with colleagues from UMG and DPZ to investigate cardiac electromechanical dysfunction in the transition to and, potentially, recovery from HF. MPI-DS researchers, in collaboration with colleagues at UMG (Zimmermann), aim to replace failing tissue with engineered heart muscle (EHM), as illustrated in Fig. 2.6. Numerical simulations and machine learning approaches are employed to optimize the design and placement of EHM for enhanced therapeutic outcomes (Sec. 8.1 and 8.2) [10].

Another major threat to the health of individual patients and our broader ability to effectively treat even seemingly simple bacterial infections is the rise in antibiotic resistance. To address this urgent issue, it is crucial not only to discover new antimicrobial compounds but also to improve our understanding of existing resistance mechanisms to better mitigate them. In collaboration with colleagues from the Geisel School of Medicine at Dartmouth, MPI-DS researchers identified a new form of "collective resistance", which contributes to the increased resistance of large bacterial populations known as biofilms compared to single cells (Sec. 6.21). The key is the self-organized spatial colony structure comprising fast-growing, slow-growing and entirely dormant cells. The reorganization of this structure in response to antibiotics leads to the formation of highly resistant cell layers (Fig. 2.7), reducing the effectiveness of subsequent drug exposures [11]. Mathematical modeling revealed that the consumption and transport of nutrients through the growing colony play an essential role: They provide an implicit coupling between metabolism in different cells, which in turn modulates their resistance to antibiotics. Stochasticity in gene expression further enhances phenotypic heterogeneity, leading to different outcomes for identical drug exposures [12]. These findings highlight the crucial roles of self-organized patterns and the coupling between biological regulation and physical interactions in shaping bacterial resistance. Our research thereby contributes to developing improved therapeutic strategies and minimizing the risk of further resistance emergence.

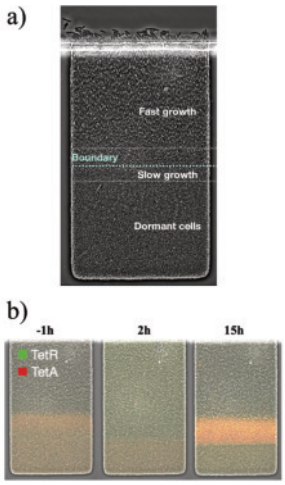

Figure 2.7: a) Microfluidic trap (100 µm × 170 µm) filled with growing bacteria. Fresh nutrients flow across at the top, leading to a distinct growth pattern. b) Upon tetracycline exposure (at 0h), the growth pattern rearranges and a layer of high antibiotic-resistance gene expression forms near the growth boundary.

Motivated by the COVID-19 pandemic, MPI-DS led one of the most comprehensive experimental studies of human respiratory particle emissions, profiling over 130 volunteers aged 5–80 years [13]. Using a unique multi-instrument platform, the study measured concentrations of exhaled particles across six orders of magnitude in size—from nanometers to millimeters—while rigorously analyzing age- and gender-dependent variability. Beyond mapping size–number distributions, the data identified the anatomical origins of distinct particle modes within the respiratory tract, establishing a mechanistic basis for exploring asymmetric pathogen-transmission dynamics. These findings formed the empirical foundation for a comprehensive interdisciplinary review, conducted with the Max Planck Institute for Chemistry and other partners, now recognized as a key reference in respiratory aerosol science and central to current epidemiological modeling and mitigation

strategy design [14].

Other global health challenges are neurological and psychiatric diseases, whose causes are multi-faceted and may have genetic underpinnings [15]. To investigate their mechanisms, researchers are turning to brain organoids, i.e. miniature neural networks grown from patient-derived pluripotent stem cells and thus carrying the same genome as the patient. Growing the neural network in a dish, with its potential malignant-regulation, enables one to investigate the mechanistic cause of the disease. Since the living neural networks in a dish are dynamic and self-organized, approaches from theoretical physics are needed to guide the self-organization to a sufficiently natural state. With our theoretical work, we derived the hypothesis that the "isolation" from the external world leads to aberrant network dynamics [16] and that reintroducing structured input could restore more physiologically relevant network states. This hypothesis spurred collaborative investigations involving groups from Göttingen (CRC1690), Spain, the UK, and Japan. The joint research confirmed that removing this isolation leads to fundamentally different, and more natural, self-organization of the neural networks [17, 18]. If we guide the network self-organization through external input in that fine manner, we will be able to detect smaller pathological aberrations, and thereby will strongly improve *in vitro* assays for testing of pharmacological, optical, and genetic interventions.

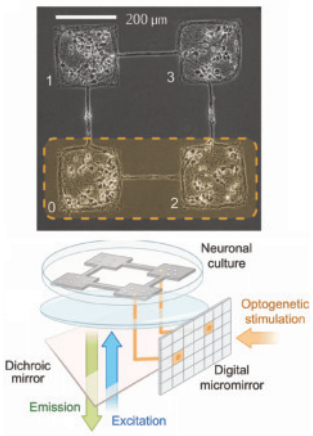

Figure 2.8: Optogenetic stimulation allows the control of neuronal cultures to induce more natural network dynamics.

[1] V.S. Zykov, E. Bodenschatz, New J. Phys. **24**, 013036 (2022)
[2] V.S. Zykov, E. Bodenschatz, Front. Appl. Math. Stat. **8**, 903563 (2022)
[3] V.S. Zykov, E. Bodenschatz, Phys. Rev. E. **110**, 064209 (2024)
[4] R. Majumder, V.S. Zykov, E. Bodenschatz, Phys. Rev. Applied **17**, 064033 (2022)
[5] T. Lilienkamp, U. Parlitz, S. Luther, Chaos **32**, 121105 (2022)
[6] D. Suth, S. Luther, T. Lilienkamp, Front. Netw. Physiol. **4**, 1401661 (2024)
[7] S. Hussaini, A. Mamyraiym Kyzy, J. Schröder-Schetelig,..., S. Luther, Chaos **34**, 031103 (2024)
[8] S. Hussaini, R. Majumder, V. Krinski, S. Luther, Pflügers Archiv: Eur. J. Phys. **475**, 1453 (2023)
[9] S. Hussaini, S.L. Lädke, J. Schröder-Schetelig,..., S. Luther, PLoS Comp. Biol. **19**, e1011660 (2023)
[10] Y. Zhang, M. Kalkhoefer-Koechling, E. Bodenschatz, Y. Wang, Front. Physiol. Phys. Rev. Applied **14**, 1195502 (2023)
[11] M. Stevanovic, T. Boukéké-Lesplulier, L. Hupe, J. Hasty, P. Bittihn, D. Schultz, Front. Microbiol. **13**, 740259 (2022)
[12] M. Stevanovic, J. Teuber Carvalho, P. Bittihn, D. Schultz, Phys. Biol. **21**, 036002 (2024)
[13] G. Bagheri, O. Schlenczek, L. Turco, B. Thiede, K. Stieger, J. Kosub, D. Clauberg, M. L. Pöhlker, C. Pöhlker, J. Moláček, S. Scheithauer, E. Bodenschatz, J. Aerosol Sci. **168**, 106102 (2023)
[14] M.L. Pöhlker, C. Pöhlker, O.O. Krüger, J.D. Förster, T. Berkemeier, W. Elbert, J. Fröhlich-Nowoisky, U. Pöschl, G. Bagheri, E. Bodenschatz, J.A. Huffman, S. Scheithauer, E. Mikhailov, Rev. Mod. Phys. **95**, 045001 (2023)
[15] F. Davenport,..., V. Priesemann, J. B. Rowe, S. W. Smye, H. Zetterberg, J. R. Soc. Interface **20**, 20220406 (2023)
[16] J. Zierenberg, J. Wilting, V. Priesemann, Phys. Rev. X **8**, 031018 (2018)
[17] H. Yamamoto, F. P. Spitzner, V. Priesemann, M. A. Muñoz, J. Zierenberg, J. Soriano, Sci. Adv. **9**, eade1755 (2023)
[18] J. M. Rowland, T. L. van der Plas, M. Loidolt,..., V. Priesemann, A. M. Packer, Nat. Neurosci. **26**, 1584 (2023)

2.3 PHYSICS AND CLIMATE

Weather and climate are essential for life on Earth. Climate change is altering our planet's climate system. Temperatures on land, in the atmosphere and in the oceans are rising. Regions that used to be frozen in summer, such as permafrost in the tundra and on mountain peaks, for example in the Alps, are thawing, as is the ice in the Antarctic and Arctic. Wind and ocean currents are changing. Precipitation patterns are shifting and rare weather events such as heavy rainfall are becoming more frequent.

Here, clouds play a pivotal role. They regulate the hydrologic cycle and also very importantly the Earth's surface temperature by reflecting visible light back into space, i.e. cooling, or by buffering the emission of infrared radiation from the Earth's surface into space, i.e. heating. For example a stratocumulus cloud cover reflects up to 35% of the incoming solar radiation back into space. Due to the lack of understanding of the complex dynamics of clouds they remain the largest source of uncertainty in future climate projections [1, 2]. Also for weather forecasting cloud process parametrization comes with strong uncertainties, as can be easily seen by comparing expected rainfall for a given region predicted from different weather forecasting models. Clouds can be distinguished on liquid-phase (warm clouds, ice clouds, or mixed-phase clouds containing both droplets and ice crystals). Warm clouds are particularly relevant for Earth's radiation budget and precipitation processes. Globally, 31% of rainfall originates from warm clouds, and in the tropics this fraction increases to 72%. Despite their utmost importance, key aspects of cloud microphysics remain unresolved, particularly the rapid growth of droplets necessary for precipitation.

With the ongoing threat of rising atmospheric and ocean temperatures, Solar Radiation Management (SRM) has been proposed as a potential means to mitigate global warming. In addition to stratospheric aerosol injection — using carefully selected aerosols to reflect sunlight — other SRM strategies include the thinning or reduction of cirrus clouds, which trap heat, and the brightening of shallow warm or mixed-phase clouds to enhance their reflectivity. The latter has the capacity to cool the planet by cloud brightening, i.e., by increasing the number of small cloud droplets by addition of aerosols [3]. While this concept has been demonstrated to some extent, the lack of knowledge regarding cloud micro-physical properties, particularly at the cloud particle scale, makes detailed scientific investigation indispensable. Without them, intervention into cloud physical processes bear great risks for the future weather and climate on our planet. Such scientific investigations have, however, the added benefit of improving weather forecasts and they might also help to mitigate the increasingly frequent occurrence of heavy rainfall. In the long run, SRM can only delay temperature increases even if we stop producing green-house gases right away. However, the deployment and effectiveness of SRM remain the subject of intense debate, as the associated uncertainties pose significant risks that require careful evaluation at the global level [4]. On

Figure 2.9: MPI-DS researchers on measurement campaingn in the Harz mountains near Göttingen.

Figure 2.10: MPI-DS researchers on measurement campaign in Pallas Finland.

Figure 2.11: CloudKite experiment from the research vessel Maria S. Merian in the trade wind region of the Atlantic Ocean.

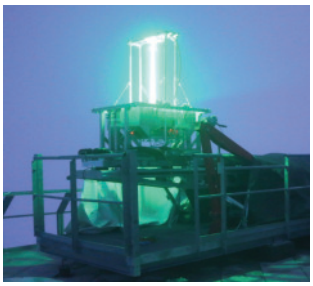

Figure 2.12: Cloud physics experiment at the Environmental Research Station Schneefernerhaus at 2650m on Mount Zugspitze in the Bavarian Alps.

Figure 2.13: Convective shallow cumulus clouds over Pallas-Yllästunturi National Park in Finland during the IMPACT Campaign of MPI-DS in spring 2024. Cloud scales range from km down to 10s of nm – the size of a single aerosol.

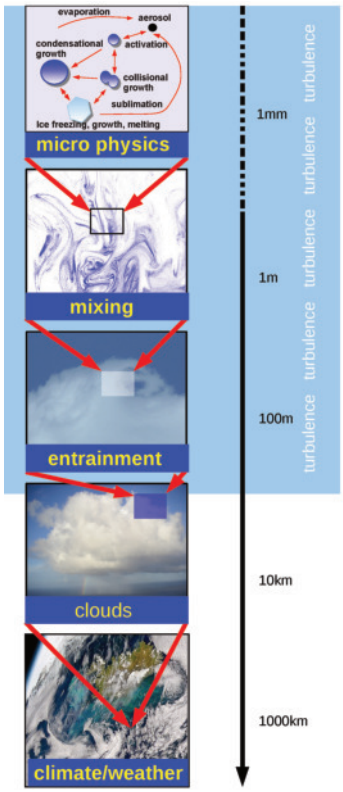

Figure 2.14: Cloud physical processes summarized analogously to Bodenschatz et al. [6].

the other hand, if cloud engineering becomes feasible, it could offer the ability to influence precipitation patterns, with significant benefits for water resources, agriculture, and ecosystems. This prospect reflects a long-standing scientific aspiration and an emerging technological objective to actively manage Earth's climate for the benefit of society.

The use of fossil carbon to generate energy and produce chemical products is the root cause of climate change. Ultimately, all of that carbon transforms into carbon dioxide and is released into the atmosphere. Since carbon dioxide is a greenhouse gas, it warms the Earth's atmosphere and with it land and oceans. To stop the accelerating warming of the planet, we must stop emitting carbon dioxide directly and indirectly into the atmosphere. However, it is important to note that even if we reach carbon neutrality, the planet will continue to heat up due to the carbon dioxide released during the past 250 years of industrialization and rapid population growth. To this end, the Max Planck Society has committed to a climate action plan to achieve full climate neutrality by 2035 [5]. Since October 2024, Director Eberhard Bodenschatz has helped lead this effort. Bodenschatz serves as the Energy Officer of the Max Planck Society in the extended presidential circle. One MPG initiative recently established three new "Max Planck Foundation Research Groups" dedicated to carbon capture technologies. Another initiative is installing photovoltaic electric power generation systems in most institutes. MPI-DS was a pioneer in this regard, installing 180 kWp of solar panels that provide approximately 10% of the institute's yearly electricity usage and are fully carbon neutral.

MPI-DS researchers contribute to projects related to the two aforementioned topics: improving our understanding of weather and climate and optimizing wind energy production to reduce the carbon footprint. These topics are closely linked to dynamical self-organization in an environments where fluid flow is complex, intermittent, locally driven, and turbulent. The facilities and technologies available at MPI-DS, as well as those being developed with the research electronics and machine shop, provide the foundation for this research. The two threads of research are presented here.

Research in Cloud Microphysics So far, our models cannot adequately explain the mechanisms that describe how micron-sized droplets and ice grow after nucleation on aerosols into multi-modal distributions of cloud particles. The up-scaling of cloud particles in size, which ultimately leads to precipitation, is not yet sufficiently well parameterized in cloud modeling. Clearly, collision, coalescence, and differential gravitational settling ultimately drive the formation of hydrometeors that lead to precipitation. The root of the difficulty lies in the complex fluid flows driven by turbulence generated by shear and buoyancy. It is important to note that condensation of moisture into liquid water and ice leads to latent heat release that drives the convection locally. In that sense a cloud is a form of active matter. Similarly evaporation and sublimation leads to cooling. This is all intertwined with the heterogeneous nucleation of drops and ice by nucleating aerosols. This was summarized by Bodenschatz and coauthers 15 years ago [6].

At MPI-DS we conduct in situ measurements resolving a cloud

from microns to km (see Secs. 5.7, 5.9, 5.14 and 5.15). Recently we have shown that the clustering in a shallow cumulus cloud is at the meter scale [7]. For atmospheric flows, large-scale transport is well understood and measured by monitoring stations and satellite observations. However, our knowledge of smaller scales and the associated concentration fluctuations, i.e., at scales of 100 m to 50 km, is very limited. To this end we simultaneously release up to 15 small (∼40 cm) balloons and track them in different atmospheric conditions, providing high-resolution data in the atmospheric boundary layer and lower troposphere. Within a Fraunhofer Max-Planck collaboration we are building a system of intelligent atmospheric tracers that are lighter and provide higher resolution data than the currently available commercial option (see Sec. 5.10).

Figure 2.15: Ballons being traced during the IMPACT Campaign of MPI-DS in spring 2024

Weather forecasting and climate models rely on the assumption that the flows are not fully chaotic and random. How solid is this assumption? The Navier-Stokes equations that describe turbulence are deterministic. Is it true that a butterfly beating in Brasil can change the weather in Germany? Recently we addressed this question in the VDTT with its active grid by repeating the same driving of the turbulence up to 30,000 times. We observed that the largest scales of the flow are predictable if the initial conditions are approximately known, while the smaller ones are completely random [8].

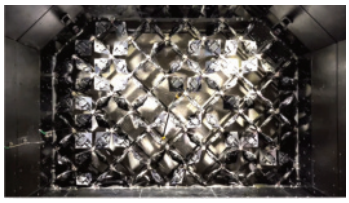

Figure 2.16: The active grid of the Max Planck Turbulence Facility allows to repeat the same turbulent driving. This way the randomness of turbulent flows can be studied.

Research in Wind Energy Wind energy has long been recognized as a crucial technology in mitigating climate change. Models suggest that a net-carbon-zero global electricity sector requires eleven times the wind energy capacity installed today. To successfully navigate this energy transition, we need to know how these increasing numbers of wind turbines will alter local land-use dynamics and existing ecosystems. In wind farms, the wakes of upstream turbines interfere with downstream turbines, reducing their performance, but also altering the microclimate. The atmospheric boundary layer is a turbulent shear flow defined by its proximity to Earth's surface and local meteorological conditions. Many quantitative questions remain unanswered because numerical simulations cannot capture its full complexity. Thus, much relies on quantitative experiments in the field and laboratory. The in-house and in-field facilities at MPI-DS offer unique opportunities in this regard. The VDTT provides one-to-one self-similarity from a model to an actual wind farm and enables particle tracking [9]. Recently, we studied the influence of shear flows and gusts on a single rotor [10]. In field experiments, we track helium-filled soap bubbles with drones for use in wind farms (see Secs. 5.20, 5.21 and 5.22).

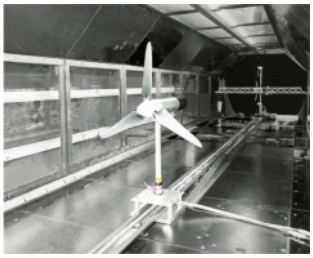

Figure 2.17: Experiments with a model in the VDTT.

Figure 2.18: Velocity measured from helium filled soap bubbles at the MPI-DS.

[1] O. Boucher et al., IPCC Report (2018)
[2] P. Forster et al., IPCC Report (2021)
[3] Action for Cooling ESA project
[4] Solar Radiation Modification, Strategic Foresight @ UNEP
[5] Climate Action Plan, Max Planck Society (2024)
[6] E. Bodenschatz, S. P. Malinowski, R. A. Shaw, F. Stratmann, Science **327**, 970 (2010)
[7] B. Tiede et al., arXiv:2502.19272, *in review*
[8] N. Clavier, E. Bodenschatz, F. Falkinhoff, *in review*
[9] C. Küchler, A. I. Landeta, J. Moláček, E. Bodenschatz, Rev. Sci. Inst. **95**, 05110 (2024)
[10] M. Grunwald, C. E. Brunner, arXiv:2502.21182, *in review*

2.4 PHYSICS AND SOCIETY

Understanding the structure of music, contributing to pandemic mitigation, designing efficient public transport, investigating the spread of information in social networks, and advising on public policy are among the less common applications of theoretical physics. Yet, these activities are central to our role as scientists and our contribution to society. Drawing on our institute's expertise in self-organization and living systems, we provide theoretical insights into these complex phenomena at the intersection of physics and society.

Music is a manifestation of complex human behavior. Music theorists have long argued that its appeal and the emotions it evokes arise from the interplay between expectation and its fulfillment or violation. Quantifying these concepts remains an open challenge. Using time series analysis on extensive collections of musical compositions and jazz improvisations, Theo Geisel demonstrated that pitch autocorrelation functions show abrupt transitions from strong predictability to unpredictability beyond characteristic cutoff times. These transitions serve as a measure of persistence and predictability in music. Geisel also addressed a central question in jazz performance: What makes jazz "swing"? While jazz musicians can sense swing, its origins were unclear. Geisel's work revealed that the microtiming of downbeats and offbeats-and their variations-play a crucial role in creating the swing feel [1–3]. This aligns with earlier findings that musical rhythms are perceived as more natural when beat microtiming exhibits long-range correlations [4]. Such correlations are common in natural phenomena, including brain activity. Identifying and quantifying these patterns in music not only deepens our understanding of music itself but also offers insights into human behavior and brain function.

Transportation in the times of climate change and the overuse of Earth's resources present existential challenges for society. Increasing mobility has driven up demand for infrastructure, materials, and energy. Public transport and ride-sharing offer promising solutions for more efficient mobility [5, 6], but effective ride-sharing—especially in rural areas—requires advanced planning algorithms. At MPI-DS, we have developed and deployed such algorithms through the "EcoBus" project, supported by the Land Niedersachsen and the Max Planck Society. Initiated by Marc Timme and further boosted by Stephan Herminghaus and his group, this project brought theoretical advances to practical application. A key metric for ride-sharing efficiency is the pooling rate, or average passengers per vehicle. While trains and trams achieve high pooling rates when full, their fixed schedules and stops often reduce convenience and demand. A sustainable transport system should combine the convenience of door-to-door service with high pooling rates. This can be realized through a bi-modal system that integrates traditional line services with ride-pooling shuttles for last-mile transport [7, 8] (Fig. 2.19). Digital twin simulations of regional transport networks demonstrate how to adapt system design to demand. This combination of theoretical optimization and detailed simulation highlights the potential to merge classical public transport

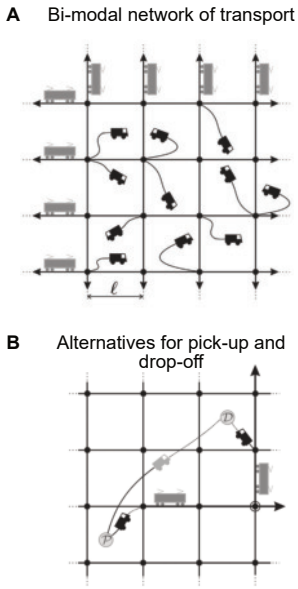

Figure 2.19: Bi-modal transport network on a square grid. A: Network with trains (grey) operating periodically at frequency μ, seating capacity k, and stations (black dots) spaced ℓ apart. Shuttles (black) provide feeder service. **B:** Pick-up ($\mathcal{P}$) and Drop-off ($\mathcal{D}$) transport request options: bi-modal (shuttle-train-shuttle with station transfers) or direct unimodal shuttle. The system dynamically selects the optimal mode. Adapted from [7].

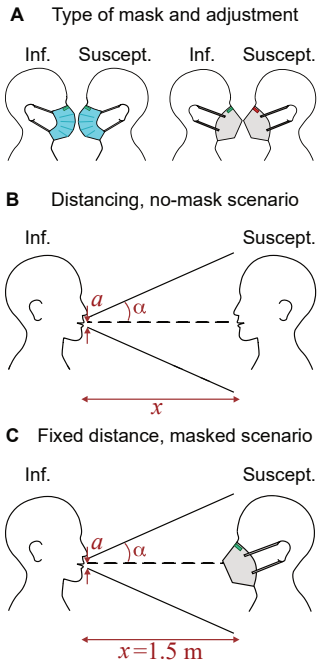

Figure 2.20: Schematics of scenarios investigated in [14]. A: Different types of masks and adjustments (fitting, determinant of the filtering effectiveness) studied. **B:** Interaction between an infectious and a susceptible individual, at arbitrary distance and without masks. **C:** Interaction between an infectious individual and a FFP2-masked susceptible individual, at the $x = 1.5\,\mathrm{m}$ distance recommended in COVID-19 mitigation guidelines. Adapted from [14].

with adaptive ride-pooling and is now being implemented in practice.

The COVID-19 pandemic demonstrated how tools originally developed for unrelated fields became crucial for understanding airborne disease transmission. Experimental setups used to study atmospheric aerosols and cloud droplets proved essential for characterizing respiratory particles produced by humans [9–11]. We also developed analytical models that more accurately describe pathogen-laden particles [11, 12], surpassing previous simplified approaches. These tools enabled precise predictions of infection transmission bounds and assessments of non-pharmaceutical interventions such as indoor ventilation [13] and face masks [14]. A pivotal study from our institute, led by Mohsen Bagheri and Eberhard Bodenschatz, provided strong evidence for the effectiveness of face masks in reducing transmission [14], supporting informed policy decisions [15] (Fig. 2.20). We also created interactive web applications to help the public assess infection risks and understand the impact of interventions in everyday scenarios [16].

From a broader perspective, pandemics exemplify spreading processes and complex contagion in living systems. The co-evolution of pathogens and the networks where they spread have shaped the ecology of societies at all scales. During the COVID-19 pandemic, large parts of the MPRG Complex Systems Theory led by Viola Priesemann actively shifted their research focus from the propagation of activity in neural networks to that of pathogens in societies. Their objective was to understand the basic mechanisms of disease spread and exploit them to mitigate the COVID-19 pandemic with the tools of theoretical physics. Viola Priesemann became a key advisor to policymakers, including the federal government, and engaged in public outreach in Germany and abroad. Her group's research encompassed three main areas: understanding COVID-19 spread and designing interventions from testing to vaccines [17–20]; inferring spreading parameters in subsampled systems [21–24]; and compiling expert knowledge for policy advice [25–28]. These efforts are interconnected and reflect our responsibility as scientists: to translate insights from nature into societal benefit. This is how theoretical concepts such as bifurcations [17, 20] were transformed into actionable guidance for policymakers [18, 28], and advances in network inference and observability [22] yielded practical information on the spread of new viral strains [24] (see Fig. 2.21).

Taken together, the research at MPI-DS demonstrates how basic research can have far-reaching and sometimes unexpected impacts on society's most pressing challenges. Whether by uncovering the mathematical foundations of music, developing algorithms that make sustainable mobility a reality, or providing critical insights and tools during a global pandemic, our work exemplifies the power of theoretical physics to inform and shape solutions well beyond its traditional boundaries. The adaptability and independence of basic research allow us to respond to new and unforeseen crises with creativity and rigor, translating deep theoretical advances into practical applications for the benefit of societies. As we face an increasingly complex and interconnected world, the continued pursuit of curiosity-driven science remains essential—not only for advancing knowledge but also for equipping

society with the understanding and tools needed to navigate future uncertainties. The MPI-DS stands as a testament to the vital role that independent, interdisciplinary research plays in building resilience, fostering innovation, and ultimately improving lives.

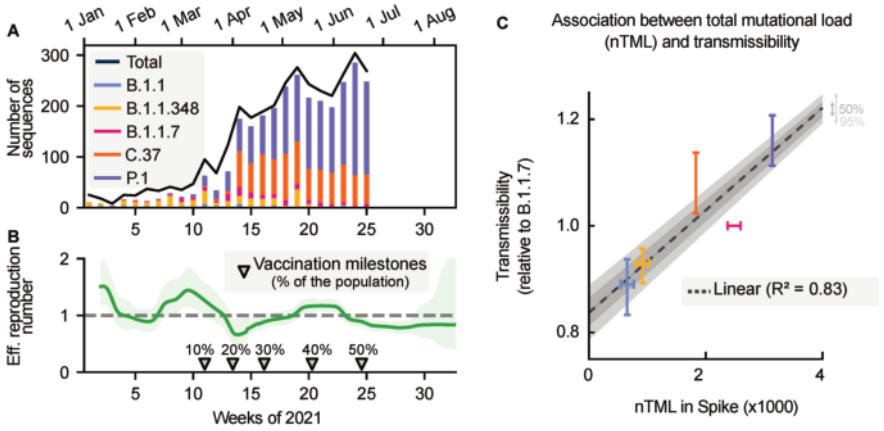

Figure 2.21: Inferring spreading parameters from subsampled genomic surveillance data. **A:** Number of COVID-19 positive samples sequenced in Chile and their corresponding SARS-CoV-2 variants. **B:** Using Bayesian inference, we calculate the overall and variant-specific spreading rate of COVID-19 in Chile. **C:** Association between the number of mutations in the Spike protein and the variants' relative transmissibility. Adapted from [24].

[1] C. Nelias, T. Geisel, Nat. Commun. **15**, 9280 (2024)
[2] C. Nelias et al., Commun. Phys. **5**, 237 (2022)
[3] C. Nelias et al., Chaos **34**, 103112 (2024)
[4] G. Datseris et al., Sci. Rep. **9**, 19824 (2019)
[5] S. Herminghaus Transp. Res. A **119**, 15 (2019)
[6] A. Minnich et al., Transp. Res. Interdiscip. Perspect. **27**, 101176 (2024)
[7] P. Sharma et al., Multimodal Transp. **2**, 100083 (2023)
[8] P. Sharma et al., Multimodal Transp. **3**, 100118 (2024)
[9] G. Bagheri et al., J. Aerosol Sci. **168**, 106102 (2023)
[10] O. Schlenczek et al., J. Aerosol Sci. **167**, 106070 (2023)
[11] M. L. Pöhlker et al., Rev. Mod. Phys. **95**, 045001 (2023)
[12] F. Nordsiek et al., PLOS ONE **16**, e0248004 (2021)
[13] B. Hejazi et al., Aerosol Air Qual. Res. **22**, 220117 (2022)
[14] G. Bagheri et al., Proc. Natl. Acad. Sci. U.S.A. **118**, e2110117118 (2021)
[15] `https://pnas.altmetric.com/details/106855773`
[16] `https://aerosol.ds.mpg.de/`
[17] S. Contreras et al., Nat. Commun. **12**, 378 (2021)
[18] S. Bauer et al., PLOS Comput. Biol. **17**, e1009288 (2021)
[19] S. Contreras et al., Chaos, Solitons & Fractals **167**, 113093 (2023)
[20] J. Wagner et al., Phys. Rev. Res. **7**, 013308 (2025)
[21] J. Dehning et al., Science **369**, eabb9789 (2020)
[22] A. Levina, V. Priesemann, J. Zierenberg, Nat. Rev. Phys. **4**, 770–784 (2022)
[23] J. Dehning et al., Nat. Commun. **14**, 122 (2023)
[24] K. Y. Oróstica et al., Sci. Rep. **14**, 16000 (2024)
[25] V. Priesemann et al., Lancet **398**, 838 (2021)
[26] V. Priesemann et al., Lancet **397**, 469 (2021)
[27] V. Priesemann et al., Lancet **397**, 92 (2021)
[28] S. Contreras et al., Lancet Reg. Health Eur. **12**, 100240 (2022)

DEPARTMENTS AND RESEARCH GROUPS

3

Contents

3.1 DEPARTMENT OF LIVING MATTER PHYSICS

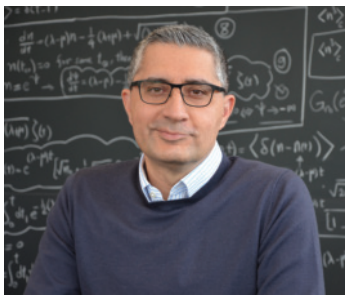

Prof. Dr. Ramin Golestanian obtained his PhD in 1998 from the Institute for Advanced Studies in Basic Sciences (IASBS) in Zanjan, under the remote supervision of Mehran Kardar from MIT. He was subsequently an independent postdoctoral research fellow at the Kavli Institute for Theoretical Physics at UCSB. He has held academic positions at IASBS, the University of Sheffield, and Oxford University, and risen through the ranks until he became a Full Professor in 2007. He is elected Fellow of APS and IoP, and the Göttingen Academy of Sciences and Humanities. He is recipient of the Holweck Medal of the Société Française de Physique and the Institute of Physics, EPJE Pierre-Gilles de Gennes Lecture Prize, Martin Gutzwiller Fellowship of the MPI-PKS, Nakamura Lecturer Award of UCSB, and 50th-Anniversary Most Distinguished Alumni Award of Sharif University of Technology. He has held many visiting positions, including CNRS Visiting Professor, Visiting Professor at College de France (hosted by the late Nobel Laureate Pierre-Gilles de Gennes), Frederic Joliot Visiting Chair at ESPCI, and Visiting Scholar at MIT. He is on the Editorial Boards of Advances in Physics and Newton (Cell Press), and was formerly Chair of IUPAP C6 Commission on Biological Physics and Divisional Associate Editor (DAE) at Physical Review Letters (APS).

The vision behind the Department of Living Matter Physics (LMP) is to study living systems as self-organized active soft matter that are away from equilibrium "just the right way". The aim is to understand the complex dynamics of living matter well enough to be able to make it from the bottom-up; i.e. from molecules to systems. The research topics cover, broadly speaking, chemical and mechanical nonequilibrium activity in Living Matter across the scales. The department is organized in such a way that allows us to study complex systems using complementary theoretical techniques that encompass multiple scales. In the last three years, the research activities at LMP have led to a number of very exciting developments. Our studies of chemically active matter start from the smallest relevant unit, namely enzymes, and systematically investigate cooperativity and emergent features in systems with multiple enzymes. These range from emergent coherence in the stochastic activity of enzymes, which has resulted in a new paradigm of molecular synchronization in barrier-crossing stochastic systems as well as a proposal for de novo enzyme design strategies, to the emergence of self-organized metabolic cycles that may have potentially played a role at the formation of early forms of life, to multifarious self-organization in suspensions of building blocks with non-reciprocal interactions. The role of non-reciprocal interactions has been further elucidated at the mesoscopic scale in the context of the non-reciprocal Cahn-Hilliard (NRCH) model that we have recently introduced. We have now put this theory on firm theoretical basis by showing that it maps to a Toner-Tu-like active polar field theory, as well as the KPZ universality class, which has allowed us to prove the existence of true long-range polar order in two dimensions and above. We have also uncovered the structure of the defects that emerge in NRCH and showed that increasing the activity in this system leads to stronger order. Moreover, we have introduced a new class of quorum-sensing active matter with non-reciprocal interactions, which bear similarities to the NRCH, but also show important differences. We have performed systematic coarse-graining of a binary mixture of active Janus colloids with non-reciprocal positional and orientational interactions, and studied glassy behavior of dense chemically active condensates. We have also studied multicomponent chemically active mixture in the limit of very large number of species within the NRCH framework using random matrix theory. We have continued to work on the area of active hydrodynamics, and made a number of breakthroughs. We have studied hydrodynamic dissipation in a number of different settings and derived rigorous bounds on the dissipation rate, which is important for understanding active matter physics in terms of the character of non-equilibrium activity, as well as a framework to derive fluctuation dissipation relations in active field theories and the appropriate generalization of the Harada-Sasa relation that satisfies momentum conservation in many-body active systems. We have elucidated the role of non-reciprocity in the hydrodynamic interactions between cilia in achieving synchronization and metachronal waves in ciliary arrays. We have investigated mixtures of

growing active matter in 2D and 3D including embryo development projects, as well as a number of projects in information processing such as micro-swimmer optimal navigation problem and quantifying the configuration entropy of tracer particles in a complex flow.

Finally, we are delighted to highlight that some of LMP alumni have moved onto faculty positions in the last three years: Dr. Jaime Agudo-Canalejo to a Lectureship at UCL (London, UK), Dr. Abdallah Daddi-Moussa-Ider to a Lectureship at the Open University (Milton Keynes, UK) and Dr. Yu Duan to an Associate Professorship position at Soochow University (Suzhou, China).

designed by
Viktoryia Novak

Group leaders

Dr. Philip Bittihn studied physics and earned his doctorate at Göttingen University in 2013 on structural complexity, pattern formation, and its control in cardiac tissue. A recipient of the Otto-Hahn Medal, his postdoctoral research as a Human Frontiers Science Program Fellow at the University of California San Diego centered on design principles of cellular dynamics in microbial populations. He joined the Department of Living Matter Physics in 2019 and has led the group Emergent Dynamics in Living Systems since August 2021, focusing on the statistical physics of multicellular systems, in particular the role of growth and division.

Dr. Benoît Mahault studied physics and obtained his Ph.D. from Université Paris-Saclay in 2018, working on the statistical physics of collective motion. After a short postdoctoral position at Tokyo University, he joined the Living Matter Physics Department in January 2019 as a postdoctoral researcher and became group leader in July 2021. His current research focuses on active matter physics problems, including self-organization driven by chemotaxis and phototaxis, as well as the energy efficiency and optimal control of microswimmers.

Dr. Supropriya Saha studied physics at the Presidency college Kolkata (India), and received her PhD from the Indian Institute of Science in 2015. Her doctoral work was on the theory of phoretic systems, with an emphasis on interacting Janus colloids. From 2015 to 2018, she was a postdoctoral fellow the Max Planck Institute for the Physics of Complex systems. She was a postdoc in MPI-DS from 2018-2021. Since 2022, she is a group leader in the Department of Living Matter Physics at the MPI-DS, working on field theories relevant to active matter, particularly on non-reciprocally interacting conserved densities.

Dr. Jaime Agudo-Canalejo studied physics at the Complutense University of Madrid, and received his PhD from the Technical University of Berlin in 2016. His doctoral work, on the physics of biomembranes, was conducted at the Max Planck Institute of Colloids and Interfaces in Potsdam. He was later a postdoctoral fellow jointly at the University of Oxford and at Penn State University and, from 2019 to 2023, a group leader in the Department of Living Matter Physics at the MPI-DS, where he worked on out-of-equilibrium processes induced by catalytic activity. Since 2024, he is Lecturer in Theoretical and Computational Biophysics at University College London.

Dr. Andrej Vilfan studied physics and received his doctorate from the Technical University Munich in 2000. He worked as a postdoctoral researcher at Cambridge University (UK) and as a visiting scientist at the Max Planck Institute for the Physics of Complex Systems in Dresden. He has been a group leader at MPI-DS from 2018-2024 and is a senior research fellow at the J. Stefan Institute in Ljubljana (Slovenia) since 2012. As a theoretical physicist, he has worked on molecular motors, auditory receptors, hydrodynamics of biological and artificial cilia, as well as other colloidal systems.

Technical and administrative staff

Yorck-Fabian Beensen studied physics at the Georg-August-University Göttingen and the University of Aarhus (Denmark). In 1997 he received his diploma from the faculty of geophysics for a work in the field of seismological data analysis which earned him a stipend from the Berliner-Ungewitter-Stiftung. He joined the institute in 2000 as an IT administrator in the former theory department. Since 2018 he has been working as an IT expert in the department of Living Matter Physics. And in 2021 he also joined the newly restructured central IT team of the institute as a Linux specialist.

Ayşe Bolik has a Higher Diploma in International Administration and Management specialising in Business Management and is also a certified translator and interpreter for English as well as a certified foreign language correspondent for English and French. She has been working at the MPI-DS since 2010 and has been assistant to Ramin Golestanian in the department of Living Matter Physics since 2018. From 2021-2024, she was Gender Equality Officer at MPI-DS.

Viktoryia Novak studied foreign languages at the Gomel State University (Belarus), International Economics at the University of Göttingen, and Higher Education and Research Management (MBA) at the University of Applied Sciences in Osnabrück. She joined the MPI-DS in 2011. Since 2018 she has been working for the department of Living Matter Physics. She is mainly responsible for scientific visualization (conceptual implementation of graphical presentation of scientific results), coordination of grant applications and third-party funded projects, management of the guest program, and implementation of activities related to societal impact of science.

Group photo of the department of Living Matter Physics in May 2024

3.2 DEPARTMENT OF FLUID PHYSICS, PATTERN FORMATION AND BIOCOMPLEXITY

The Department of Fluid Physics, Pattern Formation, and Biocomplexity was established in 2003 when Eberhard Bodenschatz became the scientific director of the institute. From the beginning, Bodenschatz planned to establish a strong, independent research group to support the department's research in the dynamics and self-organization of the heart. In 2004, while still at Cornell University, Bodenschatz hired Stefan Luther as a postdoc to work with Professor Robert Gilmour and him on cardiac dynamics experiments. In 2006, the department advertised a position (W2, equivalent to an associate professorship) with a Max Planck Research Group (MPRG) in cardiac dynamics. Following a symposium, an external hiring committee recommended Luther for the position. He accepted the tenure-track offer and was tenured by MPG in 2012. His research group, Biomedical Physics, has been part of DFPB ever since. To reflect this change, Eberhard Bodenschatz founded the Laboratory for Fluid Physics, Pattern Formation, and Biocomplexity in 2007. In 2024, Olga Shishkina became an associate professor (W2) in DFPB. She leads the MPRG Theory of Turbulent Convection. The department thus consists of three groups, which are described below.

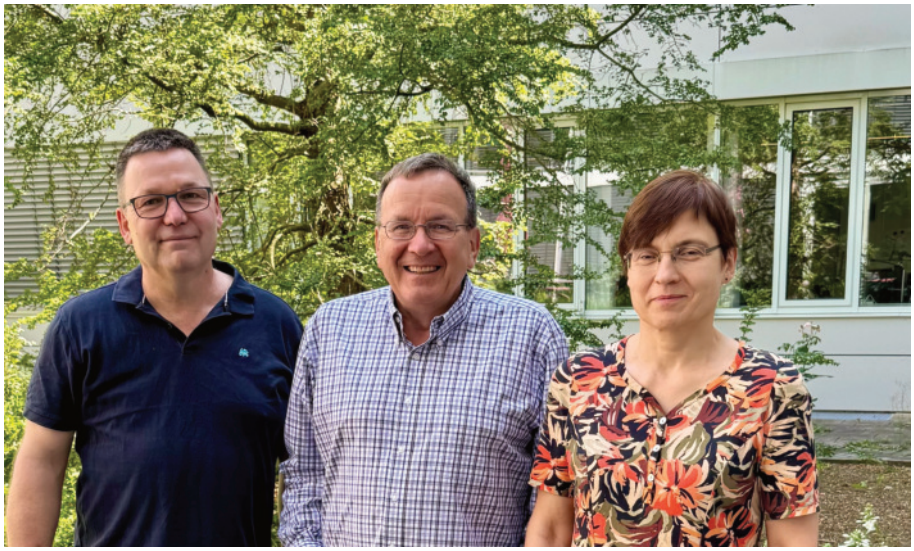

Left to right: MPRG leader Stefan Luther, director Eberhard Bodenschatz, and MPRG leader Olga Shishkina (Göttingen, June 2025).

3.2.1 *Laboratory of Fluid Physics, Pattern Formation and Biocomplexity*

We focus on the physics of dynamics and self-organization in nature. Current topics include synthetic bottom-up assembly of artificial cilia, electrical turbulence and the soft mechanics of muscle contraction in the heart, cilia-based directed transport networks in the ventricles of the mammalian brain, understanding fully developed turbulent flows (inertial/convective simple and complex fluids at the highest turbulence on Earth) with the impact on fundamental understanding of cloud physics, and human aerosols and their dispersion in the environment in the context of airborne diseases.

The department has established the Max Planck Turbulence Facility, which consists of a series of experimental systems and a pressurised gas facility to achieve ultra-high turbulence and the Max Planck Cloud Kite. Both are part of the Max Planck University of Twente Center for Complex Fluid Dynamics. Our approach is mainly experimental, supported by numerical and analytical theoretical analyses.

The department houses a microscopy facility, a cell biology laboratory and shares a class 1000 clean room with the other groups for microfluidics fabrication.. For studies of the microphysics of clouds, we have established a field laboratory at the Schneefernerhaus Environmental Research Station on the Zugspitze at 2650m, where we are also part of the Virtual Alpine Observatory. With our mobile cloud kite laboratory we investigate cloud microphysics in the field.

Our research is and will remain highly interdisciplinary, from fluid physics, statistical physics, physics of complex systems, and applied mathematics to environmental physics, synthetic biology and medicine. We link seamlessly with the other departments and research groups and are a member of the Max Planck School Matter to Life, the Centre for Cardiovascular Research (DZHK) and the Max Planck University of Twente Center of Complex Fluid Dynamics.

Prof. Dr. Dr. h.c. Eberhard Bodenschatz 1989 Dr.rer.nat. U. Bayreuth; 1989-92 postdoc UCSB; 1992 - Prof. Cornell U.; 2003 - Director MPI-DS; 2007 - Prof. U. Göttingen. Examples of service: 2008-11 Director of the MRS, 2008-12 member and chair SAB of KITP, 2012-17 vice chair and chair of the Chemistry Physics and Technology Section of MPS, 2016-20 governing board publications DPG, 2020-27 review board DFG, 2017-24 head of the Software Commission of MPS and 2024-29 energy officer of MPS in the extended presidential circle. He was Editor in Chief of NJP and on the editorial boards of Ann. Rev. Cond. Mat. Phys., EPJH, Physica D, Phys. Rev F. and SIAM JADS. He is founder and member Exec. Board of the MP-School Matter to Life, Co-director of the MP-U-Twente Center on Complex Fluid Dynamics, He is elected member in the Niedersachsen Academy of Sciences, the National Academy Leopoldina, and of AAAS. He carries a Honorary Doctorate from the ENS Lyon for his scientific work, and is Fellow of the APS, IOP, EPS, and EuroMech. He is a recipient of the Stanley Corrsin Award of the APS.

Dr. Gholamhossein (Mohsen) Bagheri studied ME at the Perisan Gulf University. He earned his PhD at the University of Geneva (Switzerland, 2015) for studying the dynamics of irregular particles transported in air. With an 18-month grant from the Swiss National Science Foundation he joined the MPI-DS in 2015 and is now group leader. His research interests include cloud microphysics and atmospheric turbulence with the Max Planck Cloud-Kites, the characterisation of respiratory particle emission and airborne disease transmission, and the numerical/experimental study of the dynamics of non-spherical particles falling in air.

Dr. Taraprasad Bhowmick earned a BA in mining engineering from IIEST (2013) and a MS from U. Alaska (2015), focusing on application of computational fluid dynamics and atmospheric sciences on mine ventilation. In 2021 he received his PhD in Physics from the Polytechnic University of Turin, Italy, collaborating with LFPB on simulations of falling hydro-meteors in turbulence and their role on aerosol activation. From 2021-24 he held a DFG Walter Benjamin position U. Göttingen working with LFPB. He investigates experimentally and numerically the fall of non-spherical atmospheric particles in air.

Dr. Venecia Chávez Medina holds a MSC in Physics from the University of Michoacán, Mexico. In 2023 she received a PhD in Physics from the U. Göttingen/MPI-DS for her work on convective atmospheric boundary layers through theoretical and computational approaches. Since 2024, she is a postdoctoral researcher within the CloudKite team. She studies turbulence in the atmospheric boundary layer, utilizing and developing airborne instrumentation to enhance in-situ measurement capabilities with the Max Planck WinDarts and CloudKites.

Dr. Florencia Falkinhoff obtained her MS in Physics at the University of Buenos Aires (Argentina) in 2019, where she specialized in direct numerical simulations of particle-laden turbulent flows. In 2023 she received her Ph.D. in Physics from ENS Lyon (France) investigating multiphase flows and the hydrodynamics of fixed beds of particles experimentally and in simulations. Since 2023 she is in LFPB. She researches two main lines of research: (1) The fundamental study of turbulent flows, especially in the dissipation range and its stochastic nature. (2) Atmospheric dispersion and mixing in the atmospheric boundary layer.

Dr. Shoba Kapoor obtained her BS in biology and MS in neurobiology at the Georg-August University in Göttingen. The Master thesis project dealt with microglial cells and their binding properties to sialic acids on neurons and was carried out at the Life and Brain center in Bonn. In 2015, she joined the MPI for Biophysical Chemistry in Göttingen as a PhD student and worked on ciliated ependymal cells in the mammalian brain. Under the supervision of Prof. G. Eichele and collaborative work with Prof. E. Bodenschatz, she graduated in 2019 from the Georg-August University in Göttingen. She joined the MPI-DS as a postdoctoral researcher in January 2021 to continue her research on fluid-dynamics within brain ventricles.

Dr. Hossein Khodamoradi received his BSc, MSc, and PhD in solid-state physics from Bu-Ali Sina University (Iran). He completed his PhD in 2017, elucidating the fundamental fluid-dynamic and thermodynamic mechanisms governing bulk crystal growth. In 2021, he joined the MPI-DS as a postdoctoral researcher, where he developed the SensoRod, a cutting-edge system for high-resolution 3D measurements of aerosol transport and turbulent mixing in enclosed environments. He later led the design of the WinDArt instruments as part of the Max Planck CloudKite, advancing experimental capabilities for high-speed atmospheric probing and providing transformative insights into the dynamics of the atmospheric boundary layer.

Dr. Yewon Kim studied mechanical engineering at Pohang University of Science and Technology (POSTECH, South Korea) where she received her bachelor's degree in 2016. She then received her PhD in 2023 at the Seoul National University (South Korea) for research on the turbulence variation in the bubbly flow. In May 2024, she joined the MPI-DS as a postdoctoral researcher to investigate cloud microphysics using in-situ data from Max Planck CloudKite.

PD Dr. Alexei Krekhov received his PhD in theoretical physics from the Perm State University (Russia) in 1990 studying defects in liquid crystals. During his Humboldt Research Fellowship at the University of Bayreuth from 1994-96 he studied pattern formation in liquid crystals. Starting 1999 he was a researcher at the University of Bayreuth working on pattern formation in complex fluids and soft matter theory. In 2010 he habilitated in theoretical physics at the University of Bayreuth. He joined the MPI-DS in October 2013. His current research interests include nonlinear dynamics in excitable media, two phase convection and modeling of cell motility. He leads the theory group on pattern formation.

Dr. Vahid Nasirimarekani studied mechanical engineering for his bachelor's degree and followed this with a master's in renewable energy. He worked for two years at the International Iberian Nanotechnology Laboratory (Portugal) on microfluidics for fabrication of multiple emulsions and the layer-by-layer formation of DNA-cation lipid complexes. He then began his doctoral thesis as an early-stage researcher as part of the Marie Curie-ETN funded European project Magnetics and Microhydrodynamics. He received his PhD in December 2021 from the University of the Basque Country (Spain). Since then, he has been a researcher at the MPI-DS. His research focuses on soft condensed matter, experimental biophysics and the origin of life.

Dr. Oliver Schlenczek studied Meteorology in Mainz. In early 2018, he received his PhD in Meteorology from the University of Mainz where he developed a new airborne holographic system for investigating the microphysical composition of liquid, mixed-phase and ice clouds. In late 2017 he joined the institute as a postdoctoral associate. From 2017 to 2020, he was involved in development of the CloudKite instrumentation and participated in field campaigns with the CloudKite (MSM 82-2, EUREC4A) and performed cloud microphysical measurements with a holographic particle spectrometer on Zugspitze. During the course of the COVID-19 pandemic, he started to examine physical properties of human exhale particles.

Dr. Puneet Sharma earned a bachelor's and master's degree in Physics from the Indian Institute of Science, Bengaluru, in 2019. For his master's thesis, he used direct numerical simulations to investigate the existence of a bounded solution of the Euler equation for an inviscid fluid. He completed his PhD in Physics at the MPI-DS in 2023. During his PhD, he worked on optimising urban transportation using mathematical modelling and agent-based simulations. As a postdoctoral researcher, he is now working on the experimental study of cloud microphysics and the numerical and experimental study of the dynamics of non-spherical particles in the atmosphere.

Dr. Stefano Villa studied physics at the University of Milan (Italy), where he obtained his master's degree in 2014. After a one-year research fellowship focused on a project in optics, he moved to Montpellier (France) in November 2015 to pursue a PhD in physics in the field of soft matter, studying the passive dynamics of colloids and developing ad hoc imaging techniques. After finishing his PhD in 2019 and a first 10-month postdoc, he moved to Milan for a 2-year postdoc at the University of Milan, working on projects related to the microrheology of soft matter and the mechanodynamics of cell monolayers. Since November 2021 he is a group leader in the LFPB department at MPI-DS, working on the dynamics of living matter.

Dr. Yong Wang studied Process Equipment & Controlling Engineering, and Applied Mathematics at Xi'an Jiaotong University (China). In 2010, he received his PhD degree (with distinction) in Engineering Thermal Physics for his development of a lattice Boltzmann method as applied to thermoacoustics and PIV measurements for oscillatory flows. From 2011–15 he was a postdoctoral researcher at UC Irvine (USA), and investigated the turbulent flow in human upper airway with DNS. He then joined the MPI-DS as a group leader in March 2015. His research interests are in biofluidics, biomechanics and complex fluid dynamics, such as failing heart regeneration and cilia coordinated flow.

Associated Scientists

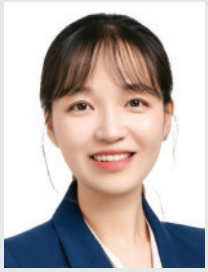

Prof. Dr. Hyejeong Kim studied mechanical engineering at Pohang University of Science and Technology (POSTECH), earning her bachelor's degree in 2012 and an integrated PhD in 2017 with the thesis "Development of Advanced Biomimetic Technologies Inspired by Leaf Transpiration." After completing a postdoc at POSTECH, she joined the MPI-DS in 2018, working on the Living Foam project until 2020. In 2021, she became an Assistant Professor in the School of Mechanical Engineering at Korea University and was promoted to Associate Professor in Fall 2024. Since 2023, she has also served as Head of the Max Planck Partner Group. Her research focuses on experimental approaches to microfluidics, soft matter, and their environmental and industrial applications.

Dr. Stephan Weiß has received his diploma in physics from the University of Bayreuth in 2005 and a PhD in experimental physics from the Georg-August University of Göttingen/MPI-DS in 2009. He worked as a postdoc at the University of California Santa Barbara (USA) (DFG-Fellowship) on turbulent thermal convection and at the University of Michigan (USA) on spirals in oscillating chemical reactions. From August 2015 to August 2021, he has led the experimental research on thermal convection. He works now at the German-Aerospace Centre (DLR) in Göttingen.

Dr. Vladimir S. Zykov studied physics at the Institute of Physics and Technology (Moscow, Russia). He graduated in 1973, received his PhD in 1979, was habilitated in 1990 and occupied the position of leading scientific researcher at the Institute of Control Sciences (Moscow, Russia). In 1992 he joined the group of Prof. S.C. Müller first at the MPI of Molecular Physiology and since 1996 at the University of Magdeburg. Since 2001 he was a research scientist at the TU Berlin and in 2010 joined the MPI-DS. His research interests include pattern formation processes in nonlinear reaction-diffusion media and control methods of self-organization.

3.2.2 *Max Planck Research Group: Biomedical Physics*

Prof. Dr. Stefan Luther studied Physics at the Georg-August-Universität Göttingen, where he received his doctoral degree in 2000. Postdoctoral research on non-ideal turbulence (University of Twente, 2001-2004) and cardiac dynamics (Cornell University, 2004-2007). Since 2007, he is head of the independent Max Planck Research Group Biomedical Physics at MPI-DS, since 2008 Honorarprofessor at the Georg-August-Universität Göttingen and since 2016 professor at the University Medical Center Göttingen. He is founding member of the the Heart and Brain Research Center Göttingen, and DZHK professor and principal investigator at the German Center for Cardiovascular Research (DZHK e.V.).

The tenured, independent Max Planck Research Group Biomedical Physics investigates the principles of dynamics and self-organization of cardiac arrhythmias, a significant cause of morbidity and mortality worldwide. Our research aims to translate fundamental scientific discoveries into innovative medical diagnostics and therapies to improve human health.

Sudden cardiac death caused by ventricular fibrillation (VF) takes the lives of hundreds of thousands of people every year. Atrial fibrillation (AF) is the most common arrhythmia and a global health epidemic, associated with an increased risk of stroke and promoted heart failure progression. Cardiac arrhythmias remain poorly understood, and therapies are often ineffective and have severe side effects, indicating a major, unmet medical need.

Our research focuses on two fundamental scientific questions: What are the essential principles underlying the spatio-temporal self-organization of cardiac arrhythmias? How can we use this knowledge to effectively control cardiac arrhythmias while mitigating side effects?

To address the first question, we are developing advanced multimodal imaging technologies to visualize cardiac electromechanical function. Our research has provided unprecedented insights into the spatio-temporal organization of cardiac fibrillation. In the preclinical experiments, we visualized for the first time 4D electromechanical rotors (scroll waves) during VF. By successfully translating this technology to clinical application, we obtained the first measurement of the spatio-temporal organization of VF in humans, a major breakthrough in cardiac research (see section 6.27 for details).

Based on these accomplishments, we aim to answer the second question. Approaching arrhythmia control from the perspective of dynamical systems, we challenge the century-old paradigm of high-energy defibrillation. Using small but optimally timed perturbations, we demonstrated efficient control of spatial-temporal complexity in the heart with unprecedented energy reduction compared to the high-energy defibrillation shock. We introduced adaptive deceleration pacing (ADP), currently the most effective algorithm for low-energy termination of VF and AF. Our recent work in cardiac optogenetics and numerical simulations indicates significant further potential for efficient control of excitable media (see section 8.8).

Our latest scientific progress brings us even closer to translating our basic research into clinical application. Supported by Max Planck Innovation GmbH, the technology transfer organization of the MPG, strategic collaborations with the MedTech industry are being established. By further advancing our technologies with clinical and industrial partners, we will pave the way for the next generation of cardiac rhythm management devices.

Our translational focus on complex cardiac dynamics and arrhythmia control is complemented and stimulated by basic research projects on general questions of analysis, control and data-driven modeling of nonlinear systems. These broad research interests include time se-

ries analysis methods and novel machine learning approaches that are applicable to many other areas of nonlinear dynamics (see section 7.9).

A characteristic feature of our current and future research is the close combination of advanced measurement and imaging techniques with innovative theoretical and conceptual approaches for the analysis and control of arrhythmias. Experimental methods such as 4D ultrasound, opto-acoustics, and opto-genetics will be applied and further improved. On a theoretical-conceptual level, we will explore innovative approaches to terminate cardiac arrhythmias through feedback control, machine learning and the targeted exploitation of the sensitive dependence of chaotic cardiac dynamics on weak perturbations.

The Research Group Biomedical Physics is committed to supporting open source and open science. For example, supported by the Max Planck Digital Library, we have introduced the open source software LinkAhead for FAIR research data and workflow management, covering the scientific process from data generation to publication. LinkAhead's large and growing user community is supported by BMPG's award-winning spin-off IndiScale GmbH.

Our research group is embedded in an interdisciplinary environment that includes the University of Göttingen, the University Medical Center Göttingen (UMG) and the German Center for Cardiovascular Research (DZHK). We are strategically expanding our national and international collaborations, including partners at Yale University, UC San Diego, McGill University, University of Freiburg, University of Applied Sciences Nuremberg, and Technical University Munich. In this vibrant community, we do not only strive for cutting-edge research but are also committed to excellence in teaching to educate and promote the next generation of scientists and physician-scientists.

apl. Prof. Dr. Ulrich Parlitz studied physics at the Georg-August-Universität Göttingen, where he received his PhD in 1987. After five years at the Inst. for Appl. Physics of the TU Darmstadt he returned to Göttingen in 1994 where he was habilitated in 1997 and was appointed apl. Prof. of Physics in 2001. He was a visiting scientist at the Santa Fe Institute (1992), the UC Berkeley (1992), and the UC San Diego (2002, 2003). His research interests include nonlinear dynamics, data analysis and cardiac dynamics. In 2010 he joined the Research Group Biomedical Physics. He is faculty member at the Inst. for the Dynamics of Complex Systems and GAUSS.

Prof. Dr. Valentin Krinski studied physics at the Institute of Physics and Technology, Moscow, where he received his PhD in 1964. After 12 years at the Institute of Biological Physics in Puschino, he was appointed Head of the Autowave Laboratory in 1976, Prof. of Biological Physics at the Institute of Physics and Technology, Moscow in 1980. He was Directeur de Recherche, CNRS, INLN, Nice, France from 1993. His research interests include rotating vortices in biological excitable tissues and arrhythmia control. In 2007 he joined the Research Group Biomedical Physics.

Dipl.-Ing. (FH) Andreas Barthel received his Diploma degree in Computer Engineering at Nordhausen University of Applied Sciences in 2004. From 2005 to 2016, he worked at the Institute for Bioprocessing and Analytical Measurement Technology e.V. (Heilbad Heiligenstadt). In 2016, he joined the Research Group Biomedical Physics as a research engineer and scientist, and since 2022 he focused on translational DZHK projects. His extensive expertise and experience in electrical and bioengineering are essential for our translational biomedical research.

Dipl.-Phys. Gisa Luther studied physics at the University of Hannover and of Oldenburg and received her Diploma degree in 1996. From 1997 to 2004, she worked as project manager in software engineering and system integration (Bull GmbH, WestLB Systems GmbH). From 2004 to 2007, she was scientific staff member at the MPI-DS and visiting scientist at Cornell University, Ithaca NY, USA. Since 2007, she has been scientific staff member in the Research Group Biomedical Physics, focusing on numerical simulations in cardiac tissue and on scientific project management.

Dr. Sayedeh Hussaini studied physics at Ferdowsi University in Mashhad, Iran. In 2015, she received her Master's degree in Nanophysics. In September 2016, she joined the Research Group Biomedical Physics, where she mainly focused on computational studies to control the dynamics of cardiac arrhythmias. She received her Ph.D. in February 2021 and then continued her research in numerical and experimental studies as a postdoctoral researcher. Her research interests focus on cardiac modeling, cardiac arrhythmia control, and cardiac optogenetics.

Dr. Alexander Schlemmer studied physics at the Georg-August-Universität Göttingen, where he received his Diploma degree in 2011. He was a research assistant at the Psychology Department of the University of Hildesheim (2011-2013) and at the Research Group Biomedical Physics at the MPI-DS (2012-2017). He received his doctoral degree in 2017. He is co-founder of IndiScale GmbH. His research interests focus on spatio-temporal dynamics of excitable media, time series analysis and machine learning for nonlinear systems, and semantic data management in complex heterogeneous scientific environments.

Dr. Johannes Schröder-Schetelig studied physics at the Georg-August-Universität Göttingen, where he received his Diploma degree in 2012. Working for the Research Group Biomedical Physics at the MPI-DS as a student assistent since 2008, he continued as a doctoral student and received his doctoral degree in 2020. His research interests focus on studying the complex spatio-temporal dynamics of the heart with simultaneous application of multiple imaging modalities including 3D panoramic optical mapping, multi-ECG, and 4D ultrasound.

3.2.3 *Max Planck Research Group: Theory of Turbulent Convection*

Turbulent thermal convection is a fundamental phenomenon that governs a wide range of astrophysical, geophysical, and industrial processes, including atmospheric circulation and ocean currents, different energy systems, and engineering applications. The interplay between buoyancy-driven turbulence, heat and momentum transport, the formation of turbulent superstructures, and the emergence of multiple states in turbulence presents intriguing challenges in fluid dynamics. These multiple states, characterized by distinct large-scale flow structures with different heat and momentum transport properties and transitions between the different turbulent regimes, have significant implications for understanding geophysical and astrophysical systems, climate modeling, numerous industrial applications, and energy efficiency.

The research of the *Theory of Turbulent Convection* Group focuses on various aspects of turbulent convection, including convection under extreme thermal driving (high Rayleigh numbers, *Ra*), known also as the ultimate regime in thermal convection; the scaling properties of the heat and momentum transport (characterized by the Nusselt number *Nu* and Reynolds number *Re*, respectively); the effects of the pressure- and temperature dependences of the fluid properties on the global heat and momentum transport (so-called non-Oberbeck–Boussinesq effects); Rayleigh–Bénard convection affected by rotation or magnetic field; and centrifugal thermal convection, where a centrifugal buoyancy determines the flow in addition to the gravitational buoyancy. The group's key research area is the emergence and properties of multiple states in different configurations of turbulent convective flows. Other key research areas include convection in liquid metals (low Prandtl number *Pr* fluids) and magnetoconvection; sheared and modulated convection; internally heated convection; and convection in viscoelastic and viscoplastic complex fluids. Additionally, the group develops advanced numerical methods for simulating and analyzing turbulent flows and algorithms for reconstructing temperature fields from experimental velocity measurements in turbulent natural convection.

PD Dr. Olga Shishkina studied mathematics at the Lomonosov Moscow State University (LMSU, 1982-1987), received her doctorate in Scientific Computing from the Moscow University for Telecommunication & Informatics (1990), habilitated in Fluid Mechanics at the TU Ilmenau (2009), and in Mathematics at the University of Göttingen (2014). She worked at the LMSU (1994-2002) and DLR (2002-2014), and joined the MPI-DS in 2014, where she leads the *Theory of Turbulent Convection* MPRG. She is a DFG Heisenberg fellow (2014), a Fellow of the American Physical Society (2020), a Fellow of EUROMECH (2022), an Expert of the Research Executive Agency (REA), European Commission, and an Associate Editor of the Journal of Fluid Mechanics.

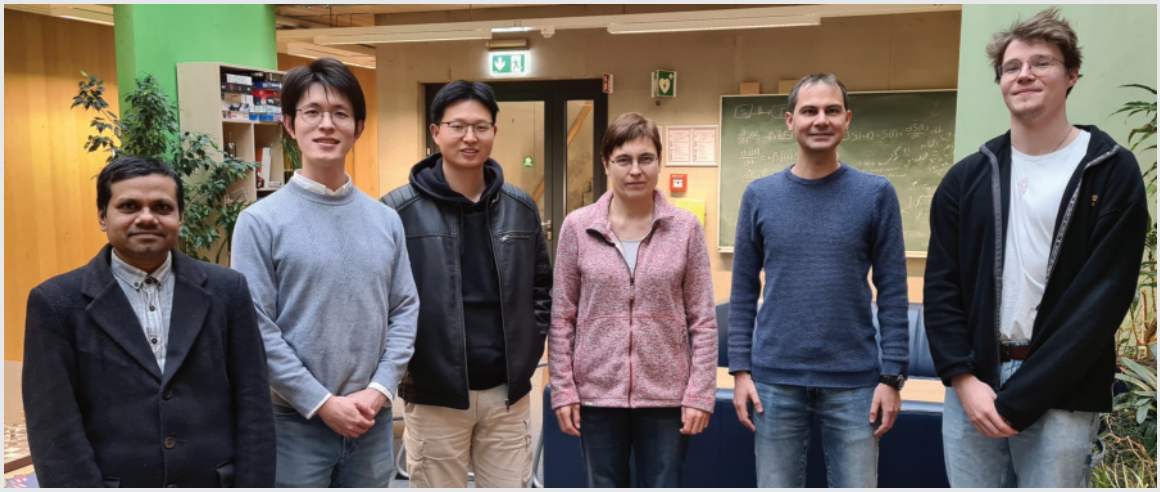

Theory of Turbulent Convection Group in February 2025

Dr. Andrei Teimurazov completed his studies in Applied Mathematics and Computer Science at Perm State Technical University (Russia) in 2009. In 2013, he received his doctorate from the Institute of Continuous Media Mechanics (Perm, Russia). His research focused on the numerical investigations of secondary flows and small-scale turbulence during convection in closed cavities. After completing PhD, he worked as a researcher at the same institute until October 2020. In November 2020, he joined the Theory of Turbulent Convection group at the MPI-DS. His research interests include investigations of turbulent flows, particularly the thermal convection of liquid metals, magnetoconvection, and rotating and internally heated convection.

Dr. Mohammad Emran studied Computational Sciences in Engineering at Braunschweig University of Technology and received an M.Sc. in June 2005. From October 2006, he was a PhD student at the Institute of Thermodynamics and Fluid Mechanics, Ilmenau University of Technology, and was awarded a PhD in turbulent convection in December 2009. After completing his PhD, he worked as a postdoctoral researcher at the same institute until February 2016. Since April 2016, he has been a postdoc in the Theory of Turbulent Convection Group at the MPI-DS. His current interest is rotational and centrifugal turbulent convection.

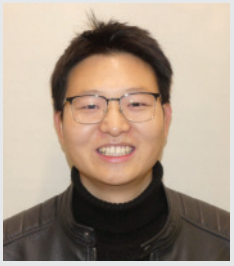

Dr. Jiaxing Song received his BA in Theoretical and Applied Mechanics from Lanzhou University in 2016 and his PhD in Fluid Mechanics from the University of Science and Technology of China in 2021. He worked as a research scientist at the Max Planck Institute for Solar System Research from 2021 to 2023 and joined the Theory of Turbulent Convection Group at the MPI-DS in January 2024 as a Humboldt Fellow. His research focuses on numerical investigation of turbulence, thermal convection, geophysical flows and complex flows of viscoelastic fluids, particularly in Rayleigh–Bénard and Taylor–Couette turbulence.

Dr. Zhongzhi Yao studied Thermal Energy and Power Engineering at the East China University of Science and Technology, graduating in 2014. He then pursued a PhD in Ocean Engineering at Zhejiang University, earning his degree in 2020. Following his PhD, he was a lecturer at Hainan Tropical Ocean University until February 2023. In March 2023, he joined the Theory of Turbulent Convection Group at the MPI-DS as a postdoctoral researcher. His recent research focuses on Rayleigh–Bénard convection, centrifugal convection and multiple states in turbulence.

Marvin Kriening studied Theoretical and Environmental Physics at Friedrich Schiller University Jena and Ruprecht Karl University of Heidelberg. After completing his master's studies in 2022, he worked as a developer at Zeiss GmbH from 2023 to 2024. In October 2024, he joined the Theory of Turbulent Convection Group at the MPI-DS as a PhD student. His research focuses on multiple states in turbulence through the theoretical and numerical investigation of rotating turbulent thermal convection and Taylor–Couette flow.

3.3 DEPARTMENT DYNAMICS OF COMPLEX FLUIDS

The arguably most important question of our time is whether (and how) humankind can devise a sustainable management of its ecological niche on planet Earth. Furthermore, it has become increasingly clear in recent years that the obstacles are not residing in a lack of technologies, but in the interaction rules (tacit or open) and incentivization structures inherent to our societies and behaviour. Societies consist of a large number of (similar) active agents in close mutual interaction, which is the defining property of a complex fluid, more precisely, of active matter. Consequently, the department Dynamics of Complex Fluids (DCF) had adopted socio-economic physics as a new focus already in 2016, in order to put our experience and expertise in complex fluids and active matter into service for humankind. From this focus, the interdisciplinary project EcoBus emerged, which evolved into public service pilot projects, and evetually to fully deployed transportation services in Leipzig and Göttingen.

During the years of the Covid19 pandemic, this focus developed theory projects on optimal strategies of pandemic management and precise forecast of infection waves. It furter branched out into more general socio-economic problems like racial profiling, and more general studies on human interaction based on the paradigm of public-goods-games.

Simultaneously, the other foci of DCF, complex fluids far from equilibrium and what has become known as active matter, continued at full strength. By the end of 2022, all of the senior researchers of the department, who were heading for an academic career, had received calls on professor positions elsewhere. As this coincided with certain health problems of the head of the department, Stephan Herminghaus decided to apply for an early retirement mid 2023, in order to give way for a swift succession. In June 2023, the institute organized a two-days closing symposium entitled 'Complex Fluids and Beyond'. Of the about thirty of our alumni who had left for professorships in many parts of the world, twenty followed the invitation to the symposium as speakers, and delivered talks about their current research projects and results.

Consequently, this 'mission statement' is actually rather a 'demission' statement; further activities by Stephan Herminghaus can be found in his statement as an Emeritus in section 4.8.

Hon. Prof. Dr. S. Herminghaus received a PhD in physics from the University of Mainz in 1989. After a postdoctoral stay at the IBM Research Center in San Jose (California, USA), he became a research associate at the University of Konstanz in 1991, where he received his habilitation in 1994. In 1996 he became head of an independent Max-Planck Research Group at the MPI for Colloids and Interfaces in Berlin. In 1998, he received calls on full professorships at the Universities of Fribourg (Switzerland) and Ulm, and decided for heading the department of Applied Physics in Ulm. Since 2003 he has been Director at the MPI-DS, and since 2005 holds an additional appointment as an adjunct professor at the University of Göttingen. He was appointed as Professeur Invité at the Université Paris VI for the winter term 2006/7 and at the Université Paris Sud for the summer term 2013. He is member of the Scientific Advisory Council of the National IOR Centre Norway and has been Scientific Advisor to the ESA (Chair of Physical Sciences).

Dr. Christian Bahr received his PhD in 1988 at the TU Berlin. After Postdoctoral work at the Raman Research Institute (Bangalore, India) and the Laboratoire de Physique des Solides of the Université Paris-Sud (Orsay, France), he received his habilitation for physical chemistry at the TU Berlin in 1992 and moved to the University Marburg as a Heisenberg-Fellow in 1996. From 2001 he worked as a software developer before he joined our institute in 2004. Research topics comprise experimental studies of soft matter, mainly thermotropic liquid crystals.

Dr. Tariq Baig-Meininghaus received his PhD in Physics from the University of Göttingen in 2017. After completing a PostDoc position in the EcoBus Project at the Max Planck Institute for Dynamics and Self-Organization, he joined the Herminghaus department as leader of the working group 'Software Infrastructure for Social Systems Research' in 2020.

Dr. Knut Heidemann received a Master of Science in physics in 2012, and a PhD in theoretical phsics in 2016, both from University of Göttingen, Germany. After two years of applied data science research at Fraunhofer IAIS (Sankt Augustin, Germany), he returned to Göttingen in 2019, as research group leader at our institute. His group 'Physics of Social Systems' studies systems involving a human component, including topics like social network dynamics and sustainable mobility.

Dr. Stefan Karpitschka received his Diploma in Physics in 2007. As a PhD student he joined the MPI of Colloids and Interfaces in Potsdam, Germany. After PostDoc projects at the University of Twente in Enschede, The Netherlands and the Stanford University, USA, he became a Research Group Leader in our department and in the Max Planck - University of Twente Center for Complex Fluid Dynmamics in 2017, investigating interfaces of complex fluids and living materials. In 2023 he was appointed as Full Professor at the University of Konstanz.

Dr. Matthias Schröter obtained his PhD in 2003 from the University of Magdeburg. During his postdoctoral stay with Harry Swinney at the Center for Nonlinear Dynamics at the University of Austin he studied the statics and dynamics of granular media. Between 2008 and 2015 he joined the Department of Dynamics of complex Fluids as a group leader. Since 2018 he is an associated researcher. Main research topics are the statistical mechanics of granular media, X-ray tomography of complex materials and applications of machine learning in physics.

3.4 MAX PLANCK RESEARCH GROUP: TURBULENCE AND WIND ENERGY

Decarbonising global energy generation is one of the greatest challenges facing humanity, and transformative advances in any renewable energy technology require a profound understanding of the underlying science. Wind turbines operate in highly turbulent atmospheric flows. Both the local meteorological conditions and the arrangement of turbines in a farm significantly impact power production. However, neither their interactions with one another nor with the surrounding flow field are well understood. Our group studies the fundamental fluid dynamics of wind power generation. Using the unique experimental facilities at the MPI-DS, we combine laboratory experiments and field measurements to optimise wind energy from the blade scale to the farm scale.

The fundamental challenge in the study of wind turbines lies in the large separation of scales. Modern wind turbines are among the largest machines ever built, spanning diameters of more than 200 m and the largest coherent structures in the turbulent atmosphere are of the same order of magnitude. Meanwhile, the smallest scales of the flow, at which the turbulence is dissipated, are $\mathcal{O}$(1mm). High Reynolds numbers are thus a defining feature of real-world wind turbines. State-of-the-art numerical simulations are nowhere near capable of resolving the full range of scales encountered in wind farms. This makes field measurements of the flows around real wind turbines crucial, but fully characterising atmospheric turbulence requires the development of new flow measurement techniques.

Atmospheric flows are heterogeneous in space and time, so that elucidating the underlying flow physics through field measurements alone is challenging. A combination of field studies and laboratory experiments is therefore necessary. However, small-scale experiments only replicate the true flow physics if dynamic similarity with real-world conditions is achieved. This is not the case in any conventional atmospheric-pressure wind tunnel. Instead, we conduct experiments in the unique Variable Density Turbulence Tunnel, housed in the Max Planck Turbulence Facility at the MPI-DS 9.8. This specialised wind tunnel uses compressed sulphur hexaflouride to create small-scale flows that accurately reproduce the flow physics of large atmospheric flows. Due to its active turbulence grid, the VDTT is the only facility worldwide that can achieve full dynamic similarity with real turbulent wind farm flows. Not only can the data from the VDTT serve as a benchmark for any numerical or experimental study of wind turbine flows. By varying the pressure we also gain an additional degree of freedom, which allows us to vary individual flow parameters while keeping all others constant. We use this to isolate and characterise specific phenomena within the complex flow field and thus elucidate the underlying flow physics.

Dr. Claudia Brunner's research focuses on experimental studies of large-scale fluid dynamics involving turbulence and unsteady effects. She is particularly interested in flows that are relevant for the fields of energy and the environment, with a particular focus on wind energy, and she supplements her fluid dynamics research with studies of relevant policy questions. Before becoming an independent group in March 2024, Dr. Brunner's group was a Minerva Fast Track Group within the department of Prof. Bodenschatz. Prior to that, Dr. Brunner was a postdoc with Prof. Bodenschatz. She received her PhD in May 2022 from the Department of Mechanical and Aerospace Engineering at Princeton University, where she was advised by Prof. Marcus Hultmark. Dr. Brunner received a National Defense Science and Engineering Graduate Fellowship from the United States Department of Defense, and a Science, Technology and Environmental Policy Fellowship from the High Meadows Environmental Institute and the School of Public and International Affairs at Princeton University. She holds an M.A. in Mechanical and Aerospace Engineering from Princeton University and a B.S. in Mechanical Engineering and a B.A. in International Relations from Stanford University.

Dr. Yuna Hattori's research in the Turbulence and Wind Energy Group focuses on experimental studies of thermal boundary layers and their interactions with wind turbines, as well as on Reynolds number effects on wind turbine performance. Dr. Hattori received her PhD in fluid mechanics from the Okinawa Institute of Science and Technology (Japan) in March 2023. Her PhD research was concerned with self-similarity in the boundary-layer flow over a dynamic boundary. She used a vertically falling soap-film experimental setup, and is specialised in Particle Image Velocimetry (PIV), Particle Tracking Velocimetry (PTV), and Laser Doppler Velocimetry (LDV). In addition to experiments, she also conducted numerical simulations using OpenFOAM and theoretical analysis. She holds a B.S. in physics from Ochanomizu University in Japan, where she conducted research in theoretical particle physics.

Dr. Hyunseok Kim is a Sejong Fellow, awarded by the National Research Foundation of South Korea for his postdoctoral research. He joined the Turbulence and Wind Energy Group in September 2024 and studies turbine blade erosion due to particle-laden atmospheric turbulence in the Variable Density Turbulence Tunnel. In his research, Dr. Kim explores ways to control fluid-related phenomena through fundamental studies of the aerodynamics of wind energy, multiphase environmental fluid mechanics, and heat transfer. He aims to address sustainability challenges through technological innovation. Prior to joining the MPI-DS, Dr. Kim worked as a staff engineer in the Environment, Health & Safety Research Center at Samsung Electronics, where he contributed to the development of next-generation greenhouse gas abatement facilities. He holds a Ph.D. in mechanical engineering and a bachelor's degree in nuclear engineering from Seoul National University.

Dr. Akhileshwar Borra joined the Turbulence and Wind Energy Group in January 2025. He is developing novel field experiments to understand the interactions between wind turbines and the atmospheric boundary layer. Dr. Borra received his Ph.D. in Aerospace Engineering from the University of Illinois Urbana-Champaign in November 2024, under the supervision of Prof. Theresa Saxton-Fox. His doctoral research focused on experimentally investigating the effects of spatially varying pressure gradients on turbulent boundary layers, as well as extending the proper orthogonal decomposition framework for near-periodic systems. He holds a B.S. in Mechanical Engineering from the University of Massachusetts Amherst, where he conducted research on vortex-induced vibrations.

Lorenn Le Turnier joined the Turbulence and Wind Energy Group as a PhD student in September 2023. She studies the flow dynamics in the wakes of wind turbines using Lagrangian particle tracking in the Variable Density Turbulence Tunnel. Ms. Le Turnier holds a Max Planck Research Fellowship from the International Max Planck Research School on the Physics of Biological and Complex Systems. Before joining the MPI-DS, she worked at ArianeGroup in France. She completed her master's degree in aeronautics and space with a specialization in energy and mechanics at the University of Paris-Saclay in 2022. She wrote her master's thesis on heat transfer in the Molecular and Macroscopic Energy and Combustion Laboratory (EM2C) at CentraleSupélec. Lorenn holds a bachelor's degree in applied physics from the University of Paris-Saclay. During her bachelor's degree, she worked in the Department of Molecular Physics at the Physics Institute of Rennes.

3.5 MAX PLANCK RESEARCH GROUP: COMPLEX SYSTEMS THEORY

Research perspective. How does information processing emerge in living systems? Information is essential to any living agent – to find food and conspecies, to avoid predators and obstacles, to venture into new territories, and, in general, to learn a model about the world and navigate it in an informed and efficient manner. With my research group, I investigate how learning and information processing emerge in living networks, with a focus on two distinct but complementary systems: (i) For living neural networks, we investigate how neurons and synapses contribute to learning a model about the world in a self-organized manner. (ii) For living social networks, we investigate how information and misinformation spread, and how their structural contact network is formed and remodeled.

The two living networks have many features in common: their local connections are ever-changing, while their global function and many of their macroscopic statistics (order parameters) are maintained. Moreover, the self-organization- and learning principles bear similarities: in both networks, connections are strengthened, respectively, (i) if neurons are co-activated ("Hebbian learning"), and (ii) if agents meet and interact regularly. Both classes of living networks are also subject to self-organization processes that regulate their basic level of activity and connectivity. By studying these two systems side by side and by abstracting from their system-specific details, our overarching goal is to develop a foundational understanding of the statistical physics of adaptive, living, and learning networks.

My Group comprises about 20 members, including Bachelor's and Master's students. I am particularly proud that I am perceived as a very supportive but still demanding mentor, and that my group is known at the campus for its collaborative spirit and high productivity. I see my strengths in the ability to identify clear, relevant, and still achievable research goals, which translate to well-structured projects; even many of the Bachelor's and Master's students achieve a first-author paper from their thesis work. Likewise, all of my PhD students graduate with several peer-reviewed papers, and many with the distinction *summa cum laude*. For example, most recently (November 15, 2024), Jonas Dehning graduated with peer-reviewed publications in Science, Nature Neuroscience, Nature Communications, and "Patterns".

Distinctions. I have received multiple awards and distinctions, including the Communitas Prize of the Max-Planck-Society, the Lise-Meitner-Lecture by the German Physical Society (DPG) and the Austrian Physical Society (ÖPG), the Lower Saxony Science Award, the Dannie Heineman Award, and the Young Investigator Award in Socio-Economic Physics (DPG). I am a member of the Präsidium of "Die Junge Akademie" of the Leopoldina and BBAW, board member of the Campus Institute for Data Science (CIDAS), and member of the Göttingen Academy of Sciences and Humanities. I have been very active in political advising and outreach, also as member of the COVID-19

Prof. Dr. Viola Priesemann is Professor in the department of physics, Göttingen, and group leader at the MPI for Dynamics and Self-Organization. She studies living and artificial neural networks, carving out their basic mechanisms of self-organization, learning, and efficient coding.

Viola studied physics at the TU Darmstadt and the U.N. Lisbon. For her PhD, she combined theoretical work at the ENS Paris with experimental neuroscience at Caltech, Pasadena, and graduated in 2013 from the MPI for Brain Research and the University Frankfurt. In 2015, she was awarded a Max Planck Research Group, which she heads at the MPI for Dynamics and Self-Organizaton, and since 2022 she is also professor of physics at the University of Göttingen.

advisory board of the German chancellor. In 2027, I will continue as a W3 professor at the Department of Physics in Göttingen after I had to decline attractive professorships and a director position, mainly for dual-career reasons. Nonetheless, Göttingen offers an ideal research environment for me with its unique strength in neuroscience, biomedical imaging, and physics of complex systems.

Funding. I have a very strong track record in acquiring third-party funding, and I am closely integrated into the research community at the Göttingen Campus. In particular, as member of the Excellence Cluster Multiscale Bioimaging (MBExC), I receive generous funding via the university, and I lead research projects in several collaborative research endeavors (SFB 1286, SFB 1528, SFB 1690, SPP 2205, RTG 2906, and more), and I am member of the Campus Institute for Data Science (CIDAS), the Center for AI in Medicine (CAIMed), and the Else-Kröner-Fresenius-Center for Optogenetic Therapies, which I co-applied for. Importantly, since 2022, I have been leading a large research consortium funded by the German Federal Ministry of Education and Research (BMBF) on pandemics and infodemics, and I have applications for the extension of that consortium, and for new consortia on disinformation and democracy pending.

Five Selected Publications (2023)

[1] J. M. Rowland, et al., Nature Neuroscience **26**, 1584 (2023)
[2] A. Kekić, et al., Patters **4**, 100739 (2023)
[3] H. Yamamoto, et al., Science Advances **9**, eade1755 (2023)
[4] J. Dehning, et al., Nature Communications **14**, 122 (2023)
[5] F. A. Mikulasch, et al., Trends in Neuroscience **46**, P45 (2023)

Dr. Sebastian "Seba" Contreras is interested in the complex interplay between human behavior and infectious diseases, studying how societies and pathogens co-evolve. He leads the research team on infectious disease modeling, focusing on behavior, feedback loops, interventions, and multi-pathogen systems for sexually transmitted infections. His work on tipping points for disease spread was highly relevant in COVID-19 mitigation in Germany, and he was granted the Berliner-Ungewitter Prize for his outstanding doctoral dissertation. Seba was also awarded the Best Graduate of the Year (Chilean Association of Engineers).

Dr. Jonas Dehning studied physics at the University of Göttingen. He is an expert in Bayesian inference and applies that to the underlying spreading dynamics of neural activity and infectious diseases. He explored the dynamical properties of neural activity from subsampled in vivo recordings. Furthermore, his work was essential during the COVID-19 pandemic, uncovering which factors influence the spread of COVID-19 in Germany and Europe. His main interest lies in improving Bayesian methods to allow the assembly of more complex models.

Anastasia Golovin studied physics and computational science at the TU Munich with a strong interest in complex systems and societal dynamics. She now investigates how the topics discussed on social media evolve over time as a complex, dynamical system. To that end, she is scraping and curating an extensive data set with over 1.8 billion messages from Telegram, and coordinates the systematic exploration of that unique data set. With approaches from statistical physics and dynamical systems, she investigates how the spread of topics self-organizes on that evolving living network.

Laura Müller's core interest is to understand how complex dynamical systems can be controlled and optimized. Using the example of infectious disease spread, she investigates how human risk perception and mitigation strategies influence the spread, and more importantly, how mitigation strategies in such complex systems can be optimized. She found that depending on disease severity, mitigation should either be perfectly balancing the reproduction rate to keep case numbers constant, or, in the case of mild diseases, mitigation should be absent. Surprisingly, there were no intermediate strategies. Thereby, she has identified a novel principle of optimal disease mitigation which she plans to further investigate.

Dr. Lucas Rudelt studied physics at the University of Göttingen, where he received his PhD in 2024 with a focus on computational neuroscience. Using variational methods of optimization, Lucas' work has uncovered a new principle for the self-organization of neural networks. He found that subcellular processes at the dendrites allow excitatory and inhibitory synapses to orchestrate their plasticity, which solves a long-standing problem of biological learning with spiking neurons. With developing approaches to infer information-theoretic measures directly from neural spike recordings, he was awarded the Berliner-Ungewitter Prize for an outstanding Master's thesis.

Andreas Schneider developed a keen interest in neuroscience and artificial intelligence while studying physics in Bayreuth. This led him to Göttingen, where he joined the group for his Master's in 2019, focusing on quantifying information processing in artificial neural networks. In his PhD project, he is advancing a novel framework for local learning that incorporates a wide variety of known strategies. Inspired by the self-organization of living neurons, this approach identifies objective functions for individual artificial neurons in order to create more robust and interpretable learning algorithms.

Dr. Johannes Zierenberg studied physics at ETH Zürich and Leipzig University, where he received his PhD in 2016 focusing on statistical physics and Monte Carlo simulations of particle and polymer systems. In January 2017, he joined the group as a postdoc and showed analytically and in data how the same self-regulation mechanisms can stabilize or destabilize neural networks, depending on context. He now heads the neural network dynamics team to uncover fundamental mechanisms underlying self-organizing processes and living computation in nature, by bridging physics-based modeling and data-driven approaches.

3.6 MAX PLANCK RESEARCH GROUP: TURBULENCE, COMPLEX FLOWS & ACTIVE MATTER

Prof. Dr. Michael Wilczek studied physics at the University of Münster from which he received his diploma in 2007 and doctorate in 2011 under the supervision of Prof. Rudolf Friedrich. During his postdoctoral time at the Institute of Theoretical Physics at the University of Münster he worked on fundamental aspects of turbulent flows. In 2013, he joined the group of Prof. Charles Meneveau at the Department of Mechanical Engineering at the Johns Hopkins University, Baltimore, extending his research portfolio to atmospheric turbulence and wind energy. In 2014 he returned to Germany and completed a short research stay with Prof. Rainer Grauer at the University of Bochum. Between 2015 and 2022 he headed an MPRG at MPI-DS. He received the 2018 Fulbright-Cottrell Award in recognition of his efforts in combining research and innovative teaching. In 2020 he was awarded an ERC Consolidator Grant. Since 2021 he has been professor of Theoretical Physics at the University of Bayreuth.

Our MPRG, which was hosted at MPI-DS from 2015 to 2022, focused on turbulence, complex flows and active matter. Collaborations with MPI-DS scientists continue until today. In the following, we showcase some select recent works.

One of the major collaborations with the Bodenschatz Department and scientists from the Fraunhofer Institute for Physical Measurement Techniques is the TWISTER project which is funded through the Fraunhofer–Max Planck cooperation program. Its main goal is the exploration of atmospheric turbulence, combining field campaigns with novel measurement techniques and simulations. This, for example, resulted in a paper quantifying how accurately the energy dissipation can be estimated using airborne measurement techniques such as the MPI-DS CloudKite (see section 5.7) [1]. More recently, we evaluated how the impact of geometric constraints for a CloudKite-mounted LiDAR system can be mitigated [2].

The investigation of particles in turbulent flows is another focus of our work. Also as part of the TWISTER project, we studied the impact of small-scale turbulence on the collision of rain droplets [3]. A similar problem arises in the context of plankton encounters in the ocean. Here, we investigated how shape affects the collision rates of particles that model phytoplankton in the ocean [4], finding enhanced collision rates for elongated species. As a characterization of the geometric properties of turbulent mixing, we investigated the evolution of material lines in turbulence and uncovered their statistical geometry [5].

We also continued our fundamental investigations of the small-scale structure of fully developed turbulence. In a collaboration led by D. Buaria, we uncovered how the vorticity can self-regulate to reduce singular behavior in turbulence [6]. We furthermore studied how important statistical properties like skewness and non-Gaussian behavior emerge in low-Reynolds number flows [7]. In a collaboration with Prof. A. Ecker, we also used machine learning techniques to develop a deterministic reduced-order model that generates quantitatively accurate velocity gradient data by design [8].

[1] M. Schröder, T. Bätge, E. Bodenschatz, M. Wilczek, G. Bagheri, Atmos. Meas. Tech. **17**, 627 (2024)
[2] W. Knöller, G. Bagheri, P. von Olshausen, M. Wilczek, Atmos. Meas. Tech. **17**, 6913 (2024)
[3] T. Bätge, I. Fouxon, M. Wilczek, Phys. Rev. Lett. **131**, 054001 (2023)
[4] J.-A. Arguedas-Leiva, J. Słomka, C.C. Lalescu, R. Stocker, M. Wilczek, Proc. Natl. Acad. Sci. U.S.A. **119**, e2203191119 (2022)
[5] L. Bentkamp, T.D. Drivas, C.C. Lalescu, M. Wilczek, Nat. Commun. **13**, 2088 (2022)
[6] D. Buaria, J.M. Lawson, M. Wilczek, Sci. Adv. **10**, eado1969 (2024)
[7] M. Carbone, M. Wilczek, J. Fluid Mech. **986**, A25 (2024)
[8] M. Carbone, V.J. Peterhans, A.S. Ecker, M. Wilczek, Phys. Rev. Lett. **133**, 184001 (2024)

3.7 MAX PLANCK RESEARCH GROUP: THEORY OF BIOLOGICAL FLUIDS

In contrast to most artificial machines, biological organisms comprise soft and often fluid-like material. How can such soft matter be controlled in space and time to fulfill precise functions? What can we learn from nature to design smart materials? To uncover the physical principles of such an organization, we analyze theoretical models of biological processes using tools from statistical physics, dynamical system theory, fluid dynamics, and information theory.

Biological cells comprise thousands of different kinds of biomolecules, which are spatially organized into organelles. Typical large organelles, like the nucleus and the mitochondria, are enclosed in a membrane, but there also exist numerous smaller organelles without membranes. These membrane-less organelles form spontaneously via phase separation, much like oil droplets form in water, and are known as biomolecular condensates. However, in contrast to oil in water, these condensates exist in the complex, non-equilibrium environment of the biological cell, where fuel molecules like ATP are constantly consumed to drive chemical reactions. Moreover, the condensates themselves and their surrounding exhibit elastic properties caused by the macro-molecular composition. Finally, cells are heterogeneous and change their behavior over time, e.g., in response to environmental cues.

A main focus of our group is to understand the influence of the complex cellular environment on condensates. In particular, we want to unveil physical mechanisms that allow cells to control condensates. Along these lines, we have shown that driven chemical reactions can be used to control droplet positions, sizes, and counts. We also already investigated how droplets grow inside elastic gels in synthetic systems. To do this, we extend the physical frameworks that are typically used for describing phase separation to accommodate the complexity of cells and we also develop new numerical methods that are suited for describing the resulting multi-scale dynamics. We discovered that chemical reactions, elasticity, and charge can all control the size of phase separated structured and influence dynamical patterns familiar from reaction-diffusion systems. All three physical principles can be interpreted as long-ranged interactions, and we currently develop a more general theory involving such interactions. We are also interested in multi-component mixtures since phase separation in cells can likely not be described by a simple theory based on binary mixtures. Alongside these more theoretical endeavors, we actively collaborate with experimentalists to apply our theories to realistic systems and help understand complex biological phenomena.

In summary, a central aim of our group is to develop insight into biological processes using theoretical modeling. Here, we relish collaborations with experimentalists and theorists both locally at our institute as well as globally to better understand the organization of biological cells and also learn about fundamentally new approaches for engineering soft materials.

Dr. David Zwicker studied physics at the Technische Universität Dresden and Lund University. After a short internship with Pieter Rein ten Wolde at AMOLF in Amsterdam, he pursued his Ph.D. in Biological Physics under the supervision of Frank Jülicher at the MPI for the Physics of Complex Systems in Dresden, where he focused on theoretical descriptions of phase separation in the non-equilibrium environment of biological cells. He then joined Michael Brenner's group at Harvard University as a postdoc to work on the information theory and fluid dynamics of olfaction. In 2017, he joined MPI-DS to start his independent Max Planck Research Group.

David is a faculty member at the Georg August University School of Science (GAUSS) and the Max Planck School Matter to Life. He is also a member of the Young Investigator Programme of the European Molecular Biology Organization and he obtained an ERC consolidator grant in 2022.

Dr. Noah Ziethen studied Physics at the Georg-August-University Göttingen. For his Bachelor thesis, he joined the group of Biological Physics and Morphogenesis at MPI-DS, where he worked on automated image analysis of biological networks. For his Master's thesis, he turned to a combination of theoretical and experimental methods investigating the role of shear stress on the growth in Physarum polycephalum in the same group and received his degree in 2019. Interested in more theoretical approaches in biological physics, he started his Ph.D. in the group Theory of Biological Fluids and investigates the influence of fluctuation on chemically driven droplets and graduated in 2024.

Marcel Ernst studied Physics at the Georg-August-University Göttingen. For his Master's thesis at the Max Planck Institute for Dynamics and Self-Organization he was researching the stability and numerical simulation of convection in dry salt lakes aiming to understand the origin of characteristic polygonal patterns in salt playa. After several years at the University of Kassel working on simulations of electrical grids and especially the integration of eMobility he joined the Zwicker group in 2021. Interested in more theoretical approaches in fluid physics he works on the physical description of condensates involved in meiosis.

Dr. Chengjie Luo focuses on systems that are out of thermodynamic equilibrium, including supercooled liquids, glasses, and living cells. He develops theories and simulations to better understand the underlying principles of these systems comprising soft and active matter. Recently, he became interested in theories describing biomolecular condensates and phase separation.

Gerrit Wellecke studied Physics at the Georg-August-University Goettingen. For his bachelor's thesis, he worked with Prof. Dr. Peter Sollich on a coarse-graining approach for stochastic dynamics. For his master's thesis, he investigated the relaxation of driven diffusive systems in the Mathematical bioPhysics Group of Aljaz Godec at the Max Planck Institute for Multidisciplinary Sciences. He then joined the Zwicker group as a Ph.D. student in 2022. He is generally interested in statistical physics and thermodynamics and how these frameworks can describe biological phenomena, such as phase separation.

Riccardo Rossetto studied Physics of Complex Systems at Politecnico di Torino. For his master thesis, he worked on a model of phase separation on fluid membranes, which coupled the self-aggregation process with surface fluctuations. He joined the Zwicker group as a PhD student in 2022. He is generally interested in statistical physics applications to biological systems, both from a theoretical and a computational perspective.

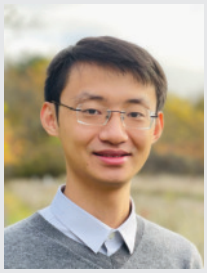

Dr. Yicheng Qiang received his Ph.D. degree from Fudan University. There, he worked on the self-assembly behavior of block copolymers and high-performance algorithms for the self-consistent field theory. He joined the Zwicker Group as a postdoc in 2022. Now he focuses on the phase separation of multicomponent mixtures, hoping to learn how to achieve robust control over the properties of biological condensates.

Dr. Oliver Paulin previously studied for his Masters and D.Phil (PhD) degrees at the University of Oxford, before joining the Zwicker Group as a postdoc in 2023. Broadly, he is interested in fluid dynamics and soft matter physics, and their application to both biological and geophysical systems. During his D.Phil, he studied multiphase fluid flow through soft porous media, with a specific focus on the formation and collapse of 'non-wetting cavities' in poroelastic materials. His current research concerns phase separation in soft systems, with application to the behaviour of biomolecular condensates in cells.

Dr. Cathelijne ter Burg obtained her Ph.D. degree at Ecole Normal Superieure (ENS) Paris where she worked on disordered systems and avalanche dynamics with Prof. Kay Wiese. She then moved to the Department of Applied Mathematics and Theoretical Physics (DAMTP) at Cambridge University for a one-year postdoc in the group of Prof. Mike Cates. At DAMPT she worked with dr. Ronojoy Adhikari on stochastic dynamics, in particular the tubular ensemble to quantify path probabilities and studying this in the context of underdamped dynamics. She then joined the Zwicker Group as a postdoc in November 2023.

Stefan Köstler studied Physics at the University of Bayreuth, with a strong focus on condensed matter systems and non-equillibrium dynamics. For his Bachelor's thesis, he investigated the effect of temperature on the dispersion of surface plasmons. For his Master's thesis, he theoretically described pattern formation and dynamic defects in ferromagnetic superconductors. He then joined the Zwicker group as a Ph.D. student in December 2023. He's genereally interested in the principles and applications of controlling the motion of biomolecular condensates.

Dr. Guido Kusters obtained his PhD degree from Eindhoven University of Technology, where he worked on modeling the (non-)equilibrium behavior of various soft and responsive materials. During this time he was also a visiting scholar at the University of Oxford and Harvard University, where he explored excursions to active matter and nanocomposite self-assembly, respectively. Having recently become increasingly interested in biological systems, he joined the Zwicker group in the autumn of 2024 to study the spatiotemporal organization of biomolecular condensates.

Dr. Filipe Thewes obtained his Ph.D. from the University of Göttingen, where he worked on the interplay between kinetic timescales and thermodynamic driving forces in multi-component mixtures. Currently, he is interested in the theoretical description of multi-component systems in biological contexts, where phase separation is combined with other biochemical/physical processes to achieve functionality. His aim is to learn how to control structure formation in biological condensates.

Henri Schmidt studied in Heidelberg, Germany and Copenhagen, Denmark before joining the Zwicker group as a PhD candidate in 2024. While for his undergraduate studies he focused on cell motility utilizing phase fields as well as optimal transport and Wasserstein distances, he investigated active turbulences modeled by nematics at the Niels-Bohr Institute in Copenhagen. Continuing researching on soft matter physics, he nowadays takes interest in phase separation within multi-component systems, e.g., inside cells, where a multitude of proteins interact with each other.

3.8 HEISENBERG GROUP: EXPERIMENTAL STATISTICAL PHYSICS

The physics of low dimensional ensembles (2D or 1D) is often much richer compared to their three dimensional (3D) counterparts. This is true for quantum systems like in the Quantum-Hall effect, in Graphene or Bose-gases as well as for classical system focusing e.g. on random walks, melting by topological defects and long wave-length fluctuations. Colloidal mono-layers my be seen as massive parallel analog computer solving the equations of motion of a enormously large number of individual particles simultaneously. Using standard video microscopy, the complete phase space information can be extracted in well equilibrated systems but also far from equilibrium. This makes colloidal ensembles ideal candidates to investigate fundamental issues in statistical physics in and out of equilibrium where self organization processes can be investigated with „atomic“ resolution.
I am especially interested in symmetry breaking and phase transition in equilibrium (Kosterlitz-Thouless transition), the 2D glass transition, low energy excitations and long wavelength fluctuations (Mermin-Wagner-Hohenberg theorem), and symmetry breaking far of thermal equilibrium (Kibble-Zurek formalism) which originally postulated topological defects to emerge in the primodial Higgs-fiels shortly after Big-Bang. Given by the two-component order parameter of the latter it turns out to have beautiful analogs in condensed matter: in quantum fluids like suprafluid Helium, normalfluid strings have to appear during symmetry breaking while in colloidal mono-layers, isolated disclinations as residuum of the high symmetry phase are frozen out. For ultra-fast quenches we identified universal behaviour in the mosaicity, independent how deep one quenches into the solid phase. For the glass transition it's been discussed widely if an analog of disclocations can be identified on an amorphous environment since they play a prominent role in softening of periodic ensembles. In an international collaboration we recently identified vortices with +1 and -1 winding number in the in the vibrational eigenspace of a 2D colloidal glass former. Presently we investigate, if they unbind at the glass transition temperature in close analogy to 2D melting of crystals. To further check the generality of topological defects in 2D melting, we investigated crystals composed of squares. A tetratic phase with quasi-long range four-fold orientational but short ranged translational order was identified, forming a liquid crystal with a four-fold director.

Priv. Doz. Dr. Peter Keim studied physics at the Universities in Frankfurt and Konstanz and received his PhD in 2005. After a two-years postdoc at the University of Graz, he went back to Konstanz to lead a Junior Research group. In 2016 he was awarded the Gustav-Hertz-Prize of the German Physical Society and got the venia legendi in experimental physics. Since 2021 he leads a Heisenberg-Group funded by the German Research Foundation and hosted at MPI-DS. 2022 he got the venia legendi from University of Göttingen and starting 2024 he holds a Representing Professorship at Heinrich-Heine-University of Düsseldorf. His research is focusing on vitrification, topological phase transitions and spontaneous symmetry breaking beyond equilibrium. His experimental technique is using the complete phase space information provided by colloidal ensembles in his group: Experimental Statistical Physics.

Alireza Valizadeh, holding a BSc in Energy Engineering from Amirkabir University of Technology, completed his MSc in Condensed Matter Physics at the University of Tehran in 2022. By focusing on the physics of critical pheomena, his master's thesis explored the universality properties of the 2D Ising model by using Random Matrix Theory. In 2023 as a PhD student, Alireza joined the Experimental Statistical Physics group where he studies the Kibble-Zurek Mechanism in two-dimensional colloidal systems within the Kosterlitz-Thouless-Halperin-Nelson-Young (KTHNY) universality class.

3.9 GÖTTINGEN CAMPUS INSTITUTE FOR DYNAMICS OF BIOLOGICAL NETWORKS

Prof. Dr. Fred Wolf studied physics and neuroscience at the University of Frankfurt, where he received his doctorate in theoretical physics in 1999. After postdoctoral research at the Interdisciplinary Center for Neural Computation of the Hebrew University of Jerusalem (Israel), he became a research associate at the MPI für Strömungsforschung in 2001 and in 2004 head of the research group Theoretical Neurophysics at the MPI-DS. He is a founding member and since 2013 the Chairperson of the Bernstein Center for Computational Neuroscience in Göttingen as well as faculty of several Physics and Neuroscience PhD programs at the University of Göttingen. From 2011 to 2015 he served as Section Coordinator for Computational Neuroscience of the German Neuroscience Society and from 2014-2018 on the review committee for research grants of the Human Frontier Science Program. Fred Wolf is a Fellow of the American Physical Society and received the Mathematical Neuroscience Prize 2017. Since 2021 he is the founding Director of the Göttingen Campus Institute for Dynamics of Biological Networks and Spokesperson of the German Research Foundation priority program *Evolutionary Optimization of Neuronal Processing*.

Biological networks perform their functions as complex dynamical systems. Be it ecosystems, networks of neurons, or the paths of information and matter inside cells, their intricate design emerges through the interplay of systems-level self-organization and long-term evolutionary remodeling. The active dynamics of biological networks and the unique sense of efficiency and beauty it elicits make these systems profoundly fascinating and scientifically challenging. It is the mission of the Göttingen Campus Institute for Dynamics of Biological Networks to advance theory-driven research into the dynamics of biological networks, pioneer novel research strategies integrating computational, mathematical and experimental approaches, and establish them through transdisciplinary research projects on the Göttingen Campus and beyond.

The Göttingen Campus Institute for Dynamics of Biological Networks (CIDBN) was established by the Max Planck Institute for Dynamics and Self-Organization and Göttingen University. The CIDBN has three departments spanning physics and biology and two central research platforms: a life science HPC unit and the Laboratory Neurophysics. To foster frontier research by young investigators, the CIDBN is designed to host young investigator groups. Currently, the Max Planck Research Group of David Zwicker and the DFG-funded Research Group of Thomas Frank are associated with the CIDBN. CIDBN research contributes to three Göttingen CRCs, the Cluster of Excellence Multiscale Bioimaging and the new cognitive science research center HuCaB. Nationally, the CIDBN is the coordination site of the DFG priority program Evolutionary Optimization of Neuronal Processing. Internationally, it is the German theory hub of the transnational research network on the evolution of the primate brain, NeuroNex, funded jointly by the National Science Foundation (USA), the Canadian Institutes of Health Research and the DFG.

The frontier between complex system dynamics and evolution is a major focus of projects at the CIDBN. Emergent phenomena and system dynamics play an important role in biological evolution, in particular for complex biological networks such as those in brains and embryonic tissues. Here our research topics range from the origins of collective computation in brain evolution, to the evolutionary optimization of the biophysics of information processing and flow, and to the emergence of compartmentalization through phase separation in eukaryotic cells.

In the past several years, we successfully expanded our research agenda beyond the dynamics of neuronal systems and uncovered intriguing connections between nervous system function and collective dynamics in developmental biology. In neurons and other cells, cell contacts are not only mechanical linkages but typically function as communication hubs. Previously primarily known from neurosensory systems underlying the perception of sound, touch and pain, we discovered force-gated ion channels in embryonic epithelia. Recently,

we became the first to demonstrate that epithelial cells use mechanosensing by force-gated ion channels to synchronize their mechanical activity in morphogenesis and orchestrate complex spatio-temporal patterns. We introduced data-driven model inference to precisely quantify the impact of channel-mediated coordination and predict large-scale consequences of local coordination. Related theoretical work led to the discovery of a novel inference phase transition in the dynamics of living systems.

In the collective dynamics of biological neural networks, we achieved major advancements ranging from the underlying biophysical dynamics of neurons and synapses to emergent phenomena. In the chaotic dynamics of neural circuits, we discovered that collective brain rhythms can boost the intensity of spiking circuit chaos and gave a comprehensive analytical characterization of the direct transition to high-dimensional extensive chaos in recurrent neural networks. We developed an analytical decomposition of dynamic gain analysis that directly links specific subcellular dynamics to information encoding in mesoscopic neuronal populations. These and related advances enabled us to directly link molecular mechanisms underlying Alzheimer disease states to cellular dynamics and network states that can serve as early warning indicators of disease progression.

Following our mission to advance paradigms integrating mathematical theory and experiment in the study of collective dynamics in biological networks, CIDBN succeeded to establish new research networks internationally and on campus. On the Göttingen Campus, CIDBN contributed as a founding member to the establishment of two large collaborative research centers dedicated to the development of optogenetic interfaces and optogenetic therapies, respectively. Among other contributions, we succeeded in recreating in vivo-like collective states in in vitro living neural networks. With funding from the Human Frontier Science Program, the German Research Foundation and DAAD, CIDBN established novel international collaborations with research centers in Bergen (Norway), Natal (Brazil), Melbourne (Australia), and the primate research facility in the Kirindy forest (Madagascar). These new international collaborations expand the scope of our research into neural circuit evolution, enabling unique studies ranging from the origin of the first neurons and synapses to the evolution of the primate brain.

Dr. Andreas Neef obtained his Diploma in physics in 2000 from the University of Jena, Germany. After work at the MRC Laboratory of Molecular Biology, Cambridge (UK), he joined the Research Centre Jülich, Germany, where he received his doctorate in 2004 (Cologne University). After postdoctoral research he became a Bernstein Fellow at the MPI for Dynamics and Self-Organization in 2006. From 2013 to 2019 he headed the research group Biophysics of Neuronal Computation at the BCCN Göttingen. In 2019 he became Head of the Laboratory Neurophysics at the Göttingen Campus Institute for Dynamics of Biological Networks.

Dr. Matthias Häring studied physics and mathematics at the TU Braunschweig and the University of Göttingen. After work at the MPI for Biophysical Chemistry, he joined the the MPI for Dynamics and Self-Organization for PhD-research from 2017-2021 on tissue morphogenesis. In 2023, after a first Postdoc he became Group Leader Developmental Dynamics at the Göttingen Campus Institute for Dynamics of Biological Networks with research focus on data analysis, stochastic dynamics and non-equilibrium statistical physics.

Prof. Dr. Kerstin Schmidt is Adjunct Professor at CIDBN and Director of the Brain Institute (ICe) at the Federal University of Rio Grande do Norte (Natal, Brazil). She did doctoral work at the MPI for Brain Research in Frankfurt, Germany. She is a recipient of the Otto Hahn Medal of the Max Planck Society, performed postdoctoral work at the Karolinska Institute (Stockholm, Sweden) and was Leader of a Max Planck Research Group from 2005 to 2010. In 2011, she moved to Brazil to become the founding director of the Instituto do Cérebro (Brain Institute, ICe). In collaboration with F. Wolf she pioneered research into neural circuit evolution in the largest rodents studied to date.

Prof. Dr. Jörg Großhans is Adjunct Professor at CIDBN and Head of the Research Group Developmental Genetics at the Department of Biology at the University of Marburg, Germany. He obtained his PhD in developmental genetics working with Nobel Laureate Christiane Nüsslein-Volhard at the Max Planck Institute for Biology (Tübingen, Germany). After research periods at the Universities of Princeton, Heidelberg and Göttingen, he moved to Philipps University Marburg. With F. Wolf he co-directs several research projects into developmental dynamics.

Dr. Bernhard Bandow obtained his diploma in physics at the TU Berlin working on MD simulations of systems with confined geometry. In 2007 he received his PhD in physical chemistry from Kiel University. After postdoctoral research, he joined the Computing Center and the North German Supercomputing Alliance (HLRN). From 2011 to 2019 he worked at the computing center of the MPI for Solar System Research in Göttingen and in 2019 joined the Göttingen Campus Institute for Dynamics of Biological Networks as HPC Coordinator.

Dr. Yvonne Reimann studied biology at the University of Göttingen and obtained her PhD with work at the MPI for Biophysical Chemistry in Göttingen. After postdoctoral research in the Department Molecular Cell Biology at the MPI for Biophysical Chemistry, she studied science management at the German University of Administrative Sciences (Speyer) from 2009 to 2010 and subsequently became scientific coordinator at the Leibniz Research Laboratories of Hannover Medical School and the Research Department of Göttingen University. Since 2012, she is Research Manager of the BCCN Göttingen and since 2018 of the Göttingen Campus Institute for Dynamics of Biological Networks.

ASSOCIATED RESEARCH GROUPS 4

Contents

4.1 MAX PLANCK FELLOW GROUP: DATA-DRIVEN MODELING OF NATURAL DYNAMICS

Prof. Dr. Alexander Ecker is trained as a computer scientist and did his PhD in systems and computational neuroscience at the University of Tübingen and Baylor College of Medicine in Houston, TX (USA). He received his PhD from the University of Tübingen in 2014. After a postdoc and group leader phase at the University of Tübingen and the Max Planck Institute for Biological Cybernetics (Tübingen, Germany), he was appointed as full professor of data science at the Institute of Computer Science and the Campus Institute Data Science at the University of Göttingen in 2019. Since May 2021, he has been a fellow of the Max Planck Society. In 2022 he received a Starting Grant from the European Research Council. Since 2025 he has been the dean of the Faculty of Mathematics and Computer Science at the University of Göttingen.

The mission of the Max Planck Fellow group "Data-Driven Modeling of Natural Dynamics" is to expand machine learning in order to empower the modeling, optimization and control of complex dynamical systems in physics and biology. Machine learning (ML) has triggered a revolution in computer vision and natural language processing a decade ago, and is now being used to solve a wide range of problems previously considered exceedingly hard or even impossible. ML techniques are currently transforming the process of scientific discovery across many scientific fields, including the quantitative natural sciences. The goal of our group is to contribute at the forefront of this transformation by establishing new machine learning approaches tailored to address some of the most challenging problems in complex system research: the dynamics of clouds and atmospheric turbulence, the modeling and control of the dynamics of the heart and understanding the design and dynamics of deep neural networks in the brain.

4.1.1 Modeling of cloud microphysics

Many microphysical processes in weather and climate, like turbulence-driven droplet collisions and radiative transfer in clouds, are not well resolved due to limited observational capabilities. A popular method for obtaining 3D measurements of particle distributions from single images is *in-line holography*, but the analysis of holograms is computationally intensive. Achieving real-time hologram reconstruction could transform applications in climate research, air quality monitoring, and environmental management.

We work in close collaboration with Eberhard Bodenschatz's Department of Fluid Physics, Pattern Formation, and Biocomplexity (DFPB) and, within that department, with Gholamhossein Bagheri's group to study and model atmospheric turbulence. Our focus over the last few years has been on developing fast and accurate 3D particle reconstruction from holographic in situ measurements in clouds. For example, during the measurement campaign EUREC4A in the trade wind region of the Atlantic, 800,000 holograms of cloud particles were taken, which have until this day not been fully analyzed due to the high computational demands on hologram reconstruction with current standard software. We are therefore developing machine learning based approaches to hologram reconstruction. These appraoches will not only speed up hologram reconstruction massively but could also enable small, low-cost holographic measurement devices with real-time 3D reconstruction capabilities.

4.1.2 Tailor-designed models for the turbulent velocity gradient through Normalizing Flow

In collaboration with the former Max Planck Research Group Turbulence, Complex Flows & Active Matter (Michael Wilczek; now Univer-

sity of Bayreuth, Germany), we have been working on the fundamental physics problem of modeling small-scale turbulence through the dynamics of the velocity gradient. Traditional models face challenges due to the nonlocal and chaotic nature of turbulence. To overcome these, we developed a novel, data-driven machine learning approach that leverages normalizing flows to learn the probability density function (PDF) of the velocity gradient from direct numerical simulation of incompressible turbulence. By using the equation for the single-time PDF of the velocity gradient, we constructed a dynamical system that features the learned steady-state PDF by design. The resulting model is deterministic, exhibits chaotic dynamics and accurately reproduces hallmark features of turbulence (Fig. 4.1). Taken together, this work contributes a new approach to modeling complex natural dynamics using machine learning.

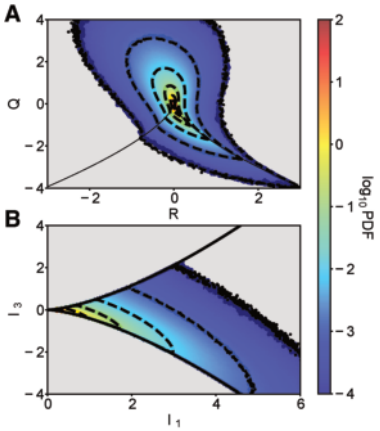

Figure 4.1: Single-time velocity gradient distributions from the direct numerical simulation (color) and from our Normalizing Flow model (black dashed lines). **A**, Joint PDF of principal invariants of the velocity gradient. **B**, Joint PDF of the strain invariants.

4.1.3 *ML-based heart simulation to support therapy with engineered heart muscle patches*

Heart attacks are among the leading causes of death in industrialized countries. They damage the heart muscle, lead to scarring, and ultimately result in heart failure. A promising treatment approach is the implantation of so-called engineered heart muscle (EHM) patches, which are composed of heart muscle cells and connective tissue cells and are surgically applied to scar tissue (Fig. 4.2). Wolfram Zimmermann's team at the University Medical Center Göttingen (UMG) recently demonstrated that this method can remuscularize the heart.

While EHMs can be optimized using tissue fusion and 3D printing methods, there are currently no algorithms capable of predicting the optimal position, size or thickness of an EHM patch for each patient. In collaboration with the DFPB (Ina Braun, Yong Wang, Eberhard Bodenschatz) and Wolfram Zimmermann's team at UMG we are currently developing a machine learning based method to design optimal patient-specific EHM patches based on routine procedures already established in clinical practice, such as cardiac computed tomography (cCT). Our goals include developing an ML-based, efficient, personalized simulation of the left ventricle, including scar tissue and EHM patches, using it to optimize patient-specific parameters and testing our methods in patients as part of a clinical trials planned for 2027.

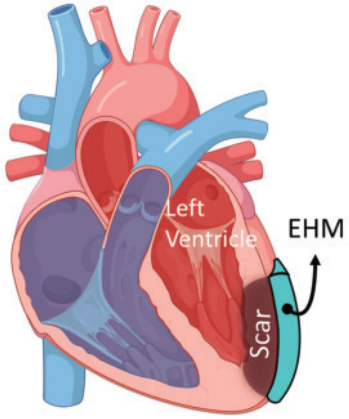

Figure 4.2: Schematic illustration of an infarcted heart with a scarred left ventricle and EHM patch over it.

4.2 MAX PLANCK FELLOW GROUP: MULTIFUNCTIONAL LIPID MEMBRANES ON SURFACES

Prof. Dr. Claudia Steinem born in 1967, got trained in Biology and Chemistry at the Westfälische Wilhelms-Universität Münster and received her PhD in 1997 in the group of Prof. Dr. Hans-Joachim Galla. After a post-doctoral stay at the Scripps Research Institute in La Jolla, CA (USA) in the group of Prof. M. Reza Ghadiri, she returned to the Institute of Biochemisty at the University of Münster as a Lise-Meitner fellow in 1999. Two years later, in 2001, she got a professorship for Bioanalytical Chemistry at the University of Regensburg and finished her habilitation. In 2005, she received an offer from the University of Göttingen for a professorship of Biomolecular Chemistry. Since 2006, she is full professor at the Institute of Organic and Biomolecular Chemistry and was a fellow of the Max Planck Society between 2017 and 2023.

For many years the chemical complexity as well as the dynamics and function of biological membranes have fascinated scientists. My group aims at generating robust and stable planar multifunctional membranes in a bottom-up approach that mimic the natural situation as closely as possible to address pressing biochemical questions and to design chip-based assays.

More than 40 years ago, biological membranes were described for the first time as a fluid mosaic based on thermodynamic principles of organization of membrane lipids and proteins and available evidence of asymmetry and lateral mobility within the membrane matrix. Over the intervening years, there is mounting evidence that the chemical and spatial complexity of biological membranes is key to understand their dynamics and functions on various length scales. It is the heterogeneity of cellular membranes that can lead to specialized functional membrane domains, enriched in certain lipids and proteins, and the interaction between lipids and proteins that limits the lateral diffusion and range of motion of membrane components thus altering their function. To be able to understand the complex interplay within a membrane on a molecular level, my research group pursues a bottom-up approach. By developing and applying model membrane systems, we aim to understand membrane-confined processes such as fusion and fission, transport processes mediated by ion channels and protein pumps as well as protein-lipid and protein-protein interactions occurring at the membrane interface. On the one hand, we use planar supported lipid bilayers (PSLBs) and vesicles, such as giant unilamellar vesicles (GUVs). On the other hand, we have developed functional lipid bilayers on highly ordered pore arrays. These so-called pore-spanning membranes (PSMs) suspend nanometer- to micrometer-sized pores in an aluminum or silicon substrate (Figure 4.2). They separate two aqueous compartments and can hence be envisioned as an intermediate between supported and freestanding membranes.

PSLBs and GUVs: Protein-membrane and protein-protein interactions

Several proteins use specific lipid receptors to attach to the plasma membrane. We are interested in the molecular interaction between these membrane-confined receptors and proteins and how this interaction influences the overall membrane structure. In this context, we focus on phosphatidylinositol phosphate binding proteins such as ezrin and the focal adhesion kinase harboring a FERM-domain as well as collybistin binding via a PH-domain. Another major target are glycosphingolipids such as Gb_3, which serve as specific receptors for bacterial toxins such as Shiga toxin.

Ezrin links the plasma membrane to the cytoskeleton in its active state. It gets activated by binding to PtdIns(4,5)P_2 in the plasma membrane and phosphorylation of a threonine. We investigated the mode of ezrin binding and its activation by using PSLBs in combination with

surface sensitive techniques such as reflectometric interference spectroscopy, and fluorescence and atomic force microscopy. We further analyzed the coupling of actin and actomyosin networks via ezrin to these membranes thus generating a minimal actin cortex. With such a system in hand, we are able to address the question how the ezrin-PtdIns(4,5)P_2 interaction influences the architecture of actin and actomyosin networks and how this impacts the dynamics, and mechanical properties of the composite system.

Collybistin is an adaptor protein that is involved, together with the scaffold protein gephyrin, in the recruitment of $GABA_A$ receptors to the postsynaptic density of inhibitory synapses. Our in vitro studies showed that full-length collybistin gets activated via an interaction with the C-terminal part of neuroligin-2 being prerequisite for binding of the PH-domain of collybistin to different phosphatidylinositol phosphates. To completely assemble the structures found at the postsynaptic membranes of inhibitory synapses, the question needs to be addressed how gephyrin, collybistin and neuroligin-2 act in concert, a process that can be further illuminated by using PSLBs in combination with reflectometric interference spectroscopy and high-resolution microscopy techniques.

In collaboration with the group of Prof. Dr. Daniel B. Werz (University of Freiburg), we investigate the influence of the fatty acid of the globoside Gb_3 on the partitioning in liquid-ordered/liquid disordered coexisting membranes, which is key to understand the primary step of Shiga toxin internalization. Shiga toxin, produced by *Shigella dysenteriae* and Shiga toxin producing *E. coli* strains gets internalized into the cell after binding of the B-subunits to Gb_3 embedded in the plasma membrane of the host. We have shown that the molecular structure of Gb_3 greatly influences its membrane partition, as well as membrane (re)organization after toxin binding.

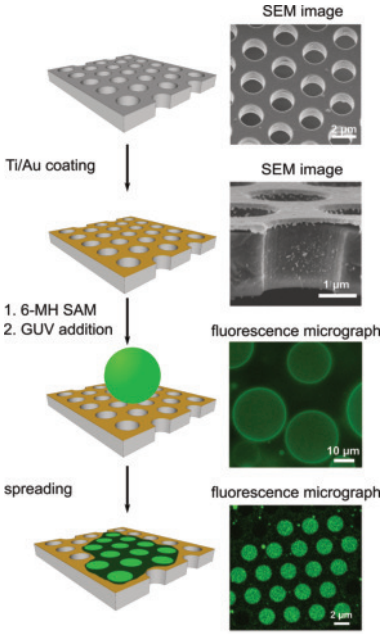

Figure 4.3: Individual steps to prepare pore-spanning membranes (PSMs) on a Si/Si_3N_4 substrate by spreading a giant unilamellar vesicle (GUV) on a 6-mercaptohexanol (6-MH) self-assembled monolayer (SAM).

PSMs: Membrane fusion and transport proteins

Membrane fusion processes, mediated by SNAREs, are a hallmark of eukaryotic life. We are especially interested in membrane fusion during neuronal exocytosis. A number of *in vitro* fusion assays with these proteins reconstituted in artificial membranes have been established in recent years. However, it has still been proven difficult to monitor intermediate states of the fusion process in a system that captures the essential features of the *in vivo* system. We develop and apply a reconstituted membrane system based on PSMs. PSMs are long-term stable and can be formed on open pore arrays as well as on cavities. These setups allow for a quantitative analysis of the different stages during fusion of a single vesicle, such as docking, intermediate states and full fusion by means of fluorescence microscopy in a time-resolved manner (Figure 4.4).

As PSMs are produced from spreading GUVs, they should also enable us to reconstitute ion channels and protein pumps with an appropriately high protein density. This is particularly important for ion channels and protein pumps that do not transport sufficient ions to

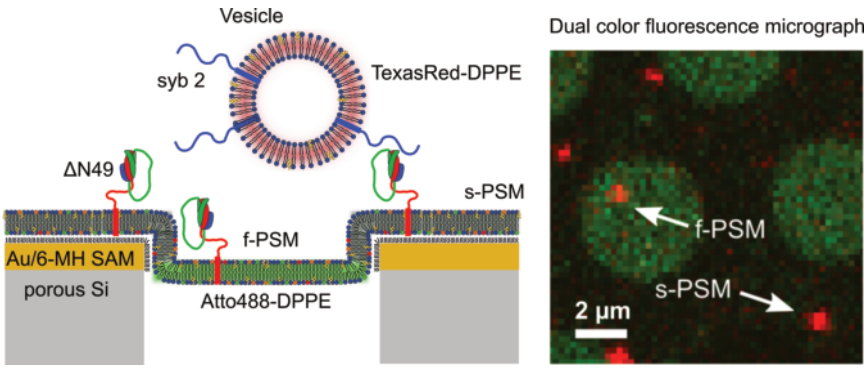

Figure 4.4: Setup to measure single vesicle fusion events (left) by means of fluorescence microscopy with high time resolution in freestanding PSMs (f-PSMs) and supported PSMs (s-PSMs) (right). The image is taken from Kuhlmann, Junius, Diederichsen, Steinem. *Biophys. J.* **112**, 2348-2356 (2017).

be detected by electrophysiological recordings on single freestanding membranes. However, classical methods to produce GUVs such as electroformation and gentle hydration do not allow for a reproducible reconstitution of transmembrane proteins in GUVs with high protein content. Thus, we search for and establish alternative methods to generate GUVs based on droplets produced in microfluidic devices. Recently, we have shown that these GUVs produced from droplet-stabilized GUVs can also be spread on porous substrates to generate PSMs. With respect to proteins, we currently focus our attention on the F_0F_1 ATP-synthase that is capable of producing ATP by using a proton gradient and which can be reversed as well as connexons that can even connect two membranes by the formation of gap junctions.

Figure 4.5: The Steinem lab during a hike.

4.3 EXTERNAL SCIENTIFIC MEMBER: BIOMEDICAL NMR

Our research is devoted to the further development and application of magnetic resonance imaging (MRI) techniques for structural and dynamic studies of biological and complex systems. Current projects focus on advanced methods that monitor human body movements and physiological functions in real time and allow for quantitative mapping of tissue parameters using model-based reconstructions. A primary aim of our Emeritus group is the translation of real-time MRI technology for scientific and medical applications. It will end 31 December 2025.

Methodological Aspects

Our breakthrough toward real-time MRI is based on spatial encoding strategies using radial trajectories, pronounced data undersampling by factors of 20 to 40, and definition of serial image reconstruction as iterative solution to a nonlinear inverse problem with temporal (or spatial) regularization. In practical terms, real-time MRI allows for recordings of the functional anatomy with image acquisition times as short as 10 to 50 milliseconds – corresponding to MRI videos at 20 to 100 frames per second.

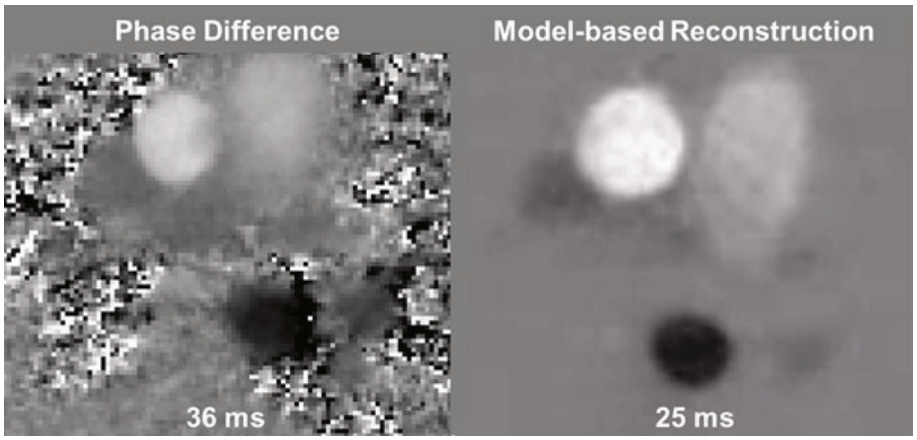

Figure 4.6: Quantitative assessment of aortic blood flow using real-time phase-contrast flow MRI. (Left) Conventional phase-difference calculation of the velocity map (28 frames per second) in comparison to (right) a model-based reconstruction with almost noiseless floor and improved spatiotemporal resolution (40 frames per second). The selected frames refer to maximum blood flow in the ascending aorta (bright circle) and descending aorta (dark circle, opposite direction). The strength of the phase signal directly corresponds to flow velocity.

Model-based reconstruction techniques are an extension of the basic reconstruction problem posed by undersampled multi-coil MRI data. It supports quantitative mapping of physical or physiological parameters by directly estimating the parameters of a known signal model from a suitable set of raw data. Thus, instead of computing a set of images which are then used for a pixel-wise fitting of the signal model, the parametric maps are obtained directly without intermediate image reconstruction. The procedure exploits redundancy in the raw data and – depending on the application – leads to much improved maps such as almost noiseless velocity maps in phase-contrast flow MRI.
In all cases, the computational demand is met by parallelization of

Prof. Dr. Jens Frahm is Director of Biomedical NMR at the Max Planck Institute for Multidisciplinary Sciences in Göttingen, Germany. He studied physics at the Georg-August-Universität in Göttingen where he received a PhD in physical chemistry in 1977. In 1982 he founded a Biomedical NMR group at the Max-Planck-Institute for Biophysical Chemistry which until 2019 operated as a non-profit research company fully financed by its MRI patents. Frahm is a recipient of the European Magnetic Resonance Award (1989), the Gold Medal of the International Society for Magnetic Resonance in Medicine (1991), the Karl Heinz Beckurts-Award (1993), the State Award of Lower Saxony for Science (1996), the Research Award of the Sobek Foundation for Multiple Sclerosis (2005), the Science Award of the Foundation for German Science (2013), the Jacob-Henle Medal (2017), the European Inventor Award (2018) and the Werner von Siemens Ring (2020). He is a member of the Academy of Science at Göttingen (2005) and the German Academy of Technical Sciences (2020) and was elected to the Hall of Fame of German Research (2016).

the corresponding algorithm and its implementation on a computer equipped with multiple graphical processing units. This computer can be fully integrated into a commercial MRI system (by a Gigabit network connection) where it serves as a by-pass system invisible to the radiological user.

Current Work

Real-time MRI applications address a broad range of hitherto impossible scientific and clinical questions. Collaborative studies focus on phonetic aspects of articulation (speech production, stuttering), brass playing (pedagogy, dystonia), swallowing dynamics (dysphagia, gastroesophageal reflux disorder), cardiac function without the need for synchronization to the electrocardiogram and during free breathing, quantitative assessments of blood flow and cerebrospinal fluid dynamics, and quantitative mapping of T1 relaxation times (brain, prostate).

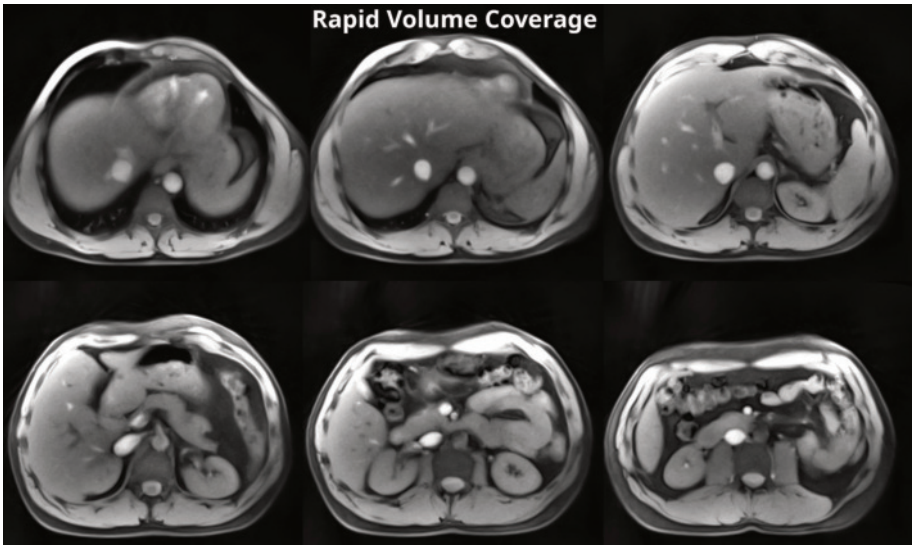

Figure 4.7: (Top left to bottom right) Selected fat-suppressed T1-weighted images (every 20th) of a 6 s real-time MRI dataset covering the entire liver (180 mm volume) of a healthy subject (free breathing) by serial cross-sectional imaging (i.e., 120 frames) at 50 ms resolution (i.e., acquisition time per frame).

Ongoing work deals with extensions of the basic concept underlying dynamic real-time MRI. In particular, we developed a new approach for motion-robust scanning of large volumes (whole organs) in only a few seconds. The method relies on the fact that the similarity of successive frames within a real-time image series holds true not only in time but also in space. In other words, temporal regularization of the nonlinear inverse problem is replaced by spatial regularization provided serial images represent neighboring cross-sections with sufficient overlap. In practice, similarity is ensured by cross-sectional real-time acquisitions that automatically advance the position of each frame by a fraction of the section thickness. Most importantly, acquisition times of tens of milliseconds per frame render individual sections robust against patient or organ movements. The method therefore proves especially valuable for pediatric radiology as it avoids the need for sedation or anesthesia.

4.4 EXTERNAL SCIENTIFIC MEMBER: PHYSICS OF FLUIDS

Scientific profile and characteristics of work

Lohse's Physics of Fluids (PoF) group presently works on a variety of aspects in the fundamentals of fluid mechanics. The subjects include turbulence and multiphase flow and micro- and nanofluidics. Both experimental, theoretical, and numerical methods are used. He closely collaborates with several companies, among them Canon and ASML. Further information, including an updated list of publications, is available at [1].

The main characteristics of Lohse's work is the direct interaction of experiment, theory, and numerics, all done in the PoF group. He is not method-driven, but problem-driven, and often had to acquire the required methods or knowledge from some neighboring fields to solve some particular research questions he had been obsessed with. This led to various fruitful interactions and collaborations with neighboring disciplines, such as engineering, mathematics, chemistry, acoustics, medicine, biology, or even computer science. As will be seen from the list below, various of his subjects have an "application perspective". Lohse and his coworkers also understand to visually present the scientific questions they are addressing and their results. This led to ten winning video entries to the Gallery of Fluid Motion from the American Physical Society, Division of Fluid Dynamics, and various television reports and newspaper articles on their work. It also makes Lohse's science very visual for laymen, with a positive effect on the outreach of science in general.

Prof. Dr. Dr. h.c. Detlef Lohse studied physics at the Universities of Kiel & Bonn (Germany), and got his PhD at Univ. of Marburg (1992). He then joined Univ. of Chicago as postdoc. After his habilitation (Marburg, 1997), in 1998 he became Chair at Univ. of Twente in the Netherlands and built up the Physics of Fluids group. Lohse is Associate Editor of J. Fluid Mech. (among others journals) and serves as Chair of the Executive Board of the Division of Fluid Dynamics of the American Physical Society and Member of the Executive Board of IUTAM. He is Member of the (American) National Academy of Engineering (2017), of the Dutch Academy of Sciences (KNAW, 2005), the German Academy of Sciences (Leopoldina, 2002) and Fellow of APS (2002). He won various scientific prizes, among which the Spinoza Prize (NWO, 2005), the Simon Stevin Meester Prize (STW, 2009), the Physica Prize of the Dutch Physics Society (2011), the AkzoNobel Science Award (2012), three European Research Council Advanced Grants (2010, 2017 & 2023), the George K. Batchelor Prize (IUTAM, 2012), the APS Fluid Dynamics Prize (2017), the Balzan Prize (2018), and the Max Planck Medal (2019). He also set up the Max-Planck Center Twente (2016, on Complex Fluid Dynamics).

Overview on present main research subjects

Turbulence

Rayleigh-Bénard (RB) flow, the flow in a box heated from below and cooled from above, and Taylor-Couette (TC) flow, the flow between two coaxial, independently rotating cylinders, are the two paradigmatic systems of physics of fluids. They are the drosophilas of the field and various new concepts in fluid dynamics have been tested with these systems. In the last few years, in joint work between Göttingen and Twente, we have succeeded to elucidate the nature of the transition between so-called classical turbulence and so-called ultimate turbulence, where the latter one has strongly enhanced transport properties. We could in particular show that the transition is in total analogy to the laminar-to-turbulence transition in boundary layers along a plate, see Fig. 4.8. In particular, it is of non-normal-nonlinear nature, i.e., subcritical, hysteretic, and with noise playing a prominent role ("double threshold behavior"). This view could unify various experimental results obtained over the last three decades, thus resolving one of the major controversies in turbulence. The results have been summarized in [2]. We also perform highly parallelized (10^5 cores) direct numerical simulations (DNS) on sheared RB flow, on double diffusion convection,

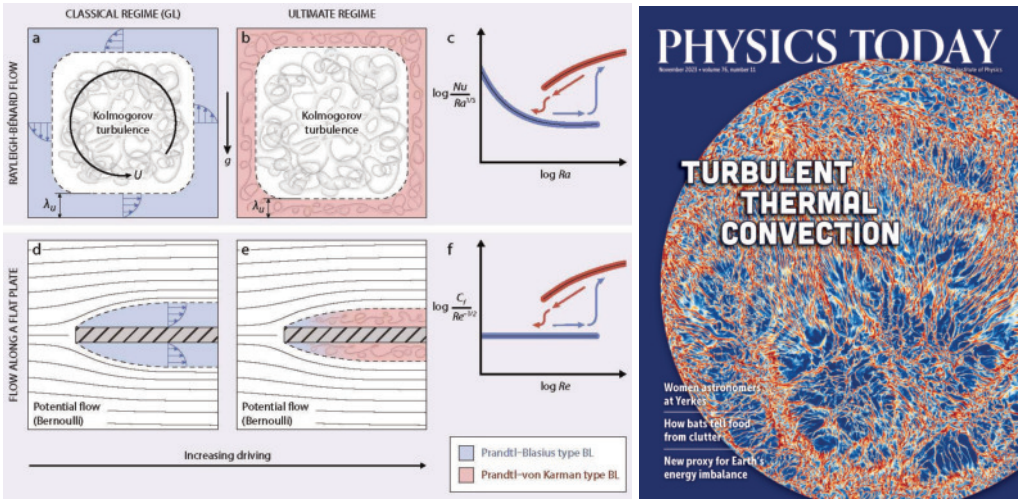

Figure 4.8: (I) The analogy between Rayleigh-Bénard flow and parallel flow along a flat plate. (a-c) In turbulent Rayleigh-Bénard convection, the core part of the flow is always turbulent (Kolmogorov turbulence), whereas the flow velocity along the wall drops to zero, as illustrated by the decreasing magnitude of blue arrows on each side in panel (a). With increasing thermal driving strength – in other words, increasing Rayleigh number Ra – the boundary layers (BLs) change from a laminar (blue) Prandtl-Blasius type BL, with velocity profiles sketched in blue, to a turbulent (red) Prandtl-von Kármán type BL. The different cases have distinct dependencies of the heat transport (expressed by the Nusselt number Nu) on Ra, as shown, respectively, by the blue and red lines in panel c. (d-f) Parallel flow along a flat plate undergoes an analogous transition between laminar and turbulent BLs, each with different dependencies of the skin-friction coefficient C_f on the Reynolds number Re, as sketched, respectively, with blue and red lines in panel (f). Figure taken from [3]. (II) Snapshot of a numerical simulation of Rayleigh-Bénard flow (done by Richard Stevens, Twente) at a Rayleigh number of $Ra = 1 \cdot 10^{13}$, a Prandtl number of $Pr = 1$, and an aspect ratio of $\Gamma = 1/2$. This image was used as Cover of our Phys. Today article [3].

and on vertical convection, focus on scaling relations for the transport quantities and on flow transitions.

Melting of ice

The insight on buoyancy driven flows (both through temperature and salinity gradients) we obtained over the last years has found direct application in our understanding of melting ice. We set up a major program (financed by an ERC-Advanced Grant) on "Melting and dissolution across scales in multicomponent systems", which has a strong bearing on climate and on the energy transition. Indeed, melting of ice induces temperature and concentration gradients in the surrounding

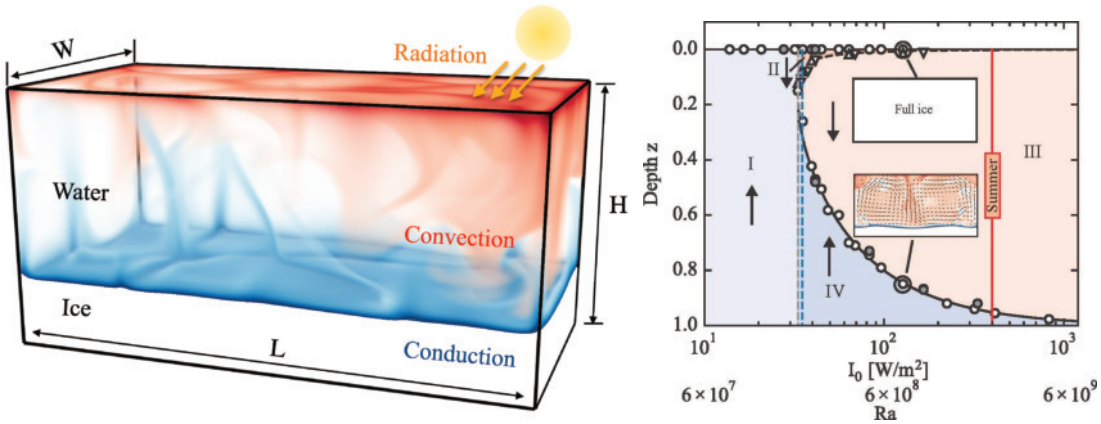

Figure 4.9: (a) Snapshot of the temperature field of our simplified simulation setup at the final stable equilibrium stages with melt pond formation. (b) Bifurcation diagram in the sun-intensity I_0 vs melt pond depth z phase space, obtained from our direct numerical simulations of melt ponds (data points) and from our theory (solid curves), with the fully frozen state (upper curve) and the melt pond state (lower curve). In between is an unstable equilibrium. Figures taken from [4].

water. These gradients induce buoyancy driven flows which locally enhance or delay the melting process and thus determine the objects shape. On large scales, a relevant example for the climate are glaciers and icebergs melting into the ocean, where cold and fresh meltwater experiences buoyant forces against the surrounding ocean water, leading to flow instabilities, thus shaping the ice and determining its melting rate. A conceptually related example is the dissolution of liquid CO_2 in brine for CO_2 sequestration. To make progress in our understanding of such processes, we have performed a number of key controlled experiments and numerical simulations for idealized setups on various length scales, inspired by above sketched problems, but allowing for a one-to-one comparison between experiments and numerics/theory. One example – the formation of a melt pond – is given in Fig. 4.9, another example – a melting ice block – in Fig. 4.10.

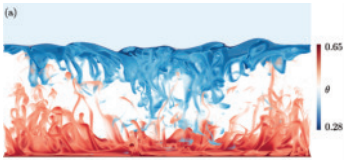

Figure 4.10: Snapshot of an ice block (light blue), melting from below in a RB geometry, with the (relative) water temperature visualized in red and in dark blue. The temperature-driven convective processes shape the ice. Figure taken from [5]

Inkjet printing and droplet impact

On this subject the PoF group very closely collaborates with Canon. We developed experimental methods and models to understand droplet formation and impact of various droplets (including non-Newtonian ones and multicomponent ones) on various substrates (including superheated & supercooled ones), focusing on heat exchange, splash formation, droplet spreading, and solidification. A stroboscopic image of the jet formation and droplet pinch-off is shown in Fig. 4.11.

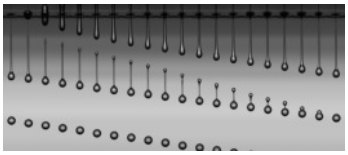

Figure 4.11: Liquid droplet formation in piezoacoustic inkjet printing generation visualized by an ultra-high-speed stroboscopic technique. Figure taken from [6].

Wetting phenomena and droplet evaporation, and the physicochemical hydrodynamics of multicomponent droplets

We work on wetting phenomena on smooth, chemically, or geometrically structured surfaces and in particular on surface nanodroplets and nanodroplets, whose counterintuitive stability we could account for. We try to better understand the nucleation and growth or the dissolution of nanobubbles and nanodroplets, either in another liquid or in a gas (then called condensation/evaporation). We also revealed the rich and often counterintuitive fluid dynamics of the evaporation process of binary, ternary, and colloidal droplets, including the crucial role of the so-called ouzo-effect. We firmly belief that major progress can be achieved at the interface between surface chemistry and fluid dynamics, by combining the methods from these two fields, both on the experimental, numerical, and theoretical side. This also holds for catalysis and electrolysis, where emerging nano- and microbubbles at the surface often cause a major problem, and for the solidification of emulsions and dispersions, which is highly relevant in the context of cryopreservation of biological cells and tissues, food engineering, and swelling of wet ground (frost heaving). An example is shown in Fig. 4.12.

Figure 4.12: Experimental snapshot of an originally spherical, water-emersed silicon droplet which was engulfed by a slowly moving freezing front (0.2 µm/s). This leads to droplet deformation, due to the competition of thermal Marangoni forces and disjoining pressure in the lubrication layer around the droplet. The red curve is from our theory, showing a perfect match with the experiments. Figure taken from [7] and the Cover of that PRL issue.

[1] https://pof.tnw.utwente.nl/
[2] D. Lohse and O. Shishkina, Rev. Mod. Phys. **96**, 035001 (2024)
[3] D. Lohse and O. Shishkina, Phys. Today **76** (11), 26-32 (2023)
[4] R. Yang et al., Phys. Rev. Lett. **131**, 234002 (2023)
[5] R. Yang et al., J. Fluid Mech. **956**, A23 (2023)
[6] D. Lohse, Annu. Rev. Fluid Mech. **54**, 349 (2022)
[7] J. G. Meijer, P. Kant, D. van Buuren, D. Lohse, Phys. Rev. Lett. **130**, 214002 (2023)

4.5 EXTERNAL SCIENTIFIC MEMBER: TURBULENT FLUIDS AND BIOPHYSICS

Prof. Dr. Alain Pumir is Research Director at the french CNRS, working in the Laboratoire de Physique at the Ecole Normale Supérieure de Lyon, France. He studied Physics at the Ecole Normale Supérieure in Paris (1979-1983), and obtained his Doctorate in 1982 under the supervision of Prof. Yves Pomeau, on problems of nonlinear dynamics in spatially extended systems. His postdoc at Cornell University, under the supervision of Prof. Eric Siggia, was devoted to the study of singularity in the fluid equations. He returned to the Ecole Normale Supérieure in Paris as a CNRS Junior Scientist, before joining the Institut Non Linéaire in Nice in 1993. He moved to the Mathematics Department in Nice (2007), and then to the Laboratoire de Physique at Ecole Normale Supérieure de Lyon (2008). He received a Humboldt Award (2013), and became fellow of the American Physical Society and. Chevalier de la Légion d'Honneur in 2014. In 2023, he gave the Lorenz lecture at the American Geophysical Union meeting, and was Gauß Professor in Göttingen.

Our research is devoted to various problems in nonlinear and statistical physics. Hydrodynamic turbulence provides a major source of inspiration, from fundamental questions to specific applications to various domains, in particular to geophysics. We also investigate nonlinear problems to describe the dynamics of biophysical systems. Although theoretical and numerical by nature, our work is largely inspired by experimental situations. In particular, we are working in close collaborations with experimental teams, at the MPI-DS and elsewhere.

Small-scale in turbulent flows

Understanding the fluid motion at very small scales in highly turbulent flows (at very large Reynolds numbers) is one of the main focus of our activity. We are particularly interested in the fundamental questions of the mechanisms of generation of small scales, and in providing a reliable statistical properties of the flow. The study of a dynamics occurring over very small spatial scales, and very short time scales, is intrinsically challenging from an experimental and numerical point of view. This difficulty is tackled in particular by the experimental group at MPI-DS. From a theoretical point of view, the analysis of the Navier-Stokes equations is hindered by the presence of nonlinear and nonlocal effects. An outstanding challenge, from the mathematical point of view, is whether the amplification of velocity gradients, known to occur in a turbulent flow, can lead to the formation of infinite gradients.

Many of our own studies dealing with these questions rest on numerical studies of the Navier-Stokes equations, in a configuration where the flow is homogeneous and isotropic. This setup can be conveniently studied using well-established numerical methods. In our numerical simulations, we insist on very high spatial and temporal resolutions, which allow us to describe accurately the properties of very intense events in turbulent flows, up to Reynolds numbers of order $R_\lambda \sim 1300$. One of the very clear results of our numerical studies is that the strain acting on vortices of size Ω grows statistically as Ω^γ, where γ is an exponent less than 1, that slightly increases with the Reynolds number. Remarkably, this empirical feature is sufficient to allow us to describe qualitatively the main features of the distribution of intense (extreme) events in turbulence.

One quantity we have been particularly interested in is pressure. In fact, in incompressible turbulence, pressure is obtained from a nonlocal expression in terms of the velocity gradient tensor, which is intrinsically difficult to handle analytically. The Hessian (second derivative) tensor of pressure is the relevant quantity to study the evolution of the velocity gradient. Our simulations show the crucial role of pressure in the evolution of the vorticity. The pressure Hessian is essential to understand vortex stretching. Simplified assumptions concerning the pressure Hessian, which have been extensively used to model the dynamics of the velocity gradient tensor, significantly inhibit vortex

stretching. Our studies have suggested improved approximations for the structure of the pressure Hessian, which capture much better the dynamics of the velocity gradients in regions of intense vorticity.

One of the reasons to study homogeneous isotropic flows comes from the postulate that turbulent flows have universal properties at very large Reynolds numbers. This postulate, although widely accepted, has received relatively little verification, beyond the properties of the spectra. In a recent study, we have considered the universality of intense gradients in turbulent flows, by comparing direct numerical simulations of homogeneous isotropic turbulent flows, of turbulent channel flows in the central plane, and experiments conducted at MPI-DS by J. Lawson in a von Karman flow. Our results demonstrate that the straight comparison of the Reynolds numbers between the different flows leads to confusing results. Estimating the level of fluctuations of the velocity gradients (such as the normalized third or fourth moments) provides an effective way to compare the turbulence intensity in different flow configurations, and allows us to demonstrate universality of the intense velocity gradient tensor in turbulence. Current studies will focus more on the structure of turbulent fluctuations in turbulent channel flows.

This work has benefited from collaborations with D. Buaria (now at Texas Tech, Lubbock, USA), H. Xu (Tsinghua University, Beijing, China), and P. Yang (Xi'an, China).

Turbulence and transport in a geophysical context

Stratified turbulence. Atmospheric and oceanographic flows involve not only very large Reynolds numbers (a consequence of the very large planetary scales) but also oftentimes a density stratification. Our interest has focused on stably stratified flows. From a fundamental point of view, the stable stratification may lead to (inertial) waves, which can interfere with turbulent eddies in determining the flow dynamics. This interplay depends on the Reynolds number of the flow, but also on the intensity of stratification. Our study has revealed a transition between a wave-dominated regime (when the stratification is important) towards an eddy-dominated regime (closer to fluid turbulence), induced by a wave instabilities, and leading to strong up- and down-drafts in the fluid. This mechanism strongly affects the transport of tracer particles, and leads to a strong increase of the energy dissipation in the fluid.

Recent work has focused on the relative motion between two or more particles. In particular, we have shown how the manifestations of flow irreversibility, well characterized in homogeneous and isotropic flows (see in particular the PhD thesis of J. Jucha, MPI-DS, 2016) are affected by rotation and stratification. Unexpectedly, we also observe that the dispersion of a group of two particles lead to a strong intermittency, the more so as the level of stratification and rotation increases.

This work, done in collaboration with R. Marino (Ecole Centrale de Lyon, France) led to the PhD thesis of S. Gallon at the Ecole Normale Supérieure de Lyon.

Transport of ice crystals in clouds. In clouds, turbulent fluid transports

small particles, droplets or small ice crystals. Collisions between these particles is an important process leading to the growth of the particles size, and therefore, to precipitation. Over the past few years, we have been particularly interested in the settling of ice crystals in mixed-phase clouds and their collisions. The description of ice crystals settling through a turbulent fluid turns out to require particular attention. Our earlier work has shown the importance of the fluid inertia (beyond the Stokes approximation) in determining the equations of motion of particles.

The subtle physical effects involved in the dynamics of anisotropic particles called for a thorough validation. Thanks to a collaboration with the group of G. Bagheri at MPI-DS, we have carefully tested the equations of motion describing the settling of small spheroids, at least in still air. Comparison between the experiments and solutions of the equations of motion leads to a very close agreement. One of the interesting observations is that the very large ratio $\rho_p/\rho_f \sim 1000$ between the density of the particles, ρ_p, and that of the fluid, ρ_f, for atmospheric particles, is responsible for oscillations as particles reach their equilibrium positions with their broad side down. This sharply contrasts with the case of particles settling in water, where the ratio ρ_p/ρ_f is much smaller, generally less than ~ 10.

With this model, we have conducted systematic study of the collision rates in turbulent suspensions of thin, prolate (disk-shaped) particles. We have also studied riming, i.e. the collision between disk-shaped crystals and water droplets. Current studies are devoted to rod-shaped particles. This work is the result of a collaboration with A. Naso, E. Lévèque (Ecole Centrale de Lyon, France), M. Z. Sheikh (Lahore, Pakistan), K. Gustavsson and B. Mehlig (University of Gothenburg, Sweden).

Other collaborations with MPI-DS

We recently collaborated with the group of A. Gholami on the motion of cargoes driven by the oscillations of axonemes, focusing in particular on the role of Calcium in the driving of the cargo. Future projects include the microphysics of clouds, in the context of the measurements performed by the cloud-kite experiments at MPI-DS.

4.6 MAX PLANCK EMERITUS GROUP RHYTHMS – BEATING CILIA AND TICKING CLOCKS

We investigate the flow of cerebrospinal fluid (CSF) through the four brain ventricles. Bundles of beating cilia that protrude from the ventricular wall drive this flow along the wall (Fig. 4.13) with a rate in the range of 0.5 mm per second. We study the composition of the cargo that the flows transports along the wall. The focus is on extracellular vesicles (EVs, red dots in Fig. 4.13. EVs are membrane-bound nanoparticles with a diameter of 50 – 100 nm and are secreted by the choroid plexus that resides in the ventricles. Mass spectrometry of EVs isolated from the choroid plexus secretome (all proteins secreted by choroid plexus cells into the extracellular space) reveals approximately 1,000 different proteins numerous of which are involved in neurogenesis (DOI: 10.1002/jev2.12276). As illustrated in Fig. 4.13, EVs flow from their site of production, the choroid plexus, towards a neural stem cell (NSC) niche (purple in Fig. 4.13). We posit that EV-borne factors control NSC differentiation.

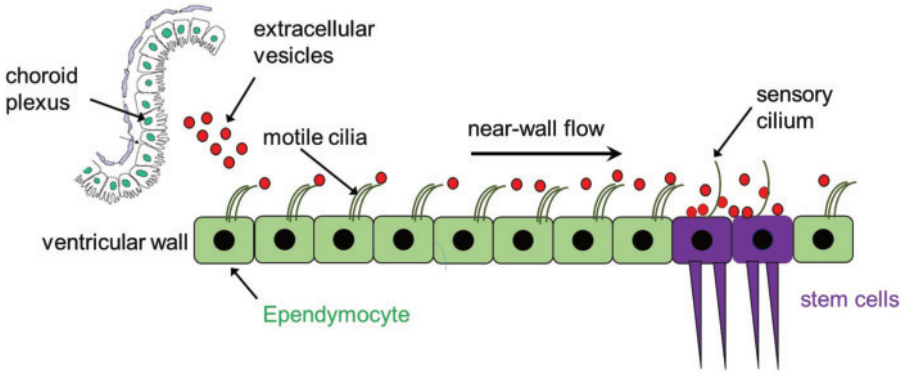

Figure 4.13

In support of this hypothesis, we found that EVs purified from the choroid plexus secretome induce neural stem cells to differentiate (Fig. 4.14). To show this, we placed brain-derived neural stem cells (NSCs) into small chambers. Left by themselves, NSCs form spherical cluster (Fig. 4.14a). However if purified EVs from Z310 cells (Z310 is a choroid plexus cell line) are added to the NSCs, these cells form protrusions and establish a network of cells (Fig. 4.14b) that express marker proteins typical for neurons (Tuj1, purple in Fig. 4.14c) and astrocytes (Gfap, orange in Fig. 4.14d). These experiments suggest that EVs transported by the ventricular flows are targeted to stem cell niches and therein are capable of evoking differentiation of NSCs as would be necessary e.g. in the case of brain injuries. The signaling concept that

Prof. Dr. Gregor Eichele's research publications cover a wide range of subjects including structural biology, developmental biology, functional genomics, human congenital diseases, neurodegeneration, circadian rhythms and most recently molecular mechanisms of transport in the brain ventricles. Eichele studied Chemistry at the University of Basel, Switzerland. After receiving his PhD in Biophysics (1980) he did postdoctoral research in developmental Biology in the laboratory of Bruce Alberts at the University of California in San Francisco. In 1985 he became Assistant and later Associate Professor at Harvard Medical School. In 1991, he joined the Biochemistry department at Baylor College of Medicine in Houston. Eichele held the Alvin Romansky Professorship at Baylor College of Medicine. From 2000 to 2020 Eichele was director first at the MPI for Experimental Endocrinology (Hanover) and starting in 2006, at the MPI for Biophysical Chemistry (now MPI for Multidisciplinary Sciences), Göttingen. Eichele is Adjunct Professor at the Baylor College of Medicine and the University of Göttingen. Since 2021, he is Emeritus Max Planck director and he is affiliated with the MPI for Multidisciplinary Sciences and the MPI for Dynamics and Self-Organization, where Eichele's research group is located.

emerges from our experiments may operate in other ciliated tissues such as the oviduct and the respiratory tract.

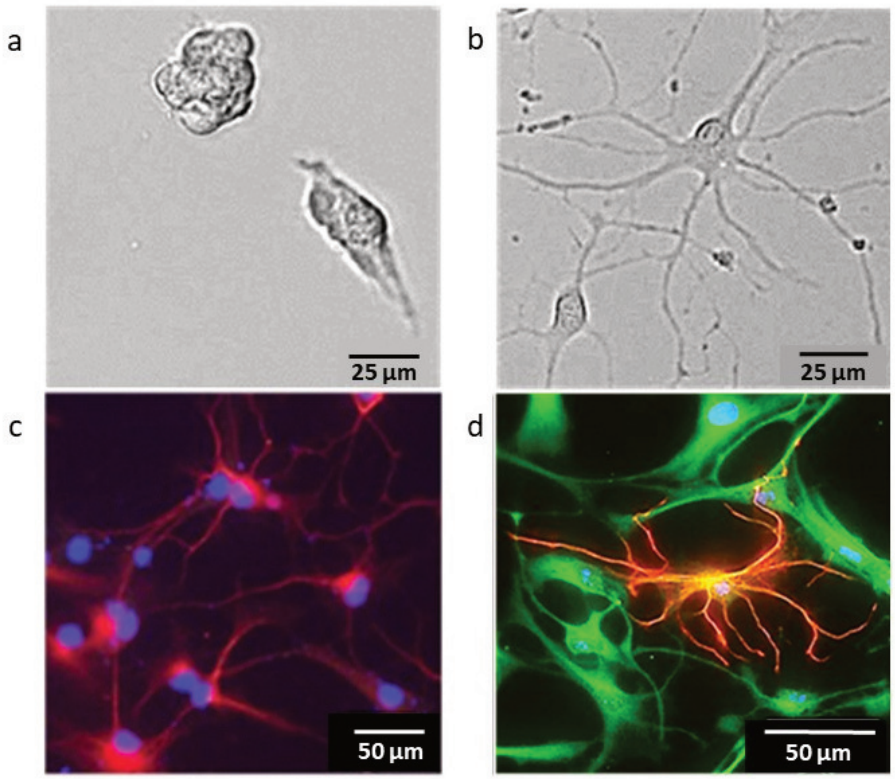

Figure 4.14

4.7 MAX PLANCK EMERITUS GROUP NONLINEAR DYNAMICS

Nature presents us with a multitude of dynamical phenomena, many of which are easy to dissect for a human observer, while others have challenged theoreticians for decades. A formidable example is the complexity of brain function, which is achieved by a plethora of dynamical states in the neural networks of our brains. The field of nonlinear dynamics has established mathematical tools for analyzing and characterizing such nontrivial dynamics in complex systems. By applying and developing such tools, the former Department of Nonlinear Dynamics was engaged in clarifying, e.g., relations between the dynamics and function of neural networks, classical and quantum mechanical transport in nanostructures, and the spatiotemporal dynamics of epidemics - activities which are continued on a smaller scale by the Max Planck Emeritus Group Nonlinear Dynamics.

The Department of Nonlinear Dynamics was founded by the Max Planck Society in 1996 to initiate a scientific reorientation of the former MPI for Flow Research towards modern nonlinear dynamics. The department initiated and hosted the federally (BMBF) funded Bernstein Center for Computational Neuroscience (BCCN) Göttingen, in which it cooperated with experimental neuroscience labs and established a high performance computing facility. The broad scope of topics in its research agenda has often led to cross-fertilization within the department, helping to meet new challenges and leading to new developments such as uncovering human travel statistics by tracking of dollar bills, modeling the spread of epidemics with Levy flight approaches, or discovering random focusing effects of propagating waves, from electrons in 2D-nanostructures to tsunamis in the oceans.

In recent years, the emeritus group has focused on data analytics of musical and psychophysical time-series, as well as cognition experiments designed to uncover the synchronization properties underlying the swing feel in jazz. The following sections summarize two of the projects completed and published in the last three years in collaboration with Corentin Nelias [1], [2]. Besides leading the research of the Emeritus Group Nonlinear Dynamics, Theo Geisel has also been providing community services such as organizing annual French-German Heraeus Seminars for the DPG and scouting for new directors of the MPG.

Prof. Dr. Theo Geisel studied physics at the Universities of Frankfurt and Regensburg, where he received his doctorate in 1975. After postdoctoral research at the MPI for Solid State Research in Stuttgart and Xerox Palo Alto Research Center (PARC), he was appointed Heisenberg Fellow in 1983. He was Professor of Theoretical Physics at the Universities of Würzburg (1988-1989) and Frankfurt (1989-1996), where he headed the DFG collaborative research center (SFB) on Nonlinear Dynamics. From 1996 to 2016 he held a dual appointment as Director at the MPI for Dynamics and Self-Organization and as Full Professor in the Physics Department of the University of Göttingen. A recipient of the Leibniz Prize and other awards, he initiated the Bernstein Center for Computational Neuroscience (BCCN) Göttingen and led it in its first decade. Director Emeritus since October 2016 he is a member of the Academy of Sciences and Humanities Göttingen. His research is driven by the fascination of complex dynamics emerging in nonlinear systems as diverse as neural networks, nanostructures, and the population dynamics of infectious diseases.

Synchronization properties underlying the swing phenomenon in jazz

The swing feel is one of the most salient features of jazz music and is considered an essential ingredient of jazz performances. Yet amazingly, a century after jazz musicians like Armstrong and Ellington came on stage, it is still controversial what is the nature of the swing feel and what are its main musical and psychoacoustical components. Jazz musicians are far from agreeing on what makes up the swing feel, as can be seen in the word cloud (Fig. 4.15) summarizing the answers

Figure 4.15: Word cloud of answers given to the question "What do you think makes a piece of music swing?" shows that among jazz musicians there is no agreement whatsoever.

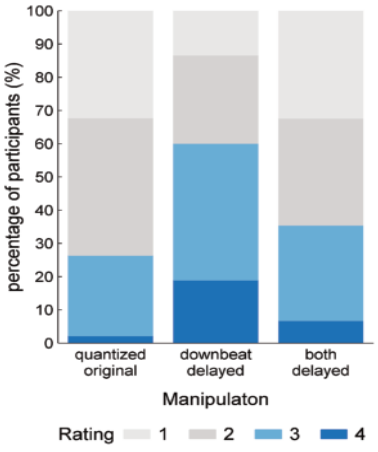

Figure 4.16: Distribution of swing ratings given by jazz musicians to different manipulated versions. Proportions of different ratings from 4 ("very much") to 1 ("not at all") were averaged over three pieces. The *downbeat delayed* manipulation in the center elicits a much larger portion of high ratings (3 and 4 in blue colors) than the quantized original and a version in which both, downbeats and offbeats, are equally delayed.

they gave in a preceding project to our question "What do you think makes a piece of music swing?".

Musicologists have hypothesized that timing effects in the form of *microtiming deviations* (MTD) play a major role for the swing feel, but this suggestion has also remained controversial: Ethnomusicologist Charles Keil (1987) and others have emphasized the importance of participatory discrepancies; i.e. *"little discrepancies within a jazz drummer's beat, between bass and drums, between rhythm section and soloists, that create 'swing' and invite us to participate"*, whereas others contested their influence and rather stressed the importance of rhythmic accuracy. Is there a way to prove that MTD can contribute substantially to the swing feel?

Adopting an operational definition of swing we have carried out the first study that is able to clarify the controversy and to rigorously demonstrate a positive effect of certain microtiming deviations on the swing feel [1]. By manipulating the timing of original piano recordings and measuring the swing feel of different manipulated versions as rated by jazz musicians we demonstrated that a playing style with *systematic* microtiming deviations, slightly *delaying downbeats* of the soloist with respect to the rhythm section while *synchronizing offbeats*, considerably enhances the swing feel - see *downbeat delayed* manipulation in Fig. 4.16. (*Downbeats* are eighth notes placed on the four beats of a 4/4-measure, while *offbeats* denote eighth notes in between two downbeats.) We compared this version with downbeat delays (of the order of 30 ms or 9% of a quarter note) to the quantized original recording and to a version in which both, downbeats and offbeats, are delayed. Fig. 4.16 shows that the latter two versions and in particular the quantized original cannot create an equally strong swing feel.

This is the result of an experiment, but do jazz musicians actually make use of this phenomenon, and to which extent? We also analyzed a large set (456) of full solo performances and determined the average downbeat delays. We found that jazz soloists generally make use of downbeat delays and that their magnitude decreases with tempo (Fig. 4.17). Taken together the results of our experimental and our observational study lead to the conclusion that *downbeat delays are a key component of the swing feel* in jazz. They underline the general importance of timing and rhythmic effects for the swing feel and resolve the long-standing controversy on the role of microtiming deviations by demonstrating that certain *systematic microtiming deviations* enhance the swing feel. Involuntary *random microtiming deviations*, on the other hand, which are present in every human performance, do not enhance but rather tend to inhibit the swing feel, as we had shown in a preceding project [3]. That downbeat delays could play such an important role for the swing feel was widely unknown. Professional and semiprofessional jazz musicians participating in our online experiment reported a pleasant friction between the soloist and the rhythm section, but were unaware of the effect and could not determine its nature, even though they have learned to intuitively create the swing feel in their performances.

Correlation properties and musical variability

Our brains are constantly making predictions about changes in our environment in response to sensory input; this is also in operation when we listen to music. Music theorists since Leonard Meyer (1956) have argued that it is the interplay between such expectations and their fulfillment or violation in the perception of musical progressions that gives music its emotional power and creates musical meaning. It would be desirable to quantify this interplay on the basis of information-theoretical concepts to compare different composers, musical genres, etc. Unfortunately the length of compositions is far from sufficient to reliably estimate entropies. This is due to the combinatorial explosion of sufficiently long n-grams of musical phrases, whose probabilities would have to be determined.

A somewhat related concept is the autocorrelation function. It can also reflect the amount of innovation, and it is possible to determine its properties through detrended fluctuation analysis (DFA) and power spectral densities (PSD). A power-law decay of the PSD implies a power-law decay of the autocorrelation function, which can be very slow depending on its exponent.

However, in PSD- and DFA-studies, several authors, following the work of Voss and Clarke have come to controversial conclusions about the functional form of the PSD, e.g. claiming $1/f$-noise, $1/f^2$-noise, or other power laws. These discrepancies may be due to numerical artifacts or large errors in the PSD-estimates. To find reliable answers about the functional form of the PSD-decay we have performed very careful PSD-analyses of pitch sequences in numerous musical compositions and improvised performances. Following other recent work of ours [4], we used a multitaper PSD-method, which allows us to reliably extend the PSD–estimates down to the smallest possible frequencies given by the bandwidth. The bandwidth is inversely proportional to the length of the time-series.

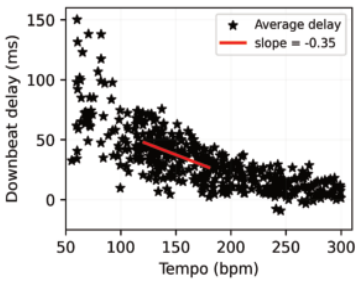

Figure 4.17: Average downbeat delays of soloists as a function of tempo. Each point in the scatter plots corresponds to one of 456 jazz solos and represents its average downbeat delays in milliseconds as a function of tempo in beats per minute. The red line delimits the tempo range of pieces used in our experiment.

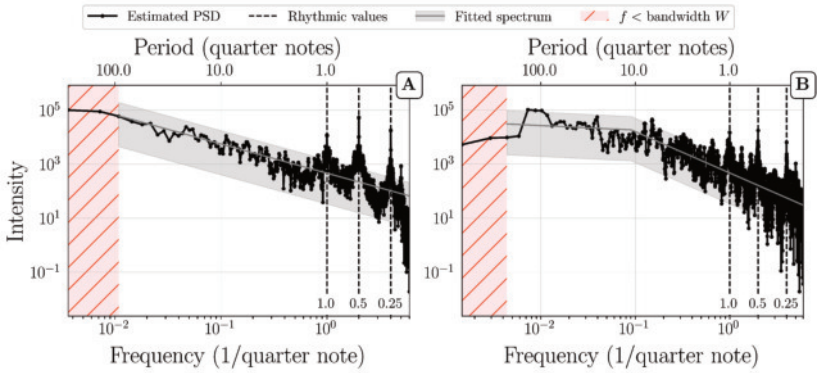

Figure 4.18: Multitaper PSD-estimation of A) Shostakovich's Prelude and Fugue in B major no. 11 op. 87 and B) Allegretto from Haydn's String Quartet in D major op.76 no. 5, Hob.III:79. The shaded gray areas represent 95% confidence intervals around the fitted PSD (gray line). For convenience dashed vertical lines indicate corresponding time periods in quarter note units. The shaded pink area represents frequencies below the bandwidth W. Example A) is representative of a PSD with power-law (PL) down to the bandwidth W, and example B) for a power-law + plateau (PL+P).

Based on such careful estimates we found that although the PSDs of musical pitch sequences exhibit inverse power laws ($1/f^{\beta}$), they terminate at a lower cutoff frequency, where the PSDs turn into flat plateaus (see Fig. 4.18). In some cases, however, we find pure power laws without plateaus and cutoff frequencies. This is only the case for relatively short musical time-series (see Fig. 4.19), where the PSD bandwidth is necessarily relatively large. Therefore, it is very likely that in these cases a true cutoff is hidden at a smaller frequency within the bandwidth and would show up if the bandwidth could be lowered.

The cutoff frequency therefore marks a transition from a $1/f^{\beta}$ to a white noise behavior at low frequencies. Correspondingly the pitch autocorrelation function exhibits slow power law decays only up to a cutoff time, beyond which the correlation vanishes. This transition from a strongly correlated to an uncorrelated time-series at large time differences thus expresses the interplay between expectation and surprise in music that has been hypothesized by music theorists. The cutoff time can serve as a measure for the degree of persistence and predictability in musical compositions. It can be used to characterize different compositions and in various cases shows differences between composers. We find, e.g., that it appears to be larger on average in Mozart's compositions than in Bach's (see Fig. 4.20). In general we obtain cutoff times in a range between 4 quarter note units and 100 quarter note units; they show an increasing trend in dependence on the lengths of the compositions.

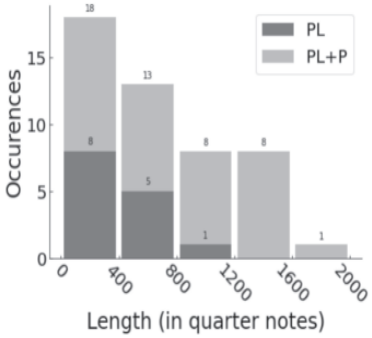

Figure 4.19: The distribution of PL and PL+P shapes as a function of piece length shows that low-frequency plateaus are absent only in relatively short pieces (see PL) and indicates that this is probably due to the lack of low-frequency resolution in these pieces.

Another parameter of interest is the power law exponent β of the power law regime, as it influences the slowness of the initial autocorrelation decay. We have determined the histogram of the exponents β over all pieces; for classical compositions it shows a pronounced peak near $\beta = 1$. Thus, in a limited sense, one can speak of $1/f$-noise in musical pitch sequences (and of very slowly decaying correlations), but only in a limited frequency range bounded by the cutoff frequency.

The spectra also show "rhythmic" peaks at multiples and fractions of inverse quarter note units (Fig. 4.18). They reflect the rhythmic structure present in the pieces. In improvised jazz solos, pure power laws are very rare and plateaus dominate at small frequencies. The rhythmic peaks are broader and less pronounced indicating larger timing variability in jazz solos.

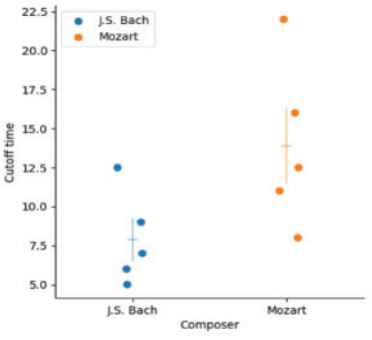

Figure 4.20: Comparison of the cutoff times for single movements of J.S. Bach and Mozart.

[1] C. Nelias, E.M. Sturm, T. Albrecht, Y. Hagmayer, and T. Geisel, Commun. Phys. **5**, 237 (2022)

[2] C . Nelias and T. Geisel, Nature Comm. **15**, 9280 (2024)

[3] G. Datseris, A. Ziereis, T. Albrecht, Y. Hagmayer, V. Priesemann, and T. Geisel, Sci. Rep. **9**, 19824 (2019)

[4] C . Nelias, B. Schulz, G. Datseris, and T. Geisel, Chaos, **34**, 103112 (2024)

4.8 MAX PLANCK EMERITUS GROUP DYNAMICS OF SOCIAL SYSTEMS

Stephan Herminghaus
(for his Curriculum Vitae, refer to the mission statement of the department Dynamics of Complex Fluids, section 3.3)

Aside from ongoing service within the Max-Planck Society (Perspectives Commission until end of 2024), emeritus activities are devoted to the continuation of experiments which had been started within the department Dynamics of Complex Fluids. This includes the investigation of switchable adhesion in *Chlamydomonas Reinhardtii*, which are considered promising for energy harvesting through photosynthesis in biological solar energy plants. Experiments are carried out in the laboratories of Prof. Oliver Bäumchen at the Universtity of Bayreuth. They are expected to continue at least until the end of 2025. A joint publication about the regulation of light-switchable adhesion in *Chlamydomonas* by animal and plant cryptochromes is presently under preparation.

Additionally, projects with socio-economic focus continue. The software codes for bi-modal public transportation systems, which had been developed within the EcoBus project (section 5.3), have meanwhile been disclosed as public domain, such that they can be used freely by public services. Accordingly, the startup company *EcoBus GmbH*, which had been created for their setup, implementation, and development, is in the process of liquidation. This expects completion by the end of next year.

Furthermore, our results on the collective behaviour of humanized agents playing public goods games (section 5.4), which displayed only very short-range spatial correlations irrespective of network topology [1], suggest that societal dynamics is mainly mirroring individual encounters, even in its collective aspects. If corroborated, this renders education of appropriate styles of interpersonal interaction particularly important for a social system. An interdisciplinary project is therefore currently being set up with the IKSK (Berlin) which aims at creating a curriculum for educating mindful encounter, even in the presence of strong power gradients, to post-adolescent young people at school. In support of outreach to the non-scientific public, other physics-related topics of general interest have also been discussed [2].

[1] P. Godara, S. Herminghaus, Chaos, Solitons & Fractals: X **107**, 100099 (2023)

[2] S. Herminghaus, Über das Fließen von Zeit und Materie in der Physik, in: M. Schulz, V. von Flemming (Hg.): Vom Fließen der Dinge, Heidelberg, arthistoricum.net (2024)

4.9 MAX PLANCK EMERITUS GROUP MOLECULAR INTERACTIONS

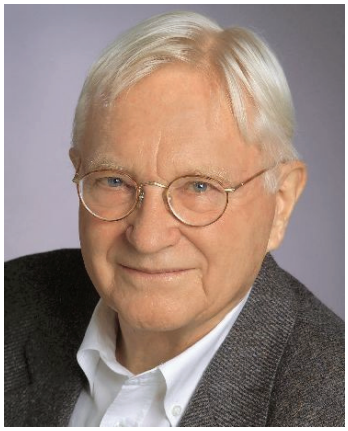

Prof. Dr. Dr. h.c. mult. J. Peter Toennies studied physics and chemistry at Brown University, Providence, USA, where he received his Ph.D.in 1957. He came to Germany in 1957 where he was a postdoc and "Assistent" 1957-1965 in Wolfgang Paul's Physics Institute in Bonn. After his habilitation (1965) he was a Dozent until becoming director at the MPI Strömungsforschung in Göttingen (1969-2002). Since 1971 he is Associate Professor at the University of Göttingen and Adjunct Professor at the University of Bonn.

Together with the late Hans Pauly (1928 - 2004) our group came to Göttingen in 1969 from the University of Bonn to establish the new research direction of molecular beam investigations of elementary collision processes between atoms and molecules. According to the Eigen-plan the idea behind our being called to the Max Planck Institute for Flow Research (Strömungsforschung) was to investigate the elementary processes behind the macroscopic fluid dynamic process and thereby achieve a better understanding. In the following years the Institute became one of the leading international centers for experimental and theoretical molecular beam research in determining with unprecedented precision the van der Waals forces and the collision dynamics between atoms and molecules. The intermolecular forces are of fundamental importance for understanding both the static and dynamic properties of gases, liquids and solids as well as their phase transitions. One of the important achievements from our Institute was the development of a new analytic model for the van der Waals interaction in place of the well-known Lennard-Jones potential. The Tang-Toennies potential, which is presently widely used for accurate simulations, has been cited 1844 times since 1984.

In the course of these studies our group observed in the late 1970's that helium free jet gas expansions behaved in a remarkable way. Instead of the usual velocity distributions with $\delta v/v \cong 10\%$ the helium atom beams had very sharp velocity distributions and were nearly monoenergetic with $\Delta v/v \leq 1\%$. This unexpected observation was found to be related to the extremely weak interatomic forces between He atoms, with the consequence that their collision cross section, at the ultra-low ambient temperatures ($\approx 10^{-3}K$) in the expanding gas rises to 259.000 Å^2, more than 4 orders of magnitude larger than the cross section at room temperature. These nearly monoenergetic helium atom beams have found widespread application. In seeded beam expansions with small concentrations of molecules the excess of helium atoms serves to cool the molecules down to temperatures of several degrees K. This became a great boon for molecular spectroscopy since at these temperatures the hot bands, that otherwise obscure the molecular spectra, are eliminated.

Our group exploited the sharp velocity helium atom beams for exploring the structures and the phonon-vibrations at the surfaces of solid crystals. In complete analogy to neutrons which are routinely used to study the structures and phonon dispersion curves inside solids, helium atoms are the ideal scattering probe method for investigating the structures and dispersion curves of phonons at solid surfaces, which are not accessible with neutrons. The study of over 200 different surfaces by inelastic helium atom scattering (HAS) and the complimentary method of inelastic electron scattering (EELS) have led to a much more profound knowledge of interatomic forces at surfaces and how atoms and molecules interact with metal surfaces, which is of basic importance

for understanding many surface phenomenon such a corrosion, friction and catalysis.

In the following years we became even more fascinated by this unusual element helium, which is the only substance which exhibits superfluidity, a collective quantum phenomena similar to superconductivity. In its superfluid state below 2.2 K liquid helium flows without friction, just as the electrons in a superconductor flow without resistance. Thus it was natural to ask if small finite-sized clusters and droplets of helium might also exhibit superfluidity. In molecular beam experiments we observed that atoms and molecules could be inserted and trapped in the droplet's interior. This opened up the possibility of employing spectroscopy to interrogate the physical properties of the trapped molecules and also the state of the helium droplets. Surprisingly the sharp spectral features of the embedded molecules indicated that the molecules were unaffected by the helium environment and could rotate freely as if they were in a vacuum and not at all strongly hindered as expected for an ordinary liquid. From the highly resolved rotational spectrum the temperature of the droplets was found to be 0.37 K. Subsequent experiments revealed that the free rotations were related to the superfluidity of these droplets. This is the first evidence that superfluidity occurs in a finite-sized system and is now called *microscopic superfluidity*.

Helium nanodroplets are now being used in more than 25 laboratories worldwide as a uniquely cold (0.15 – 0.37 K) and gentle matrix for high resolution molecular spectroscopic investigations of atoms, molecules, and "tailor made" clusters, their chemical reactions, and their response to photo-excitation. Our group used this technique to provide the first evidence that para-hydrogen molecules which, like He atoms are spinless bosons, can also exhibit microscopic superfluidity. Experiments were also directed at exploring the nature of small pure clusters consisting of a few helium and hydrogen molecules, which show large quantum effects. To this end we developed an apparatus to study the matter-wave diffraction of cluster beams from nanostructured transmission gratings. These experiments led to the first evidence for the existence of the very weakly bound dimer and the precise measurement of its size. Unexpected magic numbers were found in larger clusters ($N \leq 50$), which have led to the first insight into the elementary excitations of these nano-sized superfluids.

As an emeritus group we have been working in three main areas of research: (1) At the end of 2018 we finally completed our 600 page Springer monograph with Prof. Giorgio Benedek (University of Milan) entitled "Atomic Scale Dynamics at Surfaces: Theory and Experimental Studies with Helium Atom Scattering". This monograph provides the only up-to-date survey of the theoretical and experimental methods for studying the vibrations at the surface of single crystals and the surface vibrations of adsorbed atoms and molecules. The appendices provide a complete overview of the literature for all the systems studied and the corresponding theoretical investigations. Since then we have continued our investigations of electron-phonon coupling at the surfaces of metals and superconductors and surface plasmons. In 2022 Giorgio Benedek

and we were awarded the Enrico Prize and Medal of the Italian Physical Society for our contributions to the understanding the role of phonons at the surface of solids. Our monograph was mentioned in the Laudatio as the crowning achievement. (2) In collaboration with several bachelor students we have investigated a new modified Tang-Toennies model for describing the van der Waals potentials of the alkali diatomic molecules made up of the atoms Li, Na, K, Rb, and Cs in the weakly bound triplet state. These potentials are of great current interest for understanding the collisions in laser trapped ultra-cold gases and their Bose-Einstein Condensation. We have recently demonstrated that our model with only three parameters provides an equal or better description of all the spectroscopic data than numerical fits with up to 50 parameters. Recently in collaboration with K. T. Tang (Pacific Lutheran University, Tacoma, USA) and Xiaowei Sheng (Anhui University, Anhui, China) we have demonstrated that with an analytic extended Tang-Toennies model potential it was possible to describe the van der Waals potentials between all the homonuclear and heteronuclear rare gas dimers in excellent agreement with ab initio potentials where available (Phys. Rev. Lett. **125**, 253402 (2020)). (3) With a former PhD student, Prof. Slenczka, in 2022 we published an 11 chapter open access Springer Nature book entitled "Molecules in Superfluid Helium Nanodroplets: Spectroscopy, Structures and Dynamics". This is the first compendium covering all aspects in this emerging field of research and has been accessed 52000 times. The collaborations with Giorgio Benedek and Xiaowei Sheng are presently continuing. Recently we published in the journal "Condensed Matter" an article with Benedek and several other theoreticians entitled "The Electron-Phonon Interaction in Non-stoichiometric $Bi_2Sr_2CaCu_2O_{8+\delta}$ Superconductor from Diffuse Elastic Scattering of Helium Atoms" which was based on experiments from our group.

PART II

RESEARCH AND SUPPORT

DRIVEN SYSTEMS

5

Driven systems—maintained far from thermal equilibrium—are central to understanding many complex phenomena in physics, biology, medicine, engineering, and the environmental sciences. External or internal driving often leads to spontaneous symmetry breaking, spatio-temporal complexity, and emergent order. Despite their diversity, such systems frequently share universal behaviors that can be studied using tools from non-equilibrium physics, nonlinear dynamics, and statistical mechanics.

The systems studied here reflect the broad scope of our research, from classical fluid dynamics, droplets, and turbulence, to mechanics, phase separation, and topological defects. Applications cover an equally broad range, from atmospheric processes, wind turbines and cloud physics to societal challenges such as transmission dynamics of infections and public transport.

At MPI-DS, we combine theory, simulations, and experiments to uncover the organizing principles of driven systems and to contribute to key challenges in health, climate, and technology.

Contents

5.1 SOFT CONTACTS AND VOLATILE LIQUIDS

S. Karpitschka
Z. Xu, Y. Chao, O. Ramírez-Soto, C. Bahr, M. van Limbeek, H. Jeon, J. H. Snoeijer (Twente), H. van Brummelen (Eindhoven), S. Aland (Freiberg), K. Dalnoki-Veress (McMaster), N. Cira (Cornell)

Establishing mechanical contact between soft objects is one of the most ubiquitous processes in nature and technology, allowing humans or robots to grab fragile objects or biological cells to adhere to surfaces. Adhesion, releasing surface energy in the contact zone, generates a singularity at the edge [1] which also exists for wetting droplets [2–5]. The associated non-linear phenomena are currently not well understood. We could show how this singularity causes stick-slip motion of droplets by the interplay with dissipative forces [6], how it induces drying or indefinite swelling in poroelastic media [7] (Fig. 5.1), and how non-linear material behavior dominates in ultra-thin films [2].

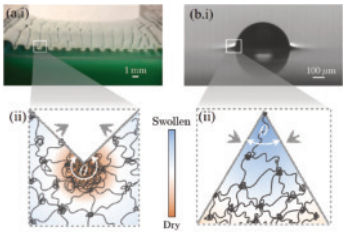

Figure 5.1: Two types of soft contacts: creases (left) and wetting ridges (right). In either case, the same singularity emerges, but with opposite sign, leading to dry-out (left) or indefinite swelling (right) of dissolved oligomers [7]

Edge singularities also dominate the dynamics of sessile droplets of volatile liquids since the local rate of evaporation diverges toward the edge of the droplet. In multicomponent droplets, this causes strong compositional gradients that in turn drive Marangoni flows [8–10] and, for partially miscible liquids, also phase separation [10]. We could demonstrate that demixing emerges in the precursor ahead of the droplet, propagating along the free surface to induce active spreading. Together with the complex flows and reversing contact line motions in ternary systems [9], these results engender new surface processing strategies, e.g. in printing or semiconductor technology.

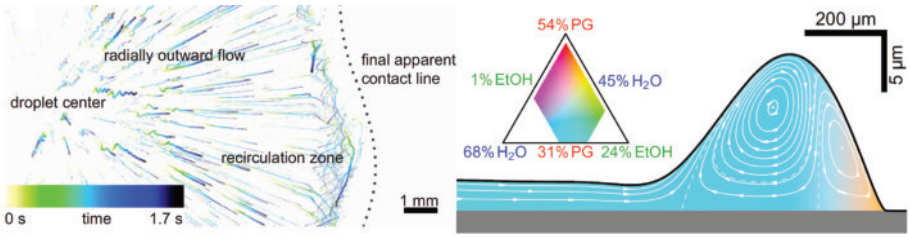

Figure 5.2: Ternary droplets of water, propylene glycol and ethanol display a boomerang-like wetting motion due to complex Marangoni flows: Evaporative depletion causes coexisting zones of reversing flows that successively dominate the flow.

[1] M. H. Essink, M. A. J. van Limbeek, A. Pandey, S. Karpitschka, and J. H. Snoeijer, Soft Matter **19**, 5160 (2023)
[2] H. K. Khattak, S. Karpitschka, J. H. Snoeijer, K. Dalnoki-Veress, Nat. Commun. **13**, 4436 (2022)
[3] H. Jeon, Y. Chao, and S. Karpitschka, Phys. Rev. E **108**, 024611 (2023)
[4] M. H. Essink, S. Karpitschka, H. K. Khattak, K. Dalnoki-Veress, H. van Brummelen, and J. H. Snoeijer, *under review*, arXiv:2402.06344 (2024)
[5] Y. Chao, H. Jeon, and S. Karpitschka, *under review*, arXiv:2411.03915 (2024)
[6] D. Mokbel, S. Aland, S. Karpitschka, Europhys. Lett. **139**, 33002 (2022)
[7] M. M. Flapper, A. Pandey, M. H. Essink, S. Karpitschka, and J. H. Snoeijer, Phys. Rev. Lett. **130**, 228201 (2023)
[8] O. Ramírez-Soto, S. Karpitschka, Phys. Rev. Fluids **7**, l022001 (2022)
[9] D. A. Baumgartner, S. Shiri, S. Sinha, S. Karpitschka, N. J. Cira, Proc. Natl. Acad. Sci. U.S.A. **119**, e2120432119 (2022)
[10] Y. Chao, O. Ramírez-Soto, C. Bahr, S. Karpitschka, Proc. Natl. Acad. Sci. U.S.A. **119**, e2203510119 (2022)

5.2 FLOW-INDUCED DISCLINATION LINES IN NEMATIC LIQUID CRYSTALS

C. Bahr

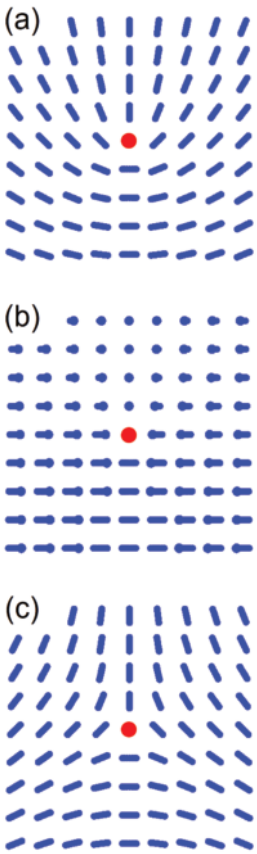

Figure 5.3: Director fields around cross sections of disclinations (red dot) with $\Omega = |\frac{\pi}{2}|$. (a): $+\frac{1}{2}$ wedge disclination, (b): twist disclination, (c): $-\frac{1}{2}$ wedge disclination. Local directors are symbolised as blue rods. Directors which are not parallel to the plane of the image are drawn with reduced length and are assigned with a dot indicating the "end" of the director pointing towards the observer (if solely a dot is displayed, the director is perpendicular to the plane of the image). Note that, in 3D, infinitely many topologically equivalent configurations exist which are distinguished by the angle between the disclination line and the rotation vector of $\vec{n}$. For the three examples shown above, this angle amounts to 0 (a), $\pi/2$ (b), and π (c).

Nematic liquid crystals (NLCs) exhibit a wealth of topological defects and provide well-suited model systems for studies of topological defects in general. For example, results obtained on NLCs may be significant for knot theory, colloid physics, or even cosmology. The most common defects in NLCs are line defects called disclinations. When crossing a disclination, the orientation of the the nematic director $\vec{n}$ changes discontinuously by a certain angle Ω which amounts in most cases to $\pi/2$. Figure 5.3 shows three common examples.

The study of disclinations is of importance from both fundamental and applied viewpoints ([1] and references therein). The common way to induce and stabilize disclinations is to confine the NLC in a cell with conflicting anchoring conditions on its walls. Here we explore a different approach: Using lattice Boltzmann simulations, we study how disclination lines can be generated and stabilized by the flow of the NLC in microfluidic channels.

For the simulations we define a straight channel with square cross section. Channel axis, width, and height are denoted with x, y, and z, respectively. We have periodic boundary conditions in x direction, top, bottom, and side walls are designed with no-slip condition. The flow of the NLC is induced by applying a body force in $+x$ direction. The strength of the flow is described by the dimensionless Ericksen number Er which specifies the ratio between viscous and elastic forces or torques: $\mathrm{Er} = \gamma_1 u L/K$. Here, γ_1 is a viscosity coefficient for director rotation, u the flow velocity, L a relevant length scale (width or depth of the channel) and K the mean elastic constant of the NLC. Highly simplified, the flow may be seen as a force which tries to align $\vec{n}$ along the flow direction. More details of the lattice Boltzmann method and nematic hydrodynamics can be found in [2, 3].

We have studied several configurations which differ by the anchoring conditions of the nematic director on the channel walls. Here, we give three examples. Case I (Fig. 5.4): perpendicular anchoring on the side walls, parallel anchoring on the top and bottom wall. Case II (Fig. 5.5): parallel on the bottom wall, perpendicular on the other three walls. Case III (Fig. 5.6): perpendicular on all four walls.

The main result of our study is the observation of a flow-induced nucleation of one or more pair(s) of twist disclination lines in those regions of the channel where the aligning forces of flow and anchoring are perpendicular to each other. Depending on the overall configuration of the director field in the channel, the newly formed disclinations either persist at higher flow rates or they annihilate with other disclinations (which were already present at zero flow or were also newly formed by the flow, more details are given in the figure captions). A necessary condition for the persistence of a flow-induced disclination line is a strong aligning force perpendicular to the shear plane of the flow. In the present study, this force is provided by one or more wall(s) with

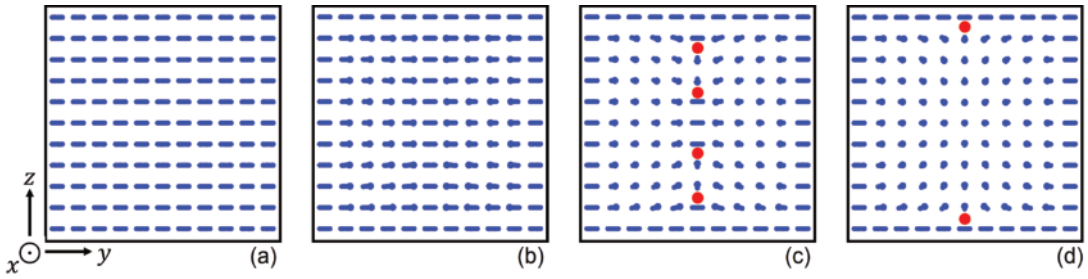

Figure 5.4: Director field in channel cross section, parallel anchoring on top and bottom wall, perpendicular anchoring on the side walls. (a) Structure at zero flow. (b) Medium flow (Er $= 30$), partial alignment of $\vec{n}$ in the direction of flow ($+x$). (c) Strong flow (Er $= 130$), nucleation of two pairs of twist disclinations (red dots, see Fig. 5.3b). Of each pair, the line closer to the center migrates towards it and annihilates in the center with the corresponding line of the other pair whereas the line closer to the top or bottom wall migrates towards the wall and persists there. (d) Final steady state at Er $= 130$.

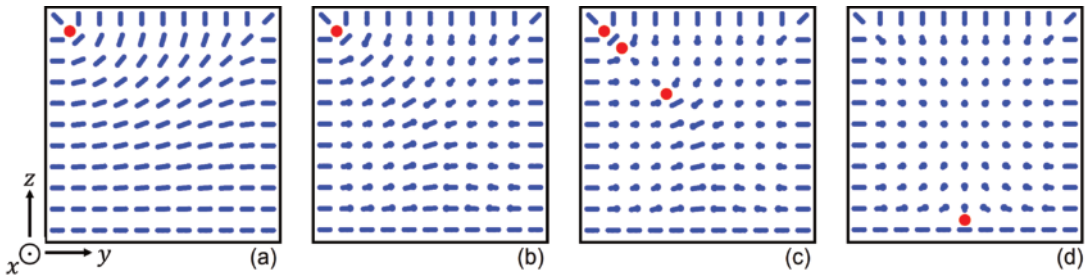

Figure 5.5: Director field in channel cross section, parallel anchoring on bottom wall, perpendicular anchoring on all other walls. (a) Structure at zero flow with a $+\frac{1}{2}$ wedge disclination (red dot) in the upper left corner. (b) Medium flow (Er $= 30$), partial alignment of $\vec{n}$ in the direction of flow ($+x$). (c) Strong flow (Er $= 80$), nucleation of one pair of twist disclinations in the upper left quarter of the channel. One of the newly formed disclinations annihilates with the disclination in the upper left corner, the other newly formed disclination migrates towards the bottom wall and persists there. (d) Final steady state at Er $= 80$.

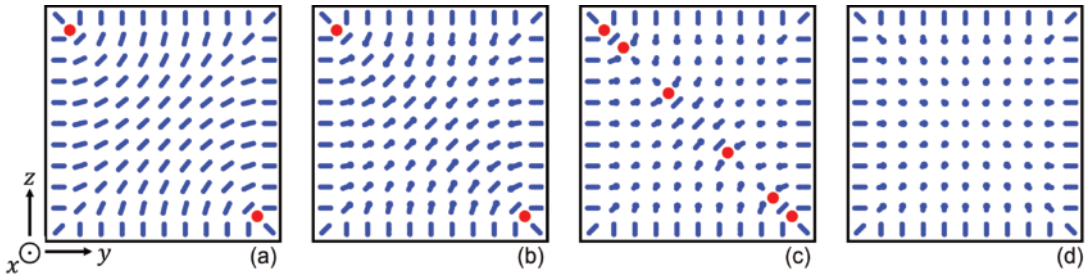

Figure 5.6: Director field in channel cross section, perpendicular anchoring on all walls. (a) Structure at zero flow with $+\frac{1}{2}$ wedge disclinations (red dots) in the upper left and lower right corner. (b) Medium flow (Er $= 30$), partial alignment of $\vec{n}$ in the direction of flow ($+x$). (c) Strong flow (Er $= 80$), nucleation of two pairs of twist disclinations in the upper left and lower right quarters of the channel. Of each pair, the line closer to the center migrates towards it and annihilates with the corresponding line of the other pair. The second line of each pair migrates towards the nearest corner where it annihilates with the line which already existed at zero flow. (d) Final steady state (escaped configuration, free of defects) at Er $= 80$.

parallel anchoring condition. In future studies we will explore if this role could be adopted also by external fields.

[1] M. Jiang, Y. Guo, R. L. B. Selinger, O. D. Lavrentovich, Q.-H. Wei, Liq. Cryst. **50**, 1517 (2023)
[2] C. Denniston, D. Marenduzzo, E. Orlandini, J. M. Yeomans, Phil. Trans. R. Soc. A **362**, 1745 (2004)
[3] C. Bahr, Phys. Rev. E **104**, 044703 (2021)

5.3 BI-MODAL DOOR-TO-DOOR PUBLIC TRANSPORT: FROM BASIC RESEARCH TO DEPLOYMENT

P. Sharma, S. Mühle, H. Heuer, T. Baig-Meininghaus, V. Cifu, B. Wacker, K. M. Heidemann, S. Herminghaus
A. Minnich, H. Herbst, T. Kneib (Uni Göttingen)
J. C. Schlüter (TU Dresden)

Although they constitute an enormous waste of resources, motorized individual vehicles (MIV) provide the predominant mode of contemporary mobility. As concerns are rising towards prudent uses of global resources, it is necessary to develop alternative transport systems. A key figure of merit is the pooling rate, b, which denotes the average number of passengers per vehicle. For a train or tram, this can be a large number if the cars are filled. However, these services have to stick to fixed service schedules and localized stations, thus compromising on service quality (and hence low demand) experienced by customers.

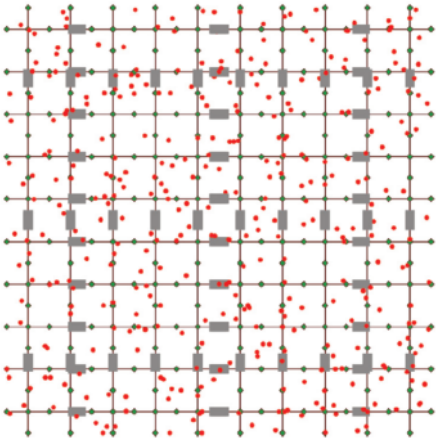

Figure 5.7: Simplified model of a bi-modal public transport, consisting of equidistant line services (black lines, tracks; grey rectangles, trains) with stops (green dots) at each intersection with another line, and in between. Line services are operated at fixed service frequency. Door-to-door service is accomplished by combining the line service with ride-pooling shuttles (red dots) which provide 'last-mile' transport to and from line service stations.

A future-proof transport system needs to provide both door-to-door service (similar to MIV) and a high pooling rate, leading to a sustainable balance of resources. A suitable way forward is a combination of a standard line service system with a fleet of ride-pooling shuttles providing last-mile service to and from the individual addresses of customers (bi-modal system). We have modeled such system on the basis of line services already in place in many large cities, taking into account our earlier results obtained for ride-pooling systems [1]. A sketch is displayed in Fig. 5.7. This setting allows so simulate the performance level of bi-model transport with variable parameters, such as demand, mesh size of line service, and the density of stations [2–4]. Pareto fronts obtained for different levels of demand, in the area spanned by energy consumption, $\mathcal{E}$, and quality of service, $\mathcal{Q}$, are displayed in Fig. 5.8. Field research suggests that $\mathcal{Q} \approx 0.5$ is acceptable for public transport. We find that in large cities ($\Lambda \geq 10^4$) energy consumption can be as low as 0.2 if the mesh size is chosen properly.

As in presently operative line service systems there are more stations than there are crossings between line services, we also studied the

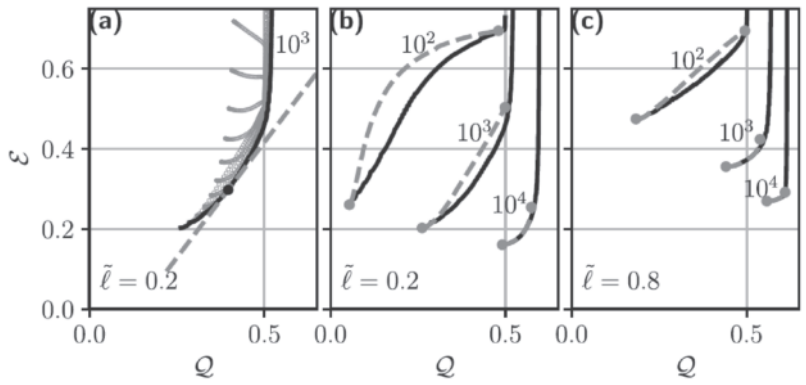

Figure 5.8: Pareto fronts for different levels of non-dimensional demand, Λ, ranging from 10^2 to 10^4. $\mathcal{E}$ is energy consumption, divided by the total energy MIV would need. $\mathcal{Q}$ is MIV transportation time, divided by the transportation time of the bimodal system. $\tilde{l}$ is the mesh size of the line service, divided by the average travel distance. Dashed grey: degenerate Pareto fronts at full train occupancy.

impact of the number of intermediate stops on system performance. As shown in Fig. 5.9, the effect on system performance is negligible for small demand (green symbols), but becomes noticeable for larger demand. In general, intermediate stops reduce both tortuosity and occupancy of shuttles. Hence we conclude that in a bi-modal system, intermediate stops can be considered advantageous for service quality.

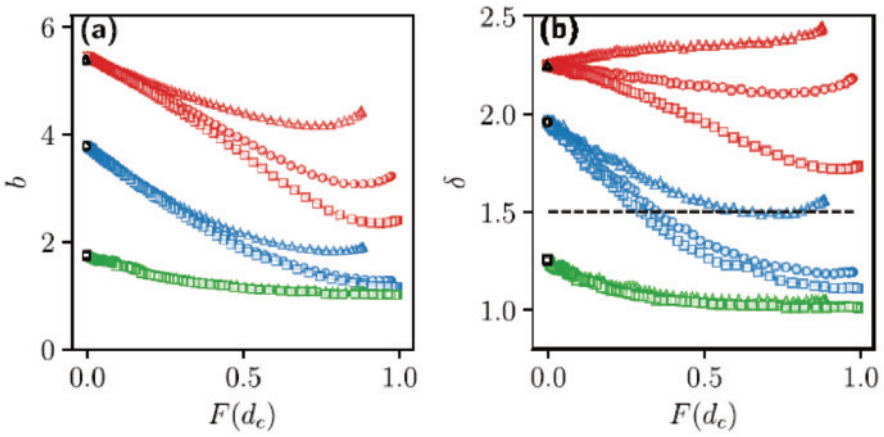

Figure 5.9: Pooling rate, b, and the average tortuosity, δ, of shuttle routes, as a function of the fraction of bi-modal routes, F. The latter was varied by varying the critical travel distance, d_c, above which service was chosen bi-modal. Triangles, circles, and squares correspond to zero, one, and three extra stations between line crossings, respectively. Green, blue, and red symbols correspond to $\Lambda = 14$, 120, and 1200, respectively.

Practical applicability of our model has been shown by successfully designing transportation systems deployed by public services, such as the shuttle service 'Flow' which is operated by *Via Transportation Inc.* in Göttingen. Similarly, we designed the bi-modal transportation system 'Flexa', which runs in Leipzig suburban areas since five years, and has been continuously augmented.

[1] S. Herminghaus, Transp. Res. A **119**, 15 (2019)
[2] A. Minnich, H. Herbst, S. Herminghaus, T. Kneib, B. Wacker, J. C. Schlüter, Transp. Res. Interdiscipl. Persp. **27**, 101176 (2024)
[3] P. Sharma, K. M. Heidemann, H. Heuer, S. Mühle, S. Herminghaus, Multimodal Transportation **2**, 100083 (2023)
[4] P. Sharma, H. Heuer, S. Herminghaus, K. M. Heidemann, Multimodal Transportation **3**, 100118 (2024)

5.4 CAN WE SIMULATE SOCIETAL DYNAMICS USING AGENTS WITH BOUNDED RATIONALITY?

P. Godara, S. Herminghaus

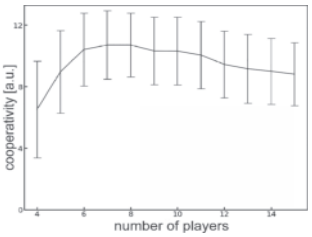

Figure 5.10: Cooperativity (average PGG investment, A) as a function of the number of bounded rational agents in a group playing a PGG.

Public-Goods-Games (PGG) are widely recognized as quite general models of human interaction within societies, making them promising candidates for predicting societal dynamics. We had already shown before that, contrary to what was commonly believed [1], learning is not necessary to explain the commonly observed declining trend of average investment in PGG [2]. In fact, the boundedness of the agent's computational power, K, accounts not only for this phenomenon, but also for the substantial game-to-game variance commonly observed with human players. We have therefore further explored to what extent such bounded rational agents resemble human behaviour in settings of socio-economic interaction. Upon varying the size of groups in which agents played PGG [3], we found that there is an optimal group size in which cooperation, as expressed in the average investment, A, reaches a maximum (see Fig. 5.10). This is in remarkable accordance with what has been reported as well from various experiments with human agents [4].

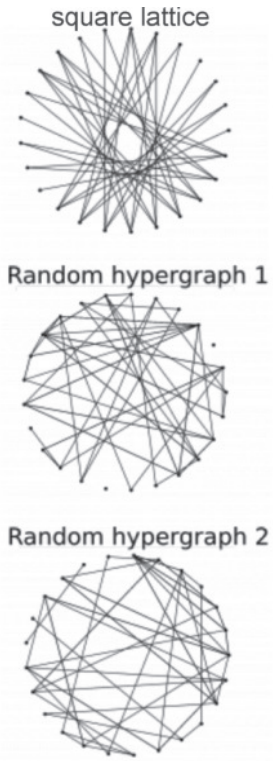

Figure 5.11: Various network topologies investigated, in circle representation.

As a natural next step, we wanted to study collective phenomena in 'societies' consisting of many such agents in mutual interaction [5]. Formally, a society whose participants interact by engaging in a large number of different PGG (associations, trade units, markets etc.) can be described as a hypergraph, as each PGG connects a (potenitally large) number of participants. However, such hypergraph can be mapped onto a simple bigraph in which the PGG are the nodes, connected by the players they share. Nodes can then be characterized by well-established metrics, such as centrality measures. We wanted to know how the topology of the PGG bigraph network influences collaboration, i.e., the average investment A, within the participating PGGs. It is well known that collective phenomena, such as phase transitions, may qualitatively depend upon the network topology of connectivity of neighbors, as encoded in, e.g., the dimensionality of the system.

We have therefore generated a large number of PGG networks with different topologies. Three examples are sketched in Fig. 5.11, in circle representation, as common in network science. The top figure represents a square lattice, the two others have been obtained by random assignment of connections. As shown in Fig. 5.12, we found that A varied in a charcteristic, and quite universal, manner with the network centrality of the group considered. The (positive) constant h depends upon the computational budget, K of the agents. Obviously, cooperation increases monotonically with group centrality.

On the other hand, we observe a general decrease of A with computational budget, K, as reflected in the behaviour of h, which is shown in Fig. 5.13. We find that the dependence of cooperativity upon group connectivity and computational budget can be expressed in a simple

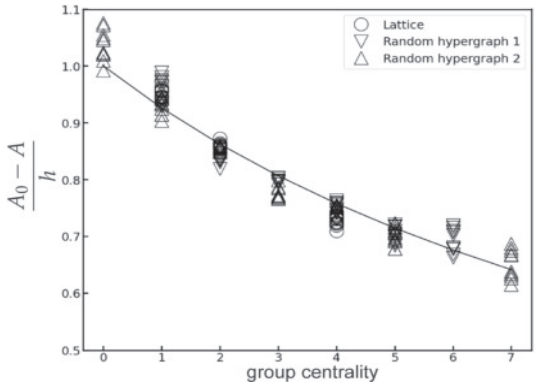

Figure 5.12: The variation of average investment as a function of group centrality, for three different network topologies. The same results were obtained for a much larger number of networks (not shown for the sake of clarty). The constant h was found to depend only on computational budget, K.

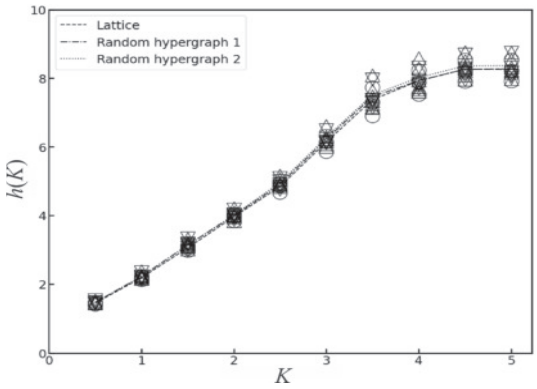

Figure 5.13: The dependence of h on K, for three different network topologies. The same results were obtained for a much larger number of networks (not shown for the sake of clarty).

formula,

$$A = A_0 - \frac{h(K)}{1 + 0.08\ c} \tag{5.1}$$

which shows that the influence of both parameters factorize. Together with Fig. 5.13, Eq. 5.1 shows that for larger computational budget, cooperativity goes down. This is in line with the known fact that Nash equilibrium (infinite computational budget) corresponds to zero cooperation for PGG. It is remarkable that the topology of the network constituted by the many PGG played in a society, which for a real society will be enormuously complex and difficult to assess, may not be decisive for collective behaviour, like cooperativity, of agents in this network. This might be very promising when it comes to simulating collective phenomena within societies.

[1] M. Burton-Chellew, S. A. West, Nat. Hum. Behav. **5**, 1330 (2021)
[2] P. Godara, T. D. Aleman, S. Herminghaus, Phys. Rev. E **105**, 024114 (2022)
[3] P. Godara, S. Herminghaus, Phys. Rev. E **107**, 054140 (2023)
[4] W. Yang et al., Proc. Natl. Acad. Sci. USA **110**, 10916 (2013)
[5] P. Godara, S. Herminghaus, Chaos, Solitons & Fractals: X **107**, 100099 (2023)

5.5 TOWARDS REALISTIC DYNAMICS OF INDOOR INFECTION TRANSMISSION

H. Khodamoradi, O. Schlenczek, E. Bodenschatz, G. Bagheri

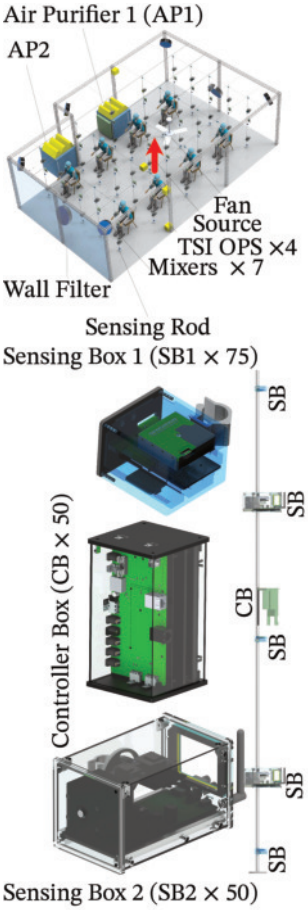

Figure 5.14: 3D schematic of the Bovenden Aerosol Test Room (BAR): A controlled semi-rectangular space with an internal volume of 146 m^3 (9.4 m × 6.3 m × 2.6 m). The 5.3 m-wide front wall has an F8 filter, simulating a large window that can be sealed with a high-density polyethylene/polypropylene (HDPE/PP) layer. Ventilation components include 2 air purifiers (AP1, AP2), 1 ceiling-mounted fan, and 8 wall-mounted mixing fans. Measurement units include 25 Sensorod units (comprising 75 Sensing Box 1, 50 Sensing Box 2, and 25 Controller Boxes). The red arrow marks the particle release point.

The well-mixed room (WMR) model, which assumes uniform aerosol distribution, is widely used to estimate infection risks in indoor spaces [1]. However, localized variations in aerosol behavior challenge this assumption [2–4]. The Bovenden Aerosol Room (BAR) was developed to investigate the validity of the WMR assumption utilizing an array of 125 sensors providing localized particle concentrations, temperature and humidity, and CO_2 in 3D (Fig. 5.14). It enables testing different ventilation layouts and particle release scenarios (pulse and continuous) under realistic occupant conditions, allowing assessment of the risk of infection transmission (RIT) in indoor environments.

The SensoRod provides 3D spatial and temporal visualization of RIT. Figure 5.15 presents results from a continuous particle release with window ventilation and eight subjects if we assume the WMR RIT at the end of experiments to be 63.21%. (A) A snapshot of infection risk highlights elevated risks near the back wall, while regions near the filter and AP2 exhibit lower risks. (B) The temporal evolution of RIT reveals that while most room locations remain below WMR predictions, certain areas near the continuous source show sharp increases around 200 seconds, persisting at elevated levels until the experiment's end, with variability exceeding 80% across locations at the end of the experiment.

Analysis of maximum RIT for different ventilation layouts reveals distinct pulse and continuous release trends. Pulse releases showed 20-60% variability with medians below WMR predictions. In contrast, continuous releases exhibited higher variability and medians exceeding WMR, suggesting the difficulty of managing continuous pathogen sources. This emphasizes the need for adaptive, location-aware ventilation strategies to manage localized and dynamic infection risks.

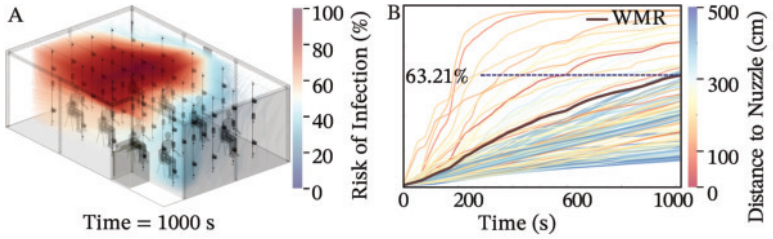

Figure 5.15: (A) 3D mean infection risk of transmission at 1000 seconds under window ventilation and with 8 subjects. (B) Mean infection risk of transmission against time.

[1] M. L. Pöhlker et al., Rev. Mod. Phys. **95**, 045001 (2023)
[2] G. Bagheri, B. Thiede, B. Hejazi, O. Schlenczek, E. Bodenschatz, PNAS **118**, e2110117118 (2021)
[3] F. Nordsiek, E. Bodenschatz, G. Bagheri, PLOS ONE **16**, e0248004 (2021)
[4] O. Schlenczek, B. Thiede, L. Turco, K. Stieger, J. Kosub, R. Müller, S. Scheithauer, E. Bodenschatz, G. Bagheri, J. Aerosol Sci. **167**, 106070 (2023)

5.6 STRESS-INDUCED CELLS MECHANODYNAMICS

S. Villa, E. Bodenschatz

Cells are complex systems probing the surrounding environment and adapting their properties to it, reacting to both biochemical and physical stimuli. The case of mechanical physical perturbation is of particular interest because of its implications in the fields of cancer development and tissue morphogenesis. We address this problem through live cell imaging, also developing custom devices for stress application (Fig. 5.16). It is known that the dynamics of cell monolayers depends on the mechanical properties of cells and their interactions [1]. At the same time, a change in the monolayer dynamics affects cells mechanical properties due to cells adaptability, e.g. by increasing nuclear stiffness to protect the nuclei from a stress increase (Fig. 5.17), as we have shown in Refs. [2, 3] by the quantitative analysis of microscopy videos of samples with different dynamic properties.

In order to decouple the terms of the problem, in an ongoing project we are investigating how external stresses affect cells dynamics. For this scope, we have developed and realized at our workshop an in-plane shearing device (Fig. 5.16) that can be mounted on commercial microscopes for live cell imaging in order to measure the effect of stress on cells shape and dynamics as a function of time.

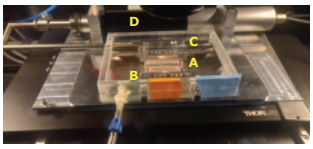

Figure 5.16: Our shearing device. Cells are in a deformable polydimethylsiloxane (PDMS) chamber (A) mounted on two series of metallic pins on the shearing device. The first series is on the stationary part of the device (B) while the second one is free to move along the shearing axis on a rail (C). Its motion is activated by a piezo motor (D) enabling the application of user defined shear protocols (step shear, sinusoidal, square wave, etc.).

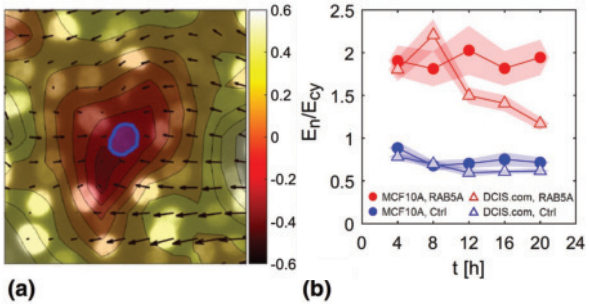

Figure 5.17: (a) Method for recovering the nuclei relative stiffness: $\nabla \cdot \vec{v}$ (colormap) is obtained from the velocity $\vec{v}$ (arrows) and locally correlated with nuclei shape (blue line). (b) Ratio between nuclei and cytoplasm moduli for two cell lines in states of low (blue) and high (red) dynamics.

Preliminary experiments are showing an increase of the cells dynamics under shear compatible with numerical results present in the literature [4].

In a different set of experiments, we are studying how stresses trigger the local detachment of the monolayer from the substrate, giving rise to 3D structures named domes (Fig. 5.18). We are showing how the size and characteristic timescales of the domes depend on cell-substrate adhesion (Fig. 5.19). A comprehensive understanding of this phenomenon can shade light on tissue morphogenesis processes, revealing the physical mechanisms behind the formation of 3D structures in real systems of cells.

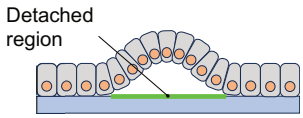

Figure 5.18: Sketch of a dome of cells locally detaching from the substrate.

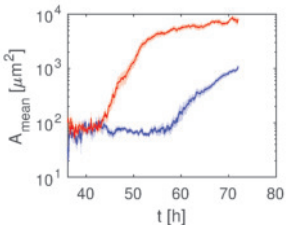

Figure 5.19: Dome average area as a function of time for MDCKII cells on a glass (strong adhesion, blue) and PDMS (low adhesion, red) substrates.

[1] D. Bi, J. H. Lopez, J. M. Schwarz, M. L. Manning, Nat. Phys. **11**, 12 (2015)
[2] S. Villa, A. Palamidessi, E. Frittoli, G. Scita, R. Cerbino, F. Giavazzi, Eur. Phys. J. E **45**, 5 (2022)
[3] E. Frittoli, et al., Nat. Mat. **22**, 5 (2023)
[4] J. Huang, J. O. Cochran, S. M. Fielding, C. Marchetti, D. Bi, Phys. Rev. Lett. **128**, 17 (2022)

5.7 THE CLOUDKITE: A FLYING TOWER INTO THE ATMOSPHERE AND CLOUDS

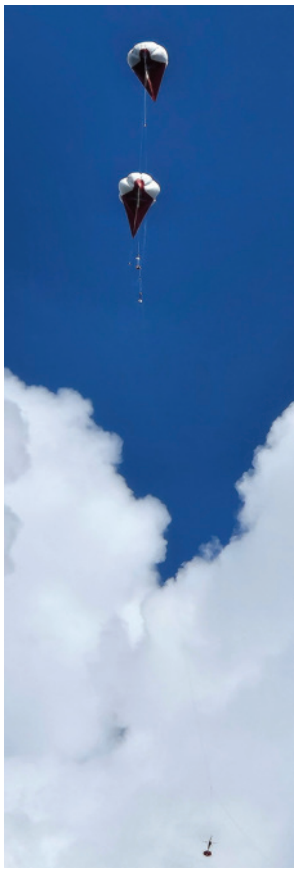

Figure 5.20: The MPCK during the IMPACT field campaign, May-June 2024. Several instruments can be seen on the line, including a WinDart at the bottom right of the picture.

G. Bagheri, F. Nordsiek, O. Schlenczek, B. Thiede, M. Schröder, V. Chávez-Medina, H. Khodamoradi, Y. Kim, E. Bodenschatz

The Max Planck CloudKite (MPCK) is an airborne platform for studying the atmospheric boundary layer and its clouds and aerosols. It uses a tethered helium-filled balloon and an attached kite (commercially known as Helikite), operated via a winch to adjust flight height, effectively functioning as a mobile 2 km tower deployable anywhere in the world. Thus far, the MPCK has undertaken four field campaigns: two over the Atlantic Ocean (MSM82-2 in March 2019 and EUREC4A [3] in January 2020) and two in northern Finland (PaCE in September 2022 and IMPACT in May–June 2024).

Over the first years of the project, we developed several unique instruments, including the Instrument Box MPCK$^+$ for high-resolution PIV and inline holography inside clouds and the Mini-MPCK [2]. We then devised methods to analyze data from these instruments, such as reliable energy-dissipation-rate estimates from velocity records [1] and hologram post-processing with speedups of up to 100 (see section 5.9). These advances allowed us to process the 500,000 holograms collected during EUREC4A — a feat once considered unattainable — and investigate particle clustering in clouds. A new generation of instruments is now ready: the WinDart (third generation of Mini-MPCK, see 5.14) and HoloTrack (Figure 5.21), a particle-tracking holography system that provides unprecedented 3D velocity, position, and size measurements. HoloTrack seamlessly links cloud microphysics and turbulence within a shared volume while providing invaluable information about the relative motion of cloud particles, for example, revealing the collision likelihood under various conditions.

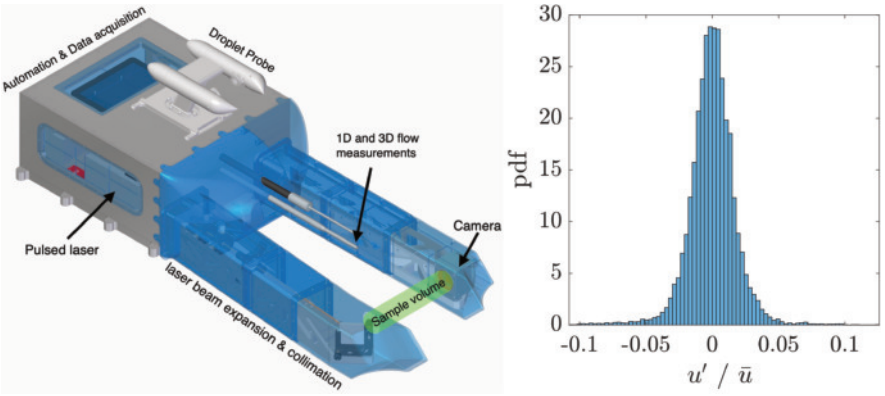

Figure 5.21: (left) CAD rendering of HoloTrack; (right) distribution of the relative droplet velocity (15–100 µm in diameter), normalized by the mean flow speed, measured in a wind tunnel at 1% turbulence intensity and 10 m/s average wind speed. Following its maiden flight during the IMPACT campaign, HoloTrack is now fully calibrated.

[1] M. Schröder, T. Bätge, E. Bodenschatz, M. Wilczek, G. Bagheri, Atmos. Meas. Tech. **17**, 627 (2024)
[2] M. Schröder, PhD thesis, University of Göttingen (2023)
[3] B. Stevens et al., Earth System Science Data **13**, 4067 (2021)

5.8 PATTERN FORMATION INSIDE AN EVAPORATING DROPLET

V. Nasirimarekani, R. Jahangir, Y. Kim

Life has evolved in the liquid phase, a phase which enables many interactions on the micrometer and submicrometer scale. Besides large water volumes, liquid droplets are abundant in nature, e.g., as aerosols, raindrops, etc. A liquid droplet can contain various components such as particles and macromolecules. Any volatile droplet on a surface exposed to the air will evaporate. We have studied evaporation to understand how it can lead to a certain self-organization of the droplet components in the presence of salt. The experiments with evaporating droplets show the following insights:
Evaporation leads to phase separation and the formation of coacervates at the interface of the evaporating droplet. Depending on the concentration of the polymeric monomers inside the droplet, the formation of regular patterns such as a lattice pattern can occur.
In an evaporating droplet containing a non-ionic polymer and salt, a phase separation occurs that is triggered by the phase separation of the polymer material in later phases of evaporation. The phase separation leads to formation of flow vortices, which can form a flower-like deposition of the droplet components.
Non-uniform evaporation of a surfactant-laden droplet can lead to symmetry breaking and the formation of polar vortices, which can drive the droplet on a solid substrate. The propulsion then resembles the creeping dynamics of a cell on a substrate and suggests that fluid physics could play an important role in the crawling of living cells.

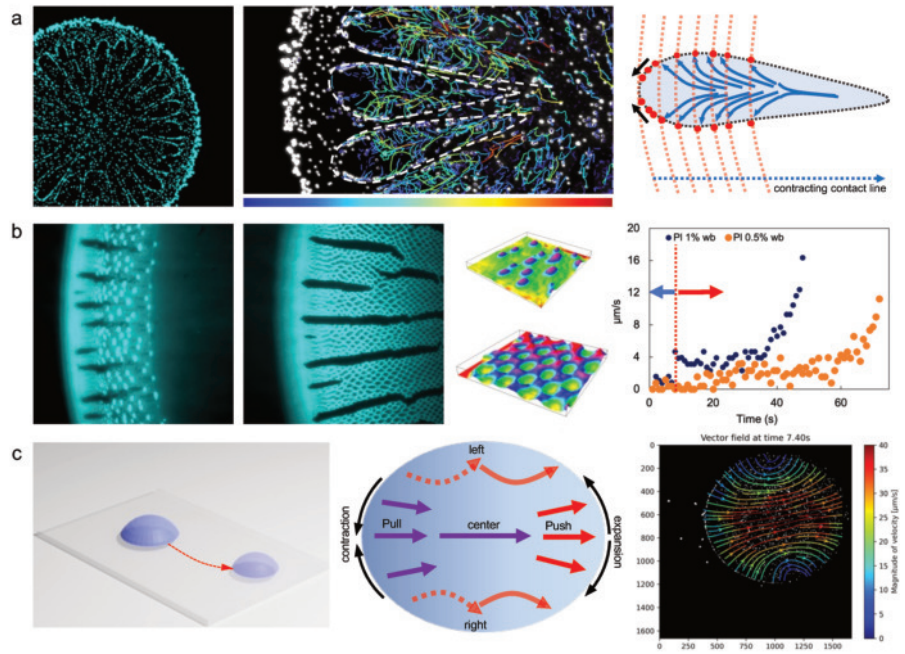

Figure 5.22: a) Phase separation, bursting, and axial symmetry breaking in an evaporating droplet due to the formation of vortices. b) Liquid-liquid phase separation at the interface of an evaporating droplet and the formation of regular patterns such as aggregates or formation of the lattice pattern. The graph shows the contraction dynamics of the interface for the two different patterns. c) Flow dynamics in a self-propelled sessile droplet that resembles the push-pull mechanism in living cells.

[1] V. Nasirimarekani, arXiv:2409.07095 (2024)
[2] V. Nasirimarekani, arXiv:2408.14129 (2024)

5.9 AIRBORNE IN-LINE HOLOGRAPHY: FROM VALIDATION TO PROCESSING OPTIMIZATION

B. Thiede, O. Schlenczek, F. Nordsiek, K. Stieger, A. Ecker, E. Bodenschatz, G. Bagheri

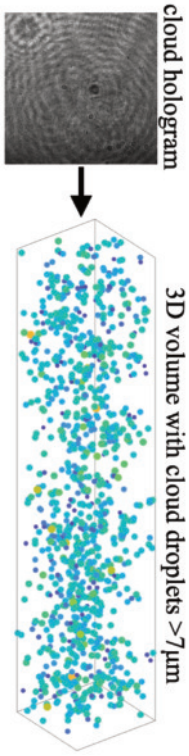

Figure 5.23: From in-situ holograms recorded with the Max-Planck-CloudKite$^+$ we extract the position and diameter of cloud droplets within a 3D sample volume.

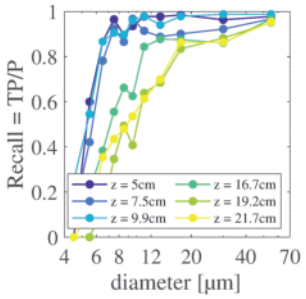

Figure 5.24: Recall as a function of droplet diameter and z-distance within the sample volume measured with our verification tool CloudTarget.

Critical gaps in understanding cloud microphysics, including cloud mixing, droplet clustering, and their effect on rain initiation, persist, despite their significant impact on Earth's weather and climate [1]. To bridge these gaps, advancements in small-scale measurement techniques are essential. In-line holography is an ideal imaging technique for the in-situ measurement of cloud droplets on small scales. It is based on recording the diffraction patterns from cloud droplets and subsequent reconstruction of the wavefront, from which the cloud droplets can be identified (Fig. 5.23). With the high sampling rates of our holographic instruments (Max-Planck-CloudKite$^+$ (MPCK$^+$) and HoloTrack), combined with the low true air-speed of the CloudKite (section 5.7), we achieve unprecedentedly low inter-hologram distances. During the EUREC4A campaign [2], the MPCK$^+$ recorded approximately 1 million holograms. The processing of this substantial amount of in-situ holograms to droplet data was a challenge. To address this, we improved the hologram noise filtering algorithms, developed a Convolutional Neural Network (CNN) classifier and the CloudTarget, a verification tool that allows accurate measurement of detection efficiency, size, and position. With CloudTarget, we were able to optimize detection, sizing, and classification thresholds, based on reliable ground truth evaluations. Our finely tuned processing now achieves over 90% recall and precision for particles larger than 7 µm within a 1.3 $\times$ 1.3 $\times$ 10 cm detection volume on MPCK$^+$ holograms (Fig. 5.24). Within this volume, we measured the average focus position uncertainty to be below 150 µm, the in-plane random position detection error to be smaller than 15 µm and a droplet sizing accuracy of $\sigma_d = 2$ µm [3]. Using our CNN classifier not only improved classification performance but yielded a 100-fold increase in classification speed compared to traditional supervised classification techniques. Overall, CloudTarget fills a crucial gap in the hologram processing verification and the improved noise filtering and the CNN classifier made the processing of our large amount of holographic data possible and accurate. These analysed holograms now provide spatially higher resolved statistics about droplet concentration, size distribution, liquid water content, and even complex statistics like the radial distribution function. Our advancements in holographic measurement and processing techniques offer promising insights into the highly intermittent nature of clouds [4].

[1] E. Bodenschatz, S.P. Malinowski, R.A. Shaw, F. Stratmann, Science **327**, 970 (2010)
[2] B. Stevens et al., Earth System Science Data **13**, 4067 (2021)
[3] B. Thiede, O. Schlenczek, K. Stieger, A. Ecker, E. Bodenschatz, G. Bagheri, EGUsphere, 2025, 1-39 (2025)
[4] B. Thiede, M.L. Larsen, F. Nordsiek, O. Schlenczek, E. Bodenschatz, G. Bagheri, arXiv:2502.19272 (2025)

5.10 SMARTIES: ATMOSPHERIC DISPERSION

G. Bagheri, T. Bhowmick, E. Bodenschatz, F. Falkinhoff
J. Josef, M. Burger, K. Ferdinand, T. Maul (Fraunhofer IIS)

The individual and relative motion of particles is fundamental to understanding transport processes in complex flows. For atmospheric flows, large-scale transport is well understood and measured by monitoring stations and satellite observations. However, our knowledge of smaller scales and the associated concentration fluctuations, i.e., at scales of 100 m to 50 km, is limited. This Fraunhofer-Max-Planck collaboration aims to build a system of intelligent atmospheric tracers so-called SMARTIES to measure information on atmospheric transport for the validation of models and numerical simulations, but also for rapid deployment in the field in cases where immediate and detailed knowledge of dispersion and transport details is needed to evaluate immediate risks to the population and the biosphere in general. SMARTIES are small and very lightweight measurement instruments consisting of environmental sensors and a wireless communication and localization unit integrated into a flight model with appropriate aerodynamic properties to maintain near-neutral buoyancy in the atmosphere for a few hours. During the flight, they transmit sensor data to a network of base stations for real-time location and data analysis with much increased time and space resolution compared to the state of the art.

A field campaign was successfully conducted with commercial sensors. To do this, we constructed a release mechanism that allows us to release up to 24 balloons simultaneously from an arbitrary altitude with the aid of the CloudKite (see Fig. 5.25).

Preliminary results show that atmospheric transport is anything but trivial, and there are different behaviours under different atmospheric and topographic conditions. Two more field campaigns are planned with the SMARTIES sensors that we are developing with the Fraunhofer IIS. This will provide better spatial resolution and will also allow us to gather more statistics under different weather conditions, and a larger number of balloons.

Figure 5.25: Left: Set of balloons attached to the CloudKite before a flight. Right: Release of balloons from an altitude of 600 m above ground level.

5.11 DIFFERENT REGIMES OF THE SPIRAL WAVE DYNAMICS IN THE BARKLEY MODEL

A. Krekhov, V. Zykov, E. Bodenschatz

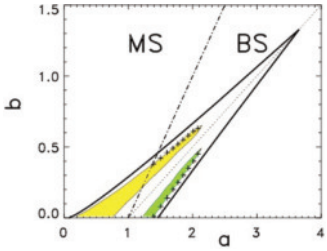

Figure 5.26: The dash-dotted line on the (a, b) parameter plane marks the boundary between the monostable region and the bistability domain, where $b < a - 1$. Within the yellow and green regions, spiral waves are meandering.

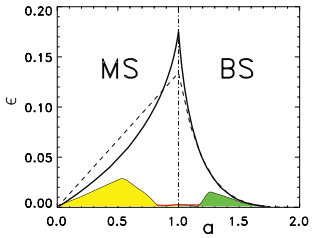

Figure 5.27: Unusual (a, ϵ) parameter plane. In the yellow and green regions, spiral waves are meandering. The narrow red region corresponds to the hysteresis domain.

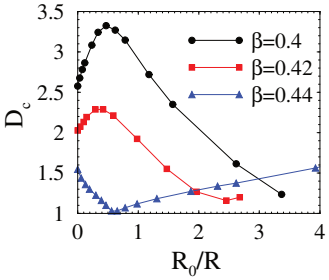

Figure 5.28: The critical values of D inside the circular region with radius R for the spiral rotating around as a function of the curvature R_0/R for various values of $\beta = b/a$.

The Barkley model has been widely used to simulate diverse reaction diffusion systems exhibiting various self-organization processes including creation of spiral waves resulting in a harmful electrical activity in cardiac or neuronal tissues. This study is concentrated on the general features of spiral wave dynamics in the Barkley model including both monostable and bistable dynamics [1–3].

The computation results clearly demonstrated the existence of the spiral waves within the bistability parameter range [1]. Moreover, the meandering spirals have been found after reducing the parameter ϵ, which characterizes the ratio between the time scales of the activator and the inhibitor, to $\epsilon = 0.01$ [3] (see Fig. 5.26). Spiral waves were observed within a triangular region in the parameters plane (a, b) bounded by two solid lines corresponding to the limiting cases of spiral waves with an infinitely large core and can be obtained analytically [3]. The dotted line shows the boundary between regions where the spiral core is positive or negative, expressed as $b = (a - 1)/2$. The spiral wave solutions obtained for (a, b) and $(a, a - b - 1)$ are symmetric and marked by crosses.

At the next step we analyzed the Barkley model with varying the parameters a and ϵ at a fixed value of $b = 0$, as shown in Fig. 5.27. The thick solid lines mark the boundaries of the region in which spiral waves are numerically observed and the dashed curves correspond to the analytical estimates [3]. The boundary between the monostable and bistable regions is now the straight line $a = 1$ and coincides with the boundary between the positive and negative core regions.

In the narrow parameter range shown in red in Fig. 5.27, the hysteresis phenomenon is found, i.e. at the same medium parameters it is possible to create rigidly rotating and meandering spiral waves depending on the initial conditions. Unusual dynamics of spiral waves and wave segments is also observed at a relatively large value of ϵ [3]. Obviously, in the future, it will be very useful and interesting to carry out similar studies within the whole 3D parameters space (a, b, ϵ).

In addition, we continue to investigate the spiral waves in an inhomogeneous medium with a sharp spatial increase in wave propagation velocity, fast propagation region (FPR) [4, 5]. For the spiral rotation around the circular FPR, our simulations based on the modified Barkley model show that the critical values of the diffusion coefficient D inside the FPR strongly depend on its radius (Fig. 5.28). In contrast to the homogeneous media, the circular FPR pins the rotating spiral.

[1] V.S. Zykov, E. Bodenschatz, New J. Phys. **24**, 013036 (2022)
[2] V.S. Zykov, E. Bodenschatz, Front. Appl. Math. Stat. **8**, 903563 (2022)
[3] V.S. Zykov, E. Bodenschatz, Phys. Rev. E. **110**, 064209 (2024)
[4] V.S. Zykov, A. Krekhov, E. Bodenschatz, PNAS **114**, 1281 (2017)
[5] V.S. Zykov, E. Bodenschatz, Annu. Rev. Condens. Matter Phys. **9**, 435 (2018)

5.12 FUNDAMENTALS OF TURBULENT FLOWS

E. Bodenschatz, F. Falkinhoff

A deep understanding of the fundamental mechanisms that drive turbulence is essential to push our knowledge of turbulent flows, which are present across various fields, including nature, technology and industry. Turbulent flows are multiscale, and can be qualitatively described through the concept of an energy cascade, where the energy is transferred at a constant rate (ε) from the bigger scales down to the smaller ones, until it is dissipated into heat. The intermediate range of scales where ε remains constant is the inertial range. These scales follow a phenomenological theory that is based on arguments on the randomness of turbulent motion, and they start at the integral scale, L, and end at the point where the energy is dissipated into heat near the Kolmogorov lengthscale η at the dissipation range. There have not been significant measurements of this range due to the lack of an appropriate measurement technique. Using the capabilities of the Variable Density Turbulence Tunnel (VDTT), we study the stochastic nature of turbulent flows and resolve their smallest scales.

Using helium, the VDTT and its active grid (GD), we have created a unique environment that allows us to measure the energy spectrum, $E(k)$, down to sub-Kolmogorov scales (see Fig. 5.29a). Future research involves the fabrication of nano-scale sensors that will be able to reach resolutions that have not yet been achieved.

Additionally, we explore how we can identify the deterministic behaviour of turbulent flows. We study this with the aid of the VDTT's AG, which makes it easy to study turbulence under controlled forcing mechanisms. We use the phase-averaged velocity signal $\langle u \rangle_{PA}$ and calculate its energy spectrum. Fig. 5.29b shows the ratio between the phase-averaged energy spectrum over N_T periods; what remains can be interpreted as the deterministic component of the velocity signal. We observe that the larger scales (smaller kL) remain deterministic, whereas the signal attenuates as $1/N_T$ in the inertial range (larger kL). Future research includes determining the universality of these results.

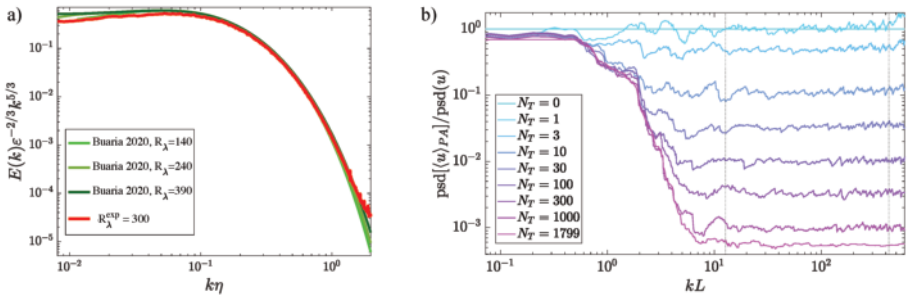

Figure 5.29: a) Energy spectrum compared to state-of-the-art simulations [1]. The energy dissipation range is well resolved up to approximately $2k\eta$. b) Attenuation of the energy spectrum for different number of phase averages.

[1] D. Buaria, K. Sreenivasan, Phys. Rev. Fluids **5**, 092601(R) (2020)

5.13 UNRAVELING THE COMPLEX DYNAMICS OF NON-SPHERICAL ATMOSPHERIC PARTICLES

T. Bhowmick, Y. Wang, J. Güttler, A. Pumir, P. Sharma, G. Bagheri, J. Latt (University of Geneva, Switzerland), K. Gustavsson (Gothenburg University, Sweden), B. Mehlig (Gothenburg University, Sweden), F. Candelier (CNRS, France), Y. Wang (ETH Zurich, Switzerland), D. Tatsii (University of Vienna), A. Stohl (University of Vienna)

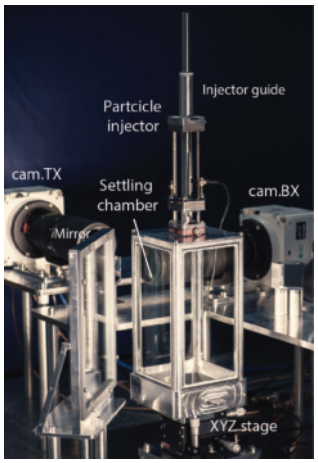

Figure 5.30: The Göttingen Turret consists of four high-speed cameras (only two cameras can be seen here) which, together with a novel particle injection mechanism, enable the three-dimensional tracking of the position and orientation dynamics of small particles in the air over a vertical distance of 60 mm from two perpendicular views. The particles are produced using a two-photon polymerisation 3D printer with sub-micron printing accuracy.

The chaotic fall of leaves or the drifting of dandelion seeds is familiar, but the behavior of smaller atmospheric particles like ice crystals, dust, volcanic ash, or microplastics is less understood. Traditional experiments in liquids suggest such particles fall smoothly, broadside down, if their Reynolds number matches that of atmospheric particles. However, our experiments and simulations in air reveal a different dynamic: small particles oscillate as they fall, creating complex trajectories. These oscillations increase the volume of air they traverse, enhancing their likelihood of interacting with other particles. The widespread presence of small, non-spherical particles and the reliance on studies in liquids or theoretical models for extremely small particles underscore the challenges in accurately characterizing their atmospheric behavior.

To address these challenges, we developed the Göttingen Turret experimental setup [1], a particle-resolved numerical framework Palabos Turret [2], and improved analytical tools [1, 3] for studying settling dynamics of arbitrarily shaped particles. Our findings reveal that heavy ellipsoids in air exhibit transient oscillatory dynamics resulting in complex settling motions [4], even in weak turbulence [1]. Non-axisymmetric ellipsoids display pronounced lateral drifts with twisting trajectories [4], while some curved fibers stabilize at oblique angles as they fall [3]. Microplastic settling velocities are highly shape-dependent, explaining their long-range atmospheric transport [5]. Ongoing work includes analyzing data from 3D-printed disk-like ice crystals and aerodynamically engineered micro-voyagers inspired by plant seeds.

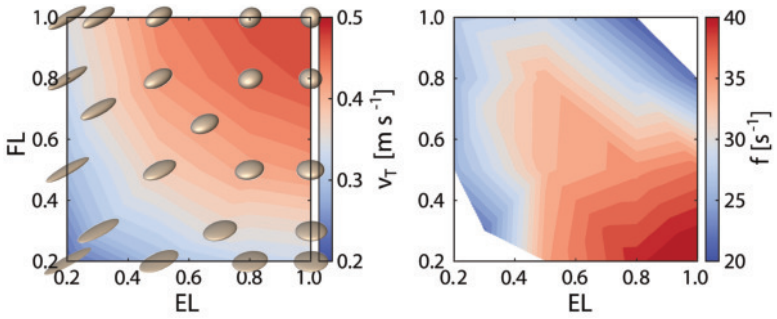

Figure 5.31: Phase space of the sinking velocity (left) and the oscillation frequency (right) of solid ellipsoids falling in air at a particle Reynolds number of about 5. The flatness, FL, is the ratio between the shortest and the intermediate axis, and the elongation, EL, is the ratio between the intermediate and the longest axis of the ellipsoid [4].

[1] T. Bhowmick, J. Seesing et al., Physical. Rev. Lett. **132**, 034101 (2024)
[2] T. Bhowmick, J. Latt, Y. Wang, G. Bagheri, arXiv:2408.15115 (2024)
[3] F. Candelier, K. Gustavsson, P. Sharma, et al, arXiv:2409.19004 (2024)
[4] T. Bhowmick, Y. Wang, J. Latt, G. Bagheri, arXiv:2408.11487 (2024)
[5] D. Tatsii, S. Bucci, T. Bhowmick, et al., Environ. Sci. Technol. **58**, 671 (2024)

5.14 THE WINDARTS: PRECISION AIRBORNE MEASUREMENTS WITHIN ATMOSPHERIC BOUNDARY LAYER

V. Chávez-Medina, H. Khodamoradi, E. Bodenschatz, G. Bagheri

The Max Planck WinDarts, developed by the CloudKite team at MPI-DS, are advanced airborne instruments designed to measure and characterize atmospheric turbulence in the boundary layer with high precision. These compact probes capture time series of temperature, pressure, humidity, wind velocity, volatile organic compounds, CO_2, and particle distributions, while also recording platform motions and geolocalization. Suspended from the tether connecting HeliKites (see 5.7) to the ground (see Fig. 5.32), WinDarts operate at altitudes up to 2 km, reaching higher frequencies than aircraft due to their zero relative velocity. Their design makes them ideal for field campaigns, overcoming the limitations of traditional setups.

During two campaigns in Pallas, Finland (September 2022 and May-June 2024, in collaboration with the Finnish Meteorological Institute), the WinDarts collected high-resolution turbulence data under diverse conditions. In the first campaign, two first-generation WinDarts recorded over 90 hours of data across 11 flights, capturing conditions such as in-cloud, free atmosphere, rain, and mixed-layer scenarios. The second campaign expanded efforts with five second-generation WinDarts, gathering 280+ hours of data across 10 flights, including shear layers, overnight measurements, and a thunderstorm. For instance, one of the most comprehensive flights from the first campaign recorded temperature, pressure, and relative humidity profiles across altitudes ranging from ground level to 841 m. This data has been instrumental in analyzing boundary layer stability and capturing the diurnal cycle. Additionally, comparisons with DNS data (Fig. 5.33) demonstrate a strong agreement, further validating the measurements [1].

The versatility of WinDarts also supports other research projects, showcasing their value as multi-purpose tools for atmospheric science.

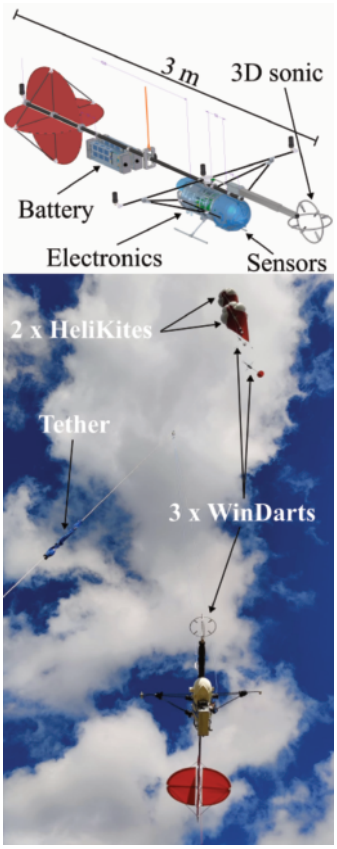

Figure 5.32: (Top) Lateral view of the second-generation WinDart showing key components. (Bottom) Two HeliKites with three WinDarts during the latest measurement campaign.

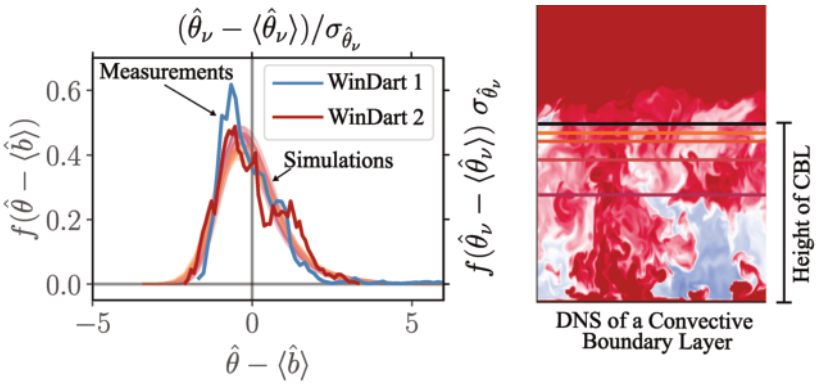

Figure 5.33: (Left) PDF of detrended and standardised virtual potential temperature fluctuations as measured by the first generation WinDarts, denoted as $(\hat{\theta}\nu - \langle\hat{\theta}\nu\rangle)/\sigma_{\hat{\theta}_\nu}$, contrasted with the PDF for buoyancy fluctuations, $\hat{\theta} - \langle\hat{b}\rangle$ from the convective boundary layer simulation. (Right) Snapshot of the buoyancy field. The coloured lines indicate the heights for which the PDFs are plotted in the left panel.

[1] V. Chávez-Medina, PhD thesis, University of Göttingen (2023)

5.15 PARTICLE DYNAMICS IN CLOUDS: INSIGHTS FROM THE ZUGSPITZE OBSERVATORY

P. Sharma, J. Moláček, G. Bertens, G. Bagheri, E. Bodenschatz

The collision-coalescence process in cloud droplets, driven by particle dynamics in turbulent environments, plays a critical role in cloud formation and precipitation. However, this process remains poorly understood due to the complex interactions influenced by turbulence.

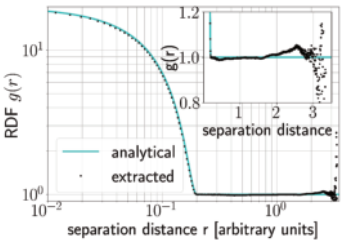

Figure 5.34: Comparison between the analytical result for RDF (g(r)) in the presence of Matérn clustering with cluster radius $r_c = 0.1$ (solid turquoise line) and the best estimate obtained by our method (black squares), on a log-log plot. A linear plot of the same is shown in the inset graph.

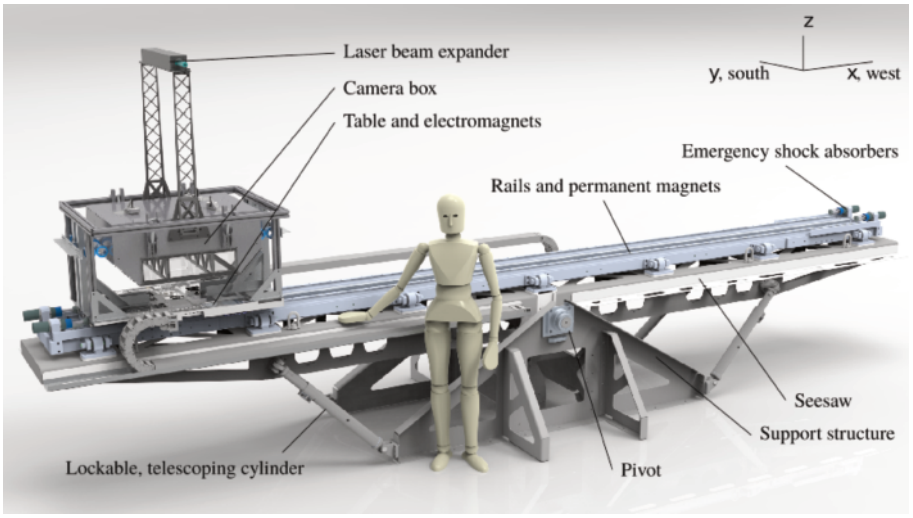

Figure 5.35: A computer render of the experimental setup. The seesaw supports a pair of 6.5 m long rails and slides an aluminium table that supports the camera box. The seesaw, rails, and table form a linear motor that makes the setup move with the mean wind. The seesaw can tilt by $\pm 15°$ [1].

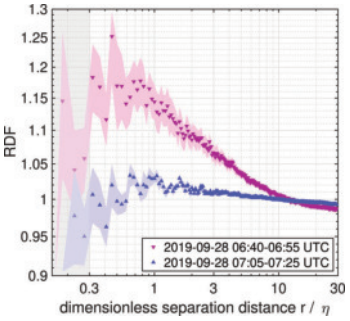

Figure 5.36: Two radial distribution functions (RDFs) of cloud droplets at Zugspitze as a function of their non-dimensional separation r/η. The purple and blue symbols are the computed experimental samples for which the Stokes number is St $\approx$ 0.1 and 0.01 respectively. The colored regions indicate the regions within one standard deviation from the mean value. The decrease for $r < 0.3\eta$ (gray shaded area) could be a measurement artefact; here, further investigation is needed.

To study cloud droplet collision rates, we built a particle tracking setup (see Fig. 5.35 and [1]) at the environmental research station Schneefernerhaus. The setup provides three-dimensional droplet positions and diameters with micrometre precision, enabling analysis of droplet spatial arrangement via the Radial Distribution Function (RDF).

The RDF provides a statistical measure of the probability of finding a droplet at a specific distance from a reference droplet, compared to a uniform distribution. If the value of RDF exceeds 1, it indicates clustering, meaning that droplets are more likely to be found at that specific distance than in a random, uniform distribution. We derive a general formula of RDF, and compare it with numerical simulations for standard geometries such as spheres, cylinders, cubes, prisms, toroids and cones (see Fig. 5.34). We leverage this methodology to study the clustering behaviour of particles in the observatory (see Fig. 5.36).

The setup also provides the droplet size information, which can be used to compute parameters related to cloud microphysics and the Stokes number, the dimensionless parameter indicating the droplets' inertia, allowing us to compare our measurements with existing in-situ measurements, numerical simulations and theoretical results.

[1] G. Bertens, G. Bagheri, H. Xu, E. Bodenschatz, J. Moláček, Rev. Sci. Instrum. **92**, 125105 (2021)

5.16 HYDRODYNAMIC CONSISTENCY IN MANY-BODY DISSIPATIVE SYSTEMS PLUS MAKING NANOMOTORS

R. Golestanian

Since the inception of the Onsager regression hypothesis, understanding the violation of the formal correspondence between fluctuations and response functions has guided many conceptual developments in non-equilibrium statistical physics, notably, the establishment of the Harada-Sasa relation.[1] In a recent work [1], the effect of hydrodynamic interactions on the non-equilibrium stochastic dynamics of particles—arising from the conservation of momentum in the fluid medium—is examined in the context of the relationship between fluctuations, response functions, and the entropy production rate. In our stochastic dynamics, the αth particle is described by position $r_i^\alpha(t)$ and force $f_i^\alpha(t)$. Here, we consider the most general case in which the individual force acting on a given particle can depend on the position of the particle itself (arbitrary external force) as well as the positions of the other particles (arbitrary interactions, including many-body interactions). The generality of the choice for the forces will enable us to apply this formalism to a variety of active and driven systems.

The multiplicative nature of the hydrodynamic interactions introduces subtleties that preclude a straightforward extension of the Harada-Sasa relation [1]. We derive a generalized Harada-Sasa relation that is consistent with the momentum conservation of the fluid medium, as follows

$$T\dot{\sigma} = \int_{-\infty}^{\infty} \frac{d\omega}{2\pi} \left[\tilde{\mathcal{C}}'^{\alpha\alpha}_{g,ii}(\omega) - 2k_{\rm B}T\tilde{\mathcal{R}}'^{\alpha\alpha}_{g,ii}(\omega) \right], \tag{5.2}$$

in terms of appropriately generalized response functions $\mathcal{R}^{\alpha\gamma}_{g,ik}(t-t') \equiv \delta \left\langle \mathcal{Z}^{\alpha\beta}_{ij}\left(\{r^\nu_l(t)\}\right)\dot{r}^\beta_j(t)\right\rangle_{f^\gamma_{k,\rm ext}} / \delta f^\gamma_{k,\rm ext}(t')\Big|_{f^\gamma_{k,\rm ext}=0}$, and appropriately generalized correlation functions $\mathcal{C}^{\alpha\gamma}_{g,ik}(t-t') \equiv \left\langle \mathcal{Z}^{\alpha\beta}_{ij}\left(\{r^\nu_l(t)\}\right)\dot{r}^\beta_j(t)\dot{r}^\gamma_k(t')\right\rangle$. Note that in this case $\tilde{\mathcal{C}}^{\alpha\alpha}_{g,ii}(\omega)$ can have both real and imaginary parts, because in general $\mathcal{C}^{\alpha\alpha}_{g,ii}(t-t') \neq \mathcal{C}^{\alpha\alpha}_{g,ii}(t'-t)$. Equation 5.2 can be understood as a balance between the work done by the viscous drag forces, the contribution from the stochastic Brownian forces, and the work done by the active driving forces. The resulting framework will enable characterization of the non-equilibrium properties of living and active matter systems, which are predominantly in suspensions.

In collaboration with the groups of C. Dekker (TU Delft) and H. Dietz (TUM), I worked on strategies to design and characterize synthetic nano-scale motors [2–4]. The work included verification of the non-equilibrium fluctuation theorem in the synthetic nano-motors.

1. The Harada-Sasa relation connects the rate of entropy production $\dot{\sigma}$ in a driven non-equilibrium system under stationary-state conditions to the spectral sum of the violation of the fluctuation-dissipation theorem, i.e. the difference between the velocity correlation function $\mathcal{C}(t)$ and the response function $\mathcal{R}(t)$ in the frequency domain. For a single particle (in 1D) with friction coefficient ζ immersed in a medium with temperature T, the Harada-Sasa relation is written as $T\dot{\sigma} = \zeta\bar{V}^2 + \zeta\int_{-\infty}^{\infty}\frac{d\omega}{2\pi}\left[\tilde{\mathcal{C}}(\omega) - 2k_{\rm B}T\tilde{\mathcal{R}}'(\omega)\right]$, where $\bar{V}$ is the mean velocity, $k_{\rm B}$ is the Boltzmann constant, and $\tilde{\mathcal{R}}'(\omega) = \frac{1}{2}[\tilde{\mathcal{R}}(\omega) + \tilde{\mathcal{R}}(-\omega)]$ is the real part of the response function.

[1] R. Golestanian, Phys. Rev. Lett. **134**, 207101 (2025)
[2] A.-K. Pumm et al., Nature **607**, 492 (2022)
[3] X. Shi et al., Nat. Phys. **18**, 1105 (2022)
[4] X. Shi et al., Nat. Nanotechnol. **19**, 338 (2023)

5.17 COMPLEX DYNAMICS IN THE SPREAD OF COVID-19

S. Contreras, J. Dehning, P. Dönges, S. Bauer, J. Wagner, J. Zierenberg, P. Spitzner, L. Müller, V. Priesemann
F. Sartori, M. Mäs (KIT), T. Krüger (Wroclaw), K.Y. Oróstica (Talca)

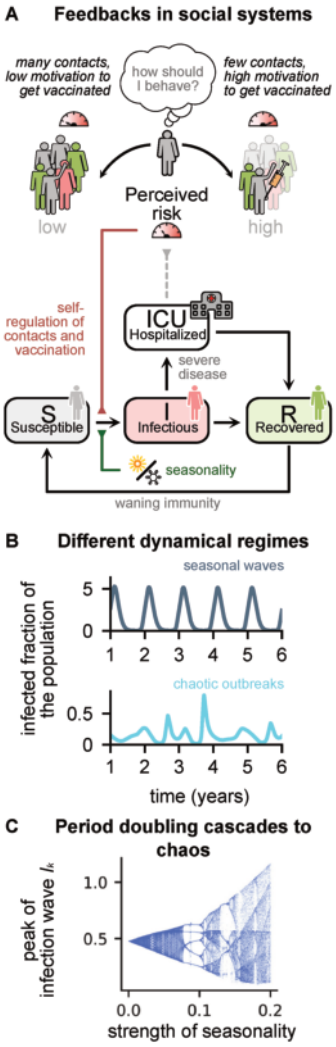

Figure 5.37: Interplay between risk perception, behavior, and disease spread. **A:** Individuals adapt their behavior according to the current state of the epidemic, thereby affecting the spreading rate of the disease through feedback loops. Behavioral feedback and seasonality combined may cause irregular epidemic waves (**B**) and feature a period-doubling cascade to chaos (**C**). Adapted from [1, 5, 15].

Understanding the basic principles behind the spreading dynamics of infectious diseases is critical for the well-being of societies. However, this is not an easy task: contagion, mediated mainly by human behavior, is complex. Examples of such complexity are the plasticity of contact networks, pathogens constantly evolving, and the fact that not all epidemiological variables and parameters can be observed from data. However, questions like "why do some pathogens exhibit biennial large surges?" or "how likely is a new emerging infectious disease to cause a global-scale outbreak?" can easily be mapped to problems of bi-stability and criticality. Consequently, statistical physics and nonlinear dynamical systems theory find broad applications in revealing, understanding, and quantifying the drivers and mechanisms behind such complexity. Our research at the MPRG Complex Systems Theory pushed forward the state-of-the-art in infectious disease modeling [1–5], simulation tools to evaluate counterfactual scenarios [6], forecast epidemic trends [7], epidemiological parameter inference [8–10], and optimization of mitigation and surveillance with limited data [11–13], besides condensing new knowledge into viable, and timely, policy recommendations [14, 15].

On short timescales (days, weeks), once a deviation from the normal levels of a disease or the emergence of a new disease with epidemic potential has been reported, policymakers and health authorities deploy a portfolio of interventions to contain the outbreak or mitigate the spread. However, what ultimately determines how effectively these interventions reduce the spreading rate of a disease is individuals' adherence to them. As information about an outbreak becomes available, individuals update their attitude toward the disease and the risk they perceive, which changes their behavior [1, 4, 5]. These behavioral changes can be reflected in different timescales: Individuals decide whether (and how properly) they wear a mask daily, while they would take longer before accepting a vaccine if hesitant (Fig. 5.37A). This behavior-driven modulation of the spreading rate results from the interplay between information, opinion, behavior, and disease spread and opens a wide variety of dynamical regimes. Mechanistically, epidemiological models can include mitigation efforts as feedback loops, featuring rich long-term dynamics, such as high-periodic wave patterns and period-doubling cascades to chaos (Fig. 5.37B, C).

On longer timescales (months, years), the evolutionary dynamics of the pathogen can play a major role, e.g., through the emergence of new variants with higher pathogenicity or transmissibility. One of the mechanisms used to monitor this evolution is genomic surveillance, where the mutational dynamics of a particular pathogen are tracked and quantified. Combining existing surveillance programs with our Bayesian inference framework to quantify the spreading rate of COVID-

19 [8], we quantified the spreading rate of the predominant SARS-CoV-2 variants in Chile [10]— a country challenged with limited sequencing capacities. Inferring global properties from limited data is not easy, as the sampling protocol selected can introduce biases in the estimations [12]. We also worked with scientists of the Chilean Public Health Institute to optimize sampling protocols for genomic surveillance using models and derived a set of simple rules for protocols to be robust and generate representative samples [13].

In general, diseases and societies interact and co-evolve. The intrinsic timescales of each can also interact and drive the epidemic dynamics. For example, periodic contact patterns in day-to-day life can resonate with the typical incubation and latent periods of a disease, thereby increasing the size of an outbreak [2]. Quantifying the disease's pace is critical to mitigate the impacts of large-scale events in an epidemic. We demonstrated that football matches in the context of a multinational championship could increase the nationwide reproduction number by as much as 3 in that day [9], which, together with the latent period of COVID-19 of about 4 days resonating with the typical distance between matches of the same country, had a major impact on the development of the pandemic (cf to Fig. 5.38). Understanding how to mitigate these impacts while still trying to maximize freedom and minimize the disruption to everyday life is thus critical. We have developed a battery of models that, given a known mechanism for the spreading dynamics of a disease (e.g., whether it follows an SIR or an SIS dynamics), determine the shape of the optimal mitigation function ([11] and Chapter 5.18). However, determining what combination of known interventions gives rise to such a mitigation function remains a non-trivial open problem with many possible solutions.

Altogether, our results were highly relevant for societies and decision-makers, making the Max Planck Institute for Dynamics and Self-Organization highly visible in the context of COVID-19 mitigation in Germany. Pandemic surveillance and control, vaccination, good public communication, international cooperation, and a holistic One Health view will remain crucial to addressing current and future pandemics.

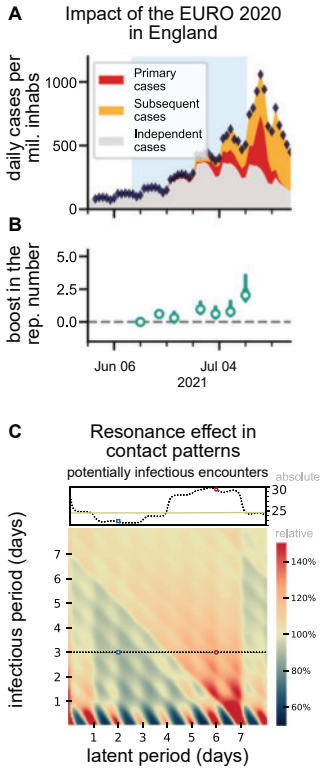

Figure 5.38: Impacts of large events in the spread of infectious diseases. **A:** The surge in COVID-19 case numbers following EURO 2020 football matches in England. **B:** Singular matches increased the country-wide reproduction number by as much as three units on the day of the match **C:** Part of this large impact can be attributed to resonance effects following contact patterns, where the frequency of the events aligns with the timescales of the disease (infectious period and latent period). Adapted from [2, 9].

[1] P. Dönges et al., Front. Phys. **10**, 842180 (2022)
[2] J. Zierenberg et al., New J. Phys. **25**, 053033 (2023)
[3] P. Dönges et al., SIAM J. Appl. Math. **84**, 1460 (2024)
[4] A. Reitenbach et al, Rep. Prog. Phys. **88**, 016601 (2024)
[5] J. Wagner et al., Phys. Rev. Res. **7**, 013308 (2025)
[6] A. Kekić et al., Patterns **4**, 100739 (2023)
[7] K. Sherratt et al., eLife **12**, e81916 (2023)
[8] J. Dehning et al., Science **369**, eabb9789 (2020)
[9] J. Dehning et al., Nat. Commun. **14**, 122 (2023)
[10] K. Y. Oróstica et al., Sci. Rep. **14**, 16000 (2024)
[11] L. Müller et al., *in preparation*
[12] A. Levina, V. Priesemann, J. Zierenberg, Nat. Rev. Phys. **4**, 770 (2022)
[13] S. Contreras et al., Chaos, Solitons & Fractals **167**, 113093 (2023)
[14] V. Priesemann et al., Lancet **398**, 838 (2021)
[15] S. Contreras, E. N. Iftekhar, V. Priesemann, Lancet Eur. **30**, 100664 (2023)

5.18 SELF-REGULATION FOR INFECTIOUS DISEASE: OPTIMAL MITIGATION IN THE ENDEMIC STATE CAN INCUR CHAOTIC DYNAMICS

S. Bauer, L. Müller, J. Wagner, J. Dehning, P. Dönges, S. Contreras, L. Fleddermann, R. Amaral Lind, U. Parlitz, V. Priesemann
F. Sartori (Karlsruhe), M. F. Eggl (Alicante)

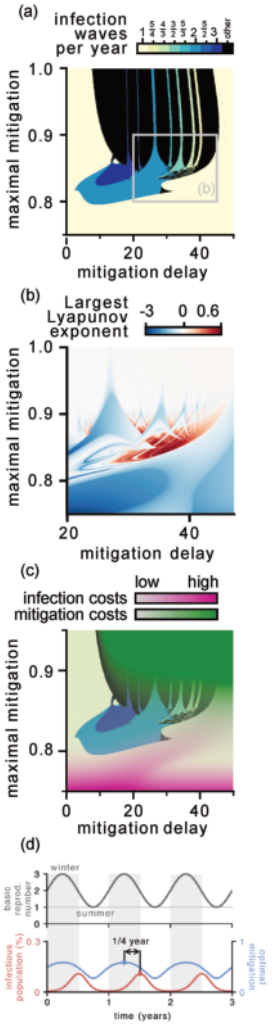

Figure 5.39: A seasonally driven SIRS model with delayed societal feedback yields highly complex dynamics, sensitive to mitigation parameters (a) and initial conditions (b). (c) The complex and chaotic regime coincides with the regime of joint low infection and low mitigation costs for society. (d) Sinusoidal seasonal fluctuations in the basic reproduction number lead to a fluctuating optimal, preemptive mitigation strategy. The infection number in this case show a single infection wave with low amplitude in spring.

Social contact behavior is a key determinant of epidemiological spread [1, 2]. If infections are severe, societies will mitigate their spread, e.g., by reducing contacts and implementing hygiene measures. This reaction can be delayed to the spread, which incurs waves of infection: People react only when infection numbers reach high levels, eventually 'breaking' the wave, and risking a rebound wave when relaxing behaviour back to normal after infection numbers have lowered again. In a compartmental SIR model that includes such a delayed feedback mechanism, periodic waves of infection emerge as a Hopf bifurcation of the endemic equilibrium. We analyzed how these human behaviour-driven oscillations interact with an external forcing induced by seasonal variations in the spreading rate [3]. Like in classic driven oscillatory systems, this interaction leads to highly complex, parameter sensitive, and chaotic dynamics (Fig. 5.39a,b). Importantly, we demonstrate that these complex dynamics occur in parameter regions where the disease burden and economical costs for society are jointly minimized (Fig. 5.39c). Data analysis of past influenza and COVID-19 infections indicate that the observed complexity of COVID-19 dynamics was due to this interplay of mitigation efforts and seasonality.

We then developed a systematic framework to derive optimal mitigation strategies [4]. The optimal mitigation is defined as the strategy that minimizes the total costs, encompassing infection and mitigation costs. By applying this framework to different scenarios, we can quantify (1) how much delaying the onset of mitigation measures entails additional costs, and (2) that the necessary mitigation strength increases with the emergence of a more infectious variant. (3) When the basic reproduction number fluctuates seasonally, optimal mitigation also varies, with stricter measures in winter and more relaxed measures in summer, preventing large infection waves during the fall and winter months (Fig. 5.39d). (4) Lastly, we show that vaccination allows for a decrease in mitigation stringency. Thus, proactive, preventative measures minimize costs, and, consequently, deaths.

[1] J. Dehning, et int., V. Priesemann, Nat. Commun. **14**, 122 (2023)
[2] P. Dönges, et int., V. Priesemann, Front. Phys. **10**, 842180 (2022)
[3] J. Wagner, et int., V. Priesemann, Phys. Rev. Research **7**, 013308 (2025)
[4] L. Müller, et int., V. Priesemann, *in preparation*

5.19 INFLUENCE OF PHYSICAL INTERACTIONS ON PHASE SEPARATION AND PATTERN FORMATION

Chengjie Luo, Yicheng Qiang, Lucas Menou, David Zwicker

Biomolecular condensates are complex droplets composed of various biomolecules, including nucleic acids and proteins. These condensates form mainly due to liquid-liquid phase separation, which is driven by short-range attraction between biomolecules. However, other complex physical interactions, such as high-order and long-range interactions, and non-linear chemical reactions between biomolecules can also significantly influence phase separation. Generally, complex spatiotemporal patterns can emerge from the interplay between chemical reactions and spatial motion like ideal diffusion. Physical interactions inevitably affect spatial motion and thus pattern formation. In this project, we systematically study the significant effects of physical interactions on phase separation and pattern formation using a few simple models.

We first focused on a multicomponent mixture described by Flory-Huggins theory extended by higher-order interactions [1]. Such interactions are typical for biomolecules, e.g., because a single molecule may interact with multiple others simultaneously. As a first step, we studied the effects of cubic interactions on phase separation. Interestingly, we observed two distinct classes of cubic interactions (Fig. 5.40): one is the binary cubic interaction $b_{ijj}\phi_i\phi_j^2$ which only involves two species, and the other is the ternary cubic interactions $b_{ijk}\phi_i\phi_j\phi_k$ between three different species. We found that the ternary cubic interactions are similar to pairwise interactions, where repulsion promotes phase separation and leads to a larger number of phases. In contrast, repulsive binary cubic interaction can oppose phase separation, whereas attraction can promote more phases. Moreover, by studying random interaction matrices, we discovered that the variance of binary cubic interactions raises the phase count more than that of ternary interactions. Importantly, the actual phase count M in equilibrium is much higher than the number of unstable modes U from a linear stability of the homogeneous state (Fig. 5.41). Higher-order interactions further increased this deviation. This hints at an enormous parameter regime with multiple locally stable states in multicomponent mixtures with higher-order interactions. In biological cells, such multistability could be used to control the formation or dissolution of droplets. Taken together, we found that higher-order interactions could play a crucial role in forming droplets in cells, and their manipulation could offer novel approaches to control multicomponent phase separation.

We next considered long-range interactions due to charges, which are typical in nucleic acids and proteins. Typically, it is thought that electrostatic interaction cannot result in long-range effects since mobile salt ions induce strong screening effects. However, when strong short-range interactions exist, phase separation can happen, which could affect the distribution of ions and thus suppressing screening. To clarify the interplay of phase separation and long-range interaction, we study a model of two polymers with short-range attraction and opposite

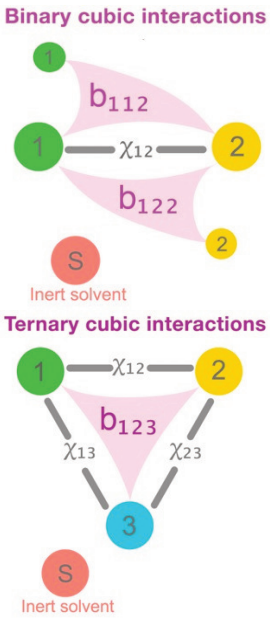

Figure 5.40: Schematics of binary cubic interactions (top) and ternary cubic interactions (bottom) b_{ijk} together with ordinary pair interactions χ_{ij}.

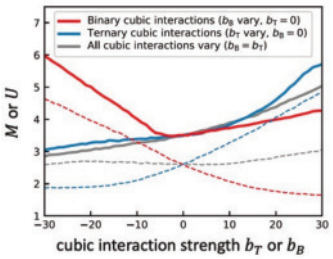

Figure 5.41: Binary and ternary cubic interactions have opposite effects on the phase count M. The mean phase count M (solid curves) and the number of unstable mode U (dashed curves) are shown as a function of the binary cubic interactions b_T or ternary cubic interactions b_B for three cases distinguished by color.

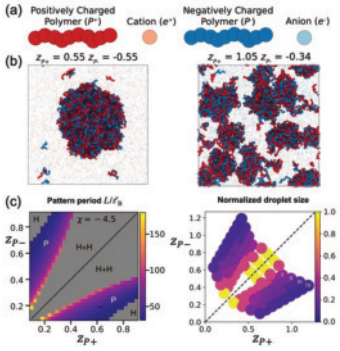

Figure 5.42: (a) Schematic of the charged polymer system. (b) Snapshots from molecular dynamic simulations at charge symmetry (left) and charge asymmetry (right). (c) Phase diagram as a function of the charge numbers z_{P+} and z_{P-} of the polymers predicted from mean-field theory revealing parameter regions with coexistence of two homogeneous phases (H+H), patterned phases (P), and homogeneous phase (H). The density plots show the droplet size from mean-field theory (left) and molecular dynamics simulation (right).

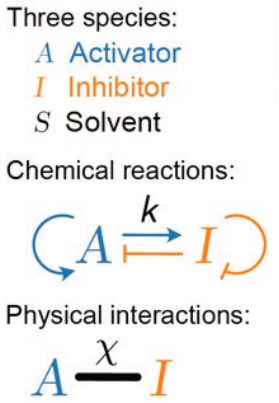

Figure 5.43: Schematic of the extended Turing model with Hill-Langmuir reactions.

charges together with small ions [2]; see Fig. 5.42a. We numerically obtained phase diagrams from an associated Flory-Huggins theory extended by the electrostatic energy. We found that charged polymers segregate from the solvent, and thus form two macrophases, when their charges are symmetric. In contrast, many droplets of equal size coexist when charge asymmetry is sufficiently strong; see Fig. 5.42b. Such patterned phases form because the short-range attraction concentrates polymers within droplets, leading to net charges, which prevents further growth. Such droplets also expel small ions, effectively weakening the screening within droplets. Moreover, the theory predicts that droplet size decreases with larger charge asymmetry, which qualitatively agrees with molecular dynamics simulation; see Fig. 5.42c. In summary, we unveiled a mechanism controlling droplet size via a trade-off between short-ranged attraction driving phase separation and long-ranged electrostatic repulsion if droplets accumulate net charges.

Finally, we investigated chemical reactions, which are ubiquitous in cells and can drive the system into nonequilibrium state. Specifically, we extended the Cahn-Hilliard equation (Model B) with active chemical reactions to investigate the influence of physical interactions on two representative nonlinear chemical reactions: the Hill–Langmuir equation, generating static Turing patterns for ideal diffusion (Fig. 5.43), and cyclic-dominant reactions, like the seminal rock-paper-scissors game, yielding dynamic spiral waves. In the Hill–Langmuir system, we found that weak repulsion substantially lowers the required differential diffusivity and reaction nonlinearity for Turing pattern formation, while strong interactions can induce phase separation [3]. For cyclic-dominant reactions, we found that weak interactions change the length- and time-scales of spiral waves [4]. In contrast, strong repulsive interactions typically generate oscillating lattices, and strong attraction leads to an interplay of phase separation and chemical oscillations, like droplets co-locating with cores of spiral waves; see Fig. 5.44. Despite the distinct nature of the two chemical reactions, physical interactions play a crucial role in pattern formation in both cases.

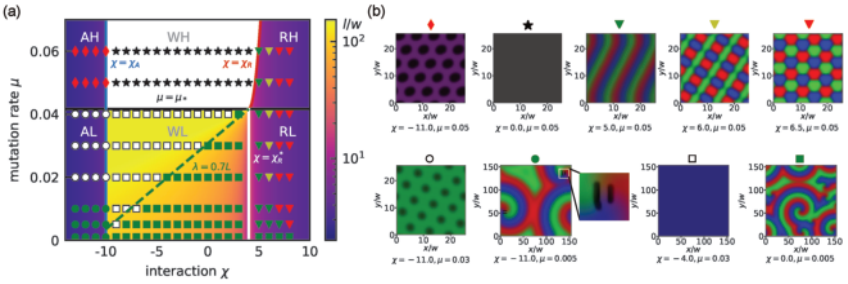

Figure 5.44: Numerical simulations reveal diverse patterns for the rock-paper-scissors model. (a) Phase diagram with (b) diverse spatiotemporal patterns.

[1] C. Luo, Y. Qiang, D. Zwicker, Phys. Rev. Research **6**, 033002 (2024)
[2] C. Luo*, N. Hess*, D. Aierken, Y. Qiang, J. A. Joseph, D. Zwicker, arXiv:2409.15599 (2024)
[3] L. Menou* , C. Luo* and D. Zwicker, J. R. Soc. Interface. **20**, 20230244 (2023)
[4] C. Luo, D. Zwicker, Phys. Rev. E **108**, 034206 (2023)

5.20 VORTEX BREAKDOWN IN WIND TURBINE WAKES

L. Le Turnier, H. Kim, M. Grunwald, C. E. Brunner

Wind turbines extract kinetic energy from the incoming flow and convert it into electricity. This leads to a momentum deficit in the wake region immediately downstream of the turbine. Turbulent entrainment of momentum into the wake re-energizes the flow over time. Due to the typical spacing between turbines in a wind farm, the wake of an upstream turbine often reaches a downstream turbine before the flow has been fully re-energized. The less kinetic energy there is in the flow, the less of it a wind turbine can extract, so the output of the downstream turbine is reduced. How to re-energize the flow behind the turbine as rapidly as possible is a central question in wind energy science. Wind turbine wakes are far more complex than canonical wakes behind bluff bodies due to the presence of tip vortices shed from the three blade tips, as well as a root vortex shed from the turbine hub. We conduct three-dimensional Lagrangian particle tracking experiments to develop a Lagrangian description of vortex breakdown in wind turbine wakes and the mechanisms involved.

5.20.1 3D Lagrangian particle tracking in the Variable Density Turbulence Tunnel

(L. Le Turnier, H. Kim, C. E. Brunner) The Variable Density Turbulence Tunnel allows us to recreate complex large-scale atmospheric flow conditions within a highly-controlled environment. Unlike in field experiments, we have full control over the flow as well as the turbine. This approach is ideal for studies which require large amounts of data for the statistics to converge, or large parameter sweeps to identify scaling laws. This experiment is unique not only in its ability to achieve dynamic similarity with real wind turbine flows, but also its ability to accommodate high particle densities, providing large amounts of information about instantaneous realisations of the flow within the measurement volume.

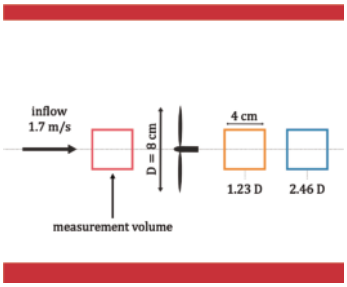

Figure 5.45: Schematic of the setup including the positions of the measurement volumes.

Experimental setup. We use the Variable Density Turbulence Tunnel (VDTT, see [1]) in the Max Planck Turbulence Facility at the MPI-DS 9.8. The tunnel can be filled with sulfur hexafluoride at up to 15 bar to match the Reynolds numbers of large-scale atmospheric flows. An active grid [2] consisting of 111 individually controllable paddles allows for precise control of spatial and temporal correlations in the turbulence. Our Lagrangian Particle Tracking (LPT) [3] setup is located in the upper test section of the VDTT. We use 30 μm cellulose particles as tracers. To illuminate the particles, we use a 300 W Nd:YLF laser. The size of the laser beam defines the dimensions of the measurement volume, resulting in a volume of $V = 4 \times 4 \times 4\,\mathrm{cm}^3$ (see Fig. 5.45). We capture the displacement of the particles using four Phantom high-speed cameras positioned at different angles. These cameras have a frame rate of up to 10 kHz and a resolution of 2560×1664 pixels. The time-resolved three-dimensional positions of the particles are obtained

using the Low Light Lagrangian Particle Tracking (L3PT) code, which was developed by scientists in the LFPB group based on the shake-the-box algorithm. An exemplary trajectory obtained with the L3PT code is shown in Fig. 5.46. From the time-resolved particle positions, we can deduce their velocities and accelerations.

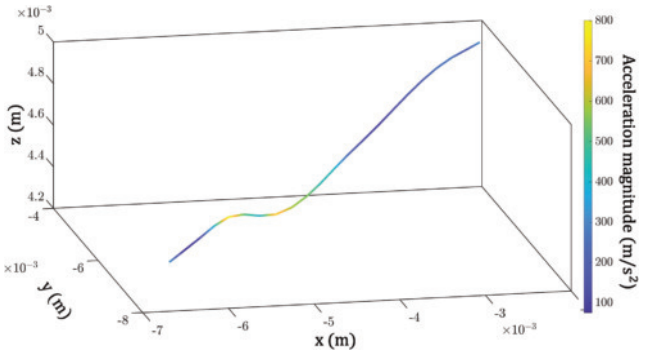

Figure 5.46: Exemplary reconstruction of the trajectory of a cellulose particle in the measurement volume using the L3PT code.

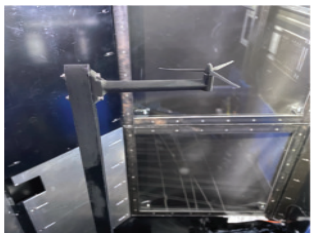

Figure 5.47: The model wind turbine used here was 3D-printed in the MPI-DS machine shop. It has a diameter of D = 8 cm.

Identifying intermittency in a wind turbine wake. Wind turbine wakes contain various coherent structures. One of these is the hub vortex, which is shed off the nacelle in the center of the rotor and convects downstream within the near-wake, dissipating quickly. Its breakdown generates turbulence within the core of the wake, thus affecting wake re-energization. In addition, these coherent structures impose unsteady loads on the nacelle and the tower, reducing the lifespan of the wind turbine. Thus, studying the formation and dissipation mechanisms of the hub vortex is crucial for understanding turbulence evolution within the wind turbine wake and enhancing wind turbine performance.
To investigate the signature of the hub vortex in the wake velocity statistics, we exposed a model wind turbine to a turbulent inflow (see Fig. 5.47) and sampled the flow at the center of the wake at multiple downstream positions. The probability density functions of the velocity fluctuations are shown in Fig. 5.48.

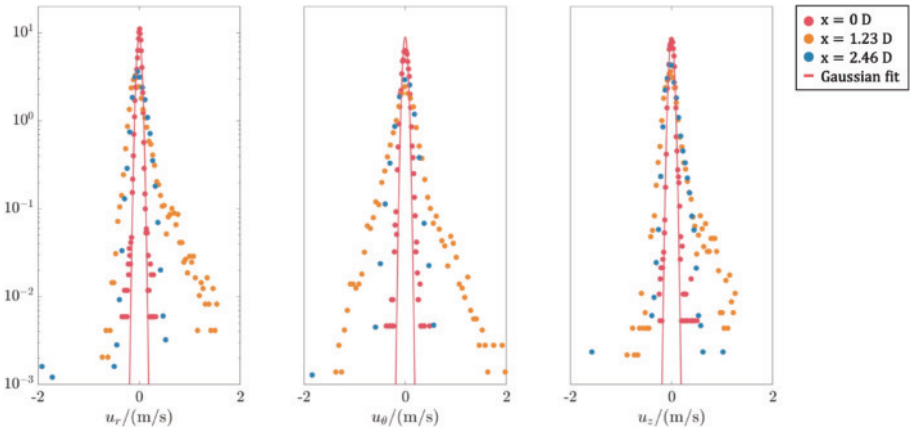

Figure 5.48: Probability density functions of the component of the velocity fluctuations in radial direction (left), angular direction (middle) and streamwise direction (right). $x = 0D$ indicates the flow at the position of the turbine rotor when the turbine absent, i.e. the inflow condition experienced by the turbine.

Under homogeneous isotropic turbulence conditions, the probability density function (PDF) of the velocity fluctuations typically resembles a Gaussian distribution. This is also observed for the PDF of the inflow ($x = 0D$). However, at a distance of $x = 1.23D$ downstream (where D

represents the wind turbine diameter), the tail of the PDF exhibits a "fatter" shape. This indicates that there is a higher occurrence of large velocity fluctuations compared to what would be expected from a Gaussian distribution. This phenomenon is known as intermittency, and it manifests as infrequent but extreme events within the flow. Furthermore, in the radial and streamwise directions, the PDF is asymmetric, which indicates that the hub vortex leads to preferential directions for fluctuations. At $x = 2.46D$, the PDF returns to a Gaussian shape, suggesting that the hub vortex has broken down, transitioning the wake back to a more homogeneous and isotropic flow.

Intermittency is particularly pronounced at small scales, highlighting the importance of examining turbulence statistics at different scales to gain insights into the persistence or decay of turbulence within the wake. Our results indicate that the hub vortex has already dissipated between $x = 1.23D$ and $x = 2.46D$. The next step is therefore to increase the spatial resolution of the measurements and analysis in order to elucidate the vortex breakdown process and mechanisms.

5.20.2 3D Lagrangian particle tracking in the atmosphere

(M. Grunwald, C. E. Brunner) Alongside our particle tracking efforts in the VDTT, we are developing a field experiment to validate the results we obtain in the laboratory experiments. A schematic of the setup is shown in Fig. 5.49. Similar to the setup in the VDTT, four cameras are used to span a measurement volume (marked in red). The flow is seeded by helium filled soap bubbles upstream of the wind turbine, which are illuminated at the position of the measurement volume. The use of helium filled soap bubbles as tracers for large measurement volumes has been investigated in laboratory environments [4] and recently in a field experiment [5].

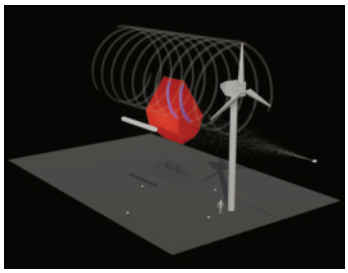

Figure 5.49: Schematic of the setup in the field experiment. The schematic is to scale.

The schematic also shows the tip vortices as one of the dominant structure in the near wake. With the presented setup, we will be able to see multiple tip vortices in the measurement volume, highlighting interaction events between the vortices. Furthermore, the setup allows us to study the entrainment of energy and therefore the re-energization of the wake, which is crucial in wind farm development.

The use of Lagrangian particle tracking will be a novel approach to the study of wind turbine wakes at field scales: Only few studies have conducted experiments at these scales. As most of them obtain only averaged velocity fields without detailed information about the particle tracks, our experiment will allow for a new perspective regarding the Lagrangian statistics of turbulence.

[1] E. Bodenschatz, G. P. Bewley, H. Nobach, M. Sinhuber, H. Xu, Rev. Sci. Instrum. **85**, 093908 (2014)
[2] K. P. Griffin, N. J. Wei, E. Bodenschatz, G. P. Bewley, Exp. Fluids **60**, 55 (2019)
[3] C. Küchler, G. Bewley, E. Bodenschatz, J. Stat. Phys. **175**, 617 (2019)
[4] J. Hou, F. Kaiser, A. Sciacchitano, D. Rival, Exp. Fluids **62**, 100 (2021)
[5] N. Conlin, H. Even, N. J. Wei, N. A. Balantrapu, M. Hultmark, Meas. Sci. Technol. **35**, 095803 (2024)

5.21 THERMAL EFFECTS ON WIND TURBINE AND FARM FLOWS

Y. Hattori, C. E. Brunner

Wind farm performance depends on the transport and redistribution of momentum from the turbulent atmospheric flow to the wind turbines. We study the effect of atmospheric stability on turbulent transport phenomena in wind turbine wakes. During daytime, thermal radiation causes the ground to be warmer than the air flow above (see Fig. 5.50). In this case, the atmospheric flow is unstable and buoyancy-generated turbulence dominates over shear-generated turbulence. Although many turbine wake models have been proposed over the last decades [1, 2], none of them include thermal effects.

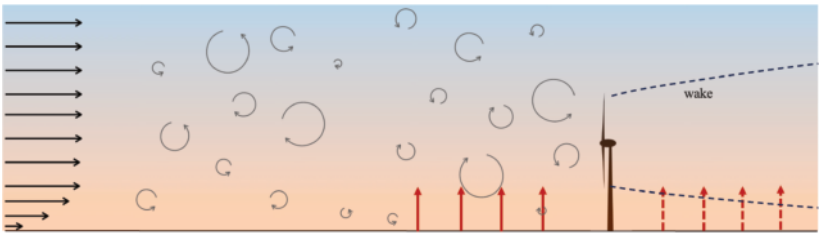

Figure 5.50: Schematic of the interaction between an unstable boundary layer flow and a wind turbine. The wake shape and turbulent transport properties differ from the neutral case.

We conduct hot-wire measurements in the Prandtl Wind Tunnel at the MPI-DS 9.8 to study the interactions of unstable boundary layers with wind turbine wakes. Fig. 5.51 shows preliminary measurements of the velocity profiles behind a model wind turbine. Future experiments will span a wide parameter space in order to develop a fundamental understanding of the interactions of temperature and momentum transport in wind turbine wakes, and ultimately to incorporate buoyancy-generated turbulence effects in wake models.

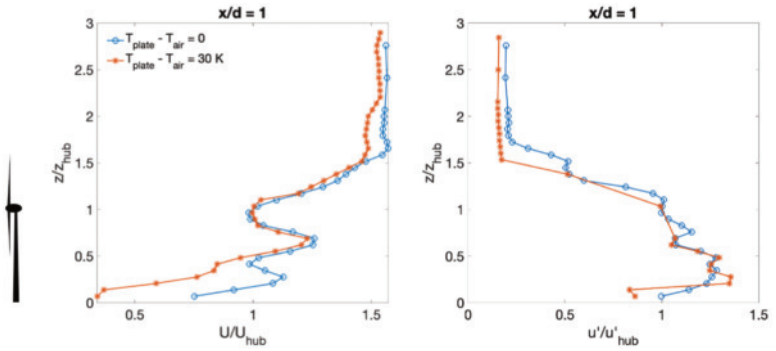

Figure 5.51: Preliminary results of mean velocity U and velocity fluctuation u' behind a wind turbine model, in an unstable boundary layer. Both quantities are normalised using the values at hub height. z is the vertical distance, z_{hub} is the hub height of the wind turbine. The blue line represents the profiles when the flow is neutral, and the red line when the flow is unstable. The data shown here were taken one diameter downstream of the rotor ($x/d = 1$).

[1] M. Bastankhah, F. Porté-Agel, Energies **10**, 923 (2017)
[2] A. Keane, Renew. Energy **171**, 687 (2021)

5.22 EFFECT OF INFLOW CONDITIONS ON TIP VORTEX BREAKDOWN

M. Grunwald, C. E. Brunner
J. Jüchter (Oldenburg)

Wind energy is one of the key technologies in the transition to green energy. Due to spatial, economical and practical reasons, wind turbines are often clustered in wind farms where the turbines are in close proximity to each other. This enables the interaction of subsequent wind turbines, as turbines located downstream encounter the wake generated by upstream turbines as their incoming flow. These interactions significantly reduce the power generated by downstream wind turbines [1] as well as their lifetime [2].

Wind turbine wakes are dominated by coherent structures: vortices are shed from roots and tips of the rotor blades and transported downstream. Due to the circular motion of the rotor, helical vortex structures are formed. While the root vortices break down close to the rotor, the tip vortices can persist for several rotor diameters. It is their evolution that determines the wake dynamics. Only when the tip vortices break down, is the wake re-energized [3]. Different mechanisms for the tip vortex breakdown have been proposed, either relying on the interaction between subsequent tip vortices or the interaction of tip vortices with the surrounding flow. The surrounding flow is often assumed to be laminar in numerical studies and laboratory experiments. However, reality is far from that - atmospheric flow is highly turbulent with large Reynolds numbers $10^6 \lesssim \mathrm{Re}_D \lesssim 10^8$. Additional complexity is added by the terrain which commonly leads to vertical shear.

$\mathrm{Re}_D = UD/\nu$ is the turbine Reynolds number based on the mean velocity U and the rotor diameter D

In our recent work, we have investigated the effect of different inflow characteristics on the wakes of wind turbines under realistic conditions. While the generation of large Reynolds number flow is generally challenging, the Variable Density Turbulence Tunnel (VDTT) at the institute is specifically designed for this purpose. With the VDTT, we can achieve realistic conditions at $\mathrm{Re}_D = 3 \times 10^6$. By additionally using an active grid, this setup enables us to adjust the incoming flow for a model wind turbine, allowing us to create various inflow conditions with different levels of shear and turbulence intensity. Furthermore, the turbine allows for control over the rotation rate and therefore the tip speed ratio, which is an important control parameter for wind turbines.

the tip speed ratio is defined as $\lambda = \omega D/(2U)$ with $\omega = 2\pi f_{\mathrm{rotor}}$ being the rotational frequency of the rotor

Having full control over shear, turbulence intensity and tip speed ratio lets us investigate the effect of these parameters on the evolution of tip vortices. The focus of our current work is not on the specific mechanism that initiates vortex breakdown, but rather the scaling of the vortex breakdown process in a turbulent shear flow. To this end, we take point measurements of the stream-wise velocity component at high temporal resolutions. The data is then analyzed in Fourier space. Fig. 5.52 shows the measured velocity spectra for one of the inflow cases. The yellow curve is taken directly upstream of the rotor to further characterize the inflow. The spectrum shows a $-5/3$-slope over almost three decades, which is indicative of a high Reynolds number

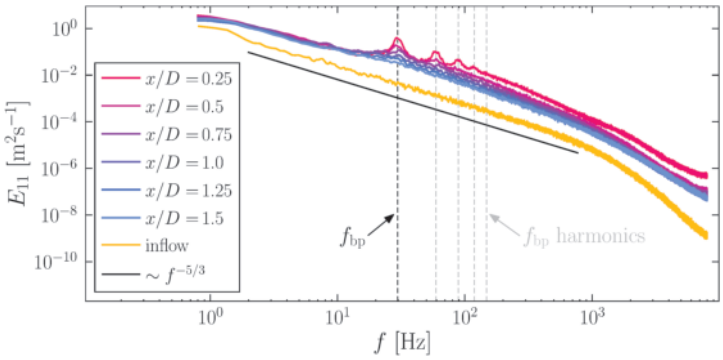

Figure 5.52: Inflow spectrum and wake spectra at different downstream positions for a single inflow condition.

the blade pass frequency is $f_{bp} = 3f_{rotor}$ for a rotor with three blades

flow. The other spectra are taken in the wake at the top of the rotor and at different downstream positions. At the blade pass frequency and its harmonics, distinct peaks emerge. They are most prominent close to the rotor but persist until $x/D \gtrsim 1$. These peaks are a signature of the tip vortices, since they are shed at the blade pass frequency. As the tip vortices break down, their signature decreases, resulting in a decrease in the peak height. To quantify the breakdown, the downstream evolution of the peak heights for different inflow cases is shown in Fig. 5.53. Here, the yellow curve corresponds to the same inflow condition in

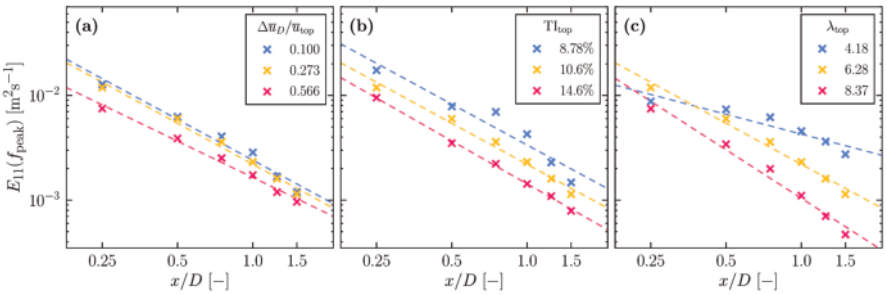

Figure 5.53: Peak height evolution for different levels of (a) shear, (b) turbulence intensity and (c) tip speed ratio

each plot. All trends are fitted with a power law $y \sim x^{\alpha}$. The exponent α corresponds to the slope of the curves. Steeper slopes indicate a faster breakdown process. Variations in tip speed ratio lead to different values for α, while variations in shear and turbulence intensity do not seem to affect the rate of breakdown much. These results suggest, that changes in the tip speed affect the tip vortex breakdown most, with higher tip speed ratios leading to a faster breakdown. Changes in the incoming flow regarding shear and turbulence intensity do not lead to significant differences in the breakdown process for the given parameter range, which does resemble the span of values for the working conditions of wind turbines.

In upcoming projects, we will investigate the tip vortex breakdown under realistic inflow conditions further. With this work, we will contribute to the improvement of current wake models, which are crucial for the development of future wind farms.

[1] R. J. Barthelmie et al., J. Atmos. Oceanic Technol. **27**, 1302 (2010)
[2] K. Thomsen, P. Sørensen, J. Wind Eng. Ind. Aerodyn. **80**, 121 (1999)
[3] L. E. M. Lignarolo et al., Renew. Energy **70**, 31 (2014)

5.23 TOPOLOGICAL DEFECTS IN PERIODIC AND AMORPHOUS ENSEMBLES AND TRANSPORT IN STEALTHY, HYPERUNIFORM STRUCTURES

Alireza Valizadeh, Peter Keim
L. Siedentop, R. Löffler, P. Dillmann, G. Maret (Konstanz), V. Vaibhav, A. Bera, A. Zaccone (Milano), G. Lui, M. Florescu (Surray), P. Steinhardt, S. Torquato (Princeton), M. Baggioli (Shanghai), A.C.Y. Liu (Clayton), P. Chaikin (New York)

Topological defects in glass

Topological defects are singularities within a field that cannot be removed by continuous transformations. The definition of these irregularities requires an ordered reference configuration, calling into question whether they exist in disordered materials, such as glasses. However, recent work suggests that well defined topological defects emerge in the dynamics of glasses, even if they are not evident in the static configuration. In this study, we reveal the presence of topological defects in the vibrational eigenspace of a two-dimensional experimental colloidal glass. These defects strongly correlate with the vibrational features and spatially correlate with each other and structural "soft spots", more prone to plastic flow. This work experimentally confirms the existence of topological defects in disordered systems revealing the complex interplay between topology, disorder, and dynamics. Fig. 5.54 shows a sketch of the results, the article is found here [1].

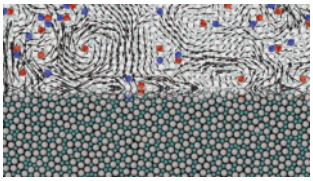

Figure 5.54: The upper half of the picture shows normal vibration modes with +1 and -1 topological defects (vortices and anti-vortices). The lower half shows the experimental system (a 2D colloidal glass)

Kibble-Zurek mechanism

Freezing and melting is typically seen to be reversible and independent of history. However, this is not the case taking critical slowing down into account: cooling an isotropic 2D fluid with a finite but nonzero rate never ends in mono-crystals. The symmetry can not be broken globally but only locally in the thermodynamic limit due to the critical slowing down of order parameter fluctuations. This results in finite sized domains with the same order parameter. For linear cooling rates, the domain size is described by the Kibble-Zurek mechanism, originally developed for the defect formation of the primordial Higgs-field shortly after the Big-Bang. Here, we investigate the limit of the deepest descent quench on a colloidal monolayer and resolve the time dependence of structure formation for (local) symmetry breaking. Quenching to various target temperatures below the melting point (deep in the crystalline phase and just close to the transition), we find universal behaviour if the timescale is re-scaled properly. Fig. 5.55 shows the mosaicity for various quenches, the results are summarized here [2].

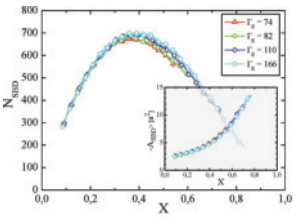

Figure 5.55: The mosaicity shows universal behaviour as function of crystallinity, independent how deep one quenches into the symmetry broken state.

Tetratic phase

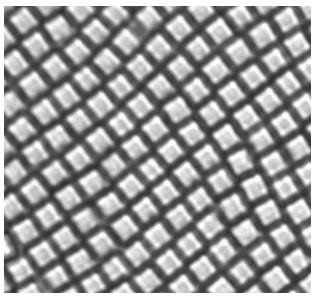

Figure 5.56: Quadratic particles arrange in square crystals and an intermediate tetratic phase shows up during melting, being a liquid crystal with four-fold director.

Isotropic particles have a hexagonal closed packed structure and show an intermediate hexatic phase during melting. Here, the melting of a quadratic, 4-fold crystal is investigated, consisting of squares of about $4 \times 4\mu$m. The anisotropic particles are manufactured from a photoresist using a 3D nanoprinter. In aqueous solution, particles sediment by gravity to a thin cover slide where they form a monolayer. The curvature of the cover slide can be adjusted from convex to concave, which allows to vary the area density of the monolayer in the field of view. For low densities, the squares are free to diffuse and form a 2D fluid while for high densities they form a quadratic crystal. Using a four-fold bond-order correlation function, we resolve the tetratic phase with quasi long ranged orientational order but short ranged translational one. Fig. 5.56 shows a crystal of squares, the manuscript will be published in Soft Matter [1].

Isotropic photonic band gap

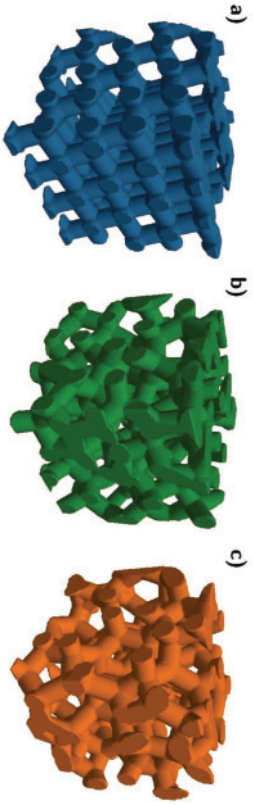

Figure 5.57: The stealthy hyperuniform pattern (green) is compared with a diamond lattice (blue) and an amorphous structure (red) and shows an isotropic photonic band gap in experiment and simulation.

In photonic crystals, the propagation of light is governed by their photonic band structure, an ensemble of propagating states grouped into bands, separated by photonic band gaps. Due to discrete symmetries in spatially strictly periodic dielectric structures their photonic band structure is intrinsically anisotropic. However, for many applications, such as manufacturing artificial structural color materials or developing photonic computing devices, but also for the fundamental understanding of light-matter interactions, it is of major interest to seek materials with long range nonperiodic dielectric structures which allow the formation of isotropic photonic band gaps. Here, we report 3D isotropic photonic band gap for an optimized disordered stealthy hyperuniform structure for microwaves. The transmission spectra are directly compared to a diamond pattern and an amorphous structure with similar node density. Results agree well with finite-difference-time-domain numerical investigations and a priori calculations of the band gap for the hyperuniform structure: the diamond structure shows gaps but being anisotropic as expected, the stealthy hyperuniform pattern shows an isotropic gap of very similar magnitude, while the amorphous structure does not show a gap at all. Since they are more easily manufactured, prototyping centimeter scaled microwave structures may help optimizing structures in the technologically very interesting region of infrared. Fig. 5.57 shows a stealthy hyperuniform structure (green), the bandgaps are reported in [4].

[1] V. Vaibhav, A. Bera, A. Liu, M. Baggioli, P. Keim, A. Zaccone, Nature Communications **16**, 55 (2025)
[2] A. Valizadeh, P. Dillmann, P. Keim, arXiv:2411.13433 (2024)
[3] R. Löffler, L. Siedentop, P. Keim, Soft Matter **21**, 2026 (2025)
[4] L. Siedentop, G. Lui, G. Maret, P. Chaikin, P. Steinhardt, S. Torquato, P. Keim, M. Florescu, PNAS Nexus **3**, pgae383 (2024)

5.24 THEORY OF TURBULENT CONVECTION

A. Teimurazov, **M. Emran**, **M. Kriening**, **P. Reiter**, **J. Song**, **C. Xu**, **Z. Yao**, **X. Zhang**, **L. Zwirner**, and **O. Shishkina**
in collaboration with G. Ahlers (University of California, SB), E. Bodenschatz (MPIDS), R. E. Ecke (Los Alamos National Laboratory), S. Eckert (Helmholtz-Zentrum Dresden-Rossendorf), M. Linkmann (University of Edinburgh), D. Lohse (University of Twente and MPIDS), R. Stevens (University of Twente), R. Verzicco (University of Rome "Tor Vergata"), S. Weiss (German Aerospace Center - DLR), X. Zhu (MPI for Solar System Research) and members of their groups

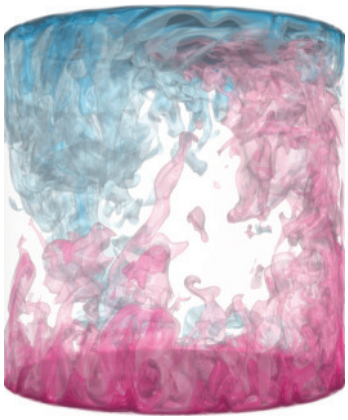

Figure 5.58: Turbulent Rayleigh–Bénard convection at $Ra = 10^9$ and $Pr = 1$ visualized with isosurfaces of the temperature.

Turbulent flows are omnipresent and their role in geophysical and astrophysical systems and many engineering applications can hardly be overestimated. Research and publications of the *Theory of Turbulent Convection* Group (led by O. Shishkina) in 2022–2024 includes four review papers [1–4], including reviews "Turbulent Rotating Rayleigh–Bénard Convection" in *Annual Review of Fluid Mechanics* (with R. E. Ecke) [3] and "Ultimate Rayleigh–Bénard Turbulence" in *Reviews on Modern Physics* (with D. Lohse) [1] and 25 research papers [5–29] devoted to different aspects of turbulent convection, including convection at very strong thermal driving (large Rayleigh number Ra) [1, 2, 5, 6], non-Oberbeck–Boussinesq effects in thermal convection [14], rotating Rayleigh-Bénard convection [3, 13, 15, 16, 18, 19, 21, 29], centrifugal convection [22, 25], convection in liquid metals [7, 10] and magneto-convection [11, 12, 23, 27], sheared convection [9, 17] and modulated convection [8], convection in viscoelastic and viscoplastic fluids [26, 28], reconstruction of the temperature field from the experimental velocity measurements in turbulent natural convection [24], and numerical methods for simulation and analysis of turbulent flows [20, 26].

Below we briefly discuss some selected topics.

5.24.1 *Magnetoconvection and convection in liquid metals*

In magnetoconvection (MC), the flow of an electromagnetically conductive fluid is driven by a combination of buoyancy forces, which create the fluid motion due to thermal expansion and contraction, and Lorentz forces, which distort the convective flow structure in the presence of a magnetic field. MC governs most astro- and geophysical systems and is relevant to various engineering applications. The former include, for instance, outer layers of stars and liquid-metal planetary cores, examples of the latter comprise liquid-metal batteries, electromagnetic brakes in continuous casting, liquid-metal cooling for nuclear fusion reactors, and semiconductor crystal growth. One of the key objectives in MC research is to provide scaling relations for the heat transport through the system, represented in dimensionless form by the ratio of total to conductive heat flux, the Nusselt number Nu, as a function of the strength of buoyancy (Rayleigh number Ra) and electromagnetic forces (Hartmann number Ha). However, the heat transport scaling relations also depend on the flow configuration, including the angle between

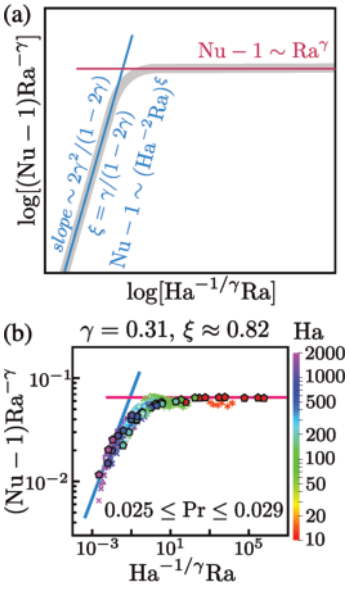

Figure 5.59: (a) The proposed heat transport (Nusselt number Nu) model for the transition from the buoyancy-dominated (pink line) to Lorentz-force-dominated (blue line) regimes in magnetoconvection. (b) Validation of the model with our DNS data and data available in the literature. Adapted from [12]. This study was highlighted in *Physik Journal*, **2** (2024), 22–23: S. Eckert, "Transport dank Wandmoden".

the magnetic field and gravity, the geometry of the container and the boundary conditions, and whether the buoyancy forces dominate over the Lorentz forces in the system or vice versa.

In [12] we proposed a theoretical model for the transition between the buoyancy-dominated (BD) and Lorentz-force-dominated (LD) regimes for the case of a static vertical magnetic field applied across a convective fluid layer confined between two isothermal, a lower warmer and an upper colder, horizontal surfaces. When the flow is turbulent with a very weak or no constraining force (BD regime), the heat transport displays a classical Rayleigh–Bénard convection (RBC) power-law dependence $Nu \sim Ra^{\gamma}$ with the scaling exponent γ. However, when the flow is strongly influenced by a constraining force (LD regime), the heat transport also displays a power-law dependence $Nu \sim (Ha^{-2}Ra)^{\xi}$ with the scaling exponent ξ. Although these scaling laws in the two extreme regimes appear disconnected, they are intrinsically linked under the assumption that they must overlap at some intermediate region, where the influence of neither the Lorentz force nor the buoyancy force on the convective heat transport can be ignored. To derive a model connecting the two scaling laws, we make two modelling assumptions, the first of which is that the transition is primarily controlled by the viscous and thermal boundary layers in the sense that at this intermediate point where the two power laws overlap, the thermal boundary layer (BL) thickness δ_T and Hartmann BL thickness δ_v, at both, the top and bottom plates, are related as $\delta_T = \lambda\delta_v$ for a constant $\lambda = \lambda(Pr)$. The second assumption is that both of these BL thicknesses scale with the control parameters in accordance with the well-established laminar theory, that is $\delta_T \propto Nu^{-1}$ and $\delta_v \propto Ha^{-1}$. Under these assumptions, we obtain the following relation between the two scaling exponents: $\xi = \gamma/(1-2\gamma)$, or $\gamma = \xi/(1+2\xi)$.

In the transitional region between the two extreme regimes, the data should satisfy the scaling relations of both regimes

$$(Nu-1)Ra^{-\gamma} \sim [Ha^{-2\xi/(\xi-\gamma)}Ra]^{s} = [Ha^{-1/\gamma}Ra]^{s}, \qquad (5.3)$$

which has been expressed only in terms of the exponent $\gamma = \gamma(\xi)$ for convenience. Notably, this form recovers the BD scaling law for $s = 0$, and the LD scaling law for $s = \xi - \gamma = 2\gamma^2/(1-2\gamma) > 0$. We validated the model using data available in the literature and obtained in our 3D direct numerical simulations (DNS) via the in-house finite-volume computational code GOLDFISH which solves the MC equations within the Oberbeck–Boussinesq and quasistatic approximations for $10 \leq Ha \leq 2000$, Prandtl number $Pr = 0.025$ and Ra up to 10^9. We wish to emphasise that the proposed model is parameter-free. For a given Prandtl number Pr and Ra-range, one can calculate the scaling exponent γ in the BD regime, using the Grossmann–Lohse (GL) theory. From this, one can calculate the scaling exponent ξ in the LD regime and collapse on a master curve the heat transport data for different values of Ha and Ra, using the coordinate transform $x = log[Ha^{-1/\gamma}Ra]$ and $y = log[(Nu-1)Ra^{-\gamma}]$, as shown in Fig. 5.59.

In [23], we derived an extended heat transport model with a single free parameter that accurately captures the smooth transition between

the BD- and LD-regimes in MC under a vertically aligned magnetic field. The model provides a simple analytic expression which asymptotes to previously observed power laws in the BD- or LD-regimes [12] and exhibits a smooth transition between these two extreme regimes. To a first approximation, the slope of the master curve, i.e. $s = s(x)$, has the general form of a sigmoid function. One can reconstruct the master curve $y = y(x)$ by directly integrating $s(x)$. We chose to model the slope of the master curve $s(x)$ by the complementary error function. This function was primarily chosen because it allowed the free parameters to be easily recovered in closed form; this property does not hold for other choices of sigmoid functions, such as a hyperbolic tangent profile. Although we have introduced several free parameters in this model, we show that only one remains independent. The value of this parameter can be obtained from a single data point in the transitional regime, or as an average over several data points if additional data is available. The model's derivation does not rely on the quasistatic approximation, so it should be applicable to full MC. The model has been validated through our DNS, and existing numerical and experimental data in the literature in both the quasistatic regime and at finite magnetic Reynolds numbers where magnetic field fluctuations must be considered. An extension of the model with an additional parameter describes the so-called overshooting effect observed at higher Prandtl numbers in the transitional region between the regimes of clear dominance of either gravitational buoyancy or the Lorentz force. The model contains a natural extension to rotating convection and offers a potential generalisation to rotating MC.

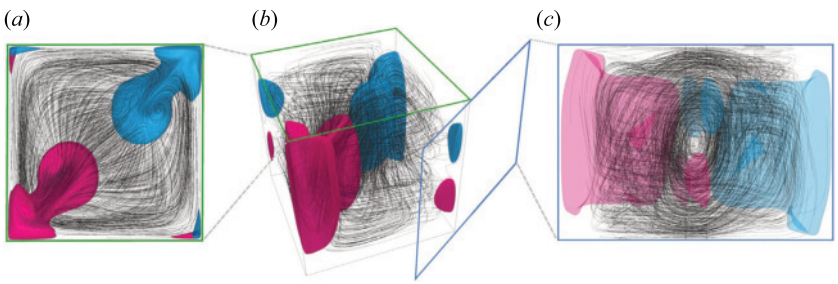

Figure 5.60: Vertical velocity isosurfaces $u_z = \pm 0.1$ (pink/blue) and instantaneous streamlines (black), showing a coexistence of wall modes and large-scale circulation at $Ha = 200$, $Ra = 10^6$: (a) top view; (b) three-dimensional view; (c) angled side view. Adapted from [11].

In [11], we investigated wall mode dynamics and transition to chaos in quasistatic MC with a vertical magnetic field in a unit-aspect-ratio box with no-slip boundaries. At high relative magnetic field strengths, given by the Hartmann number Ha, the onset of convection is known to result from a sidewall instability giving rise to the wall-mode regime. Many questions about the transition to turbulence in MC are still open, mostly concerning the various dynamics admissible by this system. Specifically, it is currently not well understood how the steady wall mode transitions to the more chaotic cellular regime, and whether other states exist in between. In [11], we carried out 3D DNS of unprecedented length to map out the parameter space at $Ha = 200$, 500, 1000, and varying the Rayleigh number over the range $6 \times 10^5 \leq Ra \leq 5 \times 10^8$. We tracked the development of stable

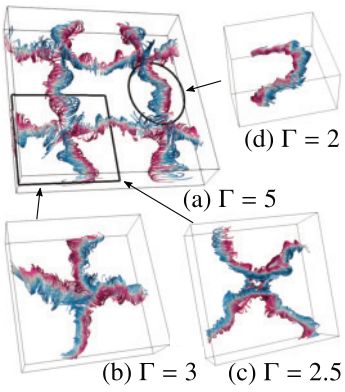

Figure 5.61: Phase-averaged streamlines for $Ra = 10^6$ and $Pr = 0.03$, as obtained in the DNS for different aspect ratios (a) $\Gamma = 5$, (b) $\Gamma = 3$, (c) $\Gamma = 2.5$ and (d) $\Gamma = 2$. The streamlines envelope the oscillating vortex. The colour scale is determined according to the vertical velocity. Adapted from [10].

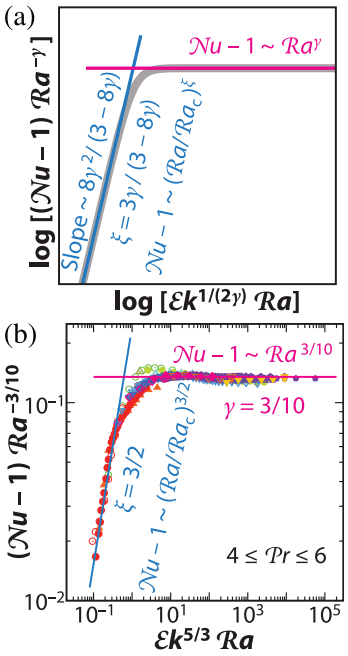

Figure 5.62: (a) Heat transport model for the transition from the rotation-dominated (blue line) to buoyancy-dominated (pink line) regimes. (b) Validation of the model with data available in the literature. Adapted from [3].

equilibria produced by this primary instability, identifying bifurcations leading to limit cycles and eventually to chaotic dynamics. At $Ha = 200$, the steady wall-mode solution undergoes a symmetry-breaking bifurcation producing a state that features a coexistence between wall modes and a large-scale roll in the centre of the domain, which persists to higher Ra (see Fig. 5.60). However, under a stronger magnetic field at $Ha = 1000$, the steady wall-mode solution undergoes a Hopf bifurcation producing a limit cycle which further develops to solutions that shadow an orbit homoclinic to a saddle point. Upon a further increase in Ra, the system undergoes a subsequent symmetry break, producing a coexistence between wall modes and a large-scale roll. However, the large-scale roll exists only for a small range of Ra, and chaotic dynamics primarily arises from a mixture of chaotic wall-mode dynamics and arrays of cellular structures. Further results suggest the presence of multiple states and hysteresis. In [27], we showed that adding insulating sidewalls and applying a vertical magnetic field in liquid metal convection changes how the conducting state loses stability, with the sidewalls allowing for stable subcritical solutions.

Turbulent thermal convection of a liquid metal (Prandtl number $Pr = 0.03$) without a presence of any external magnetic fields also exhibits rich dynamics as demonstrated in our study of vertical convection (VC), where two opposite square sidewalls are heated/cooled [7], and RBC [10]. For some aspect ratios, and at a sufficiently high values of Ra, the flow dynamics includes a 3D oscillatory mode known as a jump rope vortex (JRV). In [10], we investigated the effects of varying domain aspect ratio Γ (a ratio between the spatial length and height of the domain) on this mode, for liquid metals, at a low Prandtl number $Pr = 0.03$. DNS and experiments are carried out for a Rayleigh number range $2.9 \times 10^4 \le Ra \le 1.6 \times 10^6$ and square cuboid with different aspect ratios varying from 2 to 5. We detected the oscillatory modes for all investigated Γ. The vortices form an orthogonal cross that periodically rotates alternately clockwise and anticlockwise for domains with the aspect ratios $\Gamma = 2.5$ and 3. In a $\Gamma = 5$ cell, a lattice of four JRVs interlace each other, which oscillate in a synchronised manner. The key finding of this study is that the JRV structures are extremely robust; they adapt and reorganise dependently on the value of Γ, with the ability to form an intricate lattice of repetitive flow structures in large Γ containers (see Fig. 5.61).

5.24.2 *Rotating turbulent convection*

Rotation with thermally induced buoyancy governs many astrophysical and geophysical processes in the atmosphere, ocean, sun, and Earth's liquid-metal outer core. Rotating Rayleigh–Bénard convection (RRBC) occurs in a fluid that fills a container with heated bottom and cooled top and rotated about its vertical axis with a constant angular velocity. RRBC is an extremely rich system, with features directly comparable to geophysical and astrophysical phenomena. In [3], a unifying heat transport scaling approach for the transition between rotation-dominated (RD) and BD regimes in RRBC was proposed and validated using data

available in the literature (see Fig. 5.62).

In [18, 19], RRBC was studied using DNS in cylindrical cells for broad ranges of Ra, Γ and rotation rates (inverse Ekman number Ek). We connected linear wall-mode states that occur prior to the onset of bulk convection with the boundary zonal flow (BZF) that coexists with turbulent bulk convection in the geostrophic regime. The results confirmed that wall modes are strongly linked with the BZF being the robust remnant of nonlinear wall mode states.

In [15, 21], the DNS of RRBC in the planar geometry with no-slip top and bottom and periodic lateral boundaries were performed for Ra up to 5×10^{13} and Ek down to 5×10^{-9}. With increasing Ra, the DNS has revealed not only the typical RD regimes, namely, cellular flow, Taylor columns, plumes, geostrophic turbulence and large-scale vortices (see Fig. 5.63), but also the BD regime [15]. During the transition pathway, it is demonstrated that the thermal BL thickness decreases monotonically and becomes thinner than the viscous BL thickness in the buoyancy-dominated regime [21]. The thermal and Ekman BL statistics, scaling behaviour of the heat and momentum transport (reflected in the Nusselt Nu and Reynolds numbers Re), and the convective length scale are investigated across various flow regimes. Moreover, the global and local momentum transports are examined via the Re scaling derived from the classical theoretical balances of viscous-Archimedean-Coriolis (VAC) and Coriolis-inertial-Archimedean (CIA) forces. The VAC-based Re scaling agrees well with the data in the cellular and columnar regimes, while the CIA-based Re scaling works well in the geostrophic turbulence regime. For extremely high Ra and low Ek regimes, we derived and verified in the DNS the diffusion-free scaling relations for the heat transport (Nu), momentum transport (Re), and the convective length scale [13].

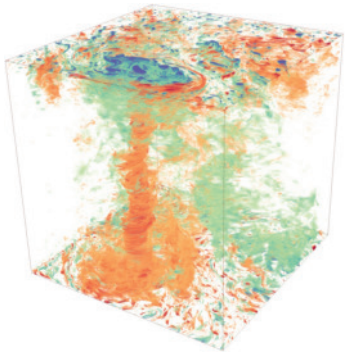

Figure 5.63: The large-scale vortices in rapidly rotating thermal convection, as obtained in DNS for $Ra = 5 \times 10^{13}$, $Ek = 5 \times 10^{-9}$ and $Pr = 1$. The colours show the dimensionless thermal fluctuations. Adapted from [15]. This work was featured on the cover of *Journal of Fluid Mechanics* **989** (2024).

5.24.3 *Centrifugal convection*

Centrifugal convection is a prosperous system that, in particular, allows the investigation of the high-Ra regime in thermal convection of Rayleigh–Bénard type, by increasing the rotation rate (i.e., by increasing the centrifugal acceleration). In addition, for any rotation rates, the system experiences gravitational acceleration, which provides additional shear to the system and thus eases a transition to the ultimate regime by relatively low Rayleigh numbers.

In [22], DNS of centrifugal convection were conducted for a range of Rayleigh numbers $2 \times 10^5 \leq Ra \leq 8.88 \times 10^8$ and Froude numbers $0 \leq Fr \leq 100$. In the setup we consider a vertically aligned cylindrical annulus with top and bottom solid walls, and cooled inner and heated outer sidewalls, all subject to a constant rotation around the vertical axis of the annulus (see Fig. 5.64). For a fixed Ra (thermal driving) and increasing Fr (centrifugal driving), the global flow structure and heat transport scaling properties undergo a transition from those typical for vertical convection, where the imposed temperature gradient is orthogonal to the driving force (gravitational buoyancy), to those typical for Rayleigh–Bénard convection, where the temperature gradient is

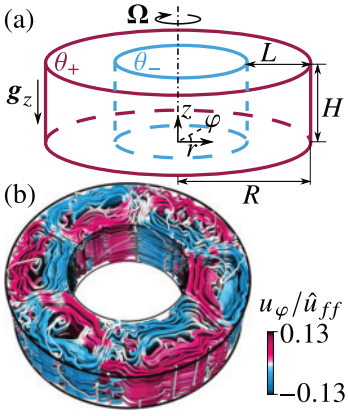

Figure 5.64: Centrifugal convection setup (a) and trajectories of passive tracer particles for $Ra = 8.88 \times 10^8$, $Fr = 6.53$, coloured by the azimuthal velocity (b). Adapted from [22].

parallel to the force (centrifugal buoyancy). With increasing centrifugal buoyancy, the flow undergoes a transition from a three-dimensional global flow structure to a quasi-two-dimensional one, which is characterized by a suppressed mixing in the vertical direction. For larger Ra values, larger values of Fr are required for the transition.

5.24.4 *Ultimate turbulent thermal convection*

While there is good agreement and understanding of the dependences $Nu(Ra, Pr, \Gamma)$ in RBC for the "classical regime" (up to $Ra \sim 10^{11}$), for even larger Ra in the so-called ultimate regime of RBC the experimental results and their interpretations are more diverse. Understanding of this transition of the flow to the ultimate regime is of the utmost importance for extrapolating the heat transfer to large or strongly thermally driven systems [1, 2]. In [6], a new scaling model for the ultimate regime in RBC was proposed, which distinguishes between four subregimes (see Fig. 5.65a). The model is consistent with the experimental data on $Nu(Ra, Pr, \Gamma)$ of various large-Ra RBC experiments (Fig. 5.65b). In this new representation, which takes the Pr dependence into account, the onset of the ultimate regime is seen in all high-Ra experimental datasets, though at different Ra, as to be expected for a non-normal-nonlinear instability [18, 19]. Here we refer also to section 4.4 of this Report.

Our findings in [5] predict also the Γ-dependence of the onset of the ultimate regime, which is consistent with almost Oberbeck–Boussinesq (OB) experiments and explains why, in small-Γ cells, much larger Ra (namely, by a factor Γ^{-3}) must be achieved to observe the ultimate regime. The influence of the temperature- and pressure-dependence of the fluid properties, i.e. the so-called non-OB effects, has been investigated in [14]. For cryogenic helium and pressurized SF6, the most popular fluids in high-Ra RBC measurements, the most critical residual is associated with the temperature dependence of specific heat at constant pressure (c_p). Our DNS showed, however, that this feature alone cannot explain a sudden and intense enhancement in the heat transport in high-Ra experiments.

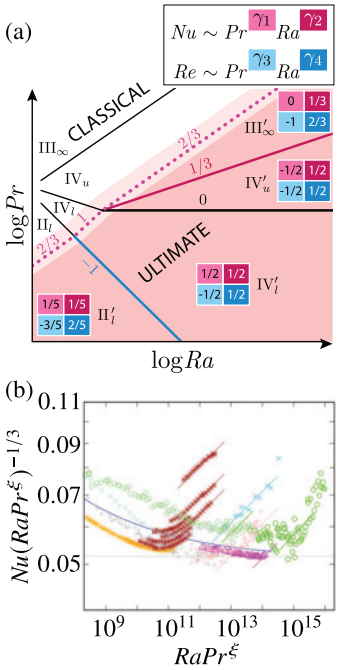

Figure 5.65: (a) A model for the ultimate regime in RBC in the $Pr - Ra$ parameter space and (b) representation of compensated Nu displaying the transition to the ultimate regime, with slopes of about $Nu \sim Ra^{0.4}$ (brown, cyan, green, pink, and magenta thin straight lines) at the highest Ra achieved in different experiments. Adapted from [6]. This study was featured on the covers of *Physics Today* **76** (11) (2023) and of *Reviews on Modern Physics* **96** (3) (2024).

5.24.5 *Turbulent thermal convection of complex fluids*

While, except for some common liquids and gases, like water and air, which can be assumed as Newtonian for practical calculations under ordinary conditions, most of the real fluids in nature and industrial processes are non-Newtonian fluids. The viscosity of non-Newtonian fluids can vary significantly with factors such as shear rate, temperature, and pressure, hence, they often exhibit more complex rheological behaviors compared to Newtonian fluids, such as viscoelasticity, plasticity, shear-thinning and shear-thickening. Among them, the elastic and plastic behaviors of the non-Newtonian fluids play a crucial role in determining the rheological properties and flow dynamics. Specifically, the relative effect of the elastic forces to the viscous forces in the viscoelastic fluids is commonly quantified by the Weissenberg number

Wi, which is proportional to the product of the elastic relaxation time λ and the shear rate of the flow, $\dot{\gamma}$. Regarding the fluid plasticity, a dimensionless Bingham number Bi is frequently used, which denotes the yield stress ratio to the viscous stress in the Saramito elastoviscoplastic model. In this case, the Bingham plastic fluid behaves as a rigid body at low stresses and as a viscous fluid at high stresses.

To study turbulent thermal convection of viscoplastic and viscoelastic fluids, in [26] an efficient and robust finite-difference algorithm for DNS of turbulent thermal convection of complex fluids was developed. Specifically, the simulated non-Newtonian fluids are modelled by either viscoelastic Oldroyd-B or FENE-P (finitely extensible nonlinear elastic-Peterlin), or Saramito elastoviscoplastic constitutive equations based on the conformation tensor. The non-Newtonian solver is built on top of the open-source AFiD (www.afid.eu) code, which uses a pencil distributed parallel strategy to handle the large-scale wall-bounded turbulence computations efficiently. The solver uses the Kurganov–Tadmor scheme for the convective term and the semi-implicit time advancement scheme for the conformation tensor equations. This algorithm was demonstrated to preserve the properties of symmetry, boundedness and positive definiteness of the conformation tensor up to large Weissenberg numbers $Wi \sim 10^2$ and high Rayleigh numbers $Ra \sim 10^{10}$. The scalability test of the code showed that the averaged wall time per step has an almost linear reduction with increasing number of CPU cores up to 10^4, and it has very good speedup to around 5000 cores for Newtonian and 2000 cores for viscoelastic calculations. Both two-dimensional (2D) and three-dimensional (3D) DNS of viscoelastic RBC were performed to validate the code [26]. A thorough comparison with the DNS data available in the literature showed an excellent agreement.

Remarkably, the results for the heat transport modification for highly turbulent thermal convection with polymer additives agreed not only qualitatively but also quantitatively with previous experiments in a similar parameter range. The 3D DNS were performed at $Ra = 10^{10}$, $Pr = 4.3$, $L = 50$, $\beta = 0.9$, $\Gamma = 1$ with Wi up to $Wi = 120$. The flow fields demonstrate that polymer additives significantly modify the Newtonian flow structures in the bulk and boundary-layer regions, where the plumes become more coherent and the boundary layers become more stable. As expected, a significant heat transport reduction up to 16.8% was obtained in our DNS of the viscoelastic flows. Previous experimental studies at $5 \times 10^9 \leq Ra \leq 7 \times 10^{10}$ and $Pr = 4.38$ also demonstrated a heat transport reduction up to 12%. This agreement between the DNS and measurements is very important since then the proposed algorithm and code can be used to determine numerically the rheological parameters of the real polymer solutions used in the experiments. This is quite complicated and still remains an elusive topic in the community.

To validate the elastoviscoplastic model used in the code, the DNS of elastoviscoplastic turbulent channel flows at friction Reynolds number $Re_\tau = 180$ and different Bingham numbers Bi were performed, which also showed a good agreement with the available results. The DNS also studied single plume dynamics of Newtonian, viscoelastic,

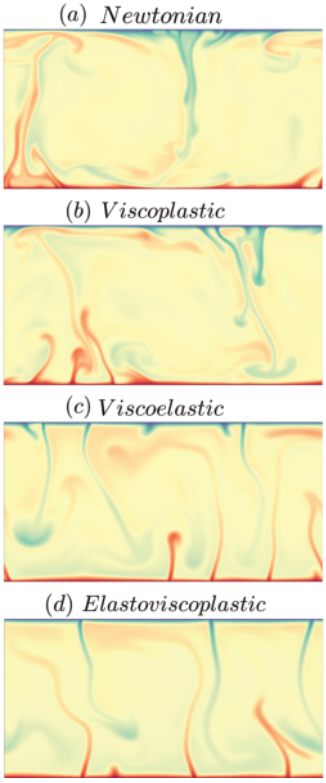

Figure 5.66: Instantaneous temperature field for (*a*) Newtonian, (*b*) viscoplastic $Bi = 50, Wi = 0.01$ (*c*) viscoelastic $Wi = 10$ and (*d*) elastoviscoplastic $Bi = 50, Wi = 10$ fluids at $Ra = 10^8$, $Pr = 7$. Adapted from [26].

and elastoviscoplastic fluids to demonstrate the code's versatility. In addition, 2D DNS of turbulent RBC of Newtonian, viscoplastic, viscoelastic and elastoviscoplastic fluids were performed to show the versatility of the code (see Fig. 5.66). The simulations were conducted for no-slip top and bottom and periodic horizontal boundary conditions. The Newtonian velocity fields were used as initial conditions for non-Newtonian flows. The considered FENE-P-related parameters were $L = 100$, $\beta = 0.97$, representing long chain and dilute polymer solutions. Compared to Newtonian fluid, all non-Newtonian fluids demonstrated a significant reduction in the heat and momentum transport in turbulent RBC. Specifically, the fluid viscoplasticity decreases the heat transport by about 6.2% by suppressing and destroying the well-organized large-scale rolls established in the Newtonian flow. For the viscoelastic fluid, the convective velocities and heat transport are further reduced to about 16.6% as the large-scale rolls in Newtonian flow are replaced by several localized thin plumes that randomly detach from the wall. The elastoviscoplastic fluid has the combined effects of both plasticity and elasticity, thus a heat transport reduction of 20.4% is obtained. Moreover, the trace field clearly supports that our method and code can faithfully resolve the sharp gradients of conformation tensor and elastic stress in turbulent flows of complex fluids [26].

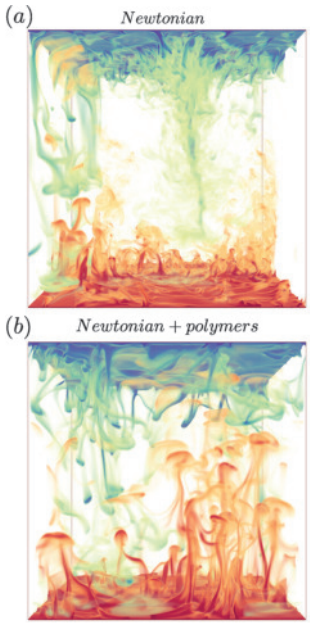

Figure 5.67: Three-dimensional instantaneous temperature fields of (*a*) Newtonian flows and (*b*) viscoelastic flows for $Wi = 10$ and $L = 50$ at $Ra = 10^{10}$ and $Pr = 4.3$. Adapted from [28].

As summarized in [28], previous experimental investigations have primarily focused on high Ra ($10^9 \sim 10^{10}$) situations, whereas simulations in the existing literature have been predominantly limited to lower Ra values, typically smaller than 10^6, due to the difficulties associated with the numerical simulations of viscoelastic flows. This lead to a gap in Ra values of several orders between experimental and numerical studies. After the above extensive validations of the new code, we studied the turbulent RBC of dilute polymeric solutions for Ra ranging from 10^6 to 10^{10} and Prandtl number $Pr = 4.3$. The viscoelastic flows were simulated by solving the incompressible Navier–Stokes equations under the Boussinesq approximation coupled with the FENE-P constitutive model. The considered Wi values were $Wi = 5$ and $Wi = 10$, with the maximum chain extensibility parameter $L = 50$, corresponding to moderate fluid elasticity. The effects of polymer additives on turbulent heat and momentum transport were investigated regarding flow structure modifications, velocity, temperature, polymeric stress statistics, thermal and kinetic energy dissipation rates.

The results demonstrated that in the studied parameter range, the presence of polymer additives reduces both heat and momentum transport. The DNS showed that the reduction of the heat and momentum transfer exhibits a nonmonotonic dependency on Ra. The heat transfer reduction is attributed to the combined effects of the boundary layers, plumes and turbulent background. For small $Ra \lesssim 10^8$, the increased effective viscosity slows down the plumes, leading to a reduced heat transfer. At the highest Ra investigated, the suppression of the velocity fluctuations (in particular, their large-scale content) and the stabilization of the boundary layers were found to be responsible for the reduced heat transfer, despite the polymers suppressing small-scale plumes and enhancing plume coherency [28].

Publications of *Theory of Turbulent Convection* Group in 2022-2024:

[1] D. Lohse and O. Shishkina, Rev. Mod. Phys. **96**, 035001 (2024)
[2] D. Lohse and O. Shishkina, Physics Today **76**, 26 (2023)
[3] R. E. Ecke and O. Shishkina, Annu. Rev. Fluid Mech. **55**, 603 (2023)
[4] O. Shishkina, Physik Journal **8**, 28 (2022)
[5] G. Ahlers, E. Bodenschatz, R. Hartmann, X. He, D. Lohse, P. Reiter, R. J. A. M. Stevens, R. Verzicco, M. Wedi, S. Weiss, X. Zhang, L. Zwirner, and O. Shishkina, Phys. Rev. Lett. **128**, 084501 (2022)
[6] O. Shishkina and D. Lohse, Phys. Rev. Lett. **133**, 144001 (2024)
[7] L. Zwirner, M. S. Emran, F. Schindler, S. Singh, S. Eckert, T. Vogt, and O. Shishkina, J. Fluid Mech. **932**, A9 (2022)
[8] P. Reiter, X. Zhang, and O. Shishkina, J. Fluid Mech. **936**, A32 (2022)
[9] G. S. Yerragolam, R. J. A. M. Stevens, R. Verzicco, D. Lohse and O. Shishkina, J. Fluid Mech. **943**, A17 (2022)
[10] A. Teimurazov, S. Singh, S. Su, S. Eckert, O. Shishkina and T. Vogt, J. Fluid Mech. **977**, A16 (2023)
[11] M. McCormack, A. Teimurazov, O. Shishkina and M. Linkmann, J. Fluid Mech. **975**, R2 (2023)
[12] A. Teimurazov, M. McCormack, M. Linkmann and O. Shishkina, J. Fluid Mech. **980**, R3 (2024)
[13] J. Song, O. Shishkina and X. Zhu, J. Fluid Mech. **984**, A45 (2024)
[14] S. Weiss, M. S. Emran, and O. Shishkina, J. Fluid Mech. **986**, R2 (2024)
[15] J. Song, O. Shishkina and X. Zhu, J. Fluid Mech. **989**, A3 (2024)
[16] A. Bhadra, O. Shishkina and X. Zhu, J. Fluid Mech. **999**, R1 (2024)
[17] G. S. Yerragolam, C. J. Howland, R. J. A. M. Stevens, R. Verzicco, O. Shishkina and D. Lohse, J. Fluid Mech. **1000**, A74 (2024)
[18] R. E. Ecke, X. Zhang, and O. Shishkina, Phys. Rev. Fluids **7**, L011501 (2022)
[19] X. Zhang, P. Reiter, O. Shishkina and R. E. Ecke, Phys. Rev. Fluids **9**, 053501 (2024)
[20] R. Yang, X. Zhang, P. Reiter, D. Lohse, O. Shishkina and M. Linkmann, GAMM-Mitteilungen **45**, e202200003 (2022)
[21] J. Song, V. Kannan, O. Shishkina and X. Zhu, Int. J. Heat Mass Transfer **232**, 125971 (2024)
[22] Z. Yao, M. S. Emran, A. Teimurazov, and O. Shishkina, Int. J. Heat Mass Transfer **236**, 126314 (2025)
[23] M. McCormack, A. Teimurazov, O. Shishkina and M. Linkmann, Int. J. Heat Mass Transfer **241**, 126641 (2025)
[24] S. Weiss, M. S. Emran, J. Bosbach, and O. Shishkina, *Int. J. Heat Mass Transfer* **242**, 126768 (2025)
[25] A. Bhadra, O. Shishkina and X. Zhu, Int. J. Heat Mass Transfer **241**, 126703 (2025)
[26] J. Song, C. Xu, and O. Shishkina, J. Comput. Phys. **525**, 113732 (2025)
[27] M. McCormack, A. Teimurazov, O. Shishkina and M. Linkmann, *submitted*
[28] C. Xu, C. Zhang, L. Brandt, J. Song and O. Shishkina, *submitted*
[29] V. Kannan, J. Song, O. Shishkina and X. Zhu, *submitted*

We acknowledge the Deutsche Forschungsgemeinschaft (DFG) for financial support of Priority Programme SPP 1881 "Turbulent superstructures" and grants Sh 405/7, Sh405/10, Sh405/16, Sh405/18, Sh405/20 and Sh405/22, and the Alexander von Humboldt Foundation Fellowship, as well as the Max Planck Computing and Data Facility (MPCDF) in Munich for providing computer time.

ACTIVE MATTER

6

Active matter systems consist of components that continuously consume energy to generate motion, mechanical stress, or chemical activity, keeping the system far from thermodynamic equilibrium. These systems—ranging from biological assemblies like enzymes, cells, and tissues to synthetic colloids and active droplets—exhibit emergent behaviors such as collective motion, pattern formation, and symmetry breaking. Their study has become a cornerstone of modern nonequilibrium statistical physics.

At MPI-DS, research in active matter spans scales from the molecular to the tissue level and bridges biological and synthetic systems. Recent work includes studies on collective dynamics in cell colonies, synchronization of cilia, mechanical and chemical self-organization in growing tissues, as well as theoretical advances in non-reciprocal interactions, stochastic thermodynamics, and field theories for active matter. This chapter highlights experimental, computational, and theoretical efforts that contribute to a deeper understanding of how active processes drive self-organization and function in complex systems.

Contents

6.1 DENSE INSECT FLIGHT DYNAMICS

T. Baig-Meininghaus

Social insects are highly suitable model organisms to study self-propelled, self-organizing active matter on the macro scale. Bees especially lend themselves as ideal research objects, not only due to the large knowledge base that exists with regard to their behavior and care, but also because, contrary to ants and wasps, their swarm flight is much less coordinated by pheromones [1].

The self-organization mechanisms that enable this coordination are the object of our current research: Although only a fraction of migrating bees possess precise knowledge of the target destination, the entire swarm successfully relocates, underscoring the importance of decentralized coordination in challenging environments [2].

To examine these dynamics, we develop a deep learning pipeline to segment images of flying bees captured by cameras on self-designed drones. By leveraging advanced image processing, we identify individual bees in flight and subsequently employ 3D triangulation methods to reconstruct their positions in space. Repeating these procedures over multiple frames yields time series data, which we then analyze to extract detailed motion trajectories of individual bees. This enables us to investigate how local interactions and limited communication support effective swarm navigation.

Our primary objective is to elucidate the principles governing the coordination of large groups of agents under communication-restricted conditions: how bees synchronize their movements, share navigational cues, and maintain group cohesion. Ultimately, this research enriches our understanding of critical pollinator species and advances the development of robust, resilient multi-agent systems.

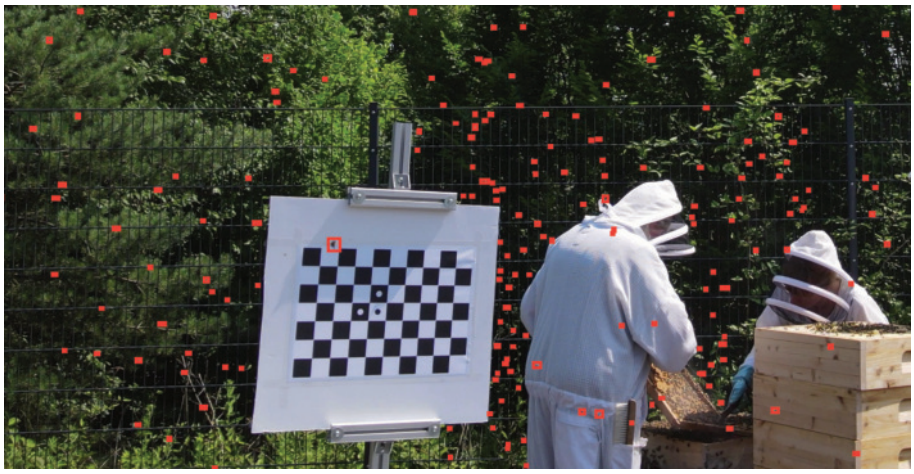

Figure 6.1: Segmented bees with calibration target. Image taken from a drone in flight.

[1] D. M. T. Nguyen, G. G. Fard, A. Atkins et al., Artif. Life Robotics **28**, 1 (2023)
[2] K. M. Schultz et al., J. Exp. Biol. **211**, 3287 (2008)

6.2 MECHANICAL INSTABILITIES AND SELF-ORGANIZATION OF LIVING FILAMENTS

S. Karpitschka
M. Kurjahn, L. Abbaspour, A. Deka, F. Papenfuß, P. Bittihn, R. Golestanian, B. Mahault, S. Klumpp (Göttingen), M. Lorenz (Göttingen), O. Bäumchen (Bayreuth)

Filamentous cyanobacteria are one of the oldest and today still most abundant lifeforms on earth, with manifold implications in ecology and economics (Fig. 6.2 a). Their flexible filaments, often several hundred cells long (Fig. 6.2 b), exhibit gliding motility in contact with solid surfaces, which allows them to aggregate into complex structures that respond collectively to environmental cues. The force generating mechanism underlying their motility remains poorly understood.

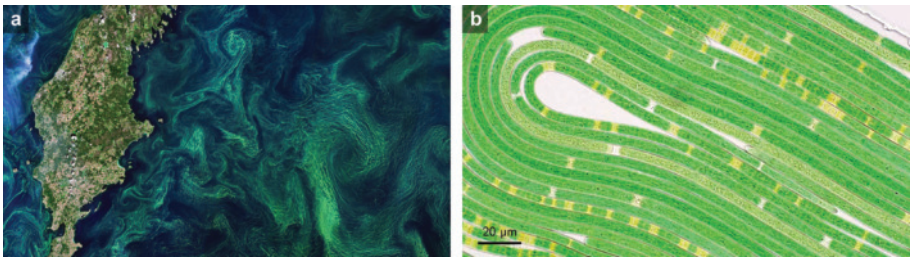

Figure 6.2: a. Cyanobacterial bloom in the baltic sea next to Gotland, a phenomenon increasing in frequency and intensity due to climate change. **b.** Ensemble of filamentous cyanobacteria confined to a monolayer in a microfluidic channel.

We directly measured their bending moduli using micropipette force sensors (Fig. 6.3 a,b), and quantified their propulsion and friction forces by analyzing their self-buckling behavior (Fig. 6.3 c,d), a mechanical instability originally described by Leonhard Euler in 1780. We discovered that propulsion and friction are strongly coupled, pointing toward an adhesion-based mechanism.

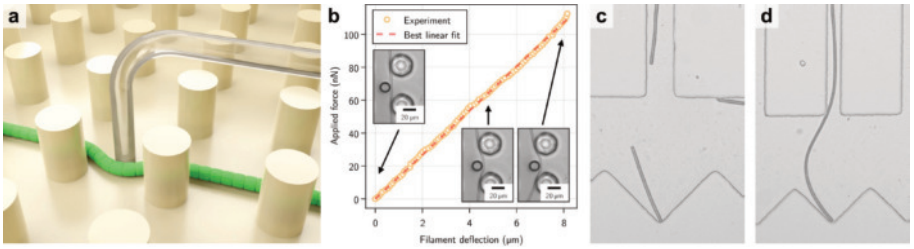

Figure 6.3: a. Microscopic three-point bending test. **b** Force-deflection curve and experiment snapshots. **c, d.** Short filaments don't, but long filaments do self-buckle upon colliding with a wall. the critical length informs about the propulsion force [1].

The unique combination of active self-propulsion, sensing-based direction reversals, and mechanical instabilities leads to intriguing self-organization phenomena that are believed to be vital to the evolutionary success of filamentous cyanobacteria, yet the underlying mechanisms remain to be explored. A particularly beautiful example, where emerging topologies that are selected by the boundary curvature of compact light patterns [2], is highlighted in section 6.15.

[1] M. Kurjahn, A. Deka, A. Girot, L. Abbaspour, S. Klumpp, M. Lorenz, O. Bäumchen, S. Karpitschka, eLife **12**, P87450 (2023)
[2] M. Kurjahn, L. Abbaspour, F. Papenfuß, P. Bittihn, R. Golestanian, B. Mahault, S. Karpitschka, Nature Communications **15**, 9122 (2024)

6.3 FLAT CELL IMAGING

V. Nasirimarekani, E. Bodenschatz
Z. Ditte (MPI-NAT)

Research in life sciences and many diagnostic methods in medicine primarily rely on imaging of living cells and the interaction of the associated molecules or particles with cellular components. As a matter of size and translucency of living cells, high resolution microscopy of the living cells is a challenging task. Although some of the techniques developed overcome the obstacle of the 3rd dimension and take images from different planes within a living cell or tissue, the spatial displacement of the living cell and cellular components cannot be avoided. Therefore, one might simply ask whether it is possible to obtain a quasi-two-dimensional configuration of a living cell in order to obtain an image of the cell in which the cell and its cellular components are largely stationary. If this is the case, the entire cell can be visualized simultaneously in a single focal plane using simple widefield microscopy. We have developed the "Flat Cell Imaging" method which enables us to flatten living cells down to 200 nm, depending on the cell type, whereby a 2D expansion of the living cells by up to 9 times is achieved. This was simply accomplished by flattening living cells in between two high-precision glass microscopy slides functionalized with a graft copolymer of poly(L-lysine) backbone and poly(ethylene glycol) side chains (PLL-g-PEG), which served as two flattening surfaces. The coating offers two main properties: (i) It blocks any plasma membrane attachment to the surfaces, as it is known to repel proteins and cell membranes, known as an antifouling property; (ii) two coated surfaces facing each other cause a high ratio spreading of the liquid between them, resulting in a nanometer depth of the flattened cell.

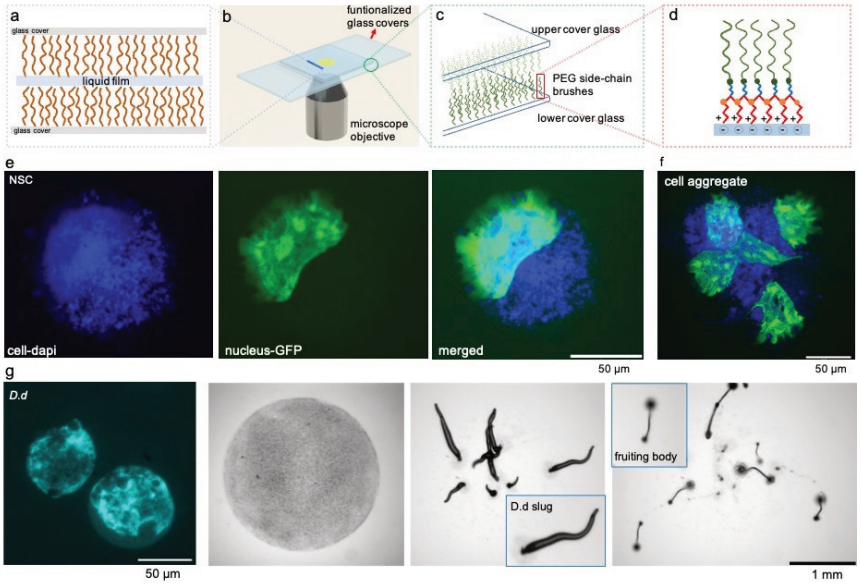

Figure 6.4: a-d) The logic of flat cell imaging as forming a thin layer of liquid in between two polymer brushes. e) example of a flattened cell with labeled nucleus and entire cell. f) examples of flattened cell aggregates. g) study the cell cycle of flattened cells, *Dictyostelium Discodium* as the model cell.

[1] V. Nasirimarekani, Z. Ditte, E. Bodenschatz, arXiv:2411.12656 (2024)

6.4 COLLECTIVE CELL MIGRATION AND SELF-ORGANIZATION IN FILAMENTOUS BACTERIA

V. Nasirimarekani

Questioning from the physics prospective, long filamentous bacteria are intriguing systems to study as they are elastic and flexible filaments and self-organize to macroscopic patterns. These mechanical properties suggest certain shape and motility changes when forces are applied on them. Although, the mechanical properties of the these active filaments are partially known but how their motility changes in different physical environments is not questioned. In other words, how physics defines their motility is not understood.

Right-handed chirality plays an important role in the self-organization of filamentous bacteria into compact aggregates. Rotation around the long axis of a flexible bacterial filament leads to clockwise bending of the filament due to partial friction on the filament. The bending can lead to the formation of bacterial spheres and to the entanglement of bacterial filaments, which then results in the formation of compact, yet dynamic, structures. Furthermore, the bending reduces the gliding velocity of the filament, which recovers when the filament retains its straight shape.

The self-organization of cyanobacteria filaments in a microfluidic channel suggests that there is filamentous self-assembly across scales. The aster formation and merging that we observed in cyanobacteria filaments (4 μm in diameter) is very similar to the aster dynamics of microtubules (20 nm in diameter). This suggests the physics play a crucial role in finally assembly of the filaments regardless of their size and activity mechanism. We are developing a model that can show there is a universal filamentous self-assembly physics in nature in gliding filaments.

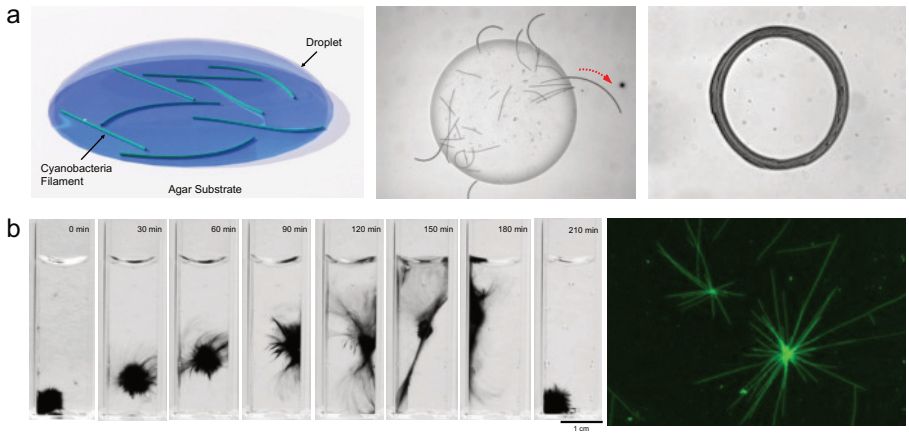

Figure 6.5: a) Clockwise bending of cyanobacteria filaments at the transition from the hydrated volume to a wet substrate. A clockwise bending bundle of the filaments form a stable active ring which preserves its shape. b) Aggregation and clustering of cyanobacteria filaments. The filament-filament interactions result in formation of compact assemblies. formation of dynamic asters in cyanobacteria filaments.

6.5 CILIA DRIVEN CSF FLOW IN THE V3V OF MOUSE BRAIN

S. Kapoor, Y. Wang, S. Villa, E. Bodenschatz, G. Eichele
C. Westendorf (Leipzig University)

Cerebrospinal fluid (CSF) is a water-like liquid that circulates through the brain's four interconnected ventricles, driven by the synchronized beating of cilia on the apical surface of ependymal cells lining the ventricular walls (Fig. 6.6).

These ciliated cells create a directional flow of CSF (Fig. 6.7). Faubel et al. [1] observed that the ventral third ventricle (v3V) in adult mice, rats, and pigs exhibits a complex network of multidirectional streams, guiding near-wall CSF flow in a consistent manner. However, the mechanisms underlying the development and maintenance of such streams remain poorly understood.

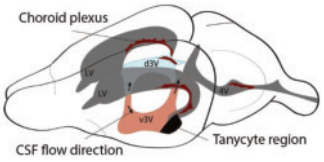

Figure 6.6: Ventricular system in the mouse brain [2], with the v3V marked in red. Within the v3V, the tanycyte region is marked in black.

Our research explores two hypotheses: 1) genetic patterning drives the establishment and maintenance of these streams, and 2) cilia-driven CSF streams serve as transport routes for solutes, modulated in an age-dependent manner by circadian clock genes.

Our findings reveal that the shape and polarity of ependymal cells, which direct ciliary beating [3, 4], are highly conserved and correlate with the stream patterns observed across mice (N > 35). To investigate how these patterns develop, we tracked the movement of fluorescent beads near v3V explants, generating stream maps of the developing v3V. Initial streams appear by postnatal day 5 (P5, Fig. 6.8) in both influx and outflux regions. If hydrodynamics alone guided ciliary orientation, fluid flow would move unidirectionally from the anterior influx to the posterior outflux (Fig. 6.9, with geometry reconstructed from micro-CT scan data [5]). Instead, a multidirectional pattern emerges (Fig. 6.10), suggesting the involvement of genetic mechanisms.

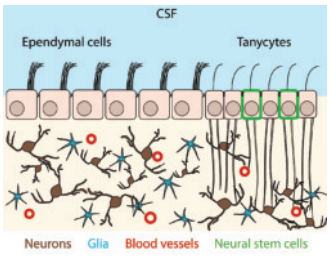

Figure 6.7: Scheme of multiciliated ependymal cells and monociliated tanycytes within the v3V wall [2].

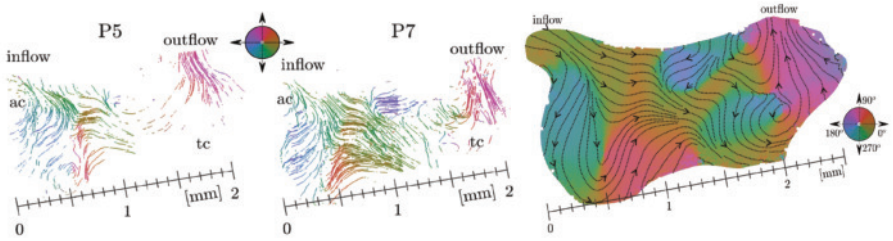

Figure 6.8: Flow maps of P5 and P7 old explants. On the right is an averaged flow map of 35 adult animals.

To test this, we examined whether ependymal cells have distinct regional identities during development. At P3, before stream patterns form, in situ hybridization revealed localized expression of specific patterning and polarity genes across the v3V wall. This suggests that each cell's gene expression profile confers a unique identity, linking genetic patterning to functional polarity and flow organization. We propose that locally expressed proteins influence cell shape and polarity,

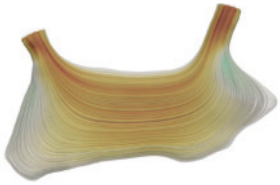

Figure 6.9: Simulation of v3V flow, without cilia. Fluid enters from the anterior duct and leaves the ventricle towards the posteriorly brain.

shaping the v3V stream network. Further research, such as targeted deletion of these genes, could elucidate their roles in flow regulation.

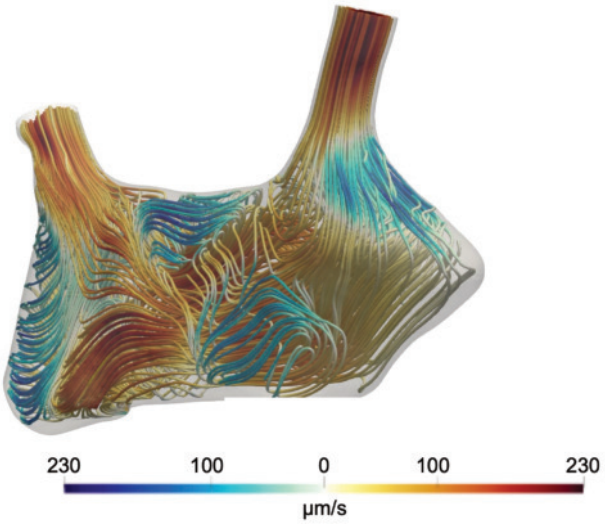

Figure 6.10: Simulation of v3V streams in wild type adult mice. Note the whirl in the lower right and difference in velocities. The areas of low velocities are where tanycytes reside. Streamlines are color-coded using the horizontal component of the local velocity, with red indicating anterior to posterior and blue indicating posterior to anterior.

Another key discovery is that, before P30, streams from both hemispheres direct fluid toward tanycytes, stem-like cells in the posterior v3V (Fig. 6.8). Tanycytes lack motile cilia but extend a primary cilium to interact with CSF and transport cargo into the brain parenchyma [6]. After P30, stream directionality changes only in the left hemisphere, diverting flow away from tanycytes. Interestingly, this hemispheric asymmetry is absent in mutant mice lacking the circadian clock proteins Period1 and Period2. Simulations of CSF fluid dynamics in these mutants resemble wild-type mice prior to P30, suggesting that circadian rhythm pathways influence the timing of stream direction changes.

[1] R. Faubel, C. Westendorf, E. Bodenschatz, G. Eichele, Science **353**, 6295 (2016)
[2] E. Eichele, E. Bodenscatz, Z. Ditte, A. K. Günther, S. Kapoor, Y. Wang, C. Westendorf, Phil. Trans. R. Soc. **375**, 1792 (2019)
[3] Z. Mirzadeh, Y. G. Han, M. Soriano-Navarro, J. M. García-Verdugo, A. Alvarez-Buylla, J. Neurosci. **30**, 7 (2010)
[4] C. Boutin, P. Labedan, J. Dimidschstein, F. Richard, H. Cremer, P. André, Y. Yang, M. Montcouquiol, A. M. Goffinet, F. Tissir, Proc. Natl. Acad. Sci. USA **111**, 30 (2014)
[5] T. Greiner, K. Manzhula, L. Baumann, H. Kaddatz, J. Runge, J. Keiler, M. Kipp, S. Joost, Front. Neuroanat. **16**, 1046017 (2022)
[6] E. Rodríguez, M. Guerra, B. Peruzzo, J. L. Blázquez, J. Neuroendocrinol. **31**, e12690 (2019)

6.6 MINIMUM DISSIPATION THEOREM FOR MICROSWIMMERS

A. Daddi-Moussa-Ider, R. Golestanian, A, Vilfan

A key question in the field of microswimmers is the energetic cost associated with their propulsion. The dissipation of a self-propelled swimmer differs profoundly from a particle pulled by an external force. In a biological context, the focus is on how swimmers have evolved to maximize efficiency and how closely they approach the theoretical limits defined by hydrodynamics. We derived a general theorem that establishes an exact lower bound on the total dissipation—both external and internal—of a microswimmer. Our approach can be applied to a variety of scenarios, including active surface-propelled droplets, swimmers with extended propulsive layers, swimmers with effective internal dissipation [1], as well as Marangoni surfers propelled by surface tension gradients [2].

Determining a lower bound on dissipation involves identifying the force distribution that minimizes dissipation while maintaining a given swimming speed for a specific swimmer type and shape. This problem can be solved by generalizing the minimum dissipation theorem originally formulated for swimmers with external dissipation only, such as those with idealized propulsion mechanisms [3]. The derivation relies on two fundamental properties of the Stokes flow: the Helmholtz minimum dissipation theorem and the Lorentz reciprocal theorem. Our approach requires defining two passive problems that satisfy the velocity boundary conditions of the original problem. One represents the flow with minimal dissipation under these boundary conditions, while the other involves passive flow with velocities orthogonal to the active forces. The lower bound on dissipation is then determined by the reciprocal difference between the two drag coefficients. For example, in the case of a surface-driven swimmer, the two passive problems correspond to a Navier-slip body and a no-slip body (Fig. 6.11).

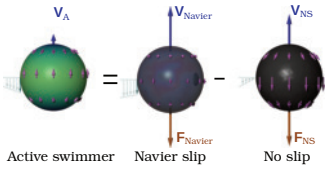

Figure 6.11: An optimal surface-driven active swimmer with both external and internal dissipation can be represented as a superposition of a passive body with Navier slip body and one with no-slip boundary.

The results have implications for the entropy production in suspensions of microswimmers, which is a fundamental question in stochastic thermodynamics and statistical physics. A common assumption in these works is to estimate the "housekeeping" work needed to propel active particles by representing autonomous propulsion as external forces acting on the particles. We have shown that this picture needs to be complemented by an unavoidable contribution that is related to the energetic cost of force generation in a fluidic environment [1].

Our work provides insights into the mechanisms of dissipation in microswimmers, offering a framework for optimizing energy efficiency and advancing the design of synthetic propulsion systems.

[1] A. Daddi-Moussa-Ider, R. Golestanian, A. Vilfan, Nat. Commun. **14**, 6060 (2023)
[2] A. Daddi-Moussa-Ider, R. Golestanian, A. Vilfan, J. Fluid Mech. **986**, A32 (2024)
[3] B. Nasouri, A. Vilfan, R. Golestanian, Phys. Rev. Lett. **126**, 034503 (2021)

6.7 HYDRODYNAMIC SYNCHRONISATION OF CILIA

A. Vilfan, D. J. Hickey, F. Meng, R. Golestanian

Biological cilia are hairlike organelles which beat periodically in order to transport or mix the surrounding fluid. When many motile cilia are arranged on a surface, their beating can synchronize with a phase lag between neighboring cilia, resulting in metachronal waves. A fundamental problem in understanding hydrodynamic synchronization is the reversible nature of the Stokes equation (the flow exactly reverses its direction upon reversal of forces), whereas the tendency of a system to reach an ordered state is by definition irreversible.

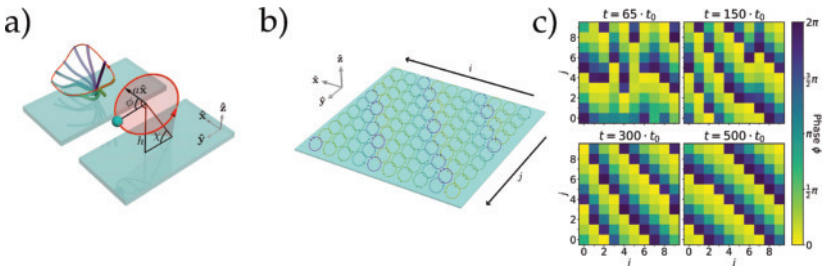

Figure 6.12: a) The model represents the motion of a cilium with a particle moving along a tilted trajectory. b) An array of model cilia subject to hydrodynamic interactions. c) The emergence of metachronal waves from an initially disordered state.

To understand the process of synchronisation, we studied a model where each cilium is represented as a spherical particle, moving along a tilted trajectory with a position-dependent active driving force and a position-dependent internal drag coefficient (Fig. 6.12a). The model thus takes into account all the essential broken symmetries of the ciliary beat. We showed that because of near-field hydrodynamic interactions, the effective coupling between cilia can become nonreciprocal: the phase of a cilium is more strongly affected by an adjacent cilium on one side than by a cilium at the same distance in the opposite direction. As a result, synchronisation starts from a seed at the edge of a group of cilia and propagates rapidly across the system (Fig. 6.12b,c), leading to a synchronisation time that scales proportionally to the linear dimension of the system. A ciliated surface is thus characterised by three different velocities: the velocity of fluid transport, the phase velocity of metachronal waves and the group velocity of order propagation. Unlike in systems with reciprocal coupling, boundary effects are not detrimental for synchronisation, but rather help to initiate the wave [1].

The role of near-field effects can also be understood analytically by performing a linear stability analysis of the metachronal wave. Hydrodynamic interactions in the far-field approximation lead to a spatially symmetric distribution of stable wave vectors [2]. Extending the model to include near-field effects to the leading order, however, breaks the symmetry such that only one direction remains stable [3].

[1] D. J. Hickey, R. Golestanian, A. Vilfan, Proc. Natl. Acad. Sci. USA **120**, e2307279120 (2023)

[2] F. Meng, R. R. Bennett, N. Uchida, R. Golestanian, Proc. Natl. Acad. Sci. USA **118**, e2102828118 (2021)

[3] Z. Cheng, A. Vilfan, Y. Wang, R. Golestanian, F. Meng, J. R. Soc. Interface **21**, 20240221 (2024)

6.8 NONEQUILIBRIUM FLUCTUATIONS IN ACTIVE MATTER

A. Bose, L. Cocconi, R. Golestanian, B. Mahault
J. Berx (Copenhagen), J. Codina (Beijing), J. Dobnikar (Beijing),
H. Chaté (Paris), P. Godara (Darmstadt),
I. Pagonabarraga (Barcelona), X.-q. Shi (Suzhou)

Active fluctuations are generally non-Brownian and have a significant impact on active systems. Understanding their influence on the dynamics is therefore crucial for assessing the robustness and potential applications of active matter.

For example, we have recently demonstrated that an isolated obstacle may have dramatic consequences on the large-scale properties of flocks [1]. Specifically, simulations of the Vicsek model and the associated kinetic theory reveal that the circular obstacle acts as a nucleation site for stochastic perturbations, which propagate throughout the flock and reverse the direction of collective motion (Fig. 6.13). In very large systems, where these events become more frequent, our results further show that the obstacle prevents the emergence of collective motion. The possibility for spontaneous nucleation of such perturbations, in particular, raises fundamental questions about the stability of flocks and related active matter systems.

Active processes may also lead to a suppressed effective temperature at macroscopic scales, which we term *diffusivity edge* [2]. Under the influence of a confining potential, this phenomenon gives rise to a nonequilibrium condensation transition that shares thermodynamic properties with Bose-Einstein condensation [2, 3]. The diffusivity edge class, described by a mean-field phenomenological equation, is of particular interest as a minimal model for active condensation. Our current work extends beyond the mean-field regime, exploring how fluctuations affect the condensation transition. We have recently found that the singular nature of the diffusivity-edge induced condensation results in a strongly non-Gaussian distribution of the condensate occupation, as well as giant fluctuations [4].

Introducing a minimal model of self-propelled particles with fluctuating motility, we have investigated the influence of fluctuations of activity on the physics of active systems [5]. We showed that fluctuating activity qualitatively modifies the segregation properties of self-propelled particles in the presence of spatial activity variations, and highlighted generic polarity-speed correlations that cannot be captured by models with deterministic motility. Moreover, our results indicate that active fluctuations can drive and reinforce motility-induced phase separation, whereby active particles self-organize into dense clusters without relying on attractive interactions.

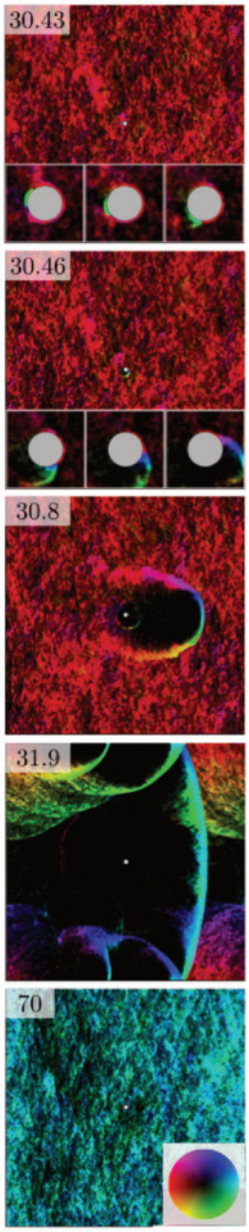

Figure 6.13: Snapshots showing the reversal of large-scale collective motion by a single obstacle (gray disk in center), time runs from top to bottom. Insets in the upper panels highlight the nucleation of the initial perturbation. The color codes for the moving direction of the particles (legend in bottom panel).

[1] J. Codina, B. Mahault et al., Phys. Rev. Lett. **128**, 218001 (2022)
[2] R. Golestanian, Phys. Rev. E **100**, 010601(R) (2019)
[3] J. Berx, A. Bose, R. Golestanian, B. Mahault, Europhys. Lett. **142**, 67004 (2023)
[4] A. Bose, L. Cocconi, R. Golestanian, B. Mahault, *in preparation*
[5] B. Mahault, P. Godara, R. Golestanian, Phys. Rev. Research **5**, L022012 (2023)

6.9 EMERGENT POLAR ORDER IN NON-RECIPROCAL ACTIVE MIXTURES

G. Pisegna, S. Saha, R. Golestanian

When a system consists of different types of active particles in a complex environment, non-conservative forces can emerge. An example is when interactions between active particles are mediated by external elements. In such cases, the effective forces often become non-reciprocal, meaning one species interacts asymmetrically with the other. To study the large-scale behavior emerging from these interactions, we use phenomenological models that allow to make concrete predictions about their universality class based on symmetries, conservation laws, and dimensionality.

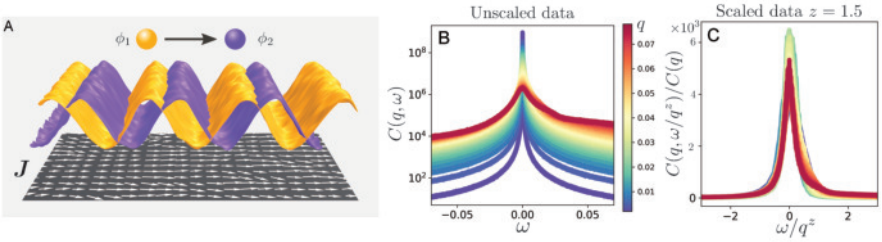

Figure 6.14: A: Density waves of species ϕ_1 chasing ϕ_2 because of non-reciprocity. In the lower plane the corresponding polar order parameter $\boldsymbol{J}$. B: dynamical correlation functions of the slow mode in $d = 1$; C: same functions as in B collapsing with the KPZ exponent.

In [1], we study a generic model for nonreciprocal interactions and we focus on the polar collective motion resulting from one species chasing the other (Fig 6.14A). Through analytical and numerical studies we establish the presence of long-range polar order in two and higher dimensions. We achieve this by developing a theory for a suitable polar order parameter, mapping our model for scalar mixtures to the Toner-Tu theory of dry polar active matter. Additionally, we show that the full effective field theory—with all soft modes and significant nonlinear terms—falls within the (Burgers-) Kardar–Parisi–Zhang universality class (Fig 6.14B,C). This classification enables us to confirm the stability of emergent polar long-range order in scalar nonreciprocal mixtures in two dimensions, hence violating the Mermin–Wagner theorem.

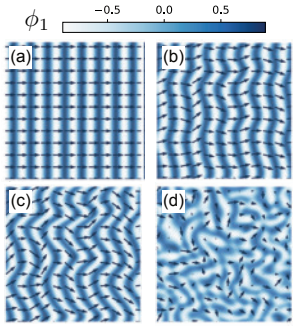

Figure 6.15: (a-d) Time series of density field ϕ_1 undergoing the hydrodynamic instability caused by active stresses. The arrows indicate the related polar order parameter field.

Natural systems are often three dimensional, leading to momentum conservation in the bulk. To study this scenario, we include in the model hydrodynamic interactions mediated by an external solvent [2]. We focus on the emergent polar ordered phase, showing the emergence of a linear instability reminiscent of polar and nematic systems in suspension. At the onset of the instability, the fluid flow pulls the densities layers apart and destroys the order (Fig. 6.15). However, there is a parameter space where order is stable and where high non-reciprocity stabilizes the propagating waves even in the unstable regime. This result confirms that the non-equilibrium polar pattern is very robust also to hydrodynamic couplings.

[1] G. Pisegna, S. Saha, R. Golestanian, Proc. Natl. Acad. Sci. USA **121**, e2407705121 (2024)
[2] G. Pisegna, N. Rana, R. Golestanian, S. Saha, arXiv:2501.01330

6.10 NONRECIPROCAL COLLECTIVE DYNAMICS IN MIXTURES OF PHORETIC JANUS COLLOIDS

G. Tucci, N. Rana, G. Pisegna, R. Golestanian, S. Saha

Our research focuses on the collective behavior of Janus colloids, a class of artificial particles characterized by anisotropic chemical or physical properties across their surface [1]. These colloids are immersed in a fluid containing a suspended chemical substrate. The coated surface of the colloids catalyzes chemical reactions, creating anisotropic local concentration gradients of the substrate. These gradients generate a slip velocity along the particle's surface, resulting in self-propulsion. Assuming an axisymmetric distribution of catalytic sites, the particles propel along their symmetry axis.

Janus colloids exhibit another fascinating feature: their response to external chemical gradients. They can exhibit (anti-)chemotactic behaviors, developing velocities aligned with (or opposing) these gradients. Additionally, they may chemotactically (anti-)align their orientation with the gradients. To analyze their collective behavior, we transition from a microscopic description to a field-theoretical framework that captures the system's slow and most relevant modes—namely, particle density, polarization, and substrate concentration.

Orientation is a key aspect of Janus colloids. We have studied how polarization effects can destabilize a homogeneous, disordered state, leading to pattern formation. This system exhibits a rich variety of phases, including stationary aster configurations, where particles radially align, and dynamic states such as traveling asters and oscillatory patterns.

A significant portion of our work investigates nonreciprocal interactions, which violate Newton's third law of action and reaction. Multi-species collections of Janus colloids, i.e., particles with varying responses to a shared chemical substrate, provide an intuitive platform for exploring these interactions. We have studied the emergent properties and phases in two-species mixtures, highlighting phenomena uniquely due to nonreciprocity.

When hydrodynamic effects become significant, we derive the corresponding hydrodynamic equations to incorporate the presence of Janus colloids. Under the assumption of Stokesian flow, we construct the stress tensor and density field equations for various colloidal species [2]. Furthermore, we establish connections between these systems and the theory of active liquid crystals, emphasizing the role of nonreciprocal interactions in shaping their behavior.

Overall, our research elucidates the intricate dynamics of Janus colloids, from self-propulsion and chemotactic responses to the emergence of complex phases driven by nonreciprocity and hydrodynamic effects. These insights contribute to a deeper understanding of active matter systems and their potential applications.

[1] G. Tucci, R. Golestanian, S. Saha, New J. Phys. **26**, 073006 (2024)
[2] G. Tucci, G. Pisegna, R. Golestanian, S. Saha, arXiv:2502.07744

6.11 EQUILIBRIUM AND NONEQUILIBRIUM EFFECTS ON DIFFUSION IN CHEMICALLY-ACTIVE SYSTEMS

J. Agudo-Canalejo, R. Golestanian
N. Rezaei-Ghaleh, C. Griesinger (Göttingen)
A. Benois, M. Jardat, V. Dahirel, V. Démery, P. Illien (Paris)
N. Bellotto, R. Colin, G. Malengo, V. Sourjik (Marburg)

Understanding diffusive processes in multicomponent systems in and out of equilibrium is necessary for further progress in the fields of intracellular dynamics, synthetic biology, and origins of life research. In a series of recent collaborations, we have studied how key features of these systems such as catalyzed chemical reactions, conformational fluctuations, or confinement affect diffusion.

In one of them, we investigated the diffusivity of molecular-scale catalysts, reactants, and products of a model click reaction [1, 2]. Contrary to existing claims that all components in this reaction undergo enhanced diffusion boosted by the energy released during catalysis, our novel analysis of the diffusion NMR experiments showed no such enhancement and instead point to the role of a relatively large intermediate species within the reaction cycle, with diffusivity lower than that of the free reactant and product molecules (Fig. 6.16).

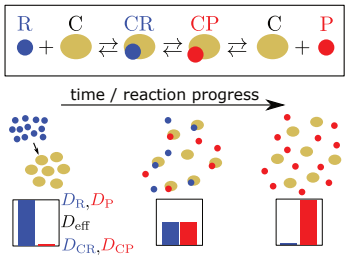

Figure 6.16: Top: Schematic of a simple catalyzed reaction. Bottom: Over the course of the reaction, the apparent diffusion coefficient of the reactant monotonically decreases from the diffusion coefficient of the free reactant D_R to that of the catalyst-reactant complex D_{CR}; while the reverse is true for the product, which monotonically increases from D_{CP} to D_P.

Catalytic activity, when combined with chemotaxis [3] in response to the same chemicals that are produced or consumed, causes effective interactions between catalysts. In systems with two distinct catalysts, these interactions can be nonreciprocal, so that e.g. catalyst A is attracted to B whereas B is repelled from A. We investigated this effect in another collaboration [4]. The analytical theory that we developed, verified by computer simulations, predicts that nonreciprocity can lead to substantial enhancements in the long time diffusion of catalysts (Fig. 6.17). This may provide an explanation for existing experimental observations showing that, in bacteria, metabolic activity fluidizes an otherwise glassy cytoplasm.

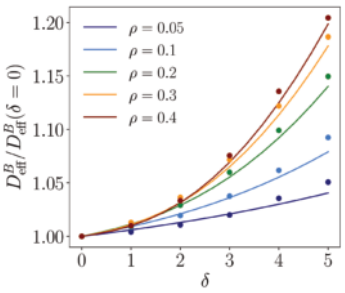

Figure 6.17: With increasing nonreciprocity of the interactions, as measured by the parameter δ, the effective diffusion coefficient of the catalyst (here, catalyst B) increases. The enhancement is more pronounced for larger catalyst concentrations ρ. Circles correspond to simulations, while lines are the (parameter-free) analytical prediction.

Finally, in another experimental collaboration, we investigated protein diffusion in the cytoplasm of *E. coli* [5]. Previous FCS studies have claimed that cytoplasmic diffusion is anomalous, and that its dependence on protein size does not satisfy the Stokes-Einstein relation. In contrast, we showed that diffusion is Brownian when one accounts for the effect of confinement within the cell boundaries in the analysis, and that the Stokes-Einstein relation is recovered when one accounts for the fluctuating dumbbell-like shape of GFP-protein fusions.

[1] N. Rezaei-Ghaleh, J. Agudo-Canalejo, C. Griesinger, R. Golestanian, J. Am. Chem. Soc. **144**, 1380 (2022)
[2] N. Rezaei-Ghaleh, J. Agudo-Canalejo, C. Griesinger, R. Golestanian, J. Am. Chem. Soc. **144**, 13441 (2022)
[3] J. Agudo-Canalejo, P. Illien, and R. Golestanian, Langmuir **38**, 2746 (2022)
[4] A. Benois, M. Jardat, V. Dahirel, V. Démery, J. Agudo-Canalejo, R. Golestanian, P. Illien, Phys. Rev. E **108**, 054606 (2023)
[5] N. Bellotto, J. Agudo-Canalejo, R. Colin, R. Golestanian, G. Malengo, V. Sourjik, eLife **11**, e82654 (2022)

6.12 MESOSCALE NEMATIC STRUCTURE OF GROWING CELL COLONIES

J. Isensee, L. Hupe, R. Golestanian, P. Bittihn

Growth as an activity defines a fascinating sub-field of active matter. Energy is injected in the form of building materials and the non-equilibrium activity to assemble them, e.g., in growing tissues or biofilms. However, many emergent phenomena that result from this activity can already be recapitulated in minimal model systems where these processes are replaced by (unconditional) volume growth of the smallest particles, which would correspond to cells in biological systems. Understanding these phenomena can not only yield insights into the self-organization processes in biology but also inform strategies for self-assembling materials in the future.

A prominent example is the collective orientation dynamics emerging from growing and dividing rod-shaped particles akin to bacteria. We conduct agent-based simulations for colonies expanding freely or confined in channel geometries resembling the conditions of microfluidic channel experiments [1, 2], where rod-like cells continuously double their length and divide. Previous work revealed microdomain formation and peculiar stress dynamics in channels [1]. During free expansion, growth leads to dense configurations with microdomains of aligned cells (Fig. 6.18B). Made up of growing cells, these microdomains expand and move with the global flow before becoming mechanically unstable and breaking up. Uncovering the underlying principles of microdomain mechanics is one of the main goals of this research.

As steric repulsion is the only interaction present in the model, all emerging dynamics must be caused by the directed addition of material and the mechanical response which depends on particle shape. To investigate the non-trivial feedback process between directed growth and mechanical response, our recent work [3] defines a modeling variant that allows for continuous variation of the tip shape towards either more *pointy* or *flat-spotted* particles (Fig. 6.18A). We find the distribution of microdomain sizes in freely expanding colonies to be heavily influenced by both tip-shape and division aspect ratio (see example snapshots in Fig. 6.18B,C). Strongly pointed tips prevent the formation of large microdomains while strongly flat-spotted cells may form large clusters even when the division aspect ratio is small (Fig. 6.18D). Using an effective master equation model, we are able to relate different microdomain size distributions to distinct breakup mechanisms.

Ongoing work is focused on finding better effective descriptions of the dynamics using the tools of continuum mechanics and consolidating existing models of varying complexity for the low-order regimes [4].

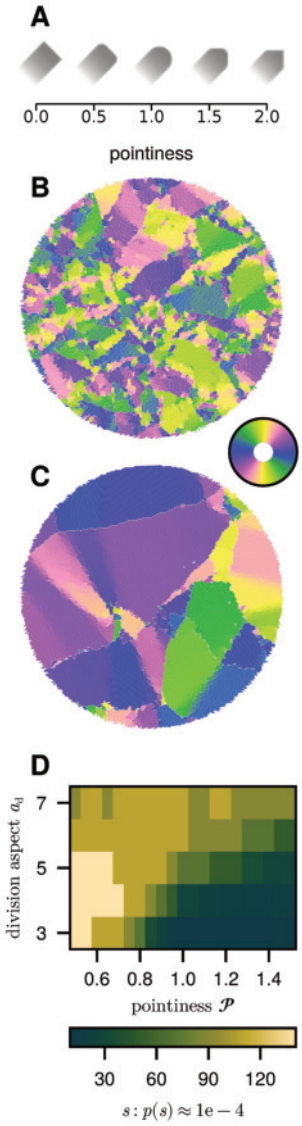

Figure 6.18: (A) A continuous variation of the tip shape form rectangular through circular to triangular tip is parameterized by a pointiness $\mathcal{P}$. (B & C) Snapshots of microdomain dynamics for regular rods ($\mathcal{P} = 1$) in (B) and $\mathcal{P} = 0.5$ in (C). (D) Approximate measure for the largest clusters appearing in freely expanding circular colonies as a function of division aspect ratio a_d and pointiness $\mathcal{P}$

[1] J. Isensee, L. Hupe, R. Golestanian, P. Bittihn, J. R. Soc. Interf. **19**, 20220512 (2022)
[2] L. Hupe*, Y.G. Pollack*, J. Isensee, A. Amiri, R. Golestanian, P. Bittihn, arXiv:2409.01959
[3] J. Isensee, P. Bittihn, Soft Matter **21**, 4233 (2025)
[4] L. Hupe, J. Isensee, R. Golestanian, P. Bittihn, arXiv:2506.10867

6.13 RE-CONFIGURING MULTIFARIOUS SYSTEMS

J. Metson, S. Osat, R. Golestanian
M. Kardar (MIT)

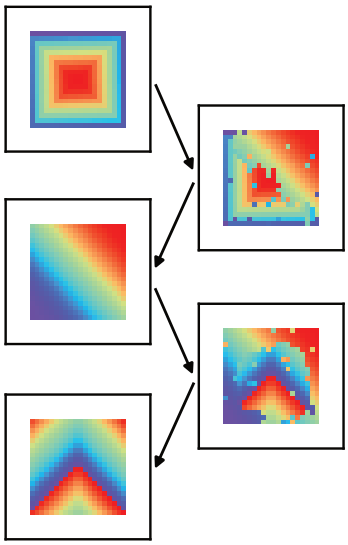

Figure 6.19: An illustration of non-reciprocal multifarious self-organization, showing shape-shifting between three different arrangements of the coloured tiles.

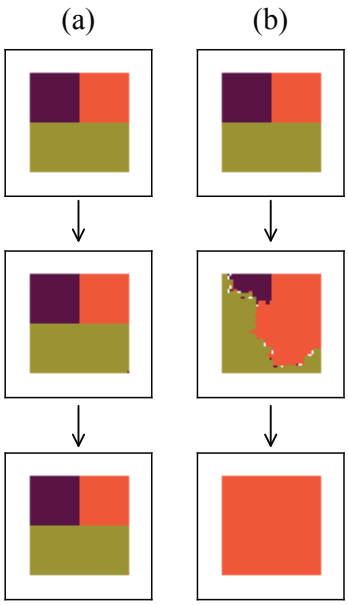

Figure 6.20: (a) In equilibrium, the system is stuck in the trapped state (mixed 'chimeric' structure). (b) Non-reciprocal interactions can be used to drive the system out of the trap and towards the desired state (fully orange structure).

The natural world is filled with intricate structures that emerge from the self-organization of individual building blocks. Harnessing these processes to develop synthetic materials has been a longstanding goal. Multifarious systems can be constructed to assemble different structures using a common set of components, mirroring the economical re-purposing of building blocks found across many natural systems. We are developing multifarious systems capable of more than just self-assembly, embedding dynamic and autonomous re-configuration into multifarious systems. For example, we have shown how to design multifarious systems with allosteric interactions to achieve shape-shifting, sorting, and self-replication [1].

Shape-shifting has also been demonstrated by the non-reciprocal multifarious self-organization (NRMSO) model [2], which is illustrated in Fig. 6.19 and presented further in Article 6.22. Building off of the initial discrete-time Monte Carlo simulations of NRMSO, we have investigated continuous-time simulations of the model using the Gillespie algorithm, both in equilibrium [3] and out of equilibrium [4]. Interestingly, for most of the parameter space we see the same boundaries using discrete-time and continuous-time simulations, even in non-equilibrium systems. There are some exceptions, which we analyse in more detail in the respective works. Moreover, we have made analytical calculations of the timescales involved in shape-shifting, which agree well with the timescales measured in our simulations, allowing us to identify the primary mechanisms governing shape-shifting under different parameter values.

A crucial issue for systems trying to find a particular energy minimum is the presence of kinetic traps. These traps correspond to deep unwanted minima in the energy landscape, in which a system can become stuck for extremely long times. Using NRMSO as a model system, we showed how non-reciprocal interactions can be used to drive systems out of a trapped state and towards a desired energy minimum [5]. This is illustrated in Fig. 6.20. We furthermore investigated the escape mechanisms in our system, uncovering Kardar–Parisi–Zhang interfaces and spiral defects. An example of defect-mediated escape is shown in Fig. 6.20(b). Deeper investigation into these dynamics in similar systems is one goal of future research.

Our findings are contributing to the rapidly growing field of non-equilibrium self-assembly, offering pathways to design systems capable of dynamic structural re-configuration.

[1] J. Metson, arXiv:2410.17807
[2] S. Osat and R. Golestanian, Nat. Nanotechnol. **18**, 79–85 (2023)
[3] J. Metson, S. Osat, R. Golestanian, arXiv:2506.07648
[4] J. Metson, S. Osat, R. Golestanian, arXiv:2506.07649
[5] S. Osat, J. Metson, M. Kardar, R. Golestanian, Phys. Rev. Lett. **133**, 028301 (2024)

6.14 A GENERAL THEORY OF NONEQUILIBRIUM DEFECT MOTION

J. Romano, B. Mahault, R. Golestanian

Many systems display the emergence of singularities (or defects) at large scale, as domain walls for magnetic materials, interfaces for phase-separating polymers and point defects for liquid crystals. Out of equilibrium the defects move, significantly affecting the evolution of the system. Our work tries to understand this dynamics and use them to characterize the large-scale properties of the system.

Defects: dynamical aspects and non-linear features Liquid crystals are passive systems that relax to equilibrium by reducing their free energy. This happens by two mechanisms: the first is the motion of the point defects, the second is the evolution of the angular field which describes the orientation of the nematogens. In [4] we provide the explicit form of this angular field in diffusive systems, uncovering how the defect trajectory affects the Schlieren texture.

In [5] we tackle the opposite problem of deriving the trajectory of a defect knowing the angular field. The approach we introduced is both simpler and more general than previous existing ones [2, 6], enabling us to investigate previously unexplored aspects of the defects motion.

In particular, for defects in liquid crystals, we have been able to analitically determine the effects of elastic anisotropy on defect motion, showing it causes defect pairs to perform curved trajectories (in place of straight ones) toward annihilation.

Interfaces in driven systems Cells use droplets of phase-separating biopolymers as membraneless organelles to achieve sub-cellular organization. Often this phase separation happens under in-homogeneous and non-stationary environmental conditions [1]. In [7] we thus extend our formalism find the equations of motion for an interface in mixtures with space and time dependent free-energy density. We show that in these systems the force of an interface gains a new normal contribution proportional to the gradient of the (space-dependent) surface tension. We apply our formalism to the study of mixtures at non-homogeneous temperatures. Remarkably, we predict that while larger droplets can be both thermophobic or thermophilic (depending on the mixture under consideration), sufficiently small ones are always thermophilic.

[1] C. P. Brangwynne, C. R. Eckmann, D. S. Courson, A. Rybarska, C. Hoege, J. Gharakhani, F. Jülicher, and A. A. Hyman, Science **324**, 1729 (2009)
[2] C. Denniston, Phys. Rev. B **54**, 6272 (1996)
[3] A. Missaoui, K. Harth, P. Salamon, and R. Stannarius, Phys. Rev. Res. **2**, 013080 (2020)
[4] J. Romano, B. Mahault, and R. Golestanian, J. Stat. Mech., 083211 (2023)
[5] J. Romano, B. Mahault, and R. Golestanian, J. Stat. Mech., 033208 (2024)
[6] Pismen, L. M. Oxford University Press (1999)
[7] J. Romano, R. Golestanian, and B. Mahault, arXiv:2506.19029

6.15 VIRTUAL CAGES: THE COLLECTIVE BEHAVIOR OF ACTIVE FILAMENTS

L. Abbaspour, M. Kurjahn, F. Papenfuß, P. Bittihn, R. Golestanian, B. Mahault, S. Karpitschka

Aggregation in response to environmental cues is a key factor in the success of many living organisms, but the physics principles governing its emergence are not yet thoroughly understood. Combining controlled experiments and numerical modelling, we investigated the photoresponse-driven aggregation of filamentous cyanobacteria induced by inhomogeneous light conditions (for more information on the biology and mechanics of these organisms, see Section 6.2).

Illuminating colonies of gliding cyanobacteria with compact light patterns (Fig. 6.21(a)), we discovered that their behaviour goes far beyond simple accumulation. Although these organisms exhibit purely one-dimensional motility, such that they avoid dark regions by reversing their direction of motion in response of a sudden decrease in illuminance (Fig. 6.21(c)), they are able to form entangled aggregates at the boundaries of illuminated regions, harnessing the boundary to establish local order (Fig. 6.21(b), left).

Remarkably, such structure formation occurs without explicit alignment mechanisms, as confirmed by numerical simulations of a minimal model of flexible active filaments [2]. Specifically, we demonstrated that soft repulsion driving alignment of the filaments and reversals at light gradients are minimal ingredients sufficient to replicate this behaviour (Fig. 6.21(b), right), therefore highlighting its emergent and generic nature.

Our results show that even the simplest organisms, incapable of active reorientation, exploit self-organization to form complex entangled structures, underscoring the importance of emergent collective phenomena in understanding their behavior in natural habitats.

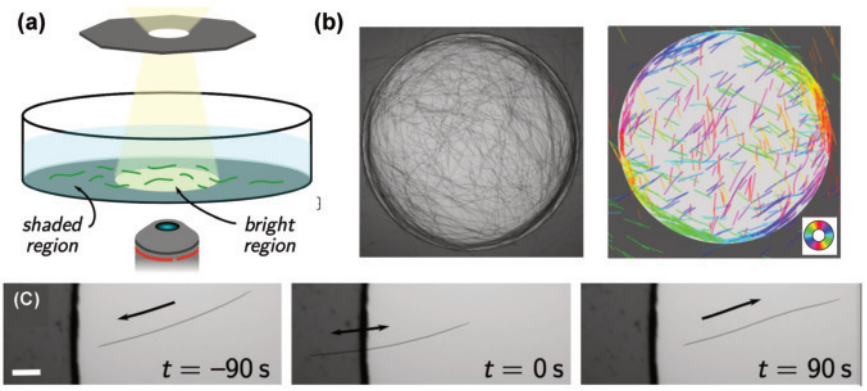

Figure 6.21: (a) Schematic of the experimental setup: Filaments glide at the bottom of a Petri dish, submerged in medium and are illuminated from above with a masked light pattern. (b) Ring formation in the experiment (left) and simulations (right), with the color wheel showing the local orientation of filaments. (c) Velocity reversal of *O. lutea* gliding into the dark. Scale bar: 100 μm.

[1] A. Wilde, and C. W. Mullineaux, FEMS Microbiol. Rev. **41**, 6 (2017)
[2] M. Kurjahn, L. Abbaspour, F. Papenfuß, P. Bittihn, R. Golestanian, B. Mahault, S. Karpitschka, Nat. Commun. **15**, 9122 (2024)

6.16 AUTONOMOUS CONTROL OF SMART ACTIVE MATTER

L. Cocconi, L. Piro, B. Mahault, A. Vilfan, R. Golestanian

Much is known about the non-equilibrium physics of motile active matter, namely of agents, such as micro-swimmers and catalytic colloids, which can locally convert environmental resources into work for the purpose of self-propulsion. Nevertheless, models that integrate such force generation with the recording, processing and/or relaying of information at the single agent level *remain comparatively less explored*. Bridging this gap is a crucial challenge that the field of active matter needs to face in order to *unlock future biological and technological applications*, from swarm robotics to targeted drug delivery.

The integration of actuation and sensing (i.e. autonomous control), comes at a thermodynamic cost, which needs to be factored into the limited energy budget of microscopic "smart" machines. While likely to give rise to fundamental tradeoffs, these costs have been consistently neglected in the field, making their characterisation an important open question. Stochastic thermodynamics is a powerful tool to address problems of this nature, having already led to the discovery of quality-dissipation bounds on a variety of fundamental biological operations, from error correction to substrate discrimination.

A promising platform for systematically exploring physical constraints associated with autonomous control through the lens of stochastic thermodynamics is offered by models of agents capable of processing environmental cues to optimize their search for nutrients and mating partners, or to escape predators. In this context, sometimes referred to as *taxis-based navigation*, regulatory feedbacks can be employed to overcome Brownian motion and confine the trajectory of the agent to a target subspace as part of a (semi)autonomous steering control mechanism. We have begun to explore this problem from the angle stochastic optimal control [1–3], however, theoretical insight of a thermodynamic nature *has been hindered by the lack of minimal, analytically tractable models*. In a more recent work [4], we have introduced such a model in the form of a generalization of the canonical process known as the Active Brownian particle (ABP), reminiscent of the dynamics of phoretic Janus colloids (see Fig. 6.22 for a schematic illustration). Our model describes an autonomous agent capable of error-prone self-steering in accordance with a pre-defined, space-dependent "steering policy" $\mathbf{u}^*(\mathbf{r})$. Crucially, it is simple enough to characterise analytically the energy dissipated by the agent into the information processing that enables its steering, establishing a new fundamental physical relation between precision and its associated energetic cost.

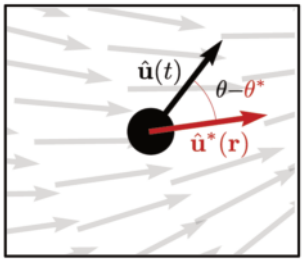

Figure 6.22: Navigation by a self-steering active Brownian particle: the agent is subject to a self-generated torque attempting to align its instantaneous self-propulsion direction (black vector) with a given position-dependent steering policy (grey vector field). In addition, the agent is subject to both positional and angular diffusion with thermal origin.

[1] L. Piro, B. Mahault, R. Golestanian, New J. Phys **24**, 093037 (2022)
[2] L. Piro, A. Vilfan, R. Golestanian, B. Mahault, Phys. Rev. Res. **6**, 013274 (2024)
[3] L. Piro, R. Golestanian, B. Mahault, Front. Phys. **10**, 1034267 (2022)
[4] L. Cocconi, B. Mahault, L. Piro, New J. Phys. **27**, 013002 (2025)

6.17 STATISTICAL PHYSICS OF PROLIFERATION

L. Hupe, S. R. Lish, J. Isensee, R. Golestanian, P. Bittihn
Y. G. Pollack (U. Göttingen), A. Amiri (MPI-PKS)

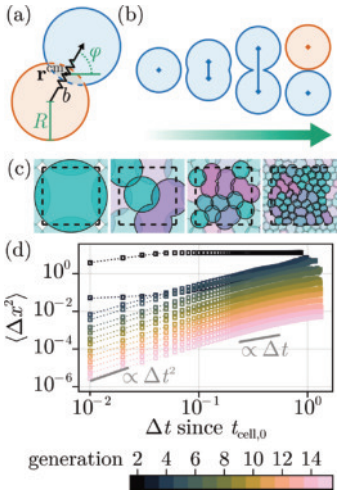

Figure 6.23: (a) Dumbbell cell with nodes and internal spring. (b) Growth and division of a cell. (c) Isovolumetrically dividing cells over six generations. (d) Intra-generational MSDs for different generations.

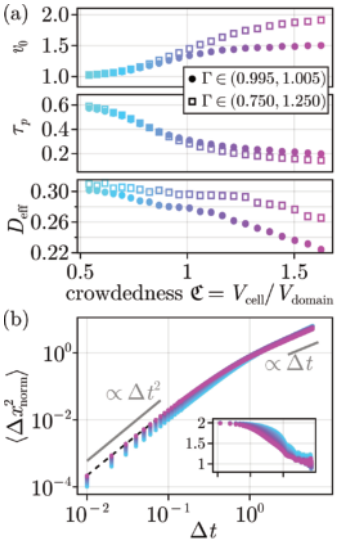

Figure 6.24: (a) Inferred self-propulsion velocity, rot. persistence time and eff. diffusion coefficient for the time-inhomogeneous active Brownian particle model. (b) Renormalized trans-generational mean squared displacements for the isovolumetric division model.

Proliferating active systems such as dense aggregates of growing and dividing cells can behave in unintuitive ways compared to their passive counterparts, e.g. by retaining fluid-like properties even at high crowdedness. While these systems can be simulated numerically using established techniques, characterising their dynamics on large timescales is challenging due to the limited lifetime of particles and often discontinuous division events. To address this issue, we developed a minimal agent-based mechanical model, explicitly designed to produce continuous trajectories and forces upon cell division [1]: Cells are modelled as dumbbells of two circular nodes of radius R_i connected by a spring of rest length b_i (Fig. 6.23a). Over the cell's lifetime, the rest length of this spring increases, pushing the two nodes apart (Fig. 6.23b). At $b_i = 2R_i$, the cell divides: its nodes are replaced with two new cells. Thus, node trajectories remain continuous across divisions.

Besides matching steric interaction force laws between internal nodes and external repulsion across divisions, all interactions are scaled by a factor that accounts for the instantaneous increase in interaction partners as a node of a dividing cell is replaced by the two nodes of its descendant.

We apply the dumbbell model to study isovolumetric division, as seen, e.g., in early embryonic development, by rescaling node radius and rest length to conserve cell volume during the cell division cycle (Fig 6.23c). Cell center mean squared displacements, measured for each individual generation of cells with respect to their time of birth, show self-similar dynamics, with exponents converging while the absolute scale decreases exponentially (Fig. 6.23d).

For insight into the dynamics on longer time scales, we consider the movement of individual nodes traced across generations. We find that an effective active Brownian particle model with an exponentially decreasing length scale can reproduce transgenerational node MSDs observed in the agent-based simulations (Fig. 6.24b), allowing us to characterize the motion of nodes in terms of effective self-propulsion, persistence time and effective diffusion. Fig. 6.24a shows how with increasing crowdedness, trajectories trends towards faster motion, while persistence and effective long-term diffusion decrease. We do not find any evidence of jamming, and wider growth rate distributions Γ (less correlated divisions) lead to higher effective diffusion.

Our results provide insights into the long-term motion statistics expected in embryo-like *isovolumetric dividing active matter* from mechanics alone. This baseline can help delineate biological mechanisms in experiments and inform design strategies for self-assembling systems.

[1] L. Hupe*, Y. G. Pollack*, J. Isensee, A. Amiri, R. Golestanian, P. Bittihn, arXiv:2409.01959
[2] S. R. Lish*, L. Hupe*, R. Golestanian, P. Bittihn, arXiv:2409.20481

6.18 ENZYMES AS STOCHASTIC OSCILLATORS: A BASIC MECHANISTIC DESCRIPTION AND NOVEL OPPORTUNITIES FOR DESIGN AND CONTROL

M. Chatzittofi, J. Agudo-Canalejo, R. Golestanian

A fundamental, interdisciplinary question is how to design biomimetic machines and to develop non-equilibrium strategies to control chemical reaction pathways. While large-scale molecular dynamics simulations can provide valuable insights into the microscopic behavior of these systems, they are often computationally expensive and may not yield simple design strategies. We have addressed this problem by

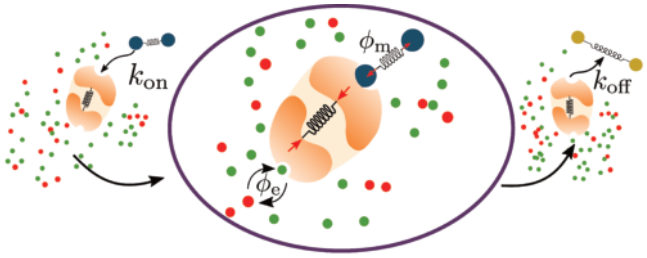

Figure 6.25: The transition state of a chemical reaction, where after the enzymatic binding of the substrate molecule a cyclic fuel-to-waste process (ϕ_e) causes a substrate-to-product reaction (described by ϕ_m).

developing a minimal mechanistic framework describing a fuelled enzymatic reaction [1]. Our theory is based two main principles, namely momentum conservation, which constraints the mechanical and the chemically-induced forces, and secondly the existence of a dissipative coupling in the slow manifold of the dynamics which couples the different reaction coordinates. The emergence of this coupling suggests that the classical Kramers' picture is not enough to capture the coupled dynamics of the reaction coordinates. In this new paradigm we use methods from dynamical systems theory (Fig. 6.26) which suggest key design rules for de novo design of enzymes. Our results can complement the pioneering works on protein design assisted by machine learning which were awarded the Nobel Prize in Chemistry in 2024.

We have also used this mechanistic framework to model the coupled dynamics of molecular oscillators and to describe reactions in enzymatic oligomeric complexes or interacting molecular rotors [2]. Importantly, the dissipative coupling leads to new mechanisms of coordinated and cooperative dynamics in the space of reaction coordinates [3, 4]. Finally, our description of molecular machines allows us to study their activity subjected to externally-applied fields [5, 6]. Strikingly, this leads to a non-monotonic chemical activity as a function of mechanical forces.

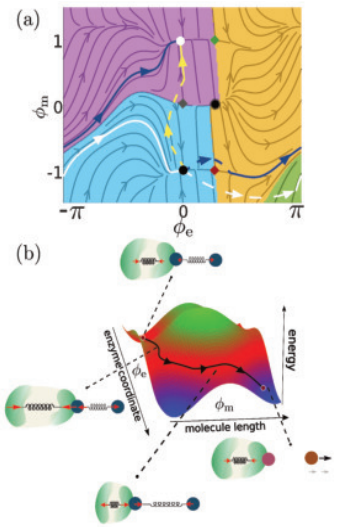

Figure 6.26: (a) Phase-portraits of the enzyme–molecule dynamical system. (b) The energy landscape of the dynamics where the dissipative coupling causes the system to overcome the substrate-to-product energy barrier.

[1] M. Chatzittofi, J. Agudo-Canalejo, R. Golestanian, Chem Catalysis (2025)
[2] M. Chatzittofi, R. Golestanian, J. Agudo-Canalejo, Phys. Rev. Research **6**, L042012 (2024)
[3] M. Chatzittofi, R. Golestanian, J. Agudo-Canalejo, New J. Phys. **25**, 090314 (2023)
[4] M. Chatzittofi, R. Golestanian, J. Agudo-Canalejo, Nat. Commun. **16**, 4835 (2025)
[5] M. Chatzittofi, J. Agudo-Canalejo, R. Golestanian, Phys. Rev. Research **6**, L022044 (2024)
[6] M. Chatzittofi, J. Agudo-Canalejo, R. Golestanian, Europhys. Lett. **147**, 21002 (2024)

6.19 FLUCTUATION DISSIPATION RELATIONS FOR ACTIVE FIELD THEORIES

M. K. Johnsrud, R. Golestanian

In equilibrium statistical physics, the underlying dynamics exhibit *time-reversal symmetry*, which results in fluctuation dissipation relations (FDRs). If we consider field theories where a set of scalar fields $\varphi_a(x,t)$ are driven by forces minimizing free energy, then one of these FDRs is $2i\mathrm{Im}\chi_{ab} = \frac{i\omega}{k_bT}C_{ab}$. Here, χ_{ab} is the linear response of the expectation value of the density, $\langle\varphi_a\rangle$, to an external perturbation, capturing the dissipation as the system relaxes back to its unperturbed state. $C_{ab} = \langle\varphi_a\varphi_b\rangle$ is the correlation function, capturing thermal fluctuations.

FDRs are invaluable tools for theorists and experimentalists alike, but they break down in active systems. In these systems, energy is consumed at the microscopic level, breaking time-reversal symmetry and leading to entropy S increasing also in steady-state. In [1], we use the time-reversal transformation in the response-field formalism to derive exact relations between χ and C out of equilibrium, such as

$$2i\mathrm{Im}\chi_{ab} - \frac{i\omega}{k_bT}C_{ab} = \Gamma\left\langle\varphi_a i\tilde{\varphi}_b\left(e^{-S}-1\right)\right\rangle \equiv \Delta_{ab}. \tag{6.1}$$

Here, Γ is the mobility and $\tilde{\varphi}$ is the response-field accounting for noise.

In [2], we consider the Non-Reciprocal Cahn-Hilliard model, a newly introduced active field theory [3]. We studied the effects of symmetry on this model in [4]. We calculate the deviation from equilibrium, Δ, using Feynman-diagrams. The first few diagrams of Δ are shown in Fig. 6.27. The black dot represents *entropy consumption*, $\langle -S\rangle$, for the time-reversed dynamics. We obtain Δ by summing all possible ways this contributes to C and χ. This task may seem hopeless, but by rearranging the sum we capture this effect in "renormalized" diagrams. The full sum then takes the form shown in Fig. 6.28.

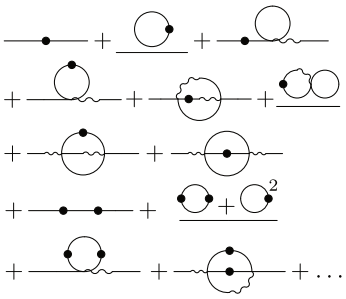

Figure 6.27: Some of the diagrams contributing to Δ.

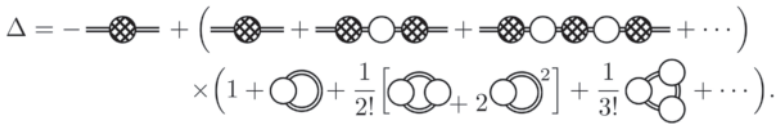

Figure 6.28: Renormalization combines all contributions to Δ.

In fact, the contribution from all the "bubbles" in the bottom parenthesis vanish! This allows us to systematically approximate Δ.

The formalism introduced here is applicable to all active, or generally out-of-equilibrium, field theories. It allows for both exact statements [1] and systematic approximations [2]. Using the tools of perturbative field theory, which have great success in high-energy physics, condensed matter and statistical mechanics, we aim to illuminate the nature of fluctuations, dissipation and entropy in active matter.

[1] M. K. Johnsrud and R. Golestanian, arXiv:2409.14977
[2] M. K. Johnsrud and R. Golestanian, arXiv:2502.02524
[3] S. Saha, J. Agudo-Canalejo, and R. Golestanian, Phys. Rev. X **10**, 041009 (2020)
[4] M. K. Johnsrud and R. Golestanian, arXiv:2503.07579

6.20 DEFECT DYNAMICS IN THE NON-RECIPROCAL CAHN-HILLIARD MODEL

N. Rana, R. Golestanian

The Non-Reciprocal Cahn-Hilliard (NRCH) model provides a coarse-grained description of phase-separation in biological systems with non-reciprocal interactions. We investigated the defect dynamics of the two-species NRCH model and found that it admits stable topologically charged spirals and neutral target solutions [1]. For a given strength of nonreciprocity (α), defect solutions with a unique asymptotic wave number $\left(k_\infty = C\sqrt{\alpha}\right)$ and amplitude $\left(R_\infty = \sqrt{1-k_\infty^2}\right)$ are selected. In our large-scale numerical simulations starting from disordered states we find a disorder-order transition at α_c (See Fig. 6.29). Below α_c, an initially disordered state evolves into quasi-stationary defect network with no global polar order and a clear preference for spirals or targets. At small α, we exclusively find spirals. As we increase α, targets start to appear as well, and close to the transition point $\alpha \lesssim \alpha_c$, we find target-dominated defect networks. Above α_c, we find travelling waves that show global polar order, rendered imperfect by mesoscopic fluctuations that decay with time and eventually lead to travelling bands. A sharp jump in the global polar order marks the onset of this transition (See Fig. 6.30).

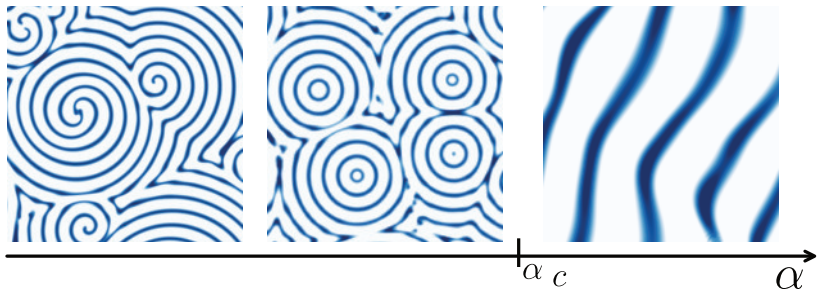

Figure 6.29: Qualitative phase portrait for the NRCH model. At small α, we find spirals. Targets appear for $\alpha \lesssim \alpha_c$ and above α_c, we find travelling waves.

We then studied pairwise interactions between defects and revealed a new class of topological interactions [2]. The stability of targets significantly affects the pairwise defect interactions. The fate of a defect pair depends upon their corresponding topological charges, initial separation, and the non-reciprocity coupling constant α. At large separations, defect interactions are small and a defect pair is stable. At very small separations, a pair of oppositely charged spirals or targets merge to form a single target. At low α, like-charged spirals form rotating bound pairs, which are however torn apart by spontaneously formed targets at high α. Similar preference for charged or neutral solutions is also seen for a spiral target pair where the spiral dominates at low α, but concedes to the target at large α. Our work sheds light on the complex phenomenology of non-reciprocal active matter systems when their collective dynamics involves topological defects.

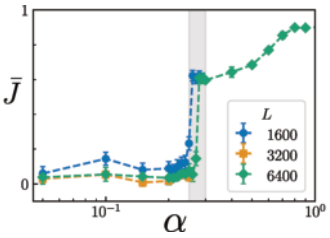

Figure 6.30: Average polar order $\bar{J}$ for different α and different box sizes. For defect networks ($\alpha < \alpha_c$), average order vanishes; whereas travelling waves ($\alpha > \alpha_c$) show an almost perfect polar order.

[1] N. Rana, R. Golestanian, Phys. Rev. Lett. **133**, 158302 (2024)
[2] N. Rana, R. Golestanian, New J. Phys. **26**, 123008 (2024)

6.21 MECHANICAL AND CHEMICAL SELF-ORGANIZATION IN GROWING CELL COLONIES

T. Sunkel, L. Hupe, P. Bittihn
M. Stevanovich, D. Schultz (Dartmouth)

Growth is a universal driver of self-organization in cellular aggregates, acting alongside processes such as motility, metabolic activity, and chemical signaling to generate complex spatiotemporal patterns. This interplay governs the behavior of systems ranging from developmental tissues and microbial colonies to engineered cellular structures. Understanding these interactions can reveal fundamental design principles[1], and, at the same time provide critical insights for applications.

1. For example, in a different collaboration with scientists from Warsaw and Edinburgh, we recently discovered a new mechanism for phase separation between motile and growing cells [1].

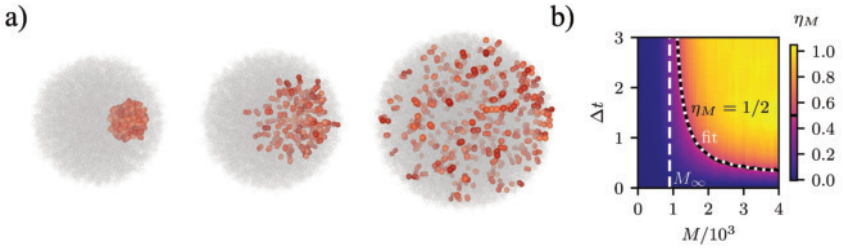

Figure 6.31: a) Any subset of cells (red) in the spheroid spreads over time. b) Mixing, quantified by $\eta_M \in [0,1]$, depends on waiting time Δt and motility M. Contour at $\eta_M = 0.5$ shows diverging time scale at critical motility M_∞.

In multicellular spheroids, growth induces mechanical interactions that drive both radial expansion and local rearrangements, which can interact with cell motility. Fig. 6.31a illustrates cell mixing that occurs above a critical motility threshold, as motile cells overcome confinement to their local environment. We found that the mixing time scale diverges near this critical point (Fig. 6.31b), highlighting a transition reminiscent of glassy dynamics [2]. The coupling between motility and growth results in structural changes and dynamic rearrangements that are crucial for understanding organization of tissues such as tumors.

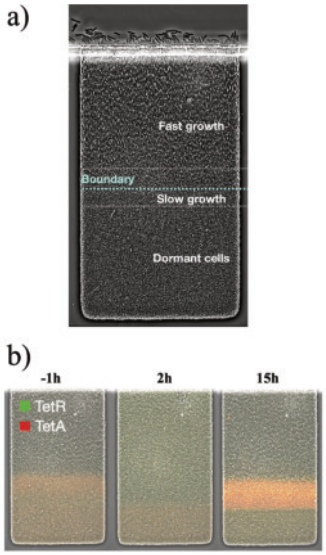

Figure 6.32: a) Microfluidic trap (100 µm × 170 µm) filled with growing bacteria. Fresh nutrients flow across at the top, leading to a distinct growth pattern. b) Upon tetracycline exposure (at 0h), the growth pattern rearranges and a layer of high antibiotic-resistance gene expression forms near the growth boundary.

In bacterial colonies subjected to stressors such as antibiotics, growth couples with metabolism and gene regulation to create complex feedback dynamics. Diffusion-limited nutrient supply can create growth zones (6.32a) with cells in different metabolic states. Upon tetracycline exposure, paradoxically, previously dormant cells start growing due to nutrient redistribution, and, after colony reorganization, preferential resistance gene expression near the boundary creates a layer of highly resistant dormant cells (6.32b) [3]. The interaction between nutrient transport, metabolic states, and gene regulation thus drives heterogeneity and adaptation, which can be further enhanced by stochasticity [4].

These studies reveal how fundamental physical principles can give rise to the extraordinary complexity observed in living systems and inform medical and biotechnological applications.

[1] L. Hupe, J. M. Materska, D. Zwicker, R. Golestanian, B. Waclaw, P. Bittihn, arXiv:2506.05288
[2] T. Sunkel, L. Hupe, P. Bittihn, Commun. Phys. **8**, 179 (2025)
[3] M. Stevanovic, T. Boukéké-Lesplulier, L. Hupe, J. Hasty, P. Bittihn, D. Schultz, Front. Microbiol. **13**, 740259 (2022)
[4] M. Stevanovic, J. Teuber Carvalho, P. Bittihn, D. Schultz, Phys. Biol. **21**, 036002 (2024)

6.22 NON-RECIPROCAL MULTIFARIOUS SELF-ORGANIZATION

S. Osat, R. Golestanian

Biological systems exhibit a unique ability to design diverse structures from a shared set of building blocks, with a plethora of proteins made from a limited set of amino acids as a prime example. Furthermore, these systems often use building blocks efficiently by introducing transformations between different structures. A self-assembled structure might undergo structural transformations, disassemble, and form a new structure with different functional purposes, without the need to discard the current structure and start anew.

To unravel this mystery, one must examine the underlying non-equilibrium processes that make this shape-shifting behavior feasible. Here, we leverage non-reciprocal interactions between building blocks to provide a foundation for designing dynamic shape-shifting structures. We used a multifarious self-assembly model, which is the molecular counterpart of the celebrated Hopfield associative memory. This model treats desired target structures as memories that should settle in the local minima of the energy landscape. The model achieves this through a set of learning rules that output the interaction matrix between building blocks. Triggering the system with a small seed leads to the proper self-assembly of the structure on demand, making the system a molecular associative memory.

By upgrading the multifarious self-assembly model to its non-equilibrium counter- part with non-reciprocal interactions, we introduce the ability to not only self-assemble different structures on demand but also facilitate shifts and transformations that lead to shape-shifting behavior. Non-reciprocal interactions between building blocks break action-reaction symmetry, providing the necessary non-equilibrium conditions that drive shape-shifting behavior.

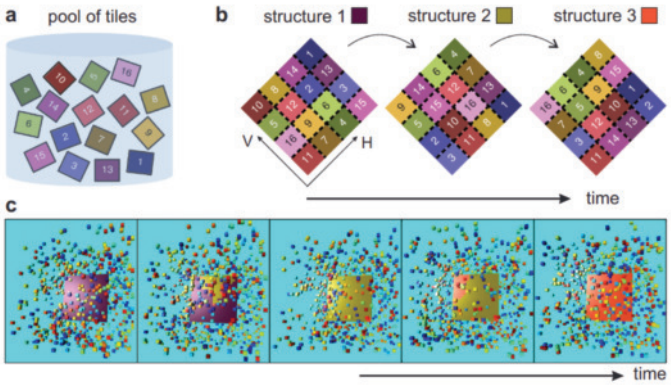

Figure 6.33: Non-reciprocal multifarious self-organization. (a) A pool of sixteen distinct building blocks can self-assemble into (b) any of three 4×4 square-shaped target structures. The goal is to introduce transformations among these structures by introducing non-reciprocal specific interactions between the building blocks. (c) Snapshots of molecular dynamics simulation capturing shape-shifting feature.

[1] S. Osat, R. Golestanian, Nat. Nanotechnol. **18**, 79 (2023)

6.23 NON-RECIPROCAL CONSERVED DYNAMICS: NONLINEARITIES, MULTI-SPECIES INTERACTIONS, AND FLUCTUATIONS

L. Parkavousi, N. Rana, J. Agudo-Canalejo, R. Golestanian, S. Saha
K. R. Prathyusha (Chicago)
B. V. Hokmabad (Princeton), C. Maass (Twente)

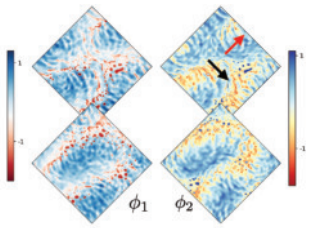

Figure 6.34: Travelling waves and phase separated unstable droplets coexisting in nonlinear non-reciprocal binary mixture.

Non-reciprocity is an exciting new ingredient to construct active matter theories that occurs naturally emerges naturally in chemically active system, or quorum-sensing systems with more than one species. We report on a continuum approach to explore the effect of non-reciprocity in number conserved densities within a theoretical framework called the non-reciprocal Cahn-Hilliard model [1] (NRCH). We also report on fluctuations in a single component chemically active systems involving tools and experimental setups that be generalised to multicomponent systems to search for signs of non-reciprocity.

As manifestation of broken parity and time reversal symmetry, travelling waves emerge in non-reciprocally interacting conserved densities. Nonlinear non-reciprocity in a binary mixture leads to a novel type of spatiotemporal chaos (termed *effervescence*) emerges in the steady state for any generic nonlinear interaction [2]. The chaotic behaviour results from a local restoration of PT symmetry in fluctuating spatial domains, which leads to the coexistence of oscillating densities and phase-separated droplets [3] that are spontaneously created and annihilated.

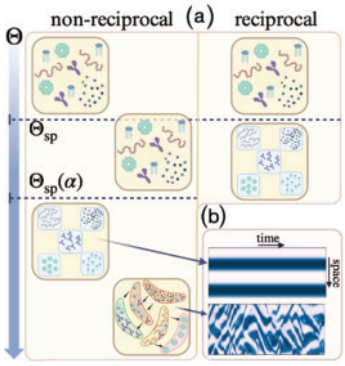

Figure 6.35: (a) Non-reciprocity is a reliable way to control LLPS, as it *always* lowers the phase separation temperature Θ. (b) Activity stirs the mixture while simultaneously stabilising it, leading to chaotic dynamics as shown in the representative kymographs.

Infinitely many interacting densities with random non-reciprocal interactions are more stable to a de-mixing transition in comparison to a reciprocal system [4]. Furthermore, the diversity in dynamical patterns increases with an increasing number of components and novel steady states such as pulsating or spatiotemporally chaotic condensates are observed.

Brownian dynamics simulations of interacting chemically active colloids uncovers a rich variety of structures and dynamical properties, including the full range of fluid-like to solid-like behaviour, and non-Gaussian positional fluctuations [5]. Self-propelling droplets as a model for chemically active particles that modify their environment by leaving chemical footprints, which act as chemorepulsive signals to other droplets [6]. These interactions lead to glassy dynamics apparent in transient dynamical arrest in active emulsions where swimmers are caged between each other's trails of secreted chemicals.

[1] S. Saha, J. Agudo-Canalejo, R. Golestanian, Phys. Rev. X, **10**, 041009 (2020)
[2] S. Saha, R. Golestanian, Nat. Commun., *in press*
[3] S. Saha, arXiv:2402.10057
[4] L. Parkavousi, N. Rana, R. Golestanian, S. Saha, Phys. Rev. Lett. **134**, 148301 (2025)
[5] R. Kokkoorakunnel, S. Saha, R. Golestanian, Phys. Rev. Lett. **133**, 058401 (2024)
[6] B. Hokmabad, J. Agudo-Canalejo, S. Saha, R. Golestanian, C. Maass, PNAS **119**, e2122269119 (2022)

6.24 SELF-ORGANIZATION THROUGH CATALYTIC ACTIVITY

V. Ouazan-Reboul, J. Agudo-Canalejo, R. Golestanian
M. Cotton (Oxford)

Many catalytic enzymes consume ATP in order to drive biochemical reactions out of equilibrium. By doing so, they perform **catalytic activity**: they locally convert a set of (substrate) chemicals into another set of (product) chemicals with a constant chemical reaction flux. Some enzymes are also chemotactic (see Sec. 6.11): they follow concentration gradients of their substrate, gradients which can themselves result from the activity of other enzymes. These two properties are often found together in catalytic systems and result in the emergence of effective chemical-field-mediated interactions between catalysts, which can be non-reciprocal if they have different properties (Fig. 6.36).

Non-reciprocal interactions are characteristic of and ubiquitous in active matter, and generically lead to dynamic self-organised steady states. Using a phenomenological field theory, we found that a simple mixture of catalysts can self-organize if it is overall self-attracting [1], forming into one or several clusters whose growth kinetics we numerically characterized [2].

To capture the complexity of the cell's chemical environment, we extended the model developed in [1] to catalysts participating in a simple metabolic cycle. This system can exhibit a great variety of novel out-of-equilibrium states depending on the cycle's structure, such as a "fireworks-like" oscillatory steady state [3] (Fig. 6.37). We also found, in the case of small cycles, that network effects can facilitate the self-organization of catalytic mixtures [4]. We are currently extending this study to more generic, non-cyclic reaction networks, which exhibit even stronger collective effects [5].

In order to go beyond the phenomenological models we studied so far, we also studied the self-organization of a single catalytic species using a Flory-Huggins-like thermodynamically consistent framework [6]. We discovered a novel mode of self-organization for this class of models, which does not rely on equilibrium interactions but only on catalytic activity, and which we termed Catalysis-Induced Phase Separation (CIPS). CIPS involves the formation of a dense, biomolecular-condensate-like structure inside of which enzymes exhibit a lowered catalytic activity, which implies that phase separation can act as a regulator of enzyme catalysis.

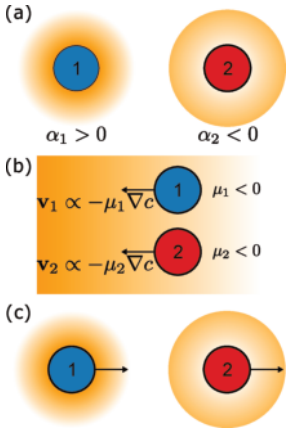

Figure 6.36: Chemical-field-mediated interactions. (a): Two catalytically active particles respectively produce and consume a chemical (orange). (b): Both particles chemotax towards higher concentration of the chemical. (c): The net results is 1 chasing after 2.

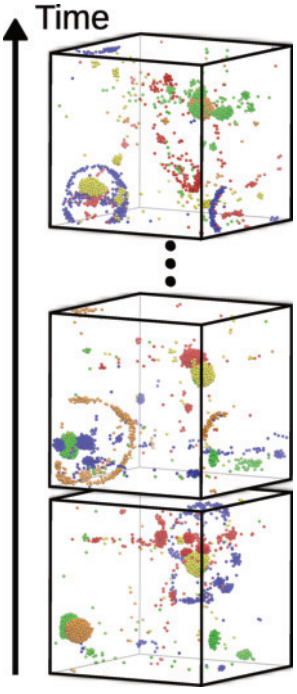

Figure 6.37: Example of an oscillatory steady state for catalytically active particles participating in a metabolic cycle. In one cycle, each species "attacks" and replaces a cluster of the previous species in the cycle.

[1] J. Agudo-Canalejo, R. Golestanian, Phys. Rev. Lett. **123**, 018101 (2019)
[2] S. Kaviani, V. Ouazan-Reboul, R. Golestanian, J. Agudo-Canalejo, *in preparation*
[3] V. Ouazan-Reboul, J. Agudo-Canalejo, R. Golestanian, Nat. Commun. **14**, 4496 (2023)
[4] V. Ouazan-Reboul, R. Golestanian, J. Agudo-Canalejo, Phys. Rev. Lett. **131**, 128301 (2023)
[5] V. Ouazan-Reboul, R. Golestanian, J. Agudo-Canalejo, *in preparation*
[6] M. W. Cotton, R. Golestanian, J. Agudo-Canalejo, Phys. Rev. Lett. **129**, 158101 (2022)

6.25 NONRECIPROCAL QUORUM-SENSING ACTIVE MATTER

Y. Duan, J. Agudo-Canalejo, R. Golestanian, B. Mahault

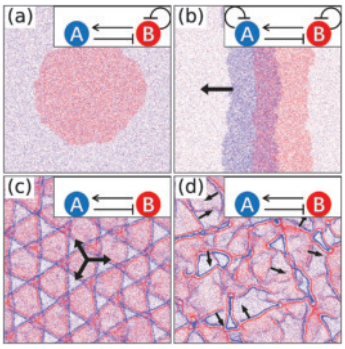

Figure 6.38: Representative simulation snapshots for strong [(a),(b)] and vanishing [(c),(d)] motility self-inhibition in the presence of chasing interactions.

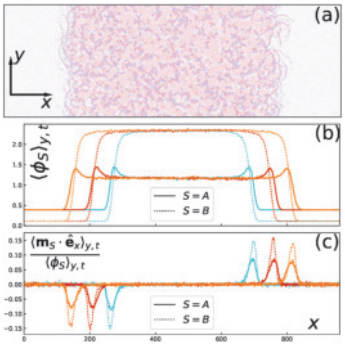

Figure 6.39: (a) Typical snapshot for the phase coexistence between chaotic dynamical phase and dilute gas. (b, c) The corresponding $y-$ and time-averaged density and polarity profiles.

Self-propelled particles often interact with each other via mediated interactions, which are not constrained by Newton's third law and are therefore generically nonreciprocal. A typical example is quorum-sensing active particles, which can regulate their motility according to nearby particle densities. Nonreciprocity naturally emerges in multi-species systems when particles from different populations respond asymmetrically to each other's presence.

A natural question is whether the interplay of self-propulsion and nonreciprocity can induce qualitatively new collective behavior not present in systems with only one of them. To this end, we study a minimal model involving two species of particles interacting via quorum-sensing rules [1, 2]. Particle i of species $S \in \{A, B\}$ moves at speed v_S controlled by the local densities of the two species, along its intrinsic polarity direction that undergoes rotational diffusion. Given that active particles tend to accumulate in regions where they move slower [3], when the motility of S particles are suppressed by the presence of S' particles, S particles shall accumulate in regions where the density of species S' is higher, as if S particles were attracted by S' particles. Similarly, motility activation will induce effective repulsion.

In the presence of effectively chasing interactions, such as when v_A is enhanced by B particles and v_B is suppressed by A, as well as sufficiently strong intra-species motility inhibition, traveling bands that break time-reversal symmetry can arise (Fig. 6.38(b)), which instead disappear when turning off the intra-species motility inhibition of one species (Fig. 6.38(a)). This is inline with the phenomenological nonreciprocal Cahn-Hilliard model [4], predicting that preconditions for the emergence of travelling bands are the presence of intra-species attraction that drives demixing, as well as chasing inter-species interactions. Strikingly, highly dynamical travelling bands can arise from the microscopic model even in the absence of intra-species motility inhibition (Fig. 6.38(c, d)), provided the strength of chasing interactions and self-propulsion are large enough. By the study of the associated coarse-grained field theory, we identify this is resulted from the non-trivial interplay between motility and nonreciprocity, which can further induce multi-scale phase separation between chaotic dynamical phase and homogeneous gas (Fig. 6.39) in the presence of intra-species motility inhibition. With much richer phase behaviors presented in [2], our research provides an example that more sources of activity are different.

[1] Y. Duan, J. Agudo-Canalejo, R. Golestanian, B. Mahault, Phys. Rev. Lett. **131**, 148301 (2023)
[2] Y. Duan, J. Agudo-Canalejo, R. Golestanian, B. Mahault, Phys. Rev. Research **7**, 013234 (2025)
[3] M. E. Cates and J. Tailleur, Annu. Rev. Condens. Matter Phys. **6**, 219 (2015)
[4] S. Saha, J. Agudo-Canalejo, R. Golestanian, Phys. Rev. X **10**, 041009 (2020)

6.26 ACTIVE TRANSPORT IN CHIRAL ACTIVE FLUIDS

Y. Hosaka, M. Chatzittofi, A. Daddi-Moussa-Ider, A. Vilfan, R. Golestanian

Chiral active fluids refer to systems with broken time-reversal and parity symmetries. Examples span a wide range of scales and include non-equilibrium active fluids composed of spinning microscopic components that break these symmetries, such as chiral biological polymer networks, spinning colloids, and magnetized plasmas. These systems are known to be described by the continuum models characterized by a dissipationless transport coefficient called *odd viscosity*. However, it is still unclear how the motile behavior of active particles, whether synthetic or living, are affected by this viscosity.

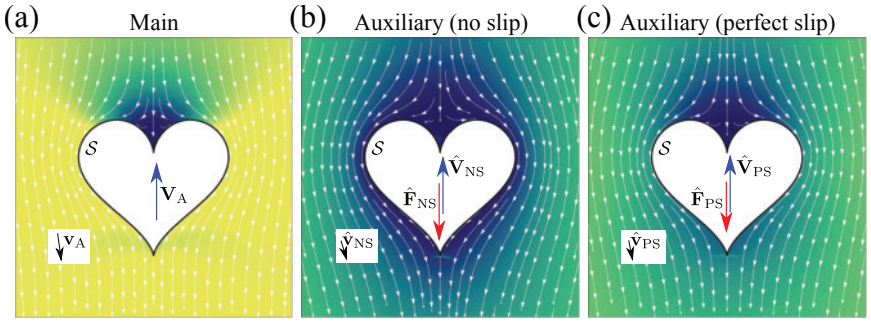

Figure 6.40: The Lorentz reciprocal theorem links the main problem (a) of a swimming body moving with velocity $\mathbf{V}_A$ with an auxiliary problem (b),(c) of a passive body with the same geometry and the velocity, $\hat{\mathbf{V}}_{NS}$ and $\hat{\mathbf{V}}_{PS}$, for the no-slip and perfect-slip boundary conditions, respectively [1].

We developed the theory that accounts for the autonomous transport of active agents in 3D [1–3] and 2D fluids [4, 5] with odd viscosity. To reveal the dynamics of micro-particles at low Reynolds number, the Lorentz reciprocal theorem is a powerful principle, which allows one to directly determine the self-propulsion speed of a microswimmer without explicitly solving the associated boundary-value problem (Fig. 6.40). Starting with the most general stress tensor, we proved that the classical theorem is still valid for fluids with odd viscosity [1]. This novel generalization allows us to determine the velocity of a microswimmer with an arbitrary surface mode. Interestingly, a microswimmer with a torque dipole on the fluid, which is otherwise stationary in normal fluids, is set in motion due to odd viscosity. Moreover, it was revealed that a swimmer with a force dipole (pusher or puller) reorients to the axis of the odd viscosity [2] (Fig. 6.41). In analogy to the tactic response of microorganisms, we denote this alignment effect along chirality as *chirotaxis*. Our findings open up new insights into autonomous transport induced by odd viscosity and may offer a novel perspective for predicting swimming motions in complex living and biological fluids, which are often dominated by broken symmetries.

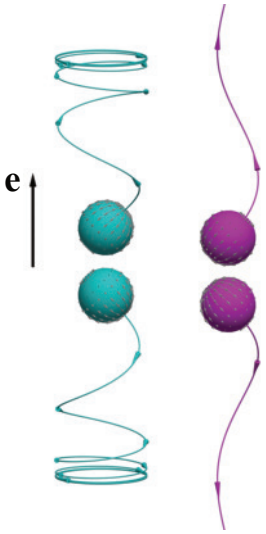

Figure 6.41: Helical trajectories followed by puller-(blue) and pusher-type swimmers (magenta) of different initial orientations. Pullers converge towards circling in a plane perpendicular to the axis of odd viscosity $\mathbf{e}$, while pushers align towards $+\mathbf{e}$ or $-\mathbf{e}$ directions, depending on their initial orientation (bimodal chirotaxis) [2].

[1] Y. Hosaka, R. Golestanian, A. Vilfan, Phys. Rev. Lett. **131**, 178303 (2023)
[2] Y. Hosaka, M. Chatzittofi, R. Golestanian, A. Vilfan, Phys. Rev. Research **6**, L032044 (2024)
[3] M. Chatzittofi*, Y. Hosaka*, A. Vilfan, R. Golestanian, *in preparation*
[4] Y. Hosaka, R. Golestanian, A. Daddi-Moussa-Ider, New J. Phys. **25**, 083046 (2023)
[5] A. Daddi-Moussa-Ider, A. Vilfan, Y. Hosaka, J. Chem. Phys. **162**, 064103 (2025)

6.27 ELECTROMECHANICAL IMAGING OF CARDIAC DYNAMICS

B. Weiss, A. Seyfried, J. Schröder-Schetelig, A. Barthel, R. Stenger, I. Kottlarz, G. Luther, B. Rüchardt, U. Parlitz, S. Luther
F. Akar, J. Akar, J. Hummel (New Haven),
M. Reiss, W.-J. Rappel, A. McCulloch (San Diego),
H. Baraki, I. Kutschka, S. Herzog (Göttingen)

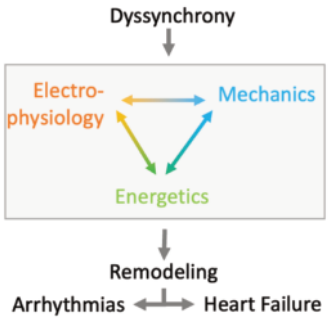

Figure 6.42: Bioenergetic-mechano-electric coupling in the heart. Alternation of the coupling may result in dyssnchrony, structural and functional remodeling of the cardiac susbstrate, leading to life-threatening arrhythmias and heart failure. The simultaneous characterization of cardiac mechanics, electrophysiology, and energetics on tissue and organ levels is a major challenge.

Cardiac tissue is an excitable and deformable medium in which tissue mechanics, cellular electrophysiology, and energetics are mutually coupled, as illustrated in Fig. 6.42. Pathophysiological perturbations in coupling may result in electrical and mechanical dysynchrony, structural and functional remodelling of the cardiac substrate, which induce or exacerbate life-threatening arrhythmias and heart failure. Despite decades of research, the fundamental principles underlying electrical, mechanical, and energetic dynamics and self-organization that contribute to the onset and progression of arrhythmias and heart failure remain largely elusive. This lack of progress is mainly because measuring cardiac mechanics, electrophysiology, and energetics simultaneously, as well as resolving wave dynamics inside the heart muscle, remain significant scientific and technological challenges. The Max Planck Research Group Biomedical Physics has pioneered the development of multi-modal imaging technologies to visualize three-dimensional electromechanical waves inside the cardiac muscle and is translating them from bench to bedside. In addition to the use of particularly powerful state-of-the-art measurement technology, new sophisticated methods of data analysis are being developed and applied, including novel approaches from the field of machine learning.

Electromechanical Imaging of Human VF

The three-dimensional spatio-temporal organization of human ventricular fibrillation is of immense scientific and medical interest. Over the past century, several hypotheses have been formulated about the nature of cardiac fibrillation [1]. However, available imaging techniques so far were only able to resolve the dynamics on the surface but not inside

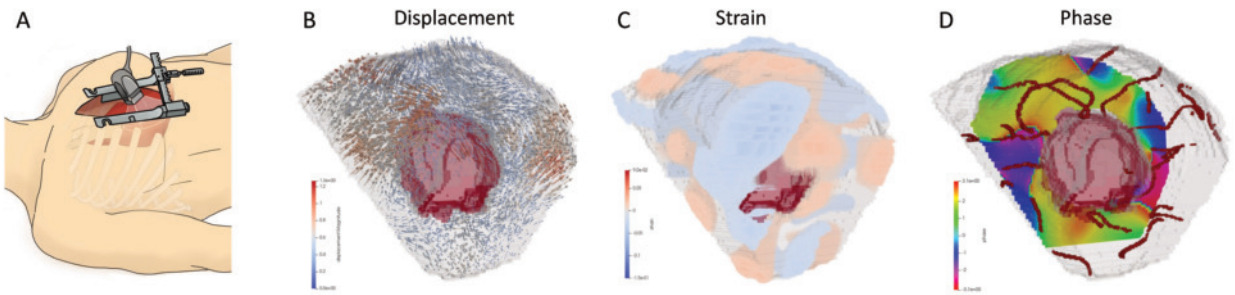

Figure 6.43: Electromechanical rotors during human VF. **A** Schematic illustration of epicardial ultrasound in patients with heart-lung machine support undergoing bypass surgery. **B** High-resolution displacement vector field (150 Mio./s). **C** Tissue strain. **D** Phase and phase singularities associated with core of scroll wave or rotor (red).

the heart muscle. We have developed advanced 4D ultrasound-based imaging technology that resolves intramural mechanical activation with unprecedented spatial-temporal resolution [2]. In an ongoing clinical study in collaboration with H. Baraki and I. Kutschka (University Medical Center, Göttingen), we demonstrate the first visualization of electromechanic waves during human ventricular fibrillation inside the heart muscle (Fig. 6.43). We are able to resolve the three dimensional dynamics and interaction of intramural rotors and phase singular filaments, and observe intermittency in spatial-temporal complexity. In collaboration with Max Planck Innovation GmbH and our clinical partners at the Yale University and UCSD, we are further advancing 4D electromechanic imaging for arrhythmia and heart failure research, and exploring further applications for advanced diagnostics and therapeutic interventions, including ventricular ablation and cardiac resynchronization therapy.

Multi-modal cardiac imaging

We have developed multi-modal optical mapping, which allows the simultaneous measurement of membrane potential, intracellular calcium, and mechanical motion in intact, isolated hearts using fluorescent dyes [2, 3]. This technique has enabled studying excitation-contraction coupling on tissue and organ level and led to the discovery of coexisting electro-mechanical vortices. We plan to further advance multi-modal optical mapping to characterize metabolic function in collaboration with our partners at Yale University. Optical mapping has been used to validate ultrasound-based 4D electromechanical imaging. Figure 6.44 shows strain wave imaging during ventricular tachycardia in an isolated, Langendorff-perfused porcine heart. The analysis of the strain enables the estimate of an mechanical activation time inside the tissue that represents the propagation of the three-dimensional mechanical wave (Fig. 6.44). The measurement of transient wave phenomena in the

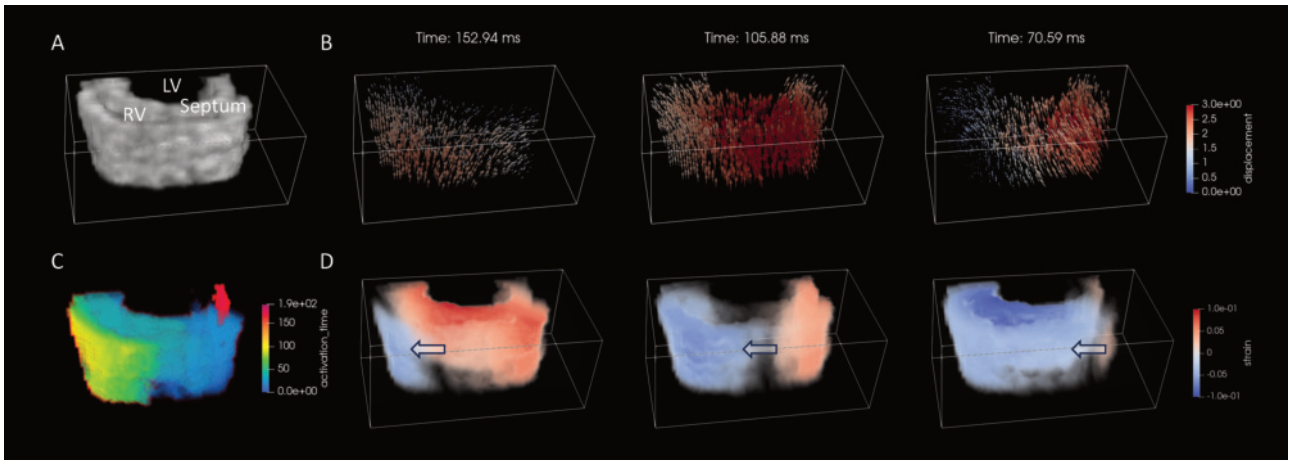

Figure 6.44: Electromechanical imaging of ventricular tachycardia. **A** 4D ultrasound during ventricular tachycardia of porcine heart (LV - left ventricle, RV - right ventricle). The measurement volume comprises the entire LV and RV; only a sub-volume is shown for better visualization. **B** Displacement vector field. **C** Mechanical activation time. **D** Strain wave, arrow indicates position of wave front.

ventricular wall transcends the capabilities of state-of-the-art cardiac mapping systems. In order to ensure reproducible and sustainable biomedical research, BMPG has developed the open source workflow data management system LinkAhead, advances data management concepts [5] and supports the MPG's OpenScience initiative.

Reconstructing in-depth activity of chaotic 3D spatio-temporal excitable media based on surface data

Motivated by potential applications in cardiac research, we set ourselves the task of reconstructing the dynamics in a spatiotemporally chaotic, excitable three-dimensional medium from partial observations at the surface [6]. Three artificial neural network methods (a spatiotemporal convolutional long-short-term-memory, an autoencoder, and a diffusion model based on the U-Net architecture) were trained to predict the dynamics in deeper layers of a cube-like three-dimensional excitable medium from observational data at the surface using data generated by the Barkley model

$$\begin{aligned} \frac{\partial u}{\partial t} &= D \cdot \nabla^2 u + \frac{1}{\varepsilon} u(1-u)\left(u - \frac{v+b}{a}\right) \\ \frac{\partial v}{\partial t} &= u^3 - v \end{aligned} \tag{6.2}$$

on a 3D domain with no-flux boundary conditions. Figure 6.45 shows that despite the high-dimensional chaotic dynamics of this system, such cross-prediction is possible, but non-trivial and as expected, its quality decreases with increasing prediction depth.

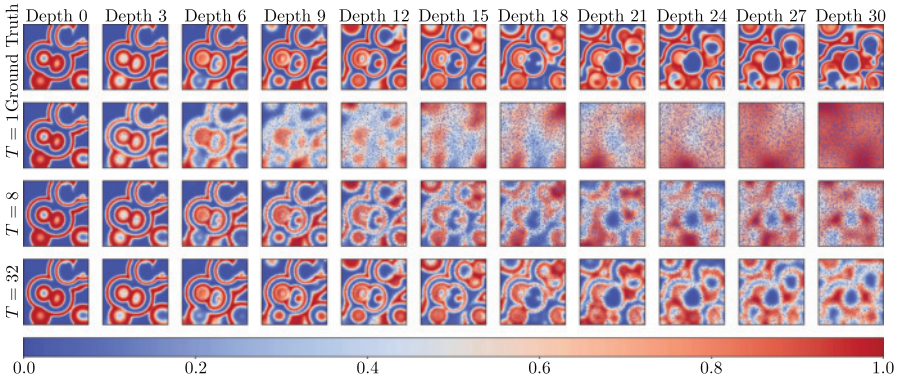

Figure 6.45: Reconstruction of dynamics in deeper layers of a 3D-cube from surface observations using a diffusion model with different input lengths $T \in \{1, 8, 32\}$ [6].

[1] W.-J. Rappel, Phys. Rep. **978**, 1 (2022)
[2] J. Christoph et al., Nature **555**, 667 (2018)
[3] V. Kappadan, A. Sohi, U. Parlitz et al., J. Physiol. **601**, 1353 (2023)
[4] S. Luther, J. Am. Coll. Cardiol. EP. **11**, 682 (2025)
[5] H. tom Wörden, F. Spreckelsen, S. Luther, U. Parlitz, A. Schlemmer, Data **9**, 24 (2024)
[6] R. Stenger, S. Herzog, I. Kottlarz, B. Rüchardt, S. Luther, F. Wörgötter, U. Parlitz, Chaos **33**, 013134 (2023)

Link to additional information: https://bmp.ds.mpg.de/research/bmp_emcoupling/

NETWORKS, GEOMETRY, AND INFORMATION

7

Living systems exhibit remarkable organizational principles that emerge across different scales, from the molecular machinery within individual cells to the complex social networks that connect human societies. These principles include emergence of patterns or the formation of networks. For example, material transport and cell coordination can be realized through emergent patterns. When this is not sufficient, networks present intricate structures that allow interactions between selected units, e.g., for sending activity or information from one agent to another, and thereby overcoming classical constraints of Euclidean geometry.

At MPI-DS, we employ theory, simulation, and data analyses to reveal how biological and artificial systems transfer and modify information. Recent results range from pattern formation in cellular systems, to learning in neural networks, to communication in social networks.

Contents

7.1 'FORWARD FORWARD' TRAINING OF CONVOLUTIONAL NEURAL NETWORKS

M. Schröter
R. Scodellaro, A. Kulkarni, F. Alves (Göttingen)

The recent successes in analyzing images with deep neural networks are in most cases achieved using Convolutional Neural Networks (CNNs). The training of these CNNs, and in fact of all deep neural network architectures, uses the backpropagation (BP) algorithm, where the output of the network is compared with the desired result, and the difference is then propagated backwards through the network in order to move the weights connecting the neurons into the right direction.

Backpropagation has a number of downsides: first, it requires the storage of intermediate results. Depending on the optimizer, the memory consumption of BP is up to 5 times larger than the requirement for storing the weights alone [1]. This becomes a problem when training large models. Second, driven by the desire to decrease power consumption and increase processing speed, there is an ongoing search of hardware alternatives to CMOS semiconductors [2]. On these alternative hardware platforms, it is often impossible to implement an analog of BP. Finally, evolution has also developed learning algorithms for neural networks such as our brain, but those algorithms seem to be quite different from BP. Given the in general high performance of evolutionary solutions to problems, the question is if deep learning could also benefit from biologically plausible alternatives to BP.

In 2022 Geoffrey Hinton suggested an alternative way of training neural networks: the Forward-Forward (FF) algorithm [3]. FF training combines two ideas: First, the weights of each layer are updated using gradients of a locally defined goodness function such as the activities in that layer. This can be done without knowing the output of the network. Second, the labels are included in the training data, which allows the neurons to learn them together. In order to understand which features of the data 'vote' for a given label, half of the data set is comprised of images combined with wrong labels. The training then happens during a forwards run: for the correctly labeled, positive data the weights are modified to maximize the goodness. In contrast, for the negative data the weights are changed in order to minimize the goodness. Both these objectives can be achieved with a local gradient descent, with no need for BP. The term Forward-Forward now refers to having two subsequent training runs, one with positive and one with negative data. Fig. 7.1 A and B shows some of the training data where the correct and false labels correspond to the position of a single white pixel in the top row of the image.

The FF algorithm has up to now only been used in fully connected networks. In [4] , we have show how the FF paradigm can be extended to CNNs. The main innovation is a spatial-extended labeling approach involving the superposition of the training data set image with a second image of identical dimensions. This additional image consists of a gray-value wave with a fixed frequency, phase, and orientation. Each

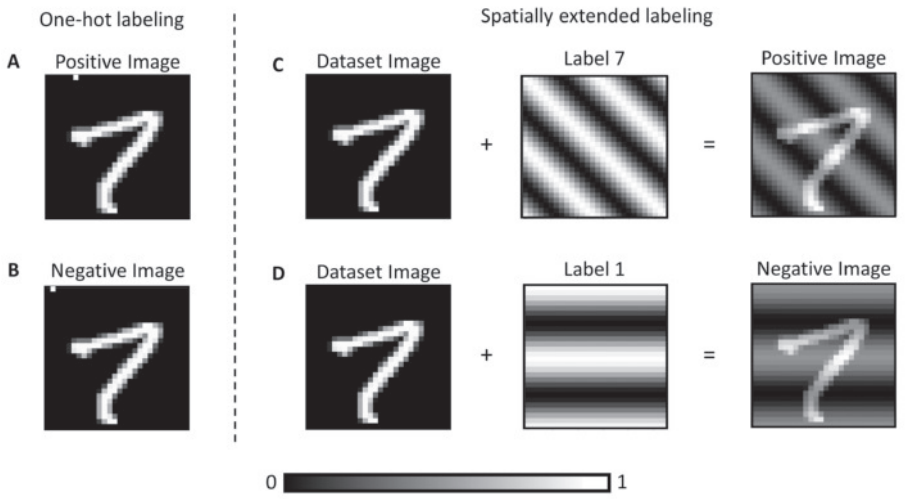

Figure 7.1: Forward Forward training requires that 1) the labels accompany the images already at the forward pass and 2) that each image is presented twice: once with the correct labels, called positive image, and once with a wrong label, the negative image. The one-hot labeling of the images in the top left corner, suggested in the original paper [3], is shown at the left. These small labels will not be not be 'visible' to most of the convolutions in a CNN. We replace these labels with spatially extended ones, created from 2D Fourier modes with different orientations and wavelengths.

FF-CNN Network	Linear Classifier Accuracy [%]	Goodness Accuracy [%]
128 filter of size 7x7, batch size 50	99.14	**99.20**
128 filter of size 5x5, batch size 50	98.93	**99.04**
128 filter of size 3x3, batch size 25	98.63	**98.74**

Table 7.1: Results from a test set not used during hyperparameter optimization

possible label is associated with a distinct configuration of these three parameters. As demonstrated in Fig. 7.1 C and D, both the positive and negative data sets are obtained by harnessing this methodology.

There are two ways how a FF trained CNN or DNN can be used for inference: the linear classifier and the goodness evaluation. In the first case, the neurons of every layer except the first are fully-connected with an output layer of N nodes, equal to the number of labels. The connecting weights are trained by evaluating the neuron activations using a cross-entropy loss. The second way is inference with goodness evaluation: each image is repeatedly presented to the network, using all possible labels. The prediction corresponds then to the label with the highest goodness value. As shown in Table 7.1 this method provides a slightly higher accuracy at the price of a tenfold increase in computation during inference.

Our achieved accuracy of 99,2 on the MNIST dataset is at eye level with similar sized CNNs trained by backpropagation.

[1] The Hugging face community: Anatomy of Model's Memory (2023)
[2] D. Christensen et al., Neuromorphic Computing and Engineering **2**, 022501 (2022)
[3] G. Hinton, arXiv:2212.13345 (2022)
[4] R. Scodellaro, A. Kulkarni, F. Alves, M. Schröter, arXiv:2312.14924 (2023)

7.2 CRITICALITY AND INFORMATION FLOW IN RECURRENT NEURAL NETWORKS

J. Dehning, L. Rudelt, D. González M., M. Loidolt, V. Priesemann
J. Rowland, A. M. Packer (Oxford), D. P. Shorten, J. Lizier (Sydney)
M. Wibral (Göttingen), R. Zeraati, A. Levina (Tübingen)

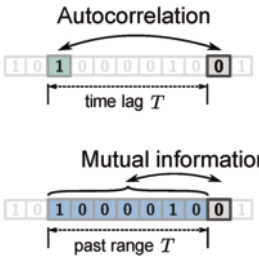

Figure 7.2: The autocorrelation quantifies the linear dependence of neural spiking in two time bins with time lag T. In contrast, the mutual information quantifies all linear and non-linear dependencies in an entire past range T. [3]

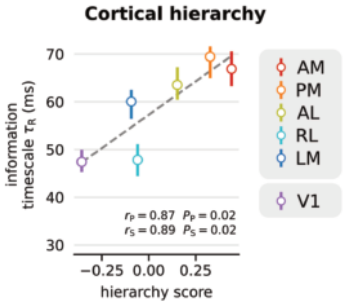

Figure 7.3: We observe a hierarchy of information timescale in mouse visual cortex [5].

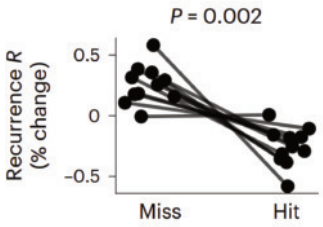

Figure 7.4: The measured recurrency of the dynamics determines the detectability of a stimulus in mice somatosensory cortex (hit=detected, miss=undetected) [7].

To directly quantify properties of information processing from neural data, we developed estimation techniques that estimate memory and information timescales from neural spiking activity using the autocorrelation and the mutual information (Fig. 7.2) [3]. In addition, we developed estimators of transfer entropy to infer the effective strength and direction of neural interactions and information flow [4].

When applying these tools to the mouse visual system we found that correlation and information timescales increase along an anatomical hierarchy (Fig. 7.3) [5]. Our results indicate that higher areas are specialized on longer integration of information, possibly due to higher recurrency in these areas. Moreover, by analyzing developing dissociated neural cell cultures using transfer entropy estimation, we found that information flow increases dramatically with development as the network grows recurrent connections [6]. Lastly, we found that information integration might also be tuned by recurrency on much faster than developmental timescales. Specifically, we found that in somatosensory cortex S1 the effective recurrency before stimulus onset is correlated with the perception probability (Fig. 7.4) [7].

To conclude, our newly developed estimation techniques provide key insights on how recurrent information flow could shape information integration on both, developmental and fast timescales.

[1] J. Wilting, J. Dehning, J. Pinheiro Neto, L. Rudelt, M. Wibral, J. Zierenberg, V. Priesemann, Front. Syst. Neurosci. **12**, 55 (2018)
[2] R. Zeraati, V. Priesemann, A. Levina, Front. in Physics **9** (2021)
[3] L. Rudelt, D. González M., M. Wibral, V. Priesemann, PLoS Comp. Biol. **17**, 6 (2001)
[4] D. P. Shorten, V. Priesemann, M. Wibral, T. Lizier, bioRxiv 2024.09.22.614302 (2024)
[5] L. Rudelt, D. González M., F. P. Spitzner, B. Cramer, J. Zierenberg, V. Priesemann, PLoS Comp. Biol. **20**, 8 (2024)
[6] D. P. Shorten, V. Priesemann, M. Wibral, T. Lizier, eLife **11**, e74651 (2022)
[7] J. M. Rowland 1, T. L. van der Plas 1, M. Loidolt,..., V. Priesemann, A. M. Packer, Nat. Neurosci. **26**, 1584 (2023)

7.3 ASSESSING PROPERTIES OF LIVING SYSTEMS DESPITE LIMITED DATA

J. Dehning, P. Spitzner, L. Rudelt, J. Neto, J. Zierenberg, V. Priesemann
A. Levina (Tübingen)

A major challenge in assessing collective properties of living systems is that often only small parts of them can be recorded without impairing their function. For example, electrode recordings in the living brain only allow the recording of a couple of thousands out of the billions of neurons due to physical constraints. There are two fundamentally different approaches to measuring the dynamical properties of networks: One can locally integrate information, e.g. through coarse measures like LFP recordings, or one can precisely record a subsample of units. But how these methods affect inference of collective properties remains an open problem.

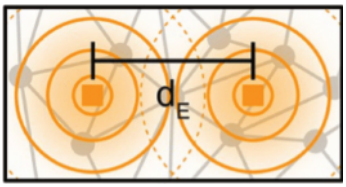

Figure 7.5: Measures of collective properties can be severely biased, when based on recording techniques that locally integrate activity, due to overlapping fields of integration [1].

To tackle this problem, we studied and developed different methods and their biases. We found that coarse sampling can severely bias measures of neural correlations due to overlapping fields of nearby electrodes (Fig. 7.5) [1]. This is particularly relevant to the ongoing scientific debate on the relevance of correlations for neural information processing. Local information-theoretic measures provide an interpretable and robust alternative, but quickly become computationally expensive [2]. Finally, we found that subsampling also biases correlation measures, but this bias can be formally derived for random and windowed sampling methods (cf. Fig. 7.6) paving the way for subsampling-invariant methods under reasonable assumptions [3].

These works showcase that measurement methods have to be well chosen and explicitly considered in the analysis to avoid making erroneous conclusions. We applied our methodology to study cortical information processing in Sec. 7.2.

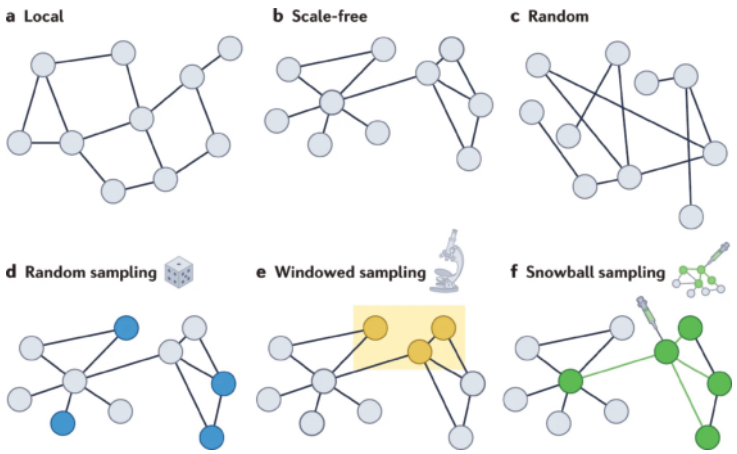

Figure 7.6: Illustration of different network types (top) and sampling strategies (bottom) that one can encounter when working with empirical data [3].

[1] J. P. Neto, F. P. Spitzner, V. Priesemann, PLoS Comput. Biol. **18**, e1010678 (2022)
[2] L. Rudelt, ..., V. Priesemann, PLoS Comput. Biol. **17**, 6 (2001)
[3] A. Levina, V. Priesemann, J. Zierenberg, Nat. Rev. Phys. **4**, 770 (2022)

7.4 INFOMORPHIC NETWORKS: DESIGNING COMPUTATION USING PARTIAL INFORMATION DECOMPOSITION

V. Neuhaus, A. C. Schneider, M. Blümel, A. S. Ecker, V. Priesemann
D. A. Ehrlich (Uni Göttingen), A. Makkeh (Uni Göttingen)
M. Wibral (Uni Göttingen)

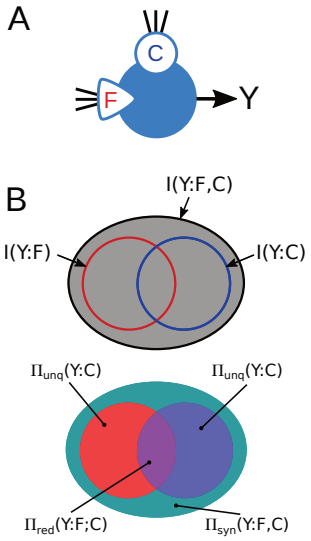

Figure 7.7: A: Schematic of a single infomorphic neuron with two input compartments (feedforward inputs F and contextual inputs C) and the resulting output Y. **B:** (Upper) Venn-diagram of the joint and the marginal mutual information terms between the input sources F and C and the neuron output Y. (Lower) The information decomposition of the joint mutual information above into unique, redundant and synergistic information contributions of the input variables.

In both biological and artificial neural networks, the roles of individual neurons and their learning mechanisms are often unclear. The precise learning mechanisms of biological neurons remain opaque and are often modeled using simplistic learning rules, while artificial neurons are usually optimizing a global goal which does not provide direct insights into the information processing at the neuronal level. To gain functional insights into learning on the neuronal level, we define goal functions for each neuron which optimize its information processing. These goal functions are defined using first principles of information theory, therefore we refer to the neurons as "infomorphic" neurons.

An infomorphic neuron, shown in Fig. 7.7**A**, processes up to three different types of inputs, each grouped into separate compartments and produces a binary output. By treating the inputs and outputs as random variables, we can use Partial Information Theory, a novel extension to information theory, to decompose the joint mutual information between the input compartments and the output of the neuron into redundant, unique, and synergistic contributions, the so called information "atoms." (see Fig. 7.7**B**). With this we can construct simple goal functions that optimize specific information atoms and thus optimizing the information processing of the neuron.

To demonstrate the generality of this approach, we solve tasks across multiple classical machine learning paradigms, such as supervised classification, associative memories and unsupervised sparse coding, with networks constructed from many infomorphic neurons that optimize certain PID goal functions [1]. We show that the goal function parameters can either be derived from intuitive reasoning or optimized using a hyperparameter optimization scheme, the latter approach giving insight into the information processing that is necessary at the local scale.

Using networks of infomorphic neurons, we solve supervised classification tasks across multiple layers. Interactions within the same layer self-organize to create efficient data encodings, achieving performance comparable to traditional global learning rules [2].

Information theory, and PID in particular, provides a robust framework for studying neural representation and computation. With our framework of infomorphic neurons, we can derive and optimize local objective functions that are effective in a variety of applications.

[1] A. Makkeh, M. Graetz, A. C. Schneider, D. A. Ehrlich, V. Priesemann, and M. Wibral, Proc. Natl. Acad. Sci. U.S.A. **122**, e2408125122 (2025)
[2] A. C. Schneider, V. Neuhaus, D. A. Ehrlich, A. Makkeh, A. S. Ecker, V. Priesemann, and M. Wibral, in Proc. 13th Int. Conf. Learn. Representations (ICLR) (2025)

7.5 SUBCELLULAR PROCESSES ENABLE SELF-ORGANIZATION IN SPIKING NEURAL NETWORKS

F. Mikulasch, L. Rudelt, V. Priesemann
M. Wibral (Uni Göttingen), S. O. Rizzoli (UMG Göttingen)

A central question in the physics of neural systems is how biological processes on various scales give rise to the sophisticated information processing and learning capabilities of the brain. Typically, studies of learning and neural network dynamics consider point neurons that linearly sum their synaptic inputs to produce sparse action potentials, so-called spikes. This is in stark contrast to the rich dynamic repertoire on the sub-cellular level of real neurons, where highly non-linear voltage dynamics enable dendritic branches to act as independent computational units [1].

In our research, we found that beyond their role for input processing, dendritic voltage dynamics play a key role for unsupervised learning. Specifically, we derived that, in conjunction with inhibitory connections, dendritic voltage dynamics compute a difference between synaptic inputs and internal predictions [2]. This difference, also called a prediction error, yields an important cue for learning that is locally available for synaptic plasticity (Fig. 7.8). We found that when representing complex spatio-temporal inputs with spikes (Fig. 7.9), learning with dendritic errors yields substantial advantages over previous Hebbian-like learning rules [2]. Moreover, we showed that dendritic error computation yields a plausible implementation of hierarchical predictive coding with spiking neurons (Fig. 7.8), which unifies several theories of unsupervised learning [3] and explains key features of voltage-dependent plasticity and so-called mismatch responses in cortex [3–5].

Next to dendrites, we also found that computations within synapses crucially shape neural information transmission and network computations. By employing a detailed model of synaptic vesicle recovery [6], we found that the vesicle cycle of hippocampal synapses implements synaptic depression on a wide range of timescales. This multi-timescale depression is particularly effective in reducing transmitter release for slow firing rate fluctuations of recorded hippocampal neurons, which improves the efficiency of synaptic transmission [7].

Our work challenges the long-held view that neural network computations and learning are mainly based on the transmission of spikes, and highlights the role of local, subcellular processes on dendrites and synapses for neural self-organization.

[1] P. Poirazi, T. Brannon, B. W. Mel, Neuron **37**, 989 (2003)
[2] F. Mikulasch, L. Rudelt, V. Priesemann, Proc. Nat. Ac. Sci. **118**, e2021925118 (2021)
[3] F. Mikulasch, L. Rudelt, M. Wibral, V. Priesemann, Trends Neurosci. **46**, 45 (2023)
[4] F. Mikulasch, L. Rudelt, V. Priesemann, Neural Comp. **35**, 27 (2023)
[5] K. van Driel, L. Rudelt, V. Priesemann, F. Mikulasch, bioRxiv 2023.11.16.567335 (2023)
[6] S. Jähne, F. Mikulasch, ..., S. O. Rizzoli, V. Priesemann, Cell Rep. **34**, 108841 (2021)
[7] F. Mikulasch, S. V. Georgiev, L. Rudelt, S. O. Rizzoli, V. Priesemann, Comm. Biol. **8**, 542 (2025)

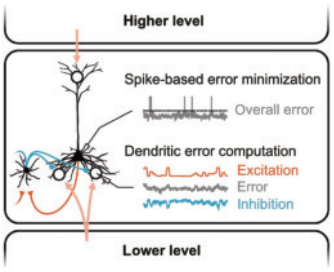

Figure 7.8: Hierarchical predictive coding for spiking neurons with dendritic error computation. Voltage dynamics of individual dendritic compartments (empty circles) can compute a prediction error that can be used locally for synaptic plasticity, as well as at the soma for a spike-based error minimization.

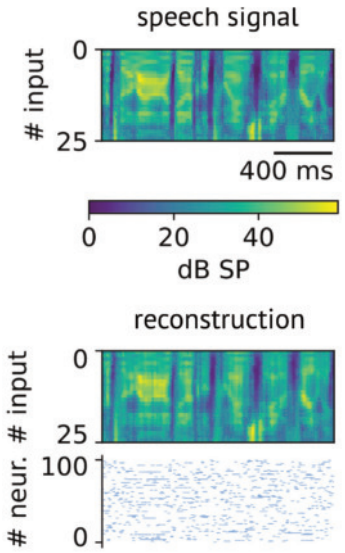

Figure 7.9: Efficient spike encoding of the power of 25 frequency bands of a speech signal learned with dendritic error computation. Top panel shows a snapshot of the input signal. Bottom panel shows a reconstruction of the input signal that was obtained from the spike responses of the model (raster plot, each dot represents a spike).

7.6 STRUCTURE AND DYNAMICS OF THE TELEGRAM COMMUNICATION NETWORK

A. Golovin, S. Mohr, R. Ventzke, A. Schneider, V. Priesemann

Figure 7.10: The Telegram network is partitioned into hierarchical clusters, for example, by language (indicated by color). Each point on the circle represents a single Telegram chat.

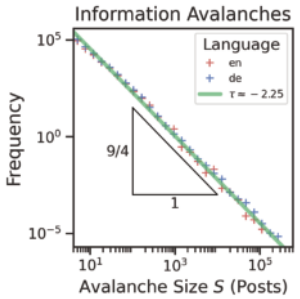

Figure 7.11: Scale-free size distribution of information avalanches with critical exponent $\tau = -\frac{9}{4}$.

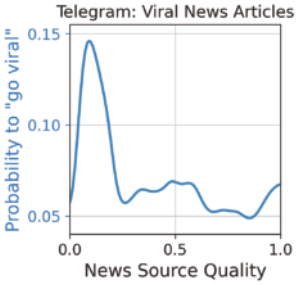

Figure 7.12: Information with a very low news quality source (0=low to 1=high) has a higher chance to "go viral" in the English speaking Telegram community.

Social media has radically changed the way information spreads. While unlimited access to information can benefit society, recent events such as the COVID-19 pandemic have exposed the danger of misinformation, fake news and conspiracy theories. At the same time, social media generates vast amounts of data that can be used in research. With advances in natural language processing, particularly transformer-based models, we can now quantitatively answer questions like: How does platform design influence the quality of discourse? Do unreliable news sources spread faster than credible ones? Can self-organization of communities help counteract misinformation spread? Our overarching goal is to understand online social media through the lens of complex adaptive networks, similar to neural systems or ecological networks.

As a source of data, we focused on Telegram, a messenger platform known for its commitment to privacy. During the COVID-19 pandemic, Telegram gained notoriety in Germany as a hub for misinformation spread, largely due to its absence of content moderation or censorship. What further distinguishes Telegram from other online social platforms is that Telegram does not use recommendation algorithms; instead, information propagates organically through word of mouth. These characteristics make Telegram an especially valuable platform for studying the dynamics of online information spread.

We developed and deployed a snowball crawler to download messages from public Telegram chats [1]. The current dataset amounts to 1.7 TB of data, which includes 1.8 billion multilingual messages from 23 million users in 132 thousand chats (Fig. 7.10). In addition to message text, we captured various Telegram features such as replies, forwarded messages, poll votes and emoji reactions under messages.

In online social networks, information tends to propagate in bursts, called avalanches – somewhat similar to neural systems. We observe scale free size and duration distributions of information avalanches on Telegram (Fig. 7.11) [2]. That is, one finds avalanches of all sizes while the statistics and temporal profiles of the avalanches are self-similar, just like a physical system at a critical point. We investigate how models from critical physical systems, especially Random Field Ising Models can be used to describe and explain information spreading phenomena in self-organized social networks. We also compare how reliable information and misinformation spread in the online community. Preliminary results indicate that on Telegram, misinformation systematically diffuses further than reliable information (Fig. 7.12).

[1] S. Mohr, "Inference of modular structures in dynamical systems and the application to Telegram data", Master's thesis (2024)

[2] R. Ventzke, "Information Spread in Telegram Communities resembles Critical Process", Master's thesis (2024)

7.7 A COARSENING MODEL EXPLAINS CROSSOVER PLACEMENT IN MEIOSIS

M. Ernst, D. Zwicker

Crossovers (COs) between female and male chromosomes mix genetic information during meiosis and play an important role in increasing genetic variability and ensuring correct segregation of homologous chromosomes. Experiments consistently reveal two key findings: First, chromosomes tend to have at least one, but rarely more than a handful, COs. Second, multiple COs on the same chromosome tend to be more widely spaced than expected by chance, a phenomenon called *CO interference*, which prevents nearby COs on a single chromosome.

A recently proposed coarsening model suggests that CO placement is determined by biomolecular condensates that coarsen by exchange and diffusion a protein along the synaptonemal complex that forms between homologous chromosomes. We have shown that this model is quantitatively consistent with experimental results [1]. In particular, the model predicts that there is an obligatory CO, i.e., the minimum number of COs is one. Using Lifshitz-Slyozov-Wagner theory, we derived scaling laws for the number of COs and predict a linear relationship with relative chromosome lengths. This result is consistent with experimental results in several species: for short chromosomes we observe the obligatory CO, and for longer chromosomes a linear relationship with length; see Fig. 7.13A.

We also developed a novel quantity, the interference length L_{int}, which quantifies changes in CO patterning due to CO interference, capturing known aspects and revealing similar behaviour across multiple species for wild type and mutations that only alter the level of the diffusing protein [2]. This behaviour show little dependence on the progress of coarsening as captured by the average CO count $\langle N \rangle$; see Fig. 7.13B. In contrast, mutations that alter the synaptonemal complex (e.g., *zyp1*, *syp-4*, *msh4* mutants) show strongly reduced CO interference, which is expected since diffusion can then only occur via the surrounding nucleoplasm. Taken together, the coarsening model successfully explains most relevant aspects of CO placement.

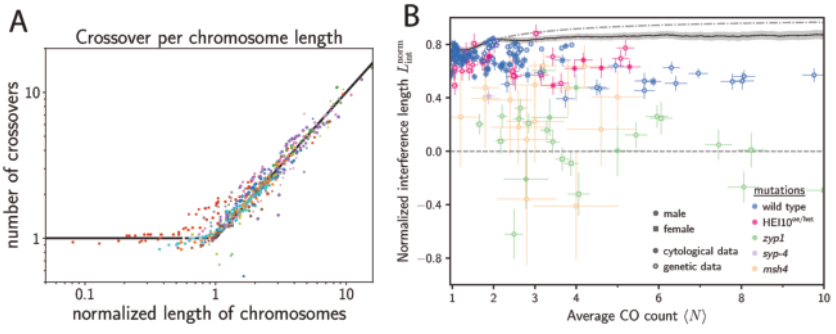

Figure 7.13: (A) Number of COs per chromosome as a function of normalized chromosome length for empirical data from 44 species [3]. (B) CO interference as a function of average CO count $\langle N \rangle$ for various species and mutations; see [2]. The dashed line marks a simple theoretical prediction and the black line shows simulation results of a simple model presented in [1].

[1] S. Durand, ..., M. Ernst, ..., D. Zwicker, R. Mercier, Nat. Comm. **13**, 5999 (2022)
[2] M. Ernst, R. Mercier, D. Zwicker, Nat. Comm. **15**, 8973 (2024)
[3] J. B. Fernandes et al., Proc. Natl. Acad. Sci. U.S.A. **115**, 2431 (2017)

7.8 NONLOCAL ELASTICITY EXPLAINS EQUILIBRIUM PATTERNS OF DROPLETS IN GELS

Y. Qiang, C. Luo, D. Zwicker

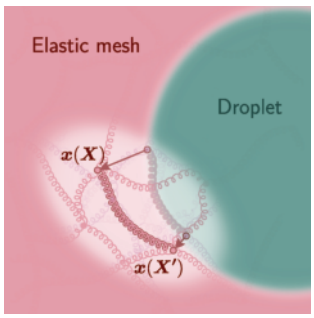

Figure 7.14: Schematic of a droplet embedded in an elastic mesh deforming elastic elements of finite length from the reference position X to $x(X)$.

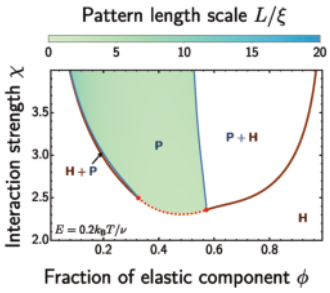

Figure 7.15: Models with nonlocal elasticity exhibit homogeneous states (H), stable patterns (P), coexisting states (H+P), and continuous phase transitions (red dotted lines).

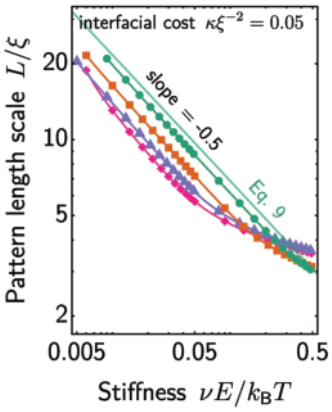

Figure 7.16: Pattern length scale exhibits scaling laws with respective to stiffness.

Phase separation in elastic material is a ubiquitous phenomenon in both synthetic systems and biological cells. Recent experiments found that regular patterns emerge in elastic gels during cooling-induced phase separation [1]. These patterns harbor potential for metamaterials and structural color, particularly since they are easier to produce compared to other systems, such as block copolymers. However, the mechanism underlying their formation is unclear, complicating further development of the method.

During the cooling of the swollen gel, the solvent phase separates from the elastic material, forms droplets, and deforms the elastic mesh (Fig. 7.14). In contrast to normal liquid-liquid phase separation, the droplets in the stiff gel do not coarsen [1]. Interestingly, this transition is reversible and the droplets disappear upon reheating, suggesting a continuous phase transition. Moreover, the droplet size is independent of the cooling rate, in contrast to previous experiments.

To explain these observations, we designed an equilibrium model of phase separation in elastic materials [2]. We showed that simple phase separation theories amended by local elasticity cannot account for equilibrium patterns, even with nonlinear elasticity and large deformation theory. Consequently, we considered a phenomenological model of higher order, yielding a nonlocal elasticity theory that takes into account the structure of the gel.

The equilibrium model with nonlocal elasticity exhibited regular periodic patterns for sufficiently large segregation parameters χ and stiffness E (Fig. 7.15). Moreover, we found a continuous phase transition from the homogeneous state to the patterned state, consistent with the experimental observations. Intuitively, the nonlocality scale ξ describes the mesh size of a regular network or the size of softer region for inhomogeneous networks. In both cases, solvent droplets inflate such a region of size ξ, leading to patterns with regular size. The optimal pattern length scale L then results from a balance between elastic and interfacial energies. Indeed, a more quantitative analysis reveals that L shows clear scaling laws with respect to stiffness and interfacial parameters (Fig. 7.16). Using an analytical approximation, we also derived that L is proportional to the geometric mean of the nonlocality scale ξ and the elastro-capillary length γ/E,

$$L \propto \sqrt{\xi\gamma/E}\,, \tag{7.1}$$

which explains the experimental data and provides guidance for further optimizations to engineer materials with defined properties.

[1] C. Fernández-Rico, S. Schreiber, H. Oudich, C. Lorenz, A. Sicher, T. Sai, V. Bauernfeind, S. Heyden, P. Carrara, L. D. Lorenzis, R. W. Style, E. R. Dufresne, Nat. Mater. **23**, 124 (2024)

[2] Y. Qiang, C. Luo, D. Zwicker, Phys. Rev. X **14**, 021009 (2024)

7.9 TIME SERIES ANALYSIS AND DATA BASED MODELLING

I. Kottlarz, L. Fleddermann, A. Schlemmer, H.F. von Koeller, G. Wellecke, U. Parlitz, S. Luther
S. Herzog (Göttingen), H. Suetani (Oita), G. Datseris (Exeter)

Time series analysis based on ordinal pattern statistics

Previous work by Rosso et al. [1] showed that time series from low-dimensional chaotic systems can be distinguished from stochastic processes ("noise") by their location in the *complexity-entropy plane* spanned by the normalized permutation entropy $H_S[P] = S[P]/S_{\max} = -\sum_{j=1}^{m!} p_j \log p_j / \log(m!)$ and the statistical complexity $C_{JS}[P] = H_s \cdot Q_{JS}[P, P_e]$, where $P = \{p_j\}$ denotes the distribution of ordinal patterns of length m (see Fig. 7.17) and $Q_{JS}[P, P_e] = D_{JS}[P, P_e]/D_{JS,max}$ stands for the normalized Jensen-Shannon divergence $D_{JS}[P, P_e] = S[\frac{P+P_e}{2}] - \frac{S[P]}{2} - \frac{S[P_e]}{2}$ quantifying the difference between P and the uniform distribution P_e.

To address the question whether this distinction is also possible for high-dimensional chaos we applied this approach to time series generated by high-dimensional systems with Kaplan-Yorke dimensions in the range from 1 to 50 and found that dense sampling of continuous signals and too few data points may lead to non-uniform ordinal pattern distributions and spuriously low entropies and high complexities [2]. In particular, phase randomized surrogate data show the same path in the CE-plane as the original data upon lag variation (variation of sampling time), as illustrated in Fig. 7.18 for the Mackey-Glass delay differential equation

$$\dot{x}(t) = \beta \frac{x(t-\tau)}{1 + x(t-\tau)^{\nu}} - \gamma x(t) \tag{7.2}$$

and the one-dimensional Kuramoto–Sivashinsky equation [5]

$$\partial_t u(x,t) = -\frac{1}{2}\nabla\left[u^2(x,t)\right] - \nabla^2 u(x,t) - \nabla^4 u(x,t) \tag{7.3}$$

with periodic boundary conditions. Therefore, the position in the complexity-entropy plane has to interpreted with caution if the null-hypothesis "data stem from a linear stochastic process" cannot be rejected [2].

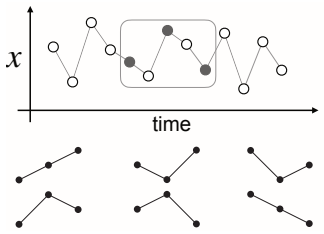

Figure 7.17: Top: Time series with ordinal pattern of length $m = 3$ and lag $l = 2$ highlighted. Bottom: 3!=6 possible ordinal patterns of length $m = 3$.

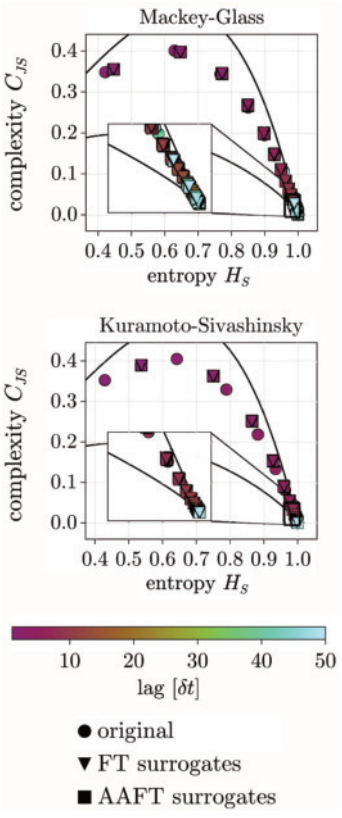

Figure 7.18: Complexity entropy values of 43 dimensional time series of length 10^6 generated by the Mackey-Glass (7.2) and the Kuramoto-Sivashinsky equation (7.3) (pattern length $m = 6$, lag varied).

Predicting chaotic time evolution using reservoir computing

Reservoir computing exploits the response of a dynamical system driven by a given (observed) input signal to predict a desired target signal or to classify the input. To achieve reproducible results the driven system has to fulfill the *echo state property* [3]. If the input signal is generated by another dynamical system the pair of unidirectional systems has to exhibit *generalized synchronization* [4] with a global basin of attraction of the response dynamics [5].

Using the Lorenz-63 system [5], the Hindmarsh-Rose model, and the Lorenz-96 equations for generating input signals and an *echo state network* as reservoir system we demonstrated that delayed values of input and reservoir state (Fig. 7.19) improve prediction performance if only partial knowledge about the state of the driving system is available or if non-optimal hyperparameters are used [6].

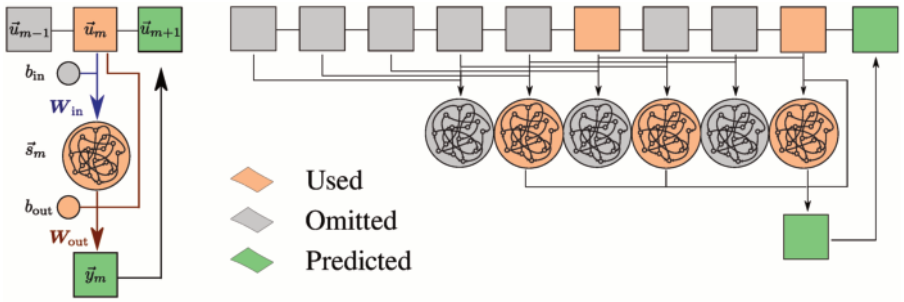

Figure 7.19: Left panel: prediction of the future value $\vec{u}_{m+1}$ of a given input time series using the current input $\vec{u}_m$ and the current state $\vec{s}_m$ of the reservoir system. Right panel: prediction based on current and past (delayed) values of the input time series and the reservoir state. The coloring marks the (dynamic) elements used or not used for computing the output [6].

Furthermore, we showed [7] that efficient iterated prediction of spatio-temporal chaos can be achieved by combining parallel reservoir computing with dimension reduction, as shown in Fig. 7.20 for the one-dimensional Kuramoto–Sivashinsky equation 7.3 with periodic boundary conditions.

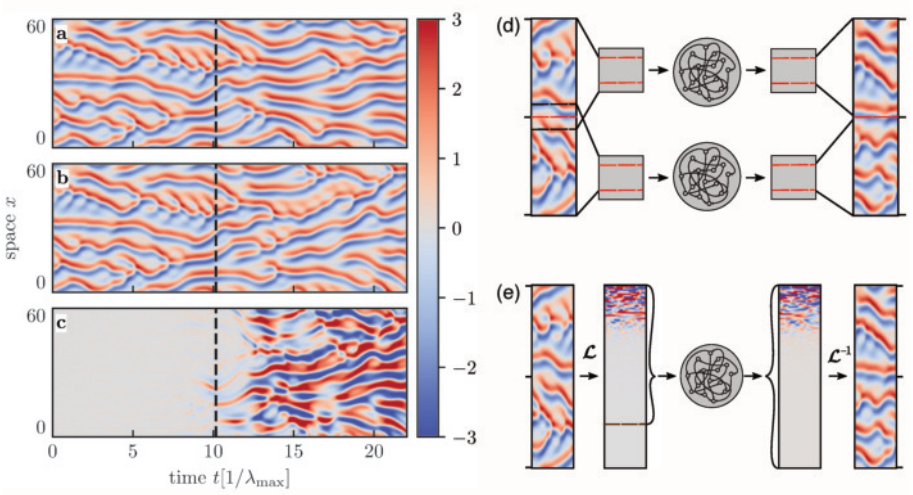

Figure 7.20: Iterative prediction of the Kuramoto–Sivashinsky equation (7.3). (a) True temporal evolution generated by solving Eq. (7.3). (b) Iterative prediction using a combined approach of parallel reservoirs with dimensionality reduction. (c) Difference between the ground truth (a) and the prediction (b). The valid time of the prediction $t_{\text{valid}} \approx 10$ Lyapunov times is marked by dashed black lines. (d) Illustration of the parallel reservoir approach for $M = 2$ reservoirs where each subdomain is predicted by its own reservoir. (e) Linear transformation $\mathcal{L}$ of the input based on principle component analysis (PCA) and dimension reduction using only the largest (75% of the) PCA components as reservoir input. The output of the reservoir is mapped back to the spatial domain by means of the inverse transformation $\mathcal{L}^{-1}$.

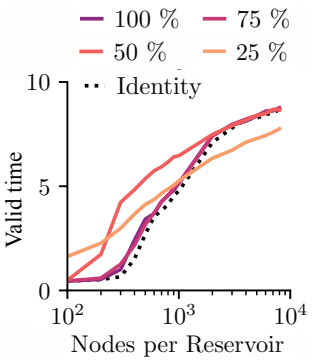

Figure 7.21: For small node numbers $N < 1000$, PCA based dimensionality reduction to 25% or 50% increases the valid times of KSE predictions using $M = 32$ parallel reservoirs

Interestingly, for small reservoir systems (< 1000 nodes), dimension reduction even improves the performance of the prediction (Fig. 7.21).

Analysing complex spiral wave dynamics using wave tracking

To analyse the creation, annihilation and break-up of (spiral) waves in excitable media we have developed a wave tracker (see Fig. 7.22) approach which provides an in-depth analysis of complex spatio-temporal dynamics which can also be applied to experimental imaging data.

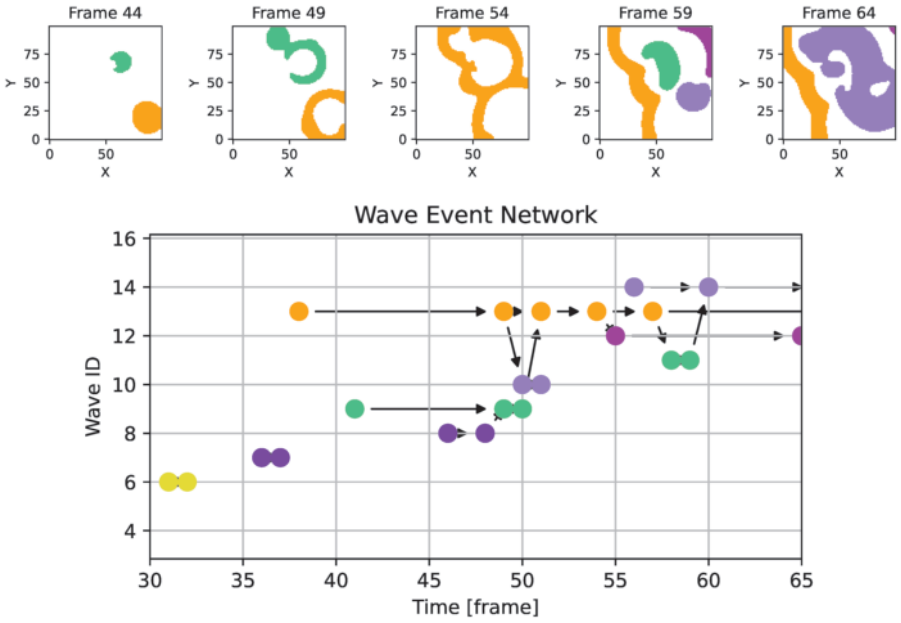

Figure 7.22: Top panel: Snapshots of spiral waves generated by the Fenton-Karma model showing connected wave parts in different colors indicating waves that remain stable and occur in different frames. Bottom panel: Graph with the colored nodes corresponding to the colored waves. Horizontal arrows show continuing waves and diagonal arrows indicate splits and merges of waves.

Further research activities and ongoing collaborations include a review on methods for estimating fractal dimensions [8], applications of adjoint optimization for parameter estimation, the development of analysis tools for real-time MRI-images to quantify the impact of heart beat and breathing on the flow in the glymphatic system of the brain, and advanced signal analysis for breathing patterns and 4D ultrasound imaging.

[1] A. Rosso, H. A. Larrondo, M. T. Martin, A. Plastino, and M. A. Fuentes, Phys. Rev. Lett. **99**, 154102 (2007)
[2] I. Kottlarz and U. Parlitz, Chaos **33**, 053105 (2023)
[3] U. Parlitz, Front. Appl. Math. Stat. **10**, 1221051 (2024)
[4] H. Suetani and U. Parlitz, (*under review*) (2025)
[5] G. Datseris and U. Parlitz, *Nonlinear Dynamics - A Concise Introduction Interlaced with Code* (Springer, 2022)
[6] L. Fleddermann, S. Herzog and U. Parlitz, Chaos **35**, 053147 (2025)
[7] L. Fleddermann, U. Parlitz and G. Wellecke, arXiv:2504.05512, *under review* (2025)
[8] G. Datseris, I. Kottlarz, A.P. Braun, U. Parlitz, Chaos **33**, 102101 (2023)

Link to additional information:
https://bmp.ds.mpg.de/
research/bmp_tsanalysis/

CONTROL AND OPTIMIZATION

8

The need to control and optimize a complex system is at the heart of many practical applications, ranging from medicine and engineering to social systems. However, this typically requires a thorough understanding of the underlying physics in order to target a specific mechanism or represent a system using reduced-order models that allow for optimization.

At MPI-DS, we work at the frontier of controlling and optimizing a broad range of dynamical systems. Which parameters control the emergence of chaos? Can we modulate the development of biological systems? Can we control the human heart to reduce failure? Can artificial intelligence improve the analysis of experimental data? How can we control turbulent flows over wind turbines and aircraft? How should wind farms be designed and operated to maximise power output? How do we design the global energy system of the future in the face of large uncertainties? This chapter highlights our most recent advances towards answering these questions.

Contents

8.1 MODELING HELPS FAILING HEART REGENERATION

Y. Wang, I. Braun, X. Gao, Y. Zhang, V. Zykov, A. Ecker, E. Bodenschatz,
J. Lotz, T. Meyer, M. Ucker, W. Zimmermann (University Medical Center Göttingen), S. Boretius, R. Hinkel (German Primate Center), L. Budde, S. Spindeldreier (Leibniz University Hannover)

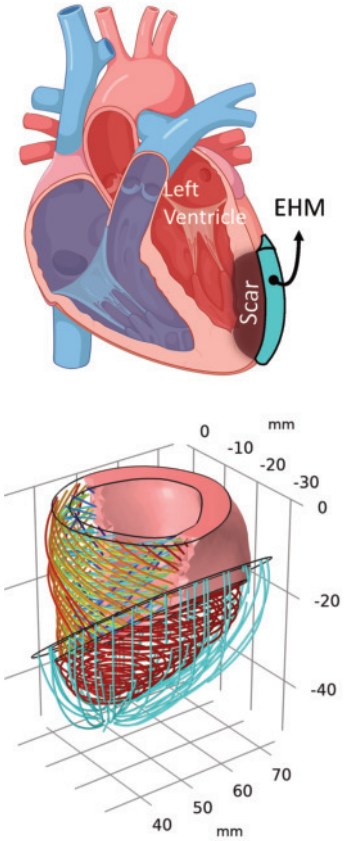

Figure 8.1: (Top) Schematic illustration of an infarcted heart with a scarred left ventricle and EHM patch over it. (Bottom) Personalized model for the left ventricle of a monkey heart reconstructed from MRI images, with scar and EHM patch. Transmural myocardiual fibers in the ventricular wall, dark red collagen fibers in the scar, and longitudinal fibers in the patch, are highlighted.

Heart failure is a common and serious condition that poses significant health and financial burdens. While mechanical assistive devices can extend life, they cannot restore heart function and may carry risks such as stroke. Emerging approaches like xenotransplantation face immune rejection challenges. Alternatively, tissue-engineered heart repair, using engineered heart muscle (EHM) patches, shows promise in enhancing heart function. Early human trials are underway, but success may rely on customized EHM designs for individual defects.

Supported by the BMBF and the DZHK, and in collaboration with the University Medical Center Göttingen, the German Primate Center, and the Leibniz University of Hanover, we developed a protocol for personalized heart modeling using medical images and finite element methods (Fig. 8.1). The model incorporates a constitutive law we proposed [1] that accounts for fiber orientation and dispersion. Simulations using this protocol identify the optimal EHM configuration and implantation site for each heart. We share these optimized designs with our collaborators, who bioprint the EHM patches for therapeutic applications.

The end-diastolic and end-systolic pressure-volume relationships (EDPVR & ESPVR), are two important indicators of the heart function. Despite extensive research, no model with physically interpretable parameters has unified these relationships. We developed a physics-based model that integrates EDPVR and ESPVR within a single framework [2]. Such model provides deeper insights into cardiac mechanics with potential applications in cardiac research and clinical practice.

Using in silico modeling, we explored the impact of the fiber architecture on cardiac function, which can guide bioprinting of artificial hearts. We proposed and numerically validated non-invasive sonogenetics treatment for cardiac defibrillation by activating stretch-sensitive ion channels in cardiomyocytes [3]. We developed a personalized stenting strategy for aortic coarctation using computational fluid dynamics [4]. We are also working on physics-informed neural networks as surrogate models for cardiac simulation. Our vision is to leverage physics-guided, computer-assisted modeling as a non-invasive tool to deepen our understanding of cardiac function and to enhance treatment outcomes.

[1] M. Kalhöfer-Köchling, E. Bodenschatz, Y. Wang, Phys. Rev. Appl. **13**, 064039 (2020)
[2] Y. Zhang, M. Kalhöfer-Köchling, E. Bodenschatz, Y. Wang, Front. Physiol. **14**, 1195502 (2023)
[3] Y. Li, X. Wang, J. Guo, Y. Wang, V. Zykov, E. Bodenschatz, X. Gao, Chaos **35**, 013127 (2025)
[4] D. Ma, Y. Wang, M. Azhar, et al., Eng. Appl. Comput. Fluid Mech. **16**, 2056 (2022)

8.2 ENGINEERED HEART MUSCLE

S. Salekdeh, L. Mamoyan, E. Bodenschatz
T. Meyer, W. Zimmermann (Göttingen)

Heart failure results in the loss of functional myocardium, replaced by non-contractile scar tissue, which compromises cardiac function. To address current challenges in clinical treatment and in cardiac tissue-engineered constructs, such as inadequate contraction force, poor integration with the host tissue, and the lack of anisotropic structure in engineered heart muscles (EHM) [1, 2], our project combines mechanoadaptation studies and 3D bioprinting to develop and engineer a functional and adaptive cardiac tissue.

To investigate how mechanical forces influence cardiac tissue organization, we employ a stepwise approach using different model systems. Freestanding monolayers serve as the simplest model to study mechanical effects on human foreskin fibroblast cells (HFFs) and cardiomyocytes (CMs) (Fig. 8.2 A). To explore how mechanical cues affect cell alignment, we use patterned substrates (Fig. 8.2 B). Finally, engineered heart muscle constructs anchored to pillars (Fig. 8.2 C), provide a biologically more native-like model. These constructs allow us to study how mechanical forces drive extracellular matrix remodeling and electrical signaling, offering valuable insights into cardiac tissue adaptation under physiological stress.

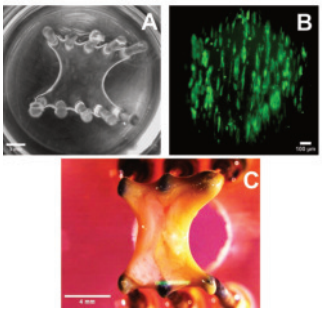

Figure 8.2: (A) Freestanding cardiac monolayer supported by pillars, scale bar 3 mm. (B) Fluorescence image demonstrating cell alignment due to patterning, scale bar 100 μm. (C) Engineered heart muscle anchored to metal rods, scale bar 4 mm.

In parallel we also pursue some efforts to translate such insights into therapeutic applications through advanced bioprinting technology. Specifically, we aim to develop an engineered myocardium using fiber-based bioprinting technique, focusing on the fabrication of cell-laden microfibers that mimic the anisotropic architecture of native cardiac tissue. A customized extrusion device was designed (Fig. 8.3 A) to assess and optimize several parameters to support: 1) the extrusion of intact core-shell fiber (Fig. 8.3 A1) in which the reconstitution mixture is surrounded by an alginate shell to generate cell-laden fiber (Fig. 8.3 A2), and 2) cell survival and functional maturation of CMs in the core part of the fiber (Fig. 8.3 B). Shortly, all the optimized printing parameters achieved by our extrusion device will be implemented in a 6-axis robotic arm to print cardiac patches based on the force pattern predicted by numerical simulations. The patch with this specific pattern is believed to result in a personalized patch that can be more efficiently integrated into the host cardiac tissue.

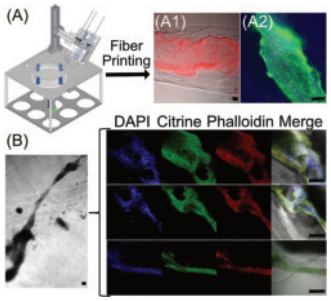

Figure 8.3: (A) The fibers printing device extruding: (A1) core-shell fiber with red fluorescent microparticles (FMPs), and (A2) cell-laden fiber with HFFs, in the core part of the fibers. (B) In vitro assessment, using specific fluorophores, to show the distribution and configuration of CMs and HFFs in different parts of a continuous cell-laden fiber after extrusion on day 28. The scale bar 100 μm.

[1] W.H. Zimmermann, T. Eschenhagen, Heart Fail Rev. **8**, 259 (2003)
[2] B. Fujita, W.H. Zimmermann, Curr. Cardiol. Rep. **19**, 78 (2017)

8.3 CONTROLLING NEURAL POPULATION DYNAMICS THROUGH STIMULATION

F. P. Spitzner, B. Cramer, J. Zierenberg, V. Priesemann
A. Neef (CIDBN), J. Schemmel (Heidelberg), A. Levina (Tübingen)
M. Muñoz (Granada), J. Soriano (Barcelona), H. Yamamoto (Sendai)

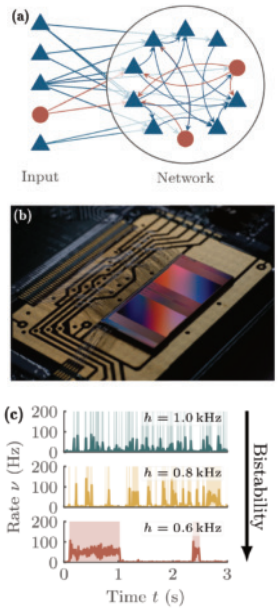

Figure 8.4: A spiking neural network that receives input of rate h and self-regulates its recurrent connections to achieve a target firing rate (a) is realized on neuromorphic hardware (b) and shows bistability for low input rates (c).

Neural networks in biological and artificial intelligence distribute computation across their neurons to solve complex tasks. Depending on the task this requires different collective properties, such as decorrelation (cf. Sec. 7.5) or memory (cf. Sec. 7.2). How neural networks self-organize to control their collective properties is an ongoing research question. With our research, we revealed the relevance of local self-regulation in controlling neural population dynamics through stimulation.

Building on our theory that homeostatic neural self-regulation shapes the correlation of population activity under varying external input strength [1], we emulated a recurrent neural network with slow homeostatic regulation on neuromorphic hardware (Fig. 8.4). We verified that reducing the stimulation rate h leads to an increase in autocorrelation time to maintain the target firing rate [2]. Since our protocol considered slow homeostatic regulation restricted to the training period, the spiking neural network implemented increasing timescales with a novel form of emergent bistability — a result of fluctuation-induced stochastic switching between metastable active and quiescent states.

On much faster timescales, we used optogenetic stimulation to induce extra spikes in a modular network of dissociated neurons in vitro (Fig. 8.5). Here, we found that stimulation can desynchronize the collective dynamics via the fast local adaptation of resource depletion [3]. Resource depletion thus acts as a quick form of negative feedback on the pre-synaptic transmission that complements the post-synaptic homeostatic regulation.

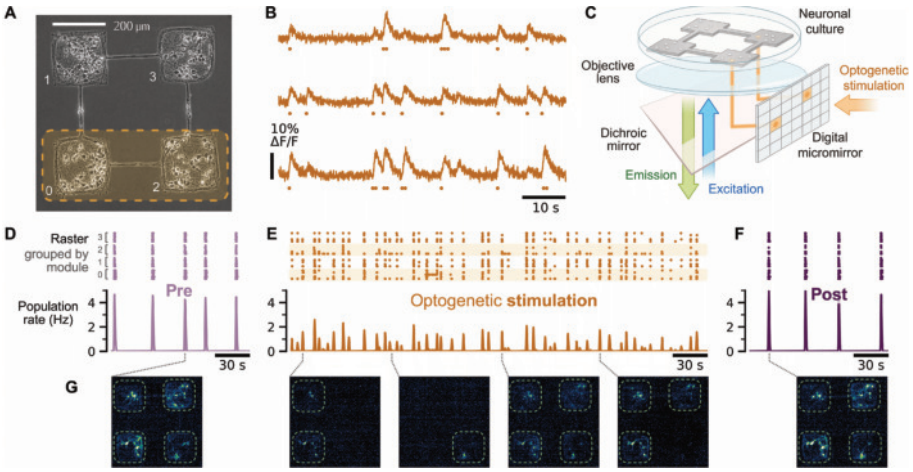

Figure 8.5: Optogenetic stimulation on modular neuronal cultures increases the variability in collective network dynamics. In silico model of spiking neurons and a mesoscopic model of stochastically coupled modules reveal that for short-term stimulation the underlying mechanism of this variability is persistent depletion of synaptic resources.

[1] J. Zierenberg, J. Wilting, V. Priesemann, Phys. Rev. X **8**, 031018 (2018)
[2] B. Cramer, ... V. Priesemann, J. Zierenberg, Phys. Rev. Research **5**, 033035 (2023)
[3] H. Yamamoto, F. P. Spitzner, ... V. Priesemann, M. A. Muñoz, J. Zierenberg, J. Soriano, Sci. Adv. **9**, eade1755 (2023)

8.4 BINDING AND DIMERIZATION CONTROL PHASE SEPARATION IN A COMPARTMENT

R. Rossetto, G. Wellecke, D. Zwicker

Biological cells exhibit a hierarchical spatial organization where various compartments harbor condensates forming by phase separation. To control the occurrence of such condensates, cells can tune the physical interactions of involved biomolecules. This directly affects binding and phase separation, but there are also indirect effects, e.g., via the formation of oligomers. To elucidate the interplay of these effects, we developed an equilibrium theory that takes into account compartment binding, unspecific interactions enabling phase separation, and dimerization as an example of oligomerization [2]; see Fig. 8.6.

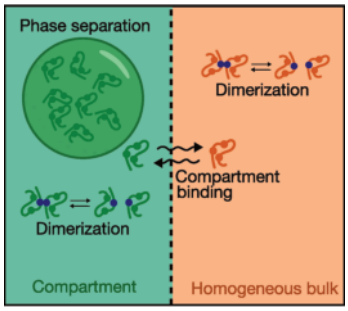

Figure 8.6: Schematic representation of the model describing compartment binding, phase separation, and dimerization of biomolecules.

Our analysis unveils a non-linear behavior, which emerges from the size disparity of the sub-systems and the fact that dimers exhibit twice the affinity of monomers. Fig. 8.7A shows that this interplay explains experimental measurements of proteins binding to membranes [1]. Moreover, compartment binding fundamentally affects equilibrium states. For instance, we find a re-entrant phase transition (Fig. 8.7B) and a multistable regime [2]. Taken together, our analysis reveals a double role of dimerization: on the one hand, it can regulate the affinity to the compartment by amplifying existing energy differences; on the other hand it amplifies the phase separation behaviour. It is thus likely that cells exploit regulated dimerization to control the formation of condensates within membranes and more generally.

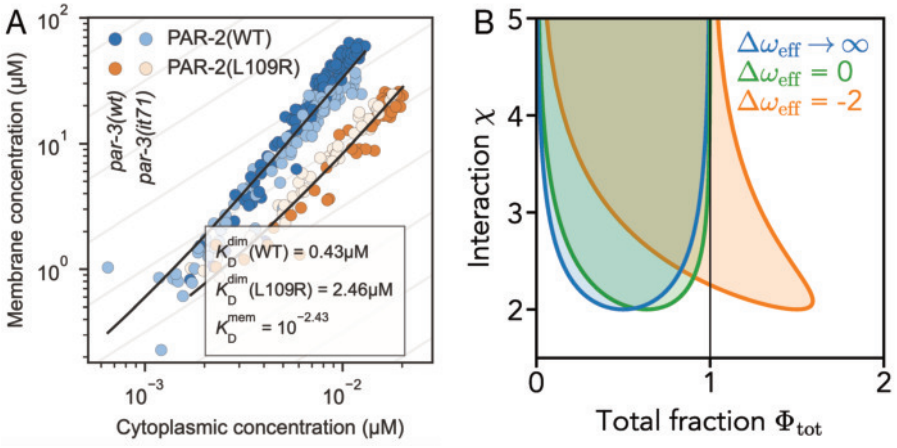

Figure 8.7: (A) Experimentally measured concentration of membrane-bound and cytoplasmic PAR-2 proteins in *C. elegans*. Solid black lines are theoretical fits of our theory [1]. (B) Phase diagram as function of total fraction of material, Φ_{tot}, and interaction strength χ for various binding affinities $\Delta\omega_{\text{eff}}$. Phase separating can occur in the compartment within the color regions.

[1] T. Bland, N. Hirani, D. C. Briggs, R. Rossetto, K. Ng, I. A. Taylor, N. Q. McDonald, D. Zwicker, N. W. Goehring, EMBO J. **43**, 3214 (2024)
[2] R. Rossetto, G. Wellecke, D. Zwicker, Phys. Rev. Res. **7**, 023145 (2025)

8.5 REYNOLDS NUMBER EFFECTS ON WIND TURBINE PERFORMANCE AND OPTIMAL PITCH ANGLE

Y. Hattori, F. Krippenstapel, C. E. Brunner,
J. Jüchter (Oldenburg)

Wind turbines are becoming larger and larger in order to meet the world's electricity demand. Modern wind turbines have diameters of more than 200 m and are able to generate up to 15 MW of electricity. To study the flow dynamics around wind turbines, it is crucial to consider the diameter-based Reynolds number, $Re_D = \rho U D/\mu$, where U is the incoming flow velocity, D is the diameter of the rotor, ρ is the density and μ is the dynamic viscosity of air. It is typically assumed that the performance of wind turbines varies with Re_D but that a threshold exists beyond which it is independent of Re_D. However, a recent study [1] observed such asymptotic Reynolds number behavior only around $Re_D \sim 10^7$, a significantly higher threshold than widely assumed.

Although many studies of wind turbine flows have been conducted using wind tunnels, traditional wind tunnels are not able to reach such high Re_D without increasing U. Increasing U can not only lead to compressibility effects, it also makes it virtually impossible to still match the tip speed ratio (TSR). This is a dimensionless time scale that is defined as $\omega R/U$, where ω is the angular velocity and R is the radius of the rotor. By using the Variable Density Turbulence Tunnel (VDTT) in the Max Planck Turbulence Facility at the MPI-DS 9.8, we are able to investigate the effects of Reynolds number on turbine performance by studying a single turbine over a Reynolds number range of $1.0 \times 10^4 \leq Re_D \leq 2.0 \times 10^7$. The VDTT achieves high Re_D at low velocities by using pressurized sulfur hexafluoride (SF_6). Thus, high TSR like real wind turbines can be achieved at easily realizable rotation rates. Results at the lower end of the range are directly comparable to results from conventional wind tunnel experiments, while results at the upper end of the range are comparable to field measurements of full-scale turbines. By spanning this wide range, our experiments help to reconcile existing studies from laboratory and field conditions. In addition, the results can serve as validation for numerical simulations. We measure turbine power output P as well as the optimal pitch angle of the turbine, O_p.

The power coefficient of a wind turbine is defined as

$$C_p = \frac{P}{\frac{1}{2}\rho U^3 \frac{\pi}{4} D^2}. \tag{8.1}$$

It is the ratio between the power that a turbine extracts as mechanical power and the available kinetic energy in the flow. We install a model wind turbine developed by the University of Oldenburg, MoWiTO 0.6 (Fig. 8.8), inside the VDTT. We obtain C_p over a wide range of Re_D by changing the pressure of the SF_6 in the tunnel from 1 to 15 bar. We determine the angle of the turbine blades which maximizes C_p. This angle is the optimal pitch angle O_p. Real wind turbines

Figure 8.8: Model Wind Turbine (MoWiTo) 0.6, developed by researchers at the University of Oldenburg [2].

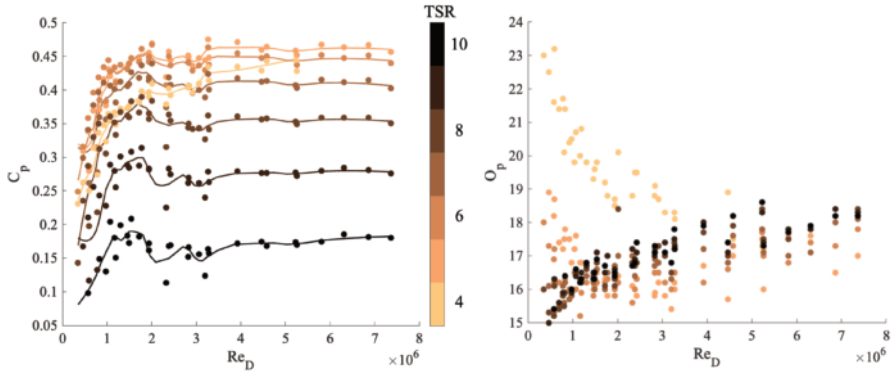

Figure 8.9: Power coefficient C_p (left) and optimal pitch angle O_p (right) over diameter-based Reynolds number Re_D.

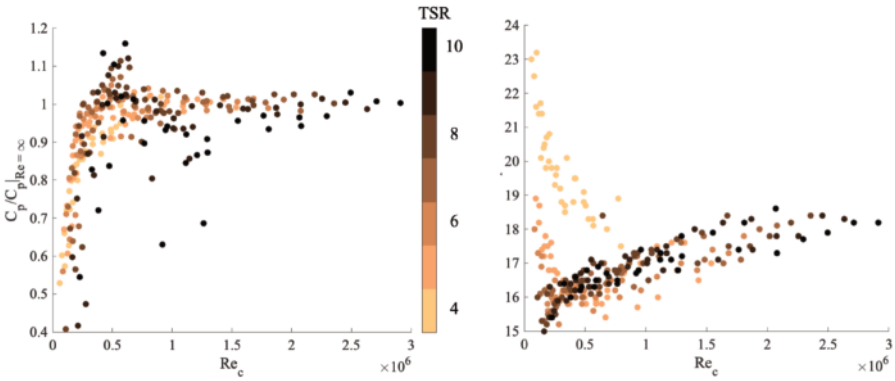

Figure 8.10: Power coefficient C_p normalised with its convergence value at high Re_D (left) and optimal pitch angle O_p over chord-based Reynolds number Re_c (right).

are designed to always operate at the optimal pitch angle for a given condition. However, the effect of Reynolds number on O_p had not previously been investigated. Fig. 8.9 shows our results for how C_p and O_p varied over Re_D at a variety of tip speed ratios. C_p is a function of TSR and becomes invariant after Re_c of $\sim 10^6$, which is consistent with previous findings [1]. Following this study, we also recast the data using the chord-based Reynolds number which captures both Re_D and TSR: $Re_c = \rho c\sqrt{U^2 + (\omega R)^2}/\mu = Re_D \frac{c}{D}\sqrt{1 + TSR^2}$, where c is the chord length of the blades. Since the blade chord c varies radially along the length of the blade, we consider the chord at $R/2$.

Rescaling the power coefficients using Re_c and normalising them by the C_p obtained over the plateau at high Reynolds numbers, a universal curve is obtained (Fig. 8.10). On the other hand, O_p surprisingly does not show Reynolds number invariance over the range of Reynolds numbers considered here. Future measurements will extend to even higher Reynolds numbers to investigate whether a plateau is reached, as well as employ additional measurement techniques to determine the physical mechanisms responsible for these Reynolds number trends.

[1] M. A. Miller, J. Kiefer, C. Westergaard, M. O. Hansen, and M. Hultmark, Phys. Rev. Fluids **4**, 110504 (2019)

[2] J. Schottler, A. Hölling, J. Peinke, and M. Hölling, J. Phys. Conf. Ser. **753**, 072030 (2016)

8.6 AIRFOIL FLOWS AS BI-STABLE DYNAMICAL SYSTEMS

C. E. Brunner
M. Hultmark (Princeton)

Wind turbines rotate due to forces generated on their blades by the surrounding flow. To study these forces, a two-dimensional cross-section of a blade (airfoil) is typically considered. Airfoil flows are the fundamental building block of aerodynamics. An understanding of airfoil flow physics is of great interest not only to the field of wind energy science, but also to aircraft and even animals (birds, insects and fish). In equilibrium, an airfoil flow adopts one of two states: attached or separated. The separated state is detrimental to most applications. We investigate the dynamics of the transitions between these two states:

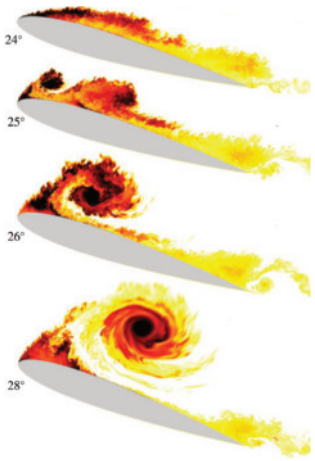

Figure 8.11: Temporal evolution of dynamic stall during increasing angle of attack, adapted from [1]. A large vortex forms over the airfoil and convects downstream.

The timescales of dynamic stall. The sheared and highly turbulent inflow conditions found in wind farms cause sudden perturbations in the flow over a blade, triggering dynamic stall - a violent transition from attached to stalled flow (Fig. 8.11). This causes extreme fluctuations in blade loads, overshooting and then rapidly undershooting those predicted by aerodynamic theory before reaching a new equilibrium. This complicates performance predictions and leads to mechanical fatigue over time. We pursue a fundamental understanding of the precursors and parameters governing dynamic stall, and elucidate scaling laws that describe these phenomena [2].

Reynolds number effects. Modern offshore wind turbines are now sufficiently large that their blades experience chord Reynolds numbers of up to $Re_c \sim 10^7$. Very few wind tunnels are capable of reproducing these conditions. Therefore, airfoil behaviour at these Reynolds numbers is not well understood, but is of large importance for wind energy science. By investigating the effect of chord Reynolds number and turbulence Reynolds number on airfoil flow behaviour in these unprecedented conditions, we determine which mechanisms are at play and whether a regime of Reynolds number invariance exists [3].

Stability and stochastics of state transitions. There is often an angle-of-attack regime in which both the attached and separated flow exist as stable states. We showed that the resulting hysteresis in angle-of-attack changes is severe and strongly dependent on Reynolds number [3]. Recently, it was shown that narrow angle-of-attack regimes exist in which the flow randomly switches between the two states and that switches are triggered by extreme events [4]. We investigate the effect of chord Reynolds number on the statistics of state transitions.

[1] S. I. Benton, M. R. Visbal, J. Fluid Mech. **861**, 860 (2018)
[2] J. Kiefer, C. E. Brunner, M. O. L. Hansen, M. Hultmark, J. Fluid Mech. **938**, A10 (2022)
[3] C. E. Brunner, J. Kiefer, M. O. L. Hansen, M. Hultmark, Exp. Fluids **62**, 178 (2021)
[4] I. Kharsansky Atallah, L. Pastur,R. Monchaux, L. Zimmer, Phys. Rev. Fluids **9**, 063902 (2024)

8.7 REPRESENTING RENEWABLE ENERGY SOURCES IN INTEGRATED ASSESSMENT MODELS

C. E. Brunner
S. A. Arora, A. Glaser (Princeton), G. Marangoni (TU Delft)

Offshore wind energy is a rapidly growing industry with the potential to contribute significantly to the clean energy transition. However, most of the complex system models used to inform long-term climate policy -so-called integrated assessment models (Fig. 8.12)- project virtually no offshore wind energy deployment due to its higher cost compared to other renewable energy sources. IAMs are cost-minimising, but real-world policy decisions are driven by a variety of factors including public opinion and grid integration, not by cost alone. We use the WITCH model [1] to investigate the impact of more realistic assumptions about renewable energy sources in IAMs.

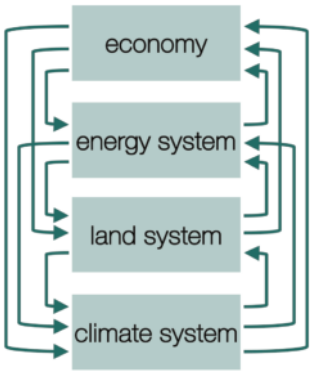

Figure 8.12: Integrated assessment models (IAMs) are complex system models that combine simplified representations of the economy, the energy system, the land system and the climate system in order to make long-term projections of policy options in the context of climate change. The latest IPCC report included results of six IAMs. One of these is the World Induced Technical Change Hybrid (WITCH) model [1]. The uncertainty in IAM projections is naturally vast, and has been a major focus of research since the inception of IAMs at the beginning of the century. Since then, they have increased significantly in complexity.

Availability. Energy systems models generally overestimate the politically feasible renewable energy resource potential: vast areas of land are technically available for renewable energy projects today, but if all of this land was in fact used, this would trigger strong public opposition, resulting in stricter siting rules. For example, some parts of Germany have imposed strict wind turbine siting rules after initial deployment. By considering a variety of assumptions regarding siting rules [2], we investigate the impact of public opposition on future renewable energy deployment. We find that for the United States, public opposition has a strong effect on model projections of onshore and offshore wind energy deployment by the end of the century.

Remoteness. Despite (inter-)national electricity grids, electricity prices can vary regionally depending on local supply and demand because grid transmission capacity is finite. For example, limited north-south transmission capacity in the German electricity grid creates a bottleneck in bringing wind energy from the north sea to industrial centers in the south. Renewable energy resources therefore vary in value depending on their distance to demand centers. IAMs have low spatial resolution and thus cannot directly model such transmission capacity constraints and regionally varying value. We are developing parameterizations of the "remoteness" of a renewable energy resource as a weighted function of its distance to the surrounding population for use in IAMs.

Model architecture. As with any complex system model, model outcomes can be highly sensitive to the model architecture and its underlying assumptions. The WITCH model traverses a decision tree of possible energy sources during its cost-minimizing optimization procedure [3]. We study the model sensitivity to various architectures for selecting renewable energy sources.

[1] V. Bosetti, C. Carraro, M. Galeotti, E. Massetti, M. Tavoni, Energy J. **27**, 13 (2006)
[2] A. Lopez, T. Mai, E. Lantz, D. Harrison-Atlas, T. Williams, G. Maclaurin, Energy **223**, 120044 (2021)
[3] S. Carrara, G. Marangoni, Energy Econ. **64**, 612 (2017)

8.8 CONTROLLING CHAOS IN EXCITABLE MEDIA

M. Aron, J. Wolter, S. Hussaini, J. Steyer, G. Luther, A. Barthel, V. Krinski, U. Parlitz, S. Luther
T. Lilienkamp, D. Suth (Nuremberg), C. Richter (Göttingen), V. Biktashev (Exeter)

With each heartbeat, electrical excitation waves propagate across the heart muscle, leading to coordinated mechanical contraction and efficient pumping. During cardiac fibrillation, however, excitation waves are chaotic, resulting in incoherent contraction and loss of mechanical function. In clinics, for lack of a better strategy, high-energy electric shocks are being used to terminate arrhythmia and restore normal function. However, these shocks have severe side effects, including tissue damage, excruciating pain, and a worsening prognosis. There is a significant need for better control of ventricular and atrial arrhythmias.

Low-energy control of fibrillation aims to replace the single high-energy shock with a sequence of weak pulses. While simple pacing sequences have shown some remarkable success, further optimization is necessary to achieve clinically relevant energy reduction. In this report, we describe recent progress in the development of adaptive and optimized pacing sequences and discuss numerical and experimental evidence demonstrating the significant potential of feedback pacing.

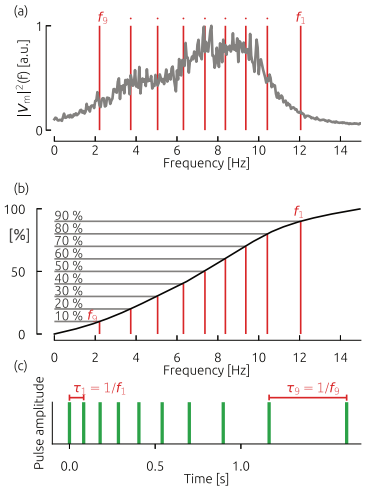

Figure 8.13: Derivation of the adaptive (spectrum-guided) deceleration pacing sequence (ADP). The power spectrum density is computed based on the dynamics of the system (a) and integrated up to a cutoff frequency (b). Frequencies are chosen such that the integrated spectrum is equidistantly covered from 10% to 90% in 10%-steps (for ten pulses) (b). The resulting frequencies f_1 to f_9 define the pulse sequence (c) covering the power spectral density (red vertical lines in (a)) [1].

Adaptive Deceleration Pacing (ADP)

Adaptive deceleration pacing (ADP) is an algorithm for determining a sequence of far-field electrical pulses based on the power spectrum of the arrhythmia [1]. In contrast to previous approaches, which often rely only on the dominant frequency of the broad spectrum of fibrillation, ADP relies on the entire spectrum as illustrated in Fig. 8.13. Starting from a high frequency, ADP gradually slows the electrical far-field pacing rate, decelerating the arrhythmia to termination. Confirmed in ex vivo experiments in isolated rabbit hearts, ADP shows robust and effective termination of ventricular and atrial arrhythmias as shown in Fig. 8.14. Supported by MPG technology transfer funds, we are conducting a preclinical in vivo validation of ADP in a large animal disease model of AF in preparation of a first-in-patient study.

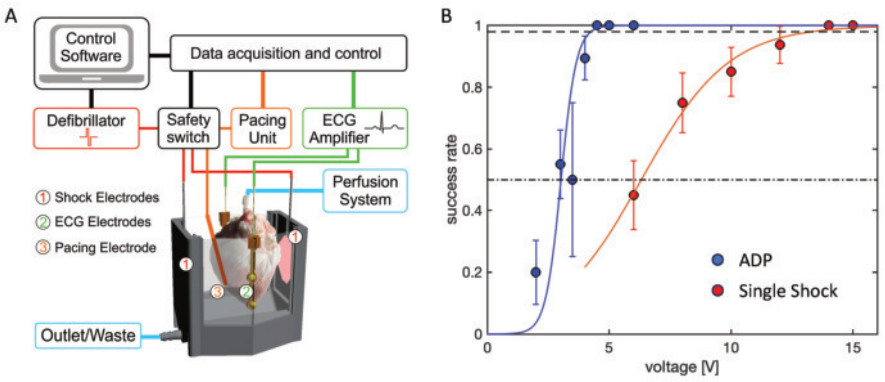

Figure 8.14: Low-energy control of atrial arrhythmias. **A** Experimental setup for Langendorff-perfused rabbit and pig hearts. **B** Dose-response for ADP and conventional single shock (N=4 rabbit hearts, $n_{ADP} = 82$ and $n_{single} = 84$ termination attempts).

The role of pulse timing in cardiac fibrillation

Success rates of simulated single and multi-pulse defibrillation protocols are sensitive to application timing with individual, protocol-specific optimal timings [3, 4] as illustrated in Fig. 8.15. Simulations of defibrillation attempts showed that such timing matters: The success rate of single- pulse protocols can vary by as much as 80 percentage points or more depending on timing, and using more shocks in succession only lessens this sensitivity up to a point [4]. The optimal application timings are found to be specific to each combination of protocol and fibrillation episode [4]. Therefore, feedback-driven inter-pulse periods may be the only feasible means of leveraging timing for improvements in treatment efficacy.

Optimizing Pulse Sequences using Genetic Algorithm

Using 2D simulations of homogeneous cardiac tissue and a genetic algorithm, we demonstrate the optimization of sequences with non-uniform pulse energies and time intervals between consecutive pulses for efficient VF termination [5]. We further identify model-dependent reductions of total pacing energy ranging from 4% to 80% compared to ADP.

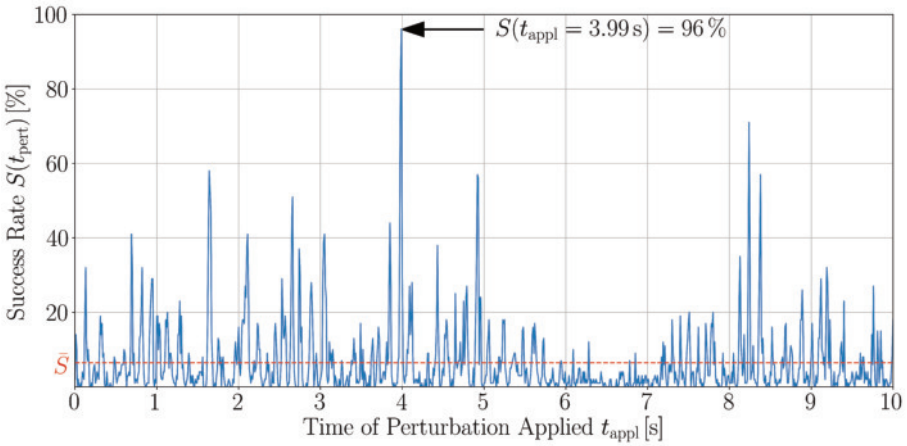

Figure 8.15: Fluctuations of success rates of single pulse defibrillation attempts vs. time when the pulse is applied [3].

Local Minima Feedback Pacing

In a numerical study, we investigated a variant of feedback pacing, in which electrical field pulses are applied after local minima in the mean value of the transmembrane potential [2]. We show that local minima pacing (LMP) can reduce the number of pulses and therefore the total electrical energy applied required to successfully terminate the underlying dynamics compared to ADP. Using different numerical models, initial conditions, and model parameters, the robustness of the effect is demonstrated. This study provides further evidence suggesting the significant potential of feedback for the termination of fibrillation.

Optogenetic Feedback Pacing

Cardiac optogenetics enables the manipulation of cellular functions using light, opening novel perspectives to study nonlinear cardiac function and control. We have investigated the efficacy of optical resonant feedback pacing to terminate ventricular tachyarrhythmias using numerical simulations and experiments in transgenic Langendorff-perfused mouse hearts [6]. We show that the effectiveness of terminating cardiac arrhythmias using feedback pacing is superior to a single optical pulse, as illustrated in Fig. 8.16. At 50% success rate, the energy per pulse is 40 times lower than with a single pulse with 10 *ms* duration. We show that even at light intensities below the excitation threshold it is possible to terminate arrhythmias by spatiotemporal modulation of excitability, that induces a spiral wave drift and dissolving spiral wave core [7, 8].

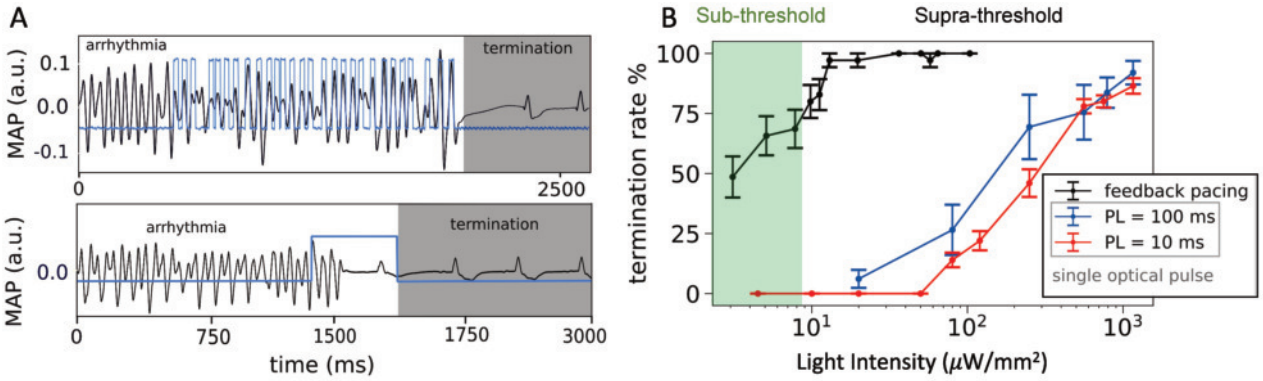

Figure 8.16: Optogenetic termination efficacy of ventricular tachyarrhythmias in ex vivo. **A** Top: Arrhythmia termination using optical resonant feedback pacing. Monophasic action potential (MAP, black) and light intensity (LI=40 $\mu W/mm^2$) with pulse length (PL=20 *ms*) triggered from MAP time series result in arrhythmia termination (gray). Bottom: Arrhythmia termination using the single optical pulse PL= 100 *ms*, LI= 560 $\mu W/mm^2$. **B** Arrhythmia termination efficacy in mouse hearts (N=5) vs. LI for optical resonant feedback pacing (black line) and single optical pulse (blue line: PL= 100 *ms*, red line: PL=10 *ms*). Green shaded area indicates sub-threshold LI, data given in mean ± SEM [6].

Link to additional information: https://bmp.ds.mpg.de/research/bmp_chaoscontrol/

[1] T. Lilienkamp, U. Parlitz, S. Luther, Chaos **32**, 121105 (2022)
[2] D. Suth, S. Luther, T. Lilienkamp, Front. Netw. Physiol. **4**, 1401661 (2024)
[3] J. Steyer, T. Lilienkamp, S. Luther, U. Parlitz, Front. Netw. Physiol. **2**, 1007585 (2023)
[4] M. Aron, S. Luther, U. Parlitz, Front. Netw. Physiol. **5**, 1572834 (2025)
[5] M. Aron, T. Lilienkamp, S. Luther, U. Parlitz, Front. Netw. Physiol. **3**, 1172454 (2023)
[6] S. Hussaini, A. Mamyraiym Kyzy, J. Schröder-Schetelig et al., Chaos **34**, 031103 (2024)
[7] S. Hussaini, R. Majumder, V. Krinski, S. Luther, Pflügers Archiv: Eur. J. Phys. **475**, 1453 (2023)
[8] S. Hussaini, S.L. Lädke, J. Schröder-Schetelig et al., PLoS Comp. Biol. **19**, e1011660 (2023)

8.9 MACHINE LEARNING FOR MICROPARTICLE DETECTION AND REAL-TIME HOLOGRAPHY

A. Paliwal, O. Schlenczek, B. Thiede, M. S. Pareira, E. Bodenschatz, G. Bagheri, A. Ecker

In weather and climate forecasting, several microphysical processes are unresolved, including turbulence-driven collision-coalescence of cloud droplets [1], radiative transfer through clouds [2]. Resolving these require instantaneous measurements of particles' spatial and size distribution in large and representative volumes. A popular method for acquiring such measurements is *in-line holography*, where a coherent light source illuminates the volume, and the 3D information about the particles within the volume can be reconstructed from a single image taken by a camera sensor [3]. However, analyzing a hologram is tedious [2] and currently takes two to four orders of magnitude longer than acquiring it [4]. Real-time hologram reconstruction could be a game changer for applications in air quality monitoring, climate research and environmental management.

We designed a two-stage neural network architecture, FLASHμ [5] (Fig. 8.20) that is able to detect small particles (6–100 μm) from holograms with large sample depths up to 20 cm. Trained only on synthetic data with added physical noise, our method reliably detects particles of at least 9 μm diameter in real holograms acquired in the lab with known ground truth (Fig. 8.17). The performance of our algorithm is comparable to the standard reconstruction-based approach while operating on smaller crops, at quarter of the original resolution and providing roughly a 600-fold speedup (Fig. 8.18). Preliminary tests on real cloud holograms suggest that the method also works well under real-world conditions when the particle density is not too high (Fig. 8.19). In addition to introducing a novel approach to a non-local object detection or signal demixing problem, our work could enable low-cost, real-time holographic imaging setups.

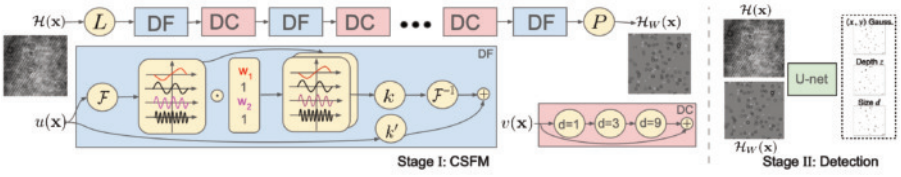

Figure 8.20: Stage I: CSFM. The hologram $\mathcal{H}$ is (L)ifted to a multi-channel image, goes through several Dilated Fourier (DF) and Dilated Convolutional (DC) blocks, and (P)rojected to Weighted Hologram $\mathcal{H}_w$. **Stage II: Detection.** The concatenated hologram, weighted-hologram $(\mathcal{H}, \mathcal{H}_w)$ pair is fed into the U-net which pinpoints (as (x, y) Gaussian blobs) the particle with limited receptive field. Additionally, depth z and size d (diameter) are regressed as separate channels.

[1] G. Bertens, Dissertation, University of Göttingen (2021)
[2] J. P. Fugal, Dissertation, Michigan Technological University (2007)
[3] J. W. Goodman, Introduction to Fourier Optics, Roberts & Co. Publishers (2005)
[4] J. P. Fugal, R. A. Shaw, E. W. Saw, A. V. Sergeyev, Appl. Opt. **43**, 5987 (2004)
[5] A. Paliwal, O. Schlenczek, B. Thiede, M. S. Pereira, K. Stieger, E. Bodenschatz, G. Bagheri, A. S. Ecker, arXiv:2503.11538 (2025)

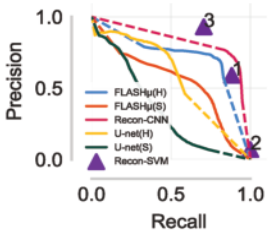

Figure 8.17: Precision-recall comparing the two methods.

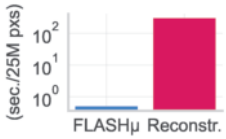

Figure 8.18: FLASHμ is 100 orders of magnitude faster than reconstr.-based approaches.

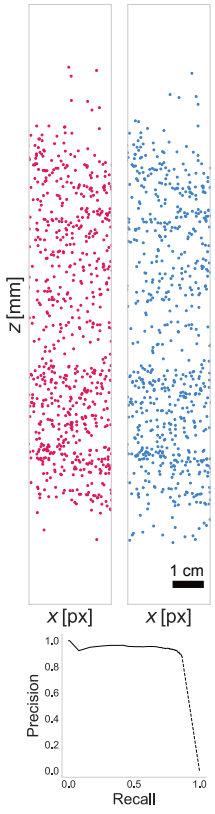

Figure 8.19: Example of FLASHμ's performance on a real cloud hologram of medium density.

FACILITIES

9

Contents

9.1 HIGH-PERFORMANCE COMPUTING FACILITY

D. Fliegner, H. Degering

The need for computing power and data storage space at MPI-DS originates from both numerical computations and simulations as well as from data acquisition and evaluation in experiments. For both purposes the HPC group provides file servers for personal and project data, HPC clusters with fast local data storage space for parallel computing and HPC systems for GPU accelerated codes. The necessary computing infrastructure scales way beyond single workstations, but well below large computing centers. As a mid-sized HPC facility it has to allow for interactive use, e.g. for developing large-scale parallel applications or directed parameter space exploration. The Linux workstations are part of the HPC systems at MPI-DS. Scientists can directly work on their data and control their jobs from their desktop systems.

The HPC group puts a lot of effort in keeping hardware as homogeneous as possible in order to minimize the maintenance workload and maximize interoperability between the scientific working groups. Currently, the HPC hardware at MPI-DS is mainly built of Lenovo systems using Intel Omnipath network interconnects for the parallel clusters. Scientists at MPI-DS have direct access to HPC clusters with

Figure 9.1: Cooling cabinets with a HPC cluster in one of the server rooms at MPI-DS. Each cabinet has a control and monitoring unit, is built in a modular way so that it can be moved, and can be customized to cool up to 36 kW if necessary.

an overall size of about 600 HPC systems (more than 26,000 CPU cores, approximately 132 TB RAM, 72 GPUs, and 10 PB of data storage capacity).

Hosting computing facilities of this size requires a very dense packing of servers which is ensured by using multicore machines and

efficient system designs like blade server enclosures. Corresponding power densities of more than 20kW per square meter cannot be cooled by traditional open air flow cooling with false floors. An efficient cooling system is required from an environmental perspective, but is mandatory from a budget point of view too, as electricity costs for cooling can be as high as one third of the total electricity costs with traditional cooling. MPI-DS was among the first institutes of the Max Planck society to solve this issue by using optimized water cooled cabinets in order to cool the necessary parts of the server rooms only, as shown in fig. 9.1.

To improve service reliability half of the MPI-DS HPC systems are located in a server room in the institute's building at Fassberg, whereas the other half is located at an external computing center site in the former 'Fernmeldezentrale' (FMZ) of Göttingen University. The smaller department server rooms at Fassberg were recently refurbished and are now used for project data file servers and infrastructure servers of all groups.

In order to manage such a complex facility at different sites, MPI-DS uses provisioning, configuration and monitoring systems based on open source software. The monitoring system collects important health data of the HPC hardware and the cooling facilities on a frequent basis. This data is summarized into a comprehensive overview and its history can be viewed for further diagnostics. In case of a cooling failure the monitoring system is able to perform an emergency shutdown autonomously in order to prevent machine damages by overheating.

9.2 UMWELTFORSCHUNGSTATION SCHNEEFERNERHAUS

G. Bagheri and E. Bodenschatz

Figure 9.2: Mast with sonic anemometers at the UFS.

Figure 9.3: A dual phase-Doppler interferometry probe.

The field measurement laboratory is a facility operated by MPI-DS at the research station Schneefernerhaus near the peak of Zugspitze mountain at an altitude of 2650 m. Location of the laboratory provides easy access to the two topmost outside platforms of the station, which are best suited for study of atmospheric turbulence and cloud dynamics.

On the top platform, we have installed a mast with a set of 3D sonic anemometers to conduct long-term year-round measurements of the wind and turbulence conditions at the UFS (Umwelt-Forschungsstation Schneefernerhaus - Environmental Research Station Schneefernerhaus).

Also situated on the top platform is a Lagrangian particle tracking apparatus dubbed the "Seesaw", consisting of a 6 m-long set of rails along which a vibration-damped box housing a set of high-speed cameras that can be driven at speeds of up to 7.5 m/s by two electromagnetic motors. Precise control of the translation velocity and tilt of the rail with respect to the horizontal make it possible to match the west-east and vertical components of the mean flow and follow cloud particles over time intervals longer than those achievable with a stationary setup. Illumination is provided by a 300 W green laser housed in the laboratory. A dual phase-Doppler interferometry probe allows measurement of cloud droplet size distribution and individual velocities.

The set of tools and equipment stored at the laboratory, together with the in-house machine shop, allows rapid development of new field experiments.

[1] G. Bertens, G. Bagheri, H. Xu, E. Bodenschatz, and J. Moláček, Rev. Sci. Inst. **92**, 125105 (2021)

9.3 RESEARCH ELECTRONICS FACILITY

L. N. Diaz-Maue, H. Nobach

Due to the unique nature of the experimental research projects carried out at MPI-DS, it is often necessary to utilize measurement devices, communication techniques and human-machine interfaces that are not commercially available. To this end, the Research Electronics Facility has a distinctive machine pool, which enables the development and construction of highly specialized electronic circuits for measurement and control tasks. These include the electronic interfaces between computers and measurement technology for scientific apparatus, all of which are produced in-house. The research electronics team works closely with the scientists throughout the process of specifying and designing the circuits required for the experimental work. Later they provide assistance to the scientists in the implementation and operation of the circuits and devices in their experiments. This allows us to provide a focused and agile response to improve devices, including on-site repair in failure cases and short development cycles for optimization and adaptation, with the highest level of professional support. Some projects in which we are especially engaged are:

- Cloudkite and HoloTrack / Physics of clouds and atmosphere,
- WinDart 1 and 2,
- Optical Particle Counters / Aerosol Dynamics,
- Low-Energy Amplifier Pulse Generators / Low-Energy Anti-Fibrillation Pacing.

Besides the support of the deparments and the various research groups in developing and building devices suiting their experimental research, the group members also pursue own research projects beyond the actual requests. These projects include:

- Micro-LED Arrays design and application [1] / Optogenetics,
- Multiwell Plate Illumination / Biological Systems,
- Hot-Wire Anemometers and Amplifiers / Measurement Devices [2],
- Pseudo-noise Generators / Secured Communication Protocols [3],
- Active Diodes / High-current Electronics [4],
- Unregular Sampling / Signal Processing [5].

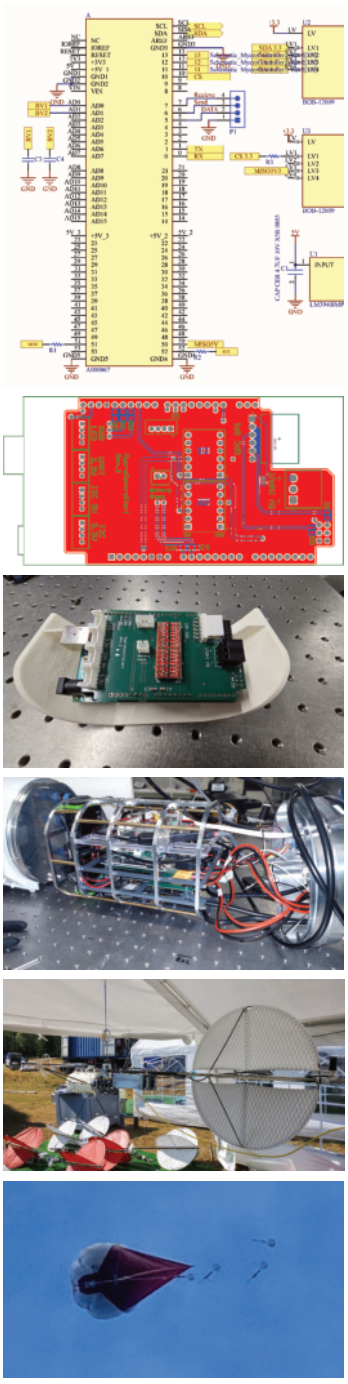

Figure 9.4: Printed Circuit Boards from Circuit Design via Prototyping, Assembly all through the Experimental Integration

[1] L. Diaz-Maue, Phys. Rev. Lett. **133**, 218401
[2] H. Nobach, arXiv:2308.03435
[3] H. Nobach, arXiv:2404.12011
[4] H. Nobach, Elektor Magazine 8/2023, p. 20
[5] N. Damaschke, V. Kühn, H. Nobach, J. Adv. Signal Process. **2024**, 17

9.4 SCIENTIFIC MECHANICAL ENGINEERING FACILITY

A. Heil

The requirements for experimental work at the Max Planck Institute for Dynamics and Self-Organization are versatile and very demanding. They require the highest quality in mechanical engineering from design and verification/certification to construction. The sizes of mechanical parts employed in the scientific experiments range from micrometers to many meters. They are used in various environments from the laboratory, to mount Zugspitze, and on research vessels like the Maria S. Merian. Parts are uniquely designed and manufactured for highly specialized experiments. Designs are conducted by the mechanical engineer, who heads the facility, in tight collaboration with the scientists. CAD 3D construction software is used not only to construct and develop the parts but also to conduct Finite Element Structural Analysis. The components created in the designs are then processed quickly, flexibly, and with high quality in the mechanical workshop according to the drawings or directly from the CAD design data with the help of a CAM interface. With a simulation integrated in the CAM software, potential errors occurring during the production process can be detected and eliminated before the actual part is machined. In addition, the 3D-CAD output can be used in scientific presentations and publications.

Figure 9.5: The scientific mechanical engineering facility.

Many of the unique experiments employ automated, integrated, computer-controlled systems. Very often, actuators, sensors, etc. with the associated control and testing devices are integrated into the mechanical components. In close cooperation with the Scientific Electronics Facility, the mechanical constructions are finetuned with the electronics.

Mechanical production is accomplished with computerized turning, milling, grinding, 3D printing, and other machines which cover the full area of precision mechanics. In order to produce precision parts with geometrically complex shapes, we have 5D-milling machines and 3D-printers.

The training of apprentices has also been an important part of the work of the facility from the very beginning. In the last ten years, our trainees have passed these examinations with distinction.

9.5 MICROFABRICATION FACILITY

S. Koschel (lab manager)

The Microfabrication Facility provides space, equipment, and assistance to design and manufacture devices for several groups within the institute and for other research institutions. The clean room (35 m2-Class 1000) is used to develop silicon masters via photo-lithography and it is equipped with a spin coater for deposing thin layers of SU-8 photoresist, hotplates for baking the resist and two mask aligners (EVG-620, UV-KUB 3) for exposing the wafers to UV illumination. Structures with features of 7-10 micrometers can be fabricated and a white light interferometer (Wyko NT1100) is used to accurately measure film thickness, surface roughness and surface features.

Microfluidic devices are assembled outside of the clean room environment after replica molding of the fabricated silicon master.

The facility is also equipped with a 3D laser lithography system (Photonic Professional GT) used to build unique 3D structures and devices with submicron resolution. Starting from the CAD model of the structure, using embedded software it is possible to rapidly print the structures with high degree of complexity via two photon polymerization of a UV curable photoresist.

Beside lithography, a high precision milling machine (DMU 50, DMG Mori Seiki) is used to pattern microchannels in hard plastic and metals for fabricating structures from 150 microns up to 10 cm.

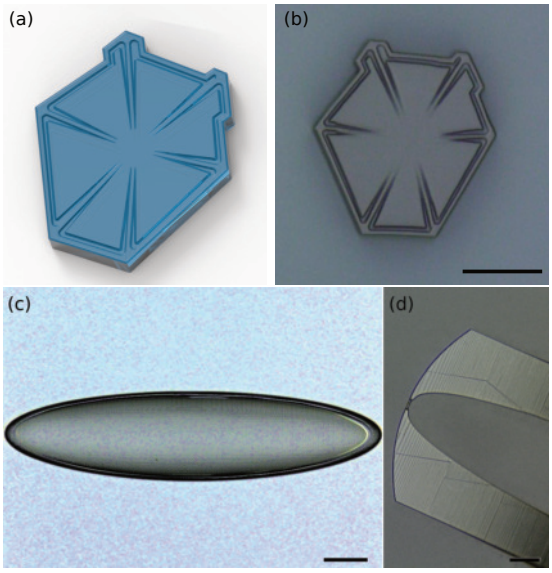

Figure 9.9: CAD Model of a snow crystal with hexagonal prism shape (a) and the fabricated 3D printing (b). Scale bar 70 microns. 3D printed elliptic particles (c) and hot wire probe (30 microns long and 4 microns thick) from measuring small-scale turbulence. Scale bar 100 microns.

The facility plays a pivotal role in developing microfluidic platforms for generating compartments that mimic cellular systems within the Max Planck Network on Synthetic Biology (MaxSynBio/cors), a joint Max-Planck-BMBF initiative. Training and assistance in microfabrication at all levels, from design to the use of microfluidic devices, is provided by the facility.

Figure 9.6: Working in the clean room.

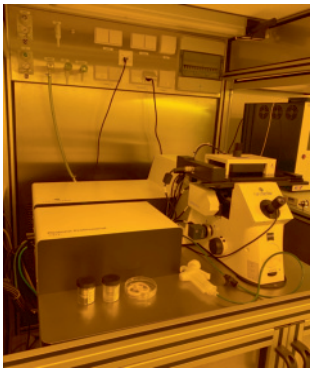

Figure 9.7: 3D printer.

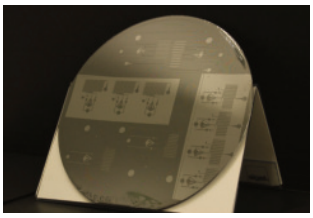

Figure 9.8: SU-8 wafer used for replica molding.

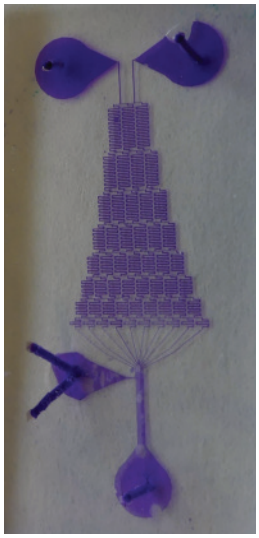

Figure 9.10: Microfluidic device fabricated by replica molding of PDMS.

9.6 MICROSCOPY FACILITY

S. Villa

The microscopy facility of the MPI-DS combines a set of advanced light- and laser based microscopes. It is operated by the LFPB department (Bodenschatz), but is open to users from the other departments as well as external users from the neighboring MPI-NAT. The current focus of the biophysical subgroups within the LFPB department are quantitative and synthetic biology. Therefore, the selection of the microscopes applies techniques of life cell imaging aided by sensitive cameras/detectors.

The backbone of the facility are two confocal laser scanning microscopes (Olympus FV1000) and a confocal spinning disk microscope (Olympus), which serve for a broad range of experiments, such as single cell stimulation and fast 3D imaging of migrating cells. These are complemented by a high precision light microscopy set-up (Deltavision), which achieves its z-resolution by deconvolution of epifluorescence z-stacks.

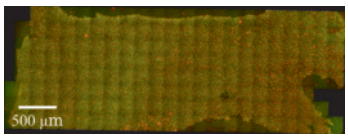

Figure 9.11: Stitched image after sequential imaging of the fixated and stained mammalian brain ventricle surface. The corresponding 184 z-stacks were recorded by spinning disk microscopy (60x, Olympus BX63 / Yokogawa). Image origin: Kapoor/Westendorf.

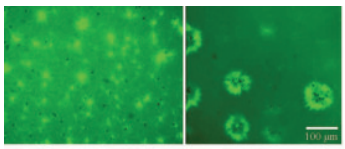

Figure 9.12: Dynamics of micron-sized bead delivery to the center of microtubule asters (4x, Olympus BX63 / Yokogawa). Image origin: Nasirimarekani.

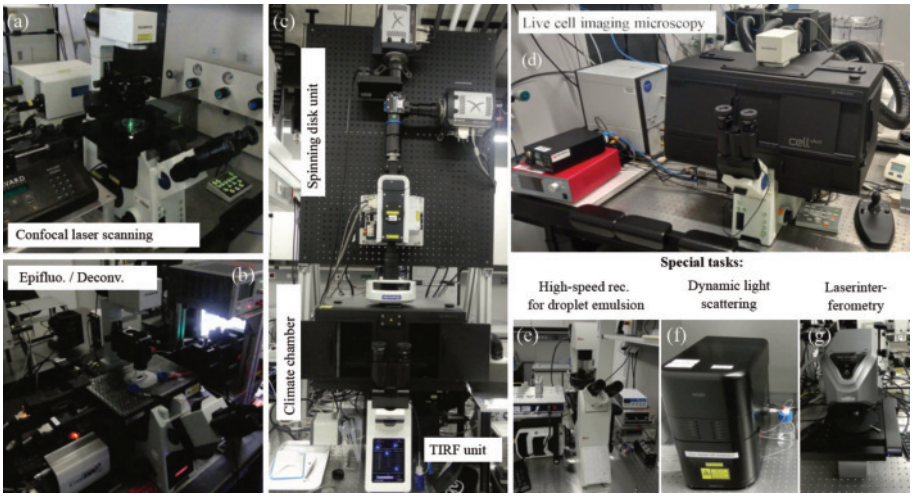

Figure 9.13: Selection of the currently operated microscopes. (a) Confocal laser scanning microscope (Olympus FV1000), (b) High precision epifluorescence (deconvolution enhanced) microscopy (Deltavision), (c) Dual set-up consisting of a spinning disk unit and a Fluorescence/TIRF unit (Olympus BX63/IX83), (d) Setup for automated live cell imaging mounted on an Olympus IX81, (e-g) Set-ups designed for special tasks.

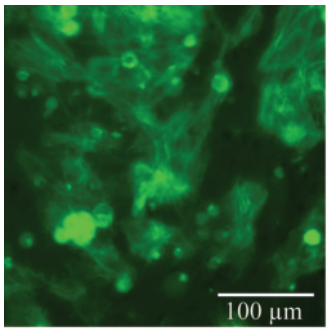

Figure 9.14: Human iPSC cardiomyocytes marked with sarcomeric α-actin. The image is part of a time lapse microscopy video series recording one week of experiment (10x, Olympus IX83). Image origin: Villa.

In the past years, we integrated multiple light and fluorescence microscopes of the now Emeritus group of Gregor Eichele. Recently, one of the confocal laser scanning microscopes and a bright field/fluorescent microscope (Olympus IX81) have been equipped with new climate chambers and some of their hardware has been updated to enable long and automated live cell imaging experiments with mammal cells.

The different set ups (see figure 9.13) allow for a variety of experiments such as large scale and long time unsupervised recordings, high speed video capture, dynamic light scattering and surface roughness measurements (see figures 9.11, 9.12, and 9.14 for examples). As in the previous period, the service of the microscopy facility also comprises the training of new users and the education of apprentices.

9.7 MOBILE CLOUD LABORATORY

O. Schlenczek, G. Bagheri, P. Höhne,
F. Nordsiek, M. Schröder, E. Bodenschatz

With our CloudKite platform, we can deploy different airborne instruments like the Advanced Max Planck CloudKite (MPCK$^+$) and the WinDarts [1], [2]. But to interpret the airborne data as well as evaluating flight safety, we need additional instruments on the ground to get the big picture in terms of cloud and boundary layer dynamics. Additionally, we need to transport the CloudKite to the field, have a location to repair instruments, and bring some computing power to do data analysis in the field. To accomplish this, we use the Mobile Cloud Laboratory (MCL), an instrumented van for transportation of the CloudKite hardware, data acquisition and instrument maintenance. An overview of the inside of the MCL is shown in Fig. 9.15 left.

The devices for ground-based measurements, weather and aispace monitoring are shown in Fig. 9.15 right. These are a 3D ultrasonic anemometer (Metek uSonic 3 Class A-MP), one compact weather station (Lufft WS500UMB), one field mill (Campbell Scientifc CS 110), one trace gas analyzer (Li-Cor LI-7500DS), and one lightning detector (Boltek LD 250). In addition, we operate a uAvionix pingStation Mode S and ADS-B receiver to locate nearby aircraft. All the data are displayed in near real time on the flight computer monitor. Airspace monitoring data as well as wind data, lightning strikes and electric field data are of particular importance for safety.

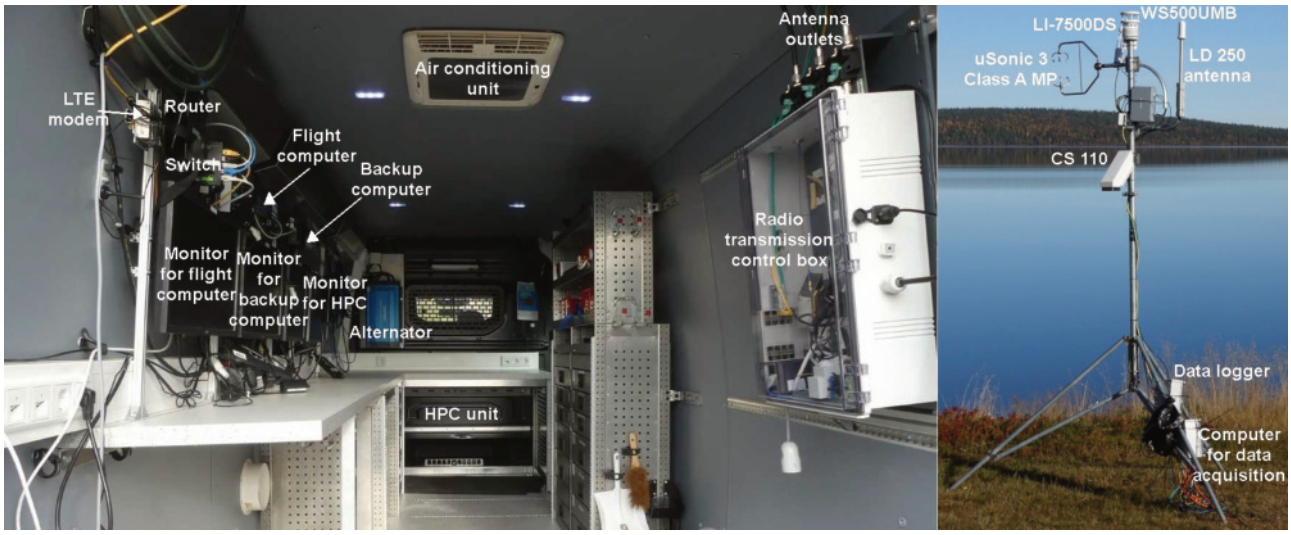

Figure 9.15: Left: Interior of the MCL van with main features annotated. Right: Ground station for weather and airspace monitoring with annotated devices. Photos were taken during the PaCE 2022 field campaign in Finland.

[1] V. Chavez-Medina, H. Khodamoradi, O. Schlenczek, F. Nordsiek, C. E. Brunner, E. Bodenschatz and G. Bagheri, Earth System Science Data, *to be published* (2025)
[2] O. Schlenczek, F. Nordsiek, C. E. Brunner, V. Chavez-Medina, B. Thiede, E. Bodenschatz and G. Bagheri, Earth System Science Data, *to be published* (2025)

9.8 THE MAX PLANCK TURBULENCE FACILITY

C. E. Brunner, L. Le Turnier, H. Kim,
M. Grunwald, F. Falkinhoff, E. Bodenschatz

Figure 9.16: The Variable Density Turbulence Tunnel (VDTT)

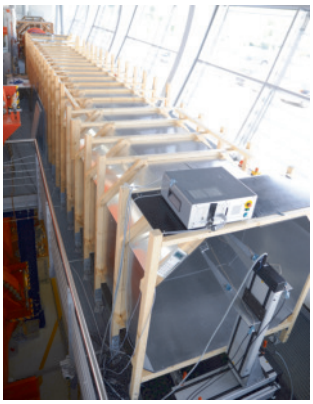

Figure 9.17: The Prandtl Tunnel

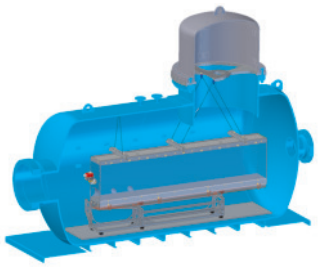

Figure 9.18: Schematic of the "U-Boot", a general-purpose pressure vessel, housing the High-Pressure Convection Facility (HPCF)

To understand turbulence in a fundamental sense and to make predictions useful in real-world applications, one needs not only to observe turbulence at high Reynolds numbers, but also to realize flows with various spatial and temporal large scale properties. These well defined flows must go hand in hand with precise measurements. In addition one must have the ability to adjust the conditions in various ways, so that dependencies can be uncovered. The Max Planck Turbulence Facility at the MPI-DS makes it possible to generate turbulence with the highest Reynolds numbers under laboratory conditions with unprecedented control. To match our achievements in controlling turbulent flows, we have advanced measurement technologies, and have even adapted these to field experiments of natural flows [1].

The Variable Density Turbulence Tunnel (VDTT) [2] is a recirculating pressurized wind tunnel that contains two measurement sections with cross-sectional areas of $1.9\,\mathrm{m}^2$ and lengths of 9 m and 7 m. The maximum flow speed is approximately 5.5 m/s. The Reynolds number is finely adjustable by changing the pressure of the gas in the tunnel, usually sulphur hexafluoride (SF_6) up to a pressure of 19 bar. An active grid consisting of 111 individually controllable flaps creates turbulence with a wide range of length scales and intensities [3, 4]. This ultimately controls the homogeneity, isotropy, and intensity of the turbulent fluctuations. The active grid allows us to reach Taylor-scale Reynolds numbers of up to 6000 with statistically homogeneous turbulence compared to maximally 1700 when a classical grid of crossed bars is used to inject turbulent kinetic energy. There exists no other wind tunnel facility that can achieve comparable Reynolds numbers. Additionally, the active grid gives us precise control over the turbulence forcing [5]. A particle-tracking system allows for Lagrangian measurements at triple the Taylor Microscale Reynolds number of any previous Lagrangian measurement. This state-of-the-art experimental system consists of high-power laser or LED illumination, an in-house particle disperser, and a vibration-damped platform holding four high-speed cameras [6].

The Prandtl tunnel is an open-circuit wind tunnel from the 1930's. The wind tunnel is 11 m long with a measurement section of 1.2 m x 1.5 m and maximum wind speed of 12 m/s. An active grid provides control over the inflow turbulence and a hot plate can be used to generate thermal boundary layer flows. Measurements are primarily conducted using hot-wire anemometry.

The High Pressure Convection Facility (HPCF) [7] uses a general-purpose pressure vessel called the "U-Boot", which is 5.3 m long and has a diameter of 2.5 m and can be filled with SF_6 up to a pressure of 19 bar. We precisely control both the temperature and the pressure in the vessel. Within the vessel is a rectangular Rayleigh-Bénard (RB) experiment of large aspect ratio (height 0.7 m, length 3.5 m and width 0.35 m) that can reach Rayleigh numbers as high as 5×10^{13}. With

its transparent sidewalls, the experiment allows for optical velocity measurements at unprecedentedly large Rayleigh numbers.

The "Cigar" is a general-purpose pressure vessel with a length of 4 m and an inner diameter of 1.5 m. It can be filled with SF_6 up to a pressure of 19 bar to perform smaller convection or turbulence experiments or to test equipment for the other pressurized facilities.

Two von Kármán mixers generate high Reynolds number turbulent water flows between two counter-rotating baffled disks. Because the average velocity of fluid particles near the middle of the mixers is close to zero, their motions can be followed for a long time. The mixers are about a half-meter in diameter, and the Taylor-scale Reynolds number can be as high as 1200. Large glass windows provide optical access for imaging techniques. The apparatus can be pumped down to reduced-pressure for the study of bubble dynamics. A frequency doubled high-power (50 W), high-repetition-rate Nd:YAG laser is devoted to measurements in this apparatus.

Theoretical knowledge is most developed for turbulence that is stationary and isotropic. But real flows are neither.

The facilities make use of state-of-the-art three-dimensional Lagrangian particle tracking (LPT) technologies that we have developed in-house. The technology relies on multiple ultra high-speed cameras viewing the same particles from different angles, with megapixel resolution and kilohertz frame rates. We also employ a Dantec hot-wire system in conjunction with nano-fabricated hot-wires from Princeton University [8], a LaVision tomographic particle image velocimetry system, and a TSI laser Doppler velocimetry and particle sizing system. All of this equipment is compatible with pressures up to 15 bar. Some of these techniques require substantial light, which is typically produced by Nd:YAG lasers or LED lights. The systems produce data at rates that necessitate high-performance computing and storage clusters.

The Max Planck Turbulence Facilities (MPTF) are open to visiting researchers. For example they were used in the European High-Performance Infrastructures in Turbulence (EuHIT) project, which integrated cutting-edge European facilities for turbulence research across national boundaries.

Figure 9.19: The "Cigar", a general-purpose pressure vessel

Figure 9.20: The von Kármán mixer

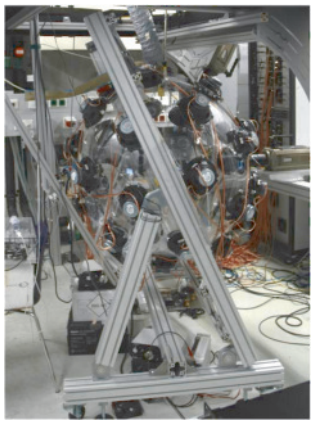

Figure 9.21: A "soccer ball"

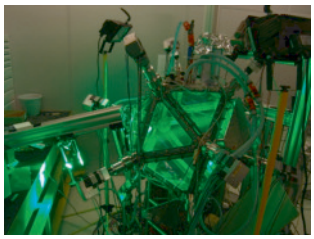

Figure 9.22: The Lagrangian Exploration Module

[1] B. Hejazi, H. Antigny, S. Huellstrunk, E. Bodenschatz, New J. Phys. **25**, 093046 (2023)
[2] E. Bodenschatz, G. P. Bewley, H. Nobach, M. Sinhuber, H. Xu, Rev. Sci. Instrum. **85**, 093908 (2014)
[3] K. P. Griffin, N. J. Wei, E. Bodenschatz, G. P. Bewley, Exp. Fluids **60**, 55 (2019)
[4] C. Küchler, G. Bewley, E. Bodenschatz, J. Stat. Phys. **175**, 617 (2019)
[5] M. Grunwald, C. E. Brunner, arXiv:2502.21182 (2025)
[6] C. Küchler, A. Ibanez Landeta, J. Moláček, E. Bodenschatz, Rev. Sci. Instrum. **95**, 105110 (2024)
[7] M. Wedi, D. van Gils, E. Bodenschatz, S. Weiss, J. Fluid Mech. **921**, A30 (2021)
[8] C. Küchler, G. P. Bewley, E. Bodenschatz, Phys. Rev. Lett. **131**, 024001 (2023)

INFRASTRUCTURE

10

Contents

10.1 OVERVIEW

The scientific creation of value at the Max Planck Institute for Dynamics and Self-Organization (MPI-DS) is supported by an efficient, high-performance and flexible infrastructural service. The so-called infrastructure management is divided into the two core areas of Administrative Service and Scientific Technical Service. The administrative service includes the areas of personnel, budget and finances, and building and operational technology, which ensure the basic operational processes. The Scientific and Technical Service includes the areas of: IT (see section 10.4 below and section 9.1), Research Electronics (see section 9.3) and Scientific Mechanical Engineering (see section 9.4), which provide direct, technical services for science.

In view of their characteristically overarching service role for the scientific organizational units and infrastructure management, the areas of Quality Management, Communication, Driving Service and General Service have been organized as staff units and assigned directly to the Chief Operations Officer. The Quality Management unit acts in a process-oriented manner and scrutinises existing organizational processes together with the existing organizational units in order to continuously ensure the quality of existing processes with regard to internal and external influencing factors.

Public relations and outreach (see section 11) work is characterized by a close proximity to the scientists of the MPI-DS. This is a key factor for the success of press and public relations work at the MPI-DS. The Institute's own driving service supports travellers in keeping appointments over short and long distances despite tight schedules in a dynamic and internationally oriented environment. The reception of our guests at the Institute location and in the WBZ (Wissenschaftliches Begegnungszentrum = Scientific Meeting Center) is ensured by the General Service. In addition to this, they take on general assistance tasks.

10.2 ADMINISTRATIVE SERVICE

The Institute's administrative service covers a wide range of responsibilities and tasks. In the past, the administrative service was divided into the areas of personnel, budget and finance, building and operating technology and IT service. With the reorganization of the entire IT at the MPI-DS (IT Service, High Performance Computing and Department IT Administration), the IT Service was combined with the other two units to form an overall IT and assigned to the Scientific Technical Service. The reorganization measures implemented in 2021 are now bearing fruits and have resulted in a noticeable increase in effectiveness and efficiency. The increasingly complex area of IT, HPC, data protection, cyber security and licensing management can thus be dealt with in the best possible way despite the same amount of resources.

Based on various legal regulations and standards, funding guidelines and federal guidelines, it is the task of the administration to ensure

a comprehensive, legally secure, science-promoting and sustainable organization of all administrative processes. The administration acts as an advisor and service provider for science in all personnel-related but also financial issues, as well as for all areas of infrastructure.

In all its activities, the MPI-DS is supported in internal and external communication by public relations and outreach work, with a value-added focus on external communication on scientific successes and processes (see section 11).

Standard instruments such as internal monthly newsletters, the organization of lecture series for a general, cross-group understanding of scientific work at MPI-DS and the new "onboarding" format for new institute members promote general understanding, identification and communication. New media are increasingly being used for the purpose of contemporary communication. For example, the video format "DO YOU HAVE A MINUTE" illustrates the scientific spectrum at the MPI-DS in a compact and targeted manner.

In 2025, special attention will be paid to the planning and organization of the main event for the 100th anniversary of MPI-DS, which will take place in July 2025.

The comprehensive professional press and public relations work of the staff unit makes a continuously valuable and important contribution to the external image of MPI-DS and to the identification and motivation of the institute's employees.

As an important anchor for a sustainable institute organization, the MPI-DS has a staff unit for quality management. Starting from the moderation of numerous meetings with the directors and senior scientists to create a common Institute vision, the staff unit accompanies and controls all Institute processes. By analyzing the individual processes, their interfaces and their respective outputs, the processes can be clearly defined and implemented in accordance with current legal regulations and standards. The standardized documentation ensures a legally compliant institute organization in the scientific and non-scientific areas.

The General Service staff unit welcomes the guests of our Institute at the Faßberg and the WBZ. In addition to this, the General Service assists with standardized processes in all departments of infrastructure management, or takes over the catering for the entire Institute within the framework of internal events. In addition to this, the post office service and the cash desk service are also provided.

The Institute's own transport service is an important service, especially in times of tight schedules and processes between the Institute's location, the numerous cooperation partners, the WBZ and the general travel locations (e.g. event venues or airports), so that deadlines can be met while those travelling can concentrate on their work.

10.2.1 Personnel

The Human Resources Division advises and supports scientists in all matters relating to employment and at all career levels, as well as infrastructure staff. This includes all personnel, legal and organiza-

tional issues such as work permits, health insurance and tax and social security benefits.

The continuous development of health promotion at MPI-DS makes a valuable contribution to balancing personal and professional interests. In addition to the development of in-house activities and sports opportunities, various courses for physical and mental health are offered on an ongoing basis.

10.2.2 Budget and Finances

The Budget and Finances section includes accounting, budget planning and taxation, asset management and annual accounts, all purchasing and customs procedures, export control, and manages third-party funds, the scientific meeting centre, the vehicle fleet, guest hospitality, event organization and all business trips.

The use of eProcurement has been expanded to all areas of our institute. In the operating activities, it is particularly pleasing that the existing procurement regulations can now be applied in such a way that contracts can also be awarded with greater consideration for sustainability criteria.

In the field of third-party funding, the acquisition of third-party and project funding continues to be successful. The experienced employees provide professional support and advice in the application and administration of the acquired funds at national and international level.

The increasing complexity of different areas of administration demands a better understanding of the applicable framework conditions by scientists. Particularly in those areas where the focus is on scientific output, such as export controls, the involvement of the scientific staff is essential.

With this in mind, the MPI-DS administration started an internal awareness-raising and training program in 2024.

10.3 BUILDING SERVICES AND OPERATING TECHNOLOGY

The service area "building services and operating technology" is divided into electrical and plant engineering. The service area is responsible for the maintenance and repair of the entire technical infrastructure of the institute, including heating, cooling, plumbing and ventilation, electrical engineering, fire alarm systems, telecommunications, gas detection systems, and emergency call systems. While small and medium-sized repairs and maintenance are carried out by team members, larger measures are outsourced and coordinated by the team. The service unit also takes care of all janitorial and cleaning tasks.

Sustainability and therefore energy efficiency are very important to MPI-DS. In addition to many energy-saving measures, the MPI-DS was the first institute of the Max Planck Society to install solar modules to generate renewable energy on its own initiative. Our initiative became a best-practice example for all institutes of the Max Planck Society.

10.4 INFORMATION TECHNOLOGY

The IT group consists of the HPC group, which is responsible for the HPC networks, HPC clusters, HPC file and project data servers and the Linux workstations (see section 9.1 High-Performance Computing Facility for details), and the IT service (ITS) group. The ITS group operates the normal institute network including the central network core and router, the firewall systems and the wireless LAN. It also runs the basic server infrastructure of the institute, which includes central file and authentification servers for Windows workstations and notebooks, and a virtualization cluster that is used to implement a broad spectrum of different IT services. The ITS group also provides Windows and macOS desktop and laptop support for the infrastructure groups and the scientific departments. Furthermore, the ITS group is responsible for the maintenance and operation of the printers and print servers.

In addition to providing IT systems, services and support the provision and licensing of software is also centrally handled by the IT group. In the case of the ITS group, this primarily involves commercial software, whereas the HPC group also handles the installation and maintenance of a wide range of open source software packages that usually need to be compiled and tailored to the existing HPC clusters. The setup of experiments is supported by both groups, depending on the respective IT requirements. This also includes the data management, backup and archiving and the provision and maintenance of the corresponding IT systems.

The IT group participates in the apprenticeship program of the institute. Few other institutions in Göttingen have got such a large variety of different IT systems that can be used in IT training courses. Currently, there are two apprentices in the IT group, in the third and first year, respectively.

COMMUNICATION

11

Contents

11.1 PUBLIC RELATIONS AND OUTREACH

Public outreach and media relations are recognized as an important part of the institute's responsibility. This is reflected by numerous press releases, by activities on social media, as well as by the institute's ongoing participation in public events and exhibitions. Both internal communication and outreach activities are coordinated by the institute's communication office.

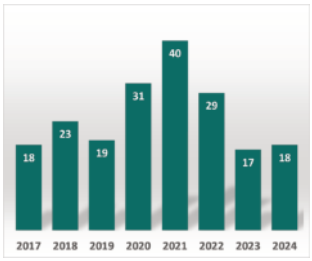

Figure 11.1: Number of MPI-DS press releases per year

11.1.1 Media relations

Press releases and news articles form the basis in communication with the local, national, and international media. These releases deal with scientific results from all departments and Max Planck Research Groups, inform the media about important prizes awarded to MPI-DS scientists, and advertise special events the institute organizes or takes part in.

Figure 11.2: Presentation of the MPI-DS at the Science Market in the Center of Göttingen

Generally, press releases are published in both German and English to reflect our national and international visibility. In recent years, the number of press releases issued per year continued to be at a high level in comparison to similar research institutions, especially during the years of the Covid-19 pandemic. These press releases frequently spark the interest of international media, industrial partners or directly other colleagues from science and research to our work. An overview of the media reports is collected by the press office and a selection is communicated to the employees in the internal newsletter.

11.1.2 75 year MPG anniversary

Figure 11.3: Science Slam in the Old Town Hall, organized by the MPI-DS

In 2023, the Max Planck Society celebrated its 75th anniversary in Göttingen. Since the society was founded in the premises of the Kaiser-Wilhelm-Institute preceding our institute, we took an active part in organizing the celebrations. Amongst others, we organized tours at the institute, contributed to the hands-on science market in the center of Göttingen and organized a Max Planck Science Slam. National and international media frequently reported on the anniversary, including also several articles on the MPI-DS in particular. Outreach and social media activities regarding the anniversary were coordinated by the central communication office of the Max Planck Society.

11.1.3 Guided Tours

Upon request, the MPI-DS offers school and student groups regular tours of the Institute. Young participants get the opportunity to learn more about the scientific work at the institute. Tours usually include the visit of the experimental hall, the computer cluster or the various laboratories. Upon request, the communication office can involve scientists to present the scientific content in a clear and target-oriented manner.

11.1.4 *Future Day*

Once a year in spring, 20 young students from Göttingen and the surrounding area visit us for the Future Day. This way, the students from grade 7 to 10 get a first-hand impression of a working day in a basic research institute. During their visit, girls and boys experienced research on dynamics and self-organization up close: self-organization of algae, simulations of emergent dynamics, or currents on a large scale such as those found in clouds. The Future Day is always a major success and great event, not only for the young visitors, but also for the scientists involved.

Figure 11.4: The Future Day 2024

11.1.5 *Social Media & Online presence*

During recent years, the MPI-DS expanded its online presence and continues to do so. The main social media channels used are LinkedIn and YouTube with currently several thousand followers and a steadily rising number of subscriptions. On X (formerly Twitter) we joined the concerted activity of German universities and research institutes in January 2025 and set our channel on hold to show that we do not agree with the increasing spread of false information via this platform.

Additionally, several group leaders also administer their own social media channels where MPI-DS research is prompted. With a clean

design, the website of the MPI-DS aims to provide information to all stakeholder groups in both, English and German. In addition to these platforms, we also focus on audiovisual presentations of the institute.

11.1.6 Video production

Figure 11.5: Video production for YouTube

To make activities at the MPI-DS more accessible, different videos and short clips were produced in house and published on YouTube. These include the presentation of our apprenticeships, interviews with scientists and insights into the daily research work, amongst others. The series 'Do you have a minute?' showcases everyday life activities and projects from individual researchers, explaining their current project in roughly one minute. Additionally, we produced a video introducing the department of Living Matter Physics in collaboration with a local media partner to highlight the growing importance of this field in physics. For the 100 year celebration in 2025, a new video about our research and history has been made.

11.1.7 Max Planck goes to school

Figure 11.6: The Night of Science 2022

In a joint project together with the other Max Planck Institutes in Göttingen, the initiative 'Max Planck geht zur Schule' takes place every year. Scientists from the institutes visit local schools on a dedicated date using one of the lessons to explain their research to the students. Each year, volunteering Max Planck scientists from Göttingen offer approximately 30 different subjects to the schools from which the teachers can select and invite a scientist for one day. By this, not only the visibility of the Max Planck Institutes is increased, but also scientific thinking and interest for contemporary research topics are promoted already at an early stage.

11.1.8 Night of Science

The Night of Science in the biggest science festival in Göttingen with 25,000 visitors during the last edition in 2022. As part of Göttingen Campus, also the MPI-DS contributes to the more than 400 activities and events throughout the city. Together with their colleagues from the other local Max Planck Institutes, our scientists volunteered to showcase their research in interactive presentations and experiments. The next edition of the Night of Science will take place in summer 2025.

11.1.9 Team event

Figure 11.7: Preparing food during the team event 2024

In addition to Christmas celebration and summer festivals organized by the employees, the institute also regularly organizes team event to promote communication across the various departments. In 2024, a cooking event was organized during which 14 professional cooks from Göttingen guided more than 200 MPI-DS employees in preparing special vegetarian dishes, using all kitchens of the institute. The activity was accompanied by talks on the physics of food, cooking and nutrition. During the subsequent gathering and introduction of the

various courses, people could connect and get to know their colleagues beyond the everyday working routines.

11.1.10 Göttinger Literaturherbst

The MPI-DS also takes part in the 'Göttinger Literaturherbst' taking place each autumn. This literature festival is one of the largest of its kind in Germany with more than 20,000 visitors each year. A key element of the festival is the scientific series where internationally renowned scientists present their latest books in the unique atmosphere of the historic Paulinerkirche in Göttingen. These lectures are introduced and chaired by scientists from the local Max Planck Institutes, leading to a vigorous exchange of ideas. The presentations of the books and the discussions are broadcasted live and provided after the event for free online to address also an audience outside Göttingen. Moreover, one of the invited speakers is awarded the Science Communication Medal to honor strong commitment to communicate current scientific results to the general public. In recent years, Prof. Gerd Gigerenzer, Katrin Böhning-Gaese and Dr. Arik Kershenbaum were awarded with the medal in 2022, 2023 and 2024, respectively.

Figure 11.8: Eberhard Bodenschatz and invited author Thomas de Padova during the Literaturherbst 2024

11.1.11 Future activities

The scientific output of the institute will continue to be accompanied by press releases and news articles. As science communication is of increasing importance, existing communication channels will be expanded and new channels may be opened. Due to a very positive perception of the recent videos produced, we will continue the series 'Do you have a minute?' providing insight to everyday life at the MPI-DS. The expansion of our Alumni-Network will help us to maintain contact with former members provided a network for exchange with current employees.

11.2 INTERNAL COMMUNICATION

In addition to the presentation of the MPI-DS to external stakeholders, we also aim to communicate our activities to our own employees. By actively maintaining communication channels and sharing information about ongoing projects internally, we aim to create a positive and enjoyable working environment.

11.2.1 Intranet

Since 2022, the Intranet of the MPI-DS was relaunched in accordance with the Max Planck Society and adapted to the MAX-platform, based on MS SharePoint. This facilitates communication across different institutes and contributes to the corporate identity while providing an interactive working platform. Documents and forms, as well as guidelines for documentations and standard operating procedures are now generally provided via MAX.

11.2.2 *Science before the weekend*

The lecture series 'Wissenschaft vorm Wochenende' (Science before the weekend) has shown to be an efficient and well received tool in order to explain the scientific work at the institute to the administrative and technical staff. In quarterly intervals, the departments of MPI-DS identify speakers who present their topics in a comprehensive and understandable manner in German language. This way, also the employees with a non-scientific background easily gain access to scientific topics from their colleagues, which supports both the mutual understanding and the team spirit. Typically, the audience consists of up to 50 people from all over the institute, indicating a high appreciation for this internal communication project.

11.2.3 *Internal newsletter*

Figure 11.9: The monthly internal MPI-DS newsletter

The internal MPI-DS newsletter is distributed monthly via mail to all employees and students at the MPI-DS. It contains important upcoming dates and events, reports latest scientific achievements and awards, as well as an overview on new employees, recent publication and media coverage. In a dedicated spotlight section, one topic is introduced and discussed in more detail each month. The newsletter is compiled and edited by the communication office; all institute members are invited to submit content that they wish to communicate to the entire MPI-DS.

11.2.4 *Onboarding*

Approximately every 3 months, the communication office organizes an onboarding where new employees who joined the institute since the last meeting get to know the organizational structure of the institute and can raise their questions. Likewise, they get to know those who are also new to enable mutual help. Representatives of the working council, gender equality office, the workshops, Human Resources as well as the ombudsperson and representative of the PhD and PostDoc community are also present during the meeting to introduce their field of work.

11.2.5 *Sustainability group*

Several employees of the MPI-DS initiated a task group to promote and encourage a more sustainable and environmental-friendly behavior at the institute. This includes regular discussions on waste and energy management as well as regular communication of recommendations via the internal news channels. The group meets once per month during lunch hours and is open to all employees, aiming to discuss measures which can be implemented to improve sustainability.

11.3 THE GÖTTINGEN CAMPUS

The Göttingen Campus was established by the university in 2006 in order to coordinate campus wide activities with the non-university

institutes. The main task of the Göttingen Campus is the consultation between the executive committees of the University (Presidential Board, University Medical Centre Board, Senate) and the non-university institutes. Topics range from joint teaching and research activities, towards the identification of research foci for the development of the Göttingen Campus. The Campus Marketing Group exists since 2016 and exchanges information once a quarter about joint activities such as the Night of Science, the Göttingen Literaturherbst, joint advertising products, the Göttingen Campus website and the Göttingen Campus Event Calendar.

11.4 MAX PLANCK CAMPUS

Together with the Max Planck Institute for Multidisciplinary Sciences (MPI-NAT), the MPI-DS forms the Göttingen Max Planck Campus. As part of the restructuring process, the Faßberg Campus is currently being expanded to include a new building ('Tower 7') to host research groups of the MPI-NAT. Common infrastructure, such as the Otto-Hahn-Library and the canteen, continue to be available to all partners of the Max Planck Campus and help cultivate an atmosphere of exchange and participation. In the past years, further efforts have been made to increase the cooperation between Max Planck Institutes and create synergistic projects. This includes regular meeting on scientific, but also on organizational and infrastructural topics.

11.4.1 Ecological projects on campus

During recent years, several ecological projects have been initiated and conducted around the Max Planck Campus. A recent example is the creation of a meadow orchard at the rear side of the MPI-DS. Together, these projects aim to support a sustainable ecology, provide living space for animals and insects and raise the consciousness for environmental care, also supported by the sustainability group of the MPI-DS.

Figure 11.10: The orchard on the backside of MPI-DS

11.4.2 Further Max Planck Campus Activities

Several tools have been established to foster the scientific exchange between researchers from the Max Planck Institutes in Göttingen. This is e.g. realized via the Campus Seminar, a biweekly lecture series with PhD and master students as speakers. Here, projects and results can be discussed with colleagues, allowing for a preliminary exchange of ideas with the aim of triggering scientific cooperation.

A more unofficial framework for getting to know other colleagues on campus is also possible during the annual summer festival on Faßberg.

HOW TO REACH US AT THE MAX PLANCK INSTITUTE FOR DYNAMICS AND SELF-ORGANIZATION

Fassberg site (main building)

Address:
Am Fassberg 17
D-37077 Göttingen
Germany

Departments:	Fluid Physics, Pattern Formation, and Biocomplexity (Prof. Eberhard Bodenschatz) Living Matter Physics (Prof. Ramin Golestanian)
Max Planck Research Groups:	Turbulence and Wind Energy (Dr. Claudia Brunner) Theory of Turbulent Convection (PD Dr. Olga Shishkina) Biomedical Physics (Prof. Stefan Luther) Neural Systems Theory (Prof. Viola Priesemann) Theory of Biological Fluids (Dr. David Zwicker)
Independent Research Units:	Dynamics in mesoscopic systems (Dr. Ragnar Fleischmann)
Emeritus Groups:	Nonlinear Dynamics (Prof. Theo Geisel) Dynamics of Social Systems (Prof. Stephan Herminghaus) Rhythms – Beating Cilia and Ticking Clocks (Prof. Gregor Eichele)
Services:	Institute Management, Administration, Facility Management, Electronics and Mechanics Workshops, IT-Services, Library, Communication Office, Stock Rooms, Lecture Hall, Göttingen Turbulence Facility, Clean Room, and Cell Biology Laboratories

By plane
From Frankfurt am Main Airport (FRA): Use one of the railway stations at the airport. Trains to Göttingen (direct or via Frankfurt) leave twice an hour during daytime (travel time: 2 hours). From Hanover Airport (HAJ): Take the suburban railway (S-Bahn) to the Central Station (»Hannover Hauptbahnhof«). From here direct ICE trains to Göttingen depart every 1/2 hour.

By train
Göttingen Station is served by the following ICE routes: Hamburg-Göttingen-Munich, Hamburg-Göttingen-Frankfurt am Main, and Berlin-Göttingen-Frankfurt. From Göttingen railway station: On arrival at Göttingen station take a taxi (15 minutes) or the bus (20 minutes). At platform D take the bus No. 21 (direction: »Nikolausberg«) or No. 23 (direction: »Faßberg« or »Universität Nord«). After about 20 minutes get off at the »Faßberg« stop, which is directly in front of the entrance of the Max Planck Campus (MPI-DS and MPI for multidisciplinary Sciences). Ask at the gate to get directions.

By car
Leave the freeway A7 (Hanover-Kassel) at the exit »Göttingen-Nord«, which is the northern of two exits. Follow the direction for Braunlage (B 27). Leave town – after about 1.5 km at the traffic light (Chinese restaurant on your right) turn left and follow the sign »Nikolausberg«. The third junction on the left is the entrance to the Max Planck Campus (MPI-DS and MPI for multidisciplinary Sciences). Ask at the gate to get directions.

Bunsenstraße site (Scientific Meeting Center)

Emeritus Group:	Molecular Interactions (Prof. Jan Peter Toennies)
Services:	Scientific Meeting Center

Address:
Bunsenstraße 10
D-37073 Göttingen
Germany

By plane
From Frankfurt am Main Airport (FRA): Use one of the railway stations at the airport. Trains to Göttingen (direct or via Frankfurt main station) leave twice an hour during daytime (travel time: 2 hours). From Hanover Airport (HAJ): Take the suburban railway (S-Bahn) to the Central Station (»Hannover Hauptbahnhof«). From here direct ICE trains to Göttingen depart every 1/2 hour.

By train
Göttingen Station is served by the following ICE routes: Hamburg-Göttingen-Munich, Hamburg-Göttingen-Frankfurt, and Berlin-Göttingen-Frankfurt. From Göttingen railway station: From the Göttingen station you can take a taxi (5 minutes) or walk (20 minutes). If you walk, you need to leave the main exit of the station and turn to the right. Follow the main street, which after the traffic lights turns into Bürgerstraße. Keep walking until you come to the Bunsenstraße. Turn right – you will reach the entrance gate of the MPI-DS after about 300 m.

By car
Leave the freeway A7 (Hanover–Kassel) at the exit »Göttingen«, which is the southern exit. Follow the direction »Göttingen Zentrum« (B3). After about 4 km you will pass through a tunnel. At the next traffic light, turn right (direction »Eschwege« B27) and follow the »Bürgerstraße« for about 600 m. The fourth junction to the right is the »Bunsenstraße«. You will reach the institute's gate after about 300 m.

Campus Institute for Dynamics of biological Networks

Max Planck Research Group:	Dynamics of Biological Networks (Prof. Dr. Fred Wolf)

Address:
Göttingen Campus Institute for Dynamics of biological Networks (CIDBN)
Heinrich-Düker-Weg 12
D-37073 Göttingen
Germany

IMPRINT

Max Planck Institute for Dynamics and Self-Organization
Am Faßberg 17
37077 Göttingen (Germany)

Editors
Eberhard Bodenschatz
Ramin Golestanian

Editorial Managers
Philip Bittihn
Holger Nobach
Christina Morgenstern
Ulrich Degenhardt
Guido Schriever

Printed by Bonifatius Druckerei, Paderborn, Germany